

# NSW coastal erosion and inundation hazards and exposure assessment

Technical report 2025



Department of Climate Change, Energy, the Environment and Water

# **Acknowledgement of Country**

Department of Climate Change, Energy, the Environment and Water acknowledges the Traditional Custodians of the lands where we work and live.

We pay our respects to Elders past, present and emerging.

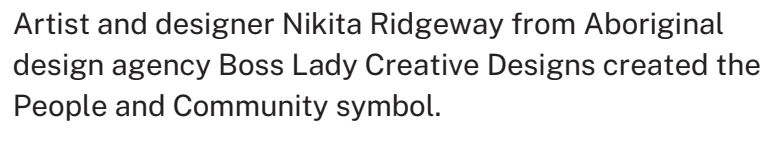
This resource may contain images or names of deceased persons in photographs or historical content.

© 2025 State of NSW and Department of Climate Change, Energy, the Environment and Water

With the exception of photographs, the State of NSW and Department of Climate Change, Energy, the Environment and Water (the department) are pleased to allow this material to be reproduced in whole or in part for educational and non-commercial use, provided the meaning is unchanged and its source, publisher and authorship are acknowledged. Specific permission is required to reproduce photographs.

Learn more about our copyright and disclaimer at www.environment.nsw.gov.au/copyright

This document should be cited as: DCCEEW (2025) NSW coastal erosion and inundation hazards and exposure assessment: technical report 2025, Department of Climate Change, Energy, the Environment and Water, Parramatta, NSW.



Cover photo: Collaroy. David Hanslow/DCCEEW

Published by:

**Environment and Heritage** 

Department of Climate Change,

Energy, the Environment and Water

Locked Bag 5022, Parramatta NSW 2124

Phone: +61 2 9995 5000 (switchboard)

Phone: 1300 361 967 (Environment and Heritage enquiries)

TTY users: phone 133 677, then ask for 1300 361 967 Speak and listen users: phone 1300 555 727, then ask for

1300 361 967

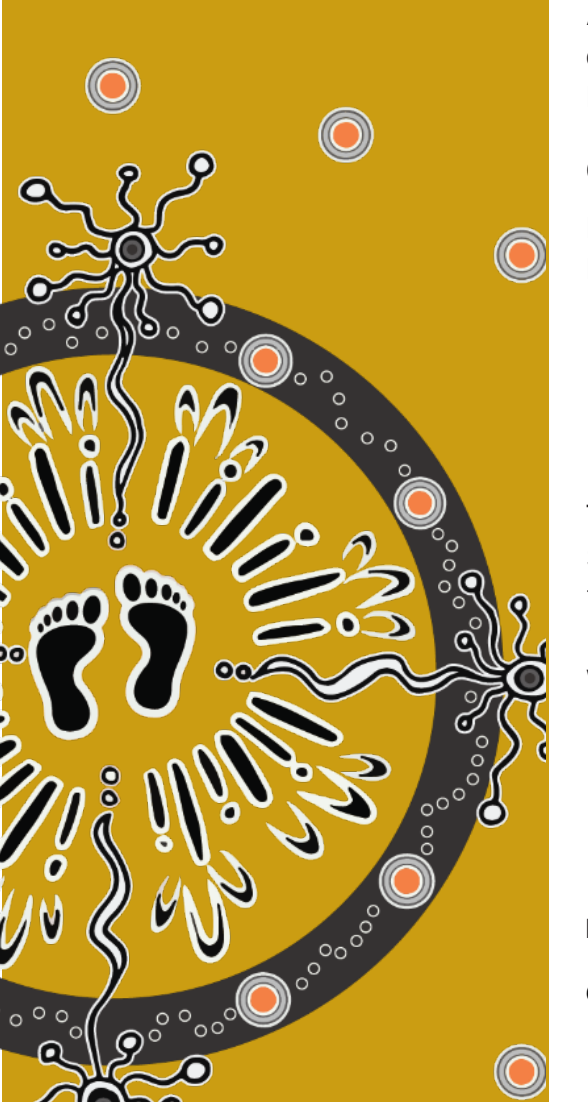
Email info@environment.nsw.gov.au

Website www.environment.nsw.gov.au

ISBN 978-1-76186-058-4 EH 2025/0391 November 2025

Find out more at:

environment.nsw.gov.au



# Contents

Lis	t of sh	ortened forms	XVIII
Ex	ecutive	e summary	xix
	Conte	ext	xix
	Clima	te scenarios	xix
	Appro	pach	XX
	Key fi	ndings	XX
	Limita	ations and assumptions	xxi
1.	Intro	duction	1
	1.1	Context	1
	1.2	Aim	2
	1.3	Outline	3
2.	Regi	onal description and coastal hazards in NSW	4
	2.1	Regional description	4
	2.2	Coastal hazards	9
3.	Meth	nods	20
	3.1	Sea level rise projections	20
	3.2	Baseline for the projections	21
	3.3	Use of scenarios	21
	3.4	Approach to uncertainty	22
	3.5	Coastal erosion methods	23
	3.6	Coastal overwash methods	29
	3.7	Estuarine inundation methods	35
	3.8	Exposure	40
4.	Results		42
	4.1	Coastal erosion	42
	4.2	Coastal overwash	61
	4.3	Estuarine inundation	75
5.	Key 1	findings	92
	5.1	Summary	92

5.2 Limitations	93
Acknowledgements	98
References	99
Appendix A: Methods	112
A.1 Timeframes and approach to uncertainty	112
A.2 Sea level rise	113
A.3 Coastal erosion methods	116
A.4 Coastal overwash	143
A.5 Estuarine inundation	153
A.6 Exposure	169
Appendix B: Datasets	171
Appendix C: Beaches modelled	173
Appendix D: Runup formula selection	185
Appendix E: Coastal overwash ensembles	188
Appendix F: NSW estuarine tidal water level gauges	189
Appendix G: Coastal erosion exposure under SSP5-8.5 (medium-	
confidence) and SSP5-8.5 (low-confidence) scenarios	201
Appendix H: Results of coastal overwash for various SSP scenari	os
and exceedance probability levels	213
Appendix I: Estuarine inundation exposure under SSP5-8.5 (med	ium-
confidence) and SSP5-8.5 (low-confidence) scenarios	226

# List of tables

Table 1	The likely ranges (17th–83rd percentile range) of sea leg projection in metres under SSP1-2.6 and SSP3-7.0 scena Yamba, Port Kembla and Eden	
Table 2	State-wide distribution (% of coastline) of current overw likelihoods for several annual exceedance probability (A levels of total water level	
Table 3	Summary of key variables in the volume-based coastal emodel – beach fluctuation	erosion 138
Table 4	Summary of key variables in the volume-based coastal emodel – sediment budget imbalance	erosion 139
Table 5	Summary of key variables in the volume-based coastal emodel – response to sea level rise	erosion 139
Table 6	Location of ocean tide gauges used within the coastal or modelling methodology	verwash 145
Table 7	Backbeach archetype classification system	149
Table 8	Classification of coastal overwash likelihoods	151
Table 9	Ocean tide gauges in New South Wales: station name, A Water Resources Code (AWRC) number, latitude, longituderation of operation	
Table 10	A list of 12 estuary models collated from different source understanding on changes to maximum water level alon different NSW estuaries and under different sea level riscenarios	g
Table 11	Summary of statistics generated for exposure to inunda erosion hazards	tion and 170
Table 12	Coastal geomorphology datasets	171
Table 13	Historical beach and shoreline change datasets	171
Table 14	Coastal waves datasets	171
Table 15	Coastal water levels datasets	172
Table 16	Beaches modelled by primary and secondary compartment number of sectors and tide gauge	ent, 173

Table 17	NSW estuarine tidal water level gauging locations by Au Water Resource Code (AWRC) number, latitude, longitud	
	duration of operation	189
Table 18	Exposure statistics for coastal erosion under present-da conditions at 1% exceedance probability level	y 201
Table 19	Results of inundation due to coastal overwash for variou	
Table 15	scenarios and probability levels from 2020 to 2150	213
Table 20	Exposure statistics for estuarine inundation under prese	nt-day
	conditions at one day/year (annual) frequency	226

# List of figures

Figure 1	Measured mean sea level at the Port Kembla baseline sea level monitoring station from 1991 to 2023 7
Figure 2	The 50-year record (1972–2022) of sand volume in the beach- foredune system at Bengello Beach (Moruya) showing a fluctuation phase exceeding 200 m³/m 10
Figure 3	Fluctuating beach erosion caused by severe storm events in (a) and undeveloped setting at Cronulla and (b) a developed setting at Wamberal, compared with sustained shoreline recession in (c) a natural setting at Woody Bay and (d) a developed setting at Old Bar. Photos: M Kinsela
Figure 4	The coastal erosion hazard zones include the beach fluctuation extent (the only component for present scenarios) as well as cumulative erosion (shoreline recession) for future forecasts. The total potential erosion extent for each scenario spans a range of distances tied to probability levels. Example years and associated probabilities shown include present (1% and 50%), 2070 (1% and 50%), and 2150 (1% and 50%)
Figure 5	Surveyed debris line on Maroubra Beach (Sydney NSW) on 7 June 2016 showing inundation elevations (m AHD) following the June 2016 east coast low
Figure 6	Damage resulting from overwash following the June 2016 East Coast Low at (a) the Clan Motel adjacent to Terrigal Lagoon and

	(b) the surf club roller doors at Terrigal Beach. Photos: DCCEE	W 16
Figure 7	Examples of tidal inundation (otherwise known as sunny day on nuisance flooding) in urban streets of (a) Marks Point, 13 May 2015, (b) Tea Gardens, 4 January 2018, (c) Woy Woy, 3 January 2018, and (d) Swansea, 2 January 2018. Photos: D Hanslow	
Figure 8	Plots of (a) days per year and (b) total annual duration (hours) nuisance street inundation (above 1 m AHD) in Sydney, 1914–2	
Figure 9	Screenshot of the NASA sea level projection tool	20
Figure 10	Conceptual diagram of the coastal erosion model used to prec the sediment volume (V) of coastal erosion, converted to the erosion distance (R) using local topography data	dict 26
Figure 11	Coastal erosion mapping for Wooli Beach showing the modelle potential erosion extent at present (2020) and for the SSP3-7 scenario in 2090	
Figure 12	Diagram showing total water level components that contribute coastal overwash	e to 30
Figure 13	Coastal overwash hazard methodology at the transect scale (1 m spaced transects)	00- 31
Figure 14	Diagram describing the transect-based overwash likelihood so (shown as inundation) used in this study. (a) Extreme value analysis (EVA) of total water level (TWL) time series using bloc maxima (1990–2020). The distribution of the 1% annual exceedance probability (AEP) (100-year) <i>TWL</i> is used in (b) to define the overwash impacts based on percentiles and local backbeach inundation thresholds. (c) The method is repeated future scenarios, where SLR distributions are now added to the original TWL distribution on a Monte-Carlo basis	ck
Figure 15	Examples of water levels representing different annual exceedance frequencies and how tidal amplification and attenuation can vary with distance from estuary entrance and different estuary types	in 37
Figure 16	Flow chart showing simplified structure of the GIS-based estuarine inundation model	39
Figure 17	Proportion of open coast and bay/estuarine beaches (by count and beach shorelines (by length) for which erosion modelling varried out in each compartment	

Figure 18	in each primary sediment compartment at the 1% exceedance probability level at (a) present (2020) conditions, and for SSP3 7.0 sea level scenario at (b) 2050, (c) 2100 and (d) 2150	
Figure 19	Box plots summarising modelled shoreline erosion distances at the 1% exceedance probability level at 2100 for the (a) SSP1-2. (b) SSP2-4.5, and (c) SSP3-7.0 scenarios	
Figure 20	State-wide counts of building exposure to coastal erosion at different exceedance probability levels (0.1%, 1%, 10%, and 50 from 2030 to 2150 under (a) SSP1-2.6, (b) SSP2-4.5 and (c) SS 7.0	
Figure 21	State-wide counts of address exposure to coastal erosion at different exceedance probability levels (0.1%, 1%, 10%, and 50 from 2030 to 2150, under (a) SSP1-2.6, (b) SSP2-4.5 and (c) SSP3-7.0	%), 49
Figure 22	State-wide exposure of road lengths (km) by type to coastal erosion at different exceedance probability levels (from right t left: 0.1%, 1%, 10% and 50%), from 2030 to 2150, under (a) SSF 2.6, (b) SSP2-4.5 and (c) SSP3-7.0	
Figure 23	State-wide exposure of path lengths (km) to coastal erosion and different exceedance probability levels (0.1%, 1%, 10%, and 50 from 2030 to 2150, under (a) SSP1-2.6, (b) SSP2-4.5 and (c) SSP3-7.0	
Figure 24	State-wide exposure of rail lengths (km) by type to coastal erosion at different exceedance probability levels (from right t left: 0.1%, 1%, 10% and 50%), from 2030 to 2150, under (a) SSF 2.6, (b) SSP2-4.5 and (c) SSP3-7.0	
Figure 25	State-wide exposure of airports by type to coastal erosion at different exceedance probability levels (from right to left: 0.1% 1%, 10% and 50%), from 2030 to 2150, under (a) SSP1-2.6, (b) SSP2-4.5 and (c) SSP3-7.0	6, 53
Figure 26	State-wide exposure of runway lengths (km) to coastal erosion different exceedance probability levels (0.1%, 1%, 10%, and 50 from 2030 to 2150, under (a) SSP1-2.6, (b) SSP2-4.5 and (c) SSP3-7.0	
Figure 27	State-wide exposure of currently identified Aboriginal cultural heritage sites to coastal erosion at different exceedance	l

	probability levels (0.1%, 1%, 10% and 50%), from 2030 to 2150, under (a) SSP1-2.6, (b) SSP2-4.5 and (c) SSP3-7.0	55
Figure 28	State-wide exposure of power lines (km) by type to coastal erosion at different exceedance probability levels (from right to left: 0.1%, 1%, 10%, and 50%), from 2030 to 2150, under (a) SSF 2.6, (b) SSP2-4.5 and (c) SSP3-7.0	
Figure 29	State-wide exposure of critical infrastructure by type to coastal erosion at different exceedance probability levels (from right to left: 0.1%, 1%, 10%, and 50%), from 2030 to 2150, under (a) SSF 2.6, (b) SSP2-4.5 and (c) SSP3-7.0	0
Figure 30	Box plot summarising the modelled shoreline erosion distances for bay/estuary beaches at a 1% exceedance probability level a present (2020), and for the SSP3-7.0 sea level scenario at 2050 2100 and 2150	at
Figure 31	State-wide exposure of (a) buildings, (b) critical infrastructure, (c) heritage sites and (d) roads (km) to coastal erosion at 1% exceedance probability, from present (2020) to 2150, under SS 2.6, SSP2-4.5, SSP3-7.0, medium-confidence SSP5-8.5 and low confidence SSP5-8.5	SP1-
Figure 32	Overview of modelling data input by primary sediment compartment, showing (a) geographical setting of the NSW region and boundaries of primary sediment compartments, (b) regional variability in beach slope by primary compartment and (c) regional variability in percentiles of the modelled distribution of 1% AEP total water levels	62
Figure 33	Distribution of backbeach archetypes by primary sediment compartment, with inset showing state-wide distribution of backbeach overwash thresholds for different archetypes	63
Figure 34	Current (2020) coastal overwash (shown as inundation) likelihoods for total water level distributions at 1% annual exceedance probability, at the state-wide level and by coastal archetype	64
Figure 35	Distribution of backbeach overwash thresholds clustered by overwash (shown as inundation) likelihood at 1% annual exceedance probability	65
Figure 36	Current (2020) coastal overwash (shown as inundation) likelihoods at (a) state-wide level and (b) by coastal archetype 100%, 20%, 5% and 1% AEP	for 66

Figure 37	Regional variability of current (2020) coastal overwash (shown as inundation) likelihoods by primary compartment 6	
Figure 38	Local scale example of 83rd and 99th percentiles of the distribution for current 1% annual exceedance probability (AEP) of total water level (TWL) and classed as overwash (shown as inundation) likelihoods at Wamberal–Terrigal Beach transects by (a) backbeach archetype, (b) different overwash likelihoods (based on elevations), and (c) mapping of current overwash likelihoods	
Figure 39	Coastal overwash and inundation event in Terrigal Beach and Lagoon after the June 2016 east coast low. Panels a (photo: Chris Drummond) and c show photos of Terrigal Lagoon (photo: DCCEEW), and panels b and d depict coastal structures in South Terrigal (photo: DCCEEW)	
Figure 40	Decadal evolution (2020 to 2150) of coastal overwash (shown as inundation) likelihoods considering present 1% annual exceedance probability of total water level distributions plus SLR, showing results for (a) low emissions (SSP1-2.6) SLR, (b) medium emissions (SSP2-4.5), and (c) high emissions (SSP3-7.0) SLR scenarios	0
Figure 41	Future evolution of sandy coastline exposure to <i>likely</i> overwash by primary compartment (1% AEP TWL plus SLR) under (a) SSP1-2.6, (b) SSP2-4.5, and (c) SSP3-7.0 scenarios for the years 2020, 2040, 2070, 2100 and 2150	1
Figure 42	Future evolution of exposure to <i>likely</i> overwash by coastal backbeach archetype (1% AEP TWL plus SLR) under (a) SSP1-2.6 (b) SSP2-4.5 and (c) SSP3-7.0 SLR scenarios for the years 2020, 2040, 2070, 2100 and 2150	
Figure 43	State-wide (a) percentage (%) and (b) kilometres of sandy coastline experiencing likely coastal overwash at 1% annual exceedance probability associated with SSP1-2.6, SSP2-4.5, SSP3-7.0, medium-confidence SSP5-8.5 and low-confidence SSP5-8.5 scenarios	4
Figure 44	Map of the northern (left), central (centre) and southern (right) sections of NSW coastline showing the current mapped extent of NSW estuaries along with the extent of inundation at 1 day per year exceedance level in 2020, 2050, 2100 and 2150 under SSP3 7.0 scenario	-

Figure 45	State-wide estuarine inundation area increasing over time (202 to 2150) for each exceedance inundation frequency under (a) SSP1-2.6, (b) SSP2-4.5 and (c) SSP3-7.0 scenarios	20 77
Figure 46	Estuaries with the greatest increases in inundated area on an annual frequency (1 day/year) by 2150 under (a) SSP1-2.6, (b) SSP2-4.5, and (c) SSP3-7.0	78
Figure 47	State-wide building counts exposed at different exceedance inundation frequencies, from 2030 to 2150, under (a) SSP1-2.6, (b) SSP2-4.5, and (c) SSP3-7.0	79
Figure 48	State-wide address counts exposed at different exceedance inundation frequencies, from 2030 to 2150, under (a) SSP1-2.6, (b) SSP2-4.5, and (c) SSP3-7.0	80
Figure 49	State-wide road lengths (km) by type exposed at different exceedance inundation frequencies (from right to left: 1 day/ye (annual), 3.6 days/year (1%), 36.5 days/year (10%) and 182.5 days/year (50%)), from 2030 to 2150, under (a) SSP1-2.6, (b) SSP2-4.5 and (c) SSP3-7.0	ar 81
Figure 50	State-wide path lengths (km) exposed at different exceedance inundation frequencies, from 2030 to 2150, under (a) SSP1-2.6, (b) SSP2-4.5 and (c) SSP3-7.0	
Figure 51	State-wide rail lengths (km) by type exposed over time (2030 to 2150) at different exceedance inundation frequencies (from rig to left: 1 day/year (annual), 3.6 days/year (1%), 36.5 days/year (10%), and 182.5 days/year (50%) exceedance) associated with (a) SSP1-2.6, (b) SSP2-4.5 and (c) SSP3-7.0	ht
Figure 52	State-wide airports by type exposed over time (2030 to 2150) a different exceedance inundation frequencies (from right to left 1 day/year (annual), 3.6 days/year (1%), 36.5 days/year (10%), ar 182.5 days/year (50%) exceedance) associated with (a) SSP1-2 (b) SSP2-4.5 and (c) SSP3-7.0	t: nd
Figure 53	State-wide runway lengths (km) exposed at different exceedar inundation frequencies, from 2030 to 2150, under (a) SSP1-2.6, (b) SSP2-4.5 and (c) SSP3-7.0	
Figure 54	State-wide exposure of Aboriginal cultural heritage sites at different exceedance inundation frequencies, from 2030 to 215 under (a) SSP1-2.6, (b) SSP2-4.5 and (c) SSP3-7.0	50, 86
Figure 55	State-wide exposure of powerline length (km) by type over time (2030 to 2150) at different exceedance inundation frequencies	

	(from right to left: 1 day/year (annual), 3.6 days/year (1%), 36.5 days/year (10%) and 182.5 days/year (50%) exceedance) associated with (a) SSP1-2.6, (b) SSP2-4.5 and (c) SSP3-7.0	87
Figure 56	State-wide counts of critical infrastructure sites, by category, exposed over time (2030 to 2150) at different exceedance inundation frequencies (from right to left: 1 day/year (annual), 3.6 days/year (1%), 36.5 days/year (10%), and 182.5 days/year (50%) exceedance) under (a) SSP1-2.6, (b) SSP2-4.5 and (c) SSP3-7.0	88
Figure 57	State-wide exposure over time (current (2020) to 2150) of (a) buildings, (b) critical infrastructure, (c) heritage sites and (d) roads (km) to estuarine inundation (at 1 day/year exceedance inundation frequency) associated with SSP1-2.6, SSP2-4.5, SS 7.0, medium-confidence SSP5-8.5 and low-confidence SSP5-8 scenarios	3P3-
Figure 58	Screenshot of the NASA sea level projection tool	114
Figure 59	Log normal sea level rise distributions for each time horizon for SSP3-7.0 at Fort Denison	r 116
Figure 60	Example of onshore and offshore coastal geomorphology sampling design in Wooli embayment, showing division of Wool Beach (nsw073) into 3 sectors, and the shorter Jones Beach (nsw074) as one sector, for erosion modelling, with wave data node (10 m water depth) for each sector also shown	oli 122
Figure 61	Example sector-average onshore profiles showing (a) the morphology of the 3 Wooli Beach sectors (nsw073a, nsw073b nsw073c) and the Jones Beach sector (nsw074) from the base to 600 m landward of the backshore line; and (b) complete profestending 2 km inland for sector nsw073a showing the difference between the full terrain profile and sediment profile (bedrock removed), and the cumulative sediment volume across the professional sectors.	line file ence
Figure 62	Examples of sector-averaged offshore profiles comparing (a) to average shoreface morphology in sector nsw074a and (b) nsw074c as shown in Figure 60	the 126
Figure 63	(a) Average recurrence interval for storm-driven beach erosion volumes (m³/m) on exposed and semi-sheltered NSW beaches and (b) the gamma probability distribution for fluctuating beacherosion	;

Figure 64	probability distribution in Wooli embayment sectors (a) nsw07 (b) nsw073b, (c) nsw073c and (d) nsw074, showing the effect sheltering from waves in the south in reducing the potential fluctuation volume	
Figure 65	Hypothetical sediment budget components for Terrigal– Wamberal Beach	131
Figure 66	Example of historical shoreline change, as captured by annual average shoreline positions from DEA Coastlines for (a) accret (b) stationary and (c) receding settings with cool colours being older and warm colours recent shorelines. The corresponding model probability distributions for annual rates of beach-volut change due to sediment budget imbalance (blue) is also show for each sector, spanning the ranges derived from DEA Coastland CoastSat data (grey)	ting, g me n
Figure 67	Illustration of beach, upper shoreface and lower shoreface promorphology typical of NSW beaches	ofile 133
Figure 68	Illustration of the profile translation method for modelling bear erosion and shoreface deposition due to sea level rise	ach 133
Figure 69	Illustration of shoreface zones linked to timescales of evolution showing the active shoreface extent increasing as habecomes deeper for longer timescales. Source: Cowell and Kinsela (201	6
Figure 70	Example input probability distributions for (a) sea level rise (m 2030 to 2150, and for (b) the active shoreface depth limit $h_a$ , which increases with the timescale from the upper shoreface closure depth (lower bound) to a maximum 35 m water depth	
Figure 71	Schematic of the coastal erosion model components applied to generalised coastal profile	o a 137
Figure 72	The Wooli Beach sector nsw073b for the scenario SSP3-7.0 in 2090 showing (a) modelled historical volume change of coasts erosion, (b) modelled estuary sediment sink, (c) modelled coast erosion translation distance, and (d) modelled shoreface sediment sink	al
Figure 73	Modelled beach volume change for Wooli embayment sector (a) nsw073a, (b) nsw073b, (c) nsw073c and (d) nsw074 for scenario SSP3-7.0 in 2090	140

Figure /4	potential erosion mapping for Wooli Beach showing the modelled potential erosion extent for the 10% and 1% exceedance probability at present (2020) and for the SSP3-7.0 scenario in 2090		
Figure 75	Total water level components that contribute to coastal over	142 wash	
rigule 70	Total water level components that contribute to coastal over	143	
Figure 76	Coastal overwash hazard assessment method at the transect scale (100-m spaced transects)	144	
Figure 77	Distribution of available LiDAR surveys (2007–2023) across 8,649 100-m spaced transects		
Figure 78	(a) Geographical distribution of marine debris line measuremen after 4 storm events in October 2014, April 2015, June 2016 and July 2020 (see legend). (b) Example of marine debris line and RTK-GNSS monitoring. Marine debris line examples for (c) Woonona beach near Port Kembla and (d) Curl Curl beach in Sydney		
Figure 79	Upper panels: examples of cross-shore transects representing coastal archetypes in New South Wales. Horizontal axes indicationage, measured from the most landward location of the transect (0 m). Lower panels: corresponding images showcas each archetype. Photos (left to right): DCCEEW, CoastSnap citizen science program, and Google Maps	cate	
Figure 80	Diagram showing extreme value analysis (EVA) of total water level (TWL) time series using block maxima (1990 to 2020) us for calculating the transect-based overwash (shown as inundation) likelihood scale. The distribution of the 1% AEP (19 year) TWL in (a) is used in (b) to define the overwash (shown a inundation) impacts based on TWL percentiles and local backbeach overwash thresholds. (c) The method is repeated to future scenarios, where SLR distributions are added to the original TWL distribution on a Monte-Carlo basis	ed 00- s	
Figure 81	Plot showing an example of a truncated estuary catchment digital elevation model (DEM) (i.e. areas below 10 m AHD) for Merimbula Lake	155	
Figure 82	Map showing location of NSW Manly Hydraulics Laboratory (MHL) tide and water level gauging network		
Figure 83	Histogram showing length (number of years) of water level records at NSW gauge locations	157	

Figure 84	Plot showing example set of empirical cumulative density functions from daily estuarine water level gauge data		
Figure 85	Plot showing empirical cumulative density functions from dail maximum data at 8 NSW ocean gauge locations	ly 159	
Figure 86	Examples of water levels in different estuary types	160	
Figure 87	Water level frequency distributions for a gauge in a non-mode estuary for a current (2020) and future case (2100; SSP3-7.0), showing (a) normalised probability density and (b) empirical cumulative density function		
Figure 88	Model grid and output for the Clarence River in Northern NSV showing maximum water levels extending from the river mount the tidal limit for each sea level rise scenario along with the percent difference in the normalised maximum water level		
Figure 89	Flow chart showing simplified structure of GIS-based estuaring inundation model	ne 165	
Figure 90	Map showing example results from water surface model, area analysis (AOA) water level surface (mm AHD)	of 166	
Figure 91	Map showing example results from the water surface model, water level surface (mm AHD)	final 167	
Figure 92	Plot showing example of primary and isolated estuarine inundation polygon layers	168	
Figure 93	Regional observations of total water levels (TWLs) from marindebris lines after 4 storm events along 40 individual beaches		
Figure 94	Summary statistics of total water level modelling (TWL = SWL + R, 472 observations) for 3 beach slope specifications a 7 runup formulas across 4 storm events	ınd 187	
Figure 95	Model sensitivity to number of ensembles based on comparing the LiDAR accuracy with the variability (standard deviation) of different total water level exceedances for different numbers ensemble members	f	
Figure 96	Box plots summarising modelled shoreline erosion distances in 1% exceedance probability level in 2100 for (a) SSP5-8.5 med confidence and (b) SSP5-8.5 low-confidence scenarios		
Figure 97	State-wide building counts exposed to coastal erosion over ti at different exceedance probability levels (0.1%, 1%, 10%, and 50%) associated with (a) medium-confidence SSP5-8.5 and (b) low-confidence SSP5-8.5 scenarios		

Figure 98	State-wide address counts exposed to coastal erosion over time at different exceedance probability levels (0.1%, 1%, 10%, and 50%) associated with (a) medium-confidence SSP5-8.5 and (b) low-confidence SSP5-8.5 scenarios	
Figure 99	State-wide road lengths (km) by type exposed to coastal erosion over time at different exceedance probability levels (from right to left: 0.1%, 1%, 10%, and 50%) associated with (a) medium-confidence SSP5-8.5 and (b) low-confidence SSP5-8.5 scenarios 20	:0 S
Figure 100	State-wide path lengths (km) exposed to coastal erosion over time at different exceedance probability levels (0.1%, 1%, 10%, and 50%) associated with (a) medium-confidence SSP5-8.5 and (b) low-confidence SSP5-8.5 scenarios	6
Figure 101	State-wide rail lengths (km) exposed by type to coastal erosion over time at different exceedance probability levels (from right t left: 0.1%, 1%, 10%, and 50%) associated with (a) medium-confidence SSP5-8.5 and (b) low-confidence SSP5-8.5 scenarios 20	s
Figure 102	State-wide airports by type exposed to coastal erosion over time at different exceedance probability levels (from right to left: 0.1%, 1%, 10%, and 50%) associated with (a) medium-confidence SSP5-8.5 and (b) low-confidence SSP5-8.5 scenarios	
Figure 103	State-wide runway lengths (km) exposed to coastal erosion over time at different exceedance probability levels (0.1%, 1%, 10%, and 50%) associated with (a) medium-confidence SSP5-8.5 and (b) low-confidence SSP5-8.5 scenarios	
Figure 104	State-wide Aboriginal cultural heritage sites exposed to coastal erosion over time at different exceedance probability levels (0.1%, 1%, 10%, and 50%) associated with (a) medium-confidence SSP5-8.5 and (b) low-confidence SSP5-8.5 scenarios	9
Figure 105	State-wide lengths (km) of electricity transmission lines, by type exposed to coastal erosion over time at different exceedance probability levels (from right to left: 0.1%, 1%, 10%, and 50%) associated with (a) medium-confidence SSP5-8.5 and (b) low-confidence SSP5-8.5 scenarios	
Figure 106	State-wide critical infrastructure assets, by type, exposed to coastal erosion over time at different exceedance probability levels (from right to left: 0.1%, 1%, 10%, and 50%) associated with	h

	(a) medium-confidence SSP5-8.5 and (b) low-confidence SSP5-8.5 scenarios	o- 212
Figure 107	Bar charts of increasing inundated area for each exceedance inundation frequency and climate change scenario under (a) medium-confidence SSP5-8.5 and (b) low-confidence SSP5-8.5 scenarios	5- 227
Figure 108	Bar charts showing the top 10 estuaries with the greatest increases on an annual exceedance frequency (1 day/year) in inundated area for medium-confidence SSP5-8.5	227
Figure 109	State-wide counts of buildings exposed to inundation over time different exceedance frequencies associated with (a) medium-confidence SSP5-8.5 and (b) low-confidence SSP5-8.5 scenar	-
Figure 110	State-wide counts of addresses exposed to inundation over tinat different exceedance frequencies associated with (a) mediu confidence SSP5-8.5 and (b) SSP5-8.5 low-confidence scenar	ım-
Figure 111	Bar plots of the 10 estuaries most exposed to inundation (defining in terms of building counts) in 2150 under (a) SSP1-2.6, (b) SSP 4.5, (c) SSP3-7.0 and (d) medium-confidence SSP5-8.5 scenar	2-
Figure 112	State-wide road lengths (km) by type exposed to inundation of time at different exceedance frequencies (from right to left: 1 day/year (annual), 3.6 days/year (1%), 36.5 days/year (10%), and 182.5 days/year (50%) exceedance) under (a) medium-confidence SSP5-8.5 and (b) SSP5-8.5 low-confidence scenarios	d
Figure 113	State-wide path lengths (km) exposed to inundation over time different exceedance frequencies under (a) medium-confidence SSP5-8.5 and (b) low-confidence SSP5-8.5 scenarios	
Figure 114	Bar plots of the 10 estuaries most exposed to inundation (defining in terms of road lengths) in 2150 associated with various exceedance frequencies under (a) SSP1-2.6, (b) SSP2-4.5, (c) SSP3-7.0 and (d) medium-confidence SSP5-8.5 scenarios 2	
Figure 115	Bar plots of the 10 estuaries most exposed to inundation (defining in terms of path lengths) in 2150 associated with various exceedance frequencies under (a) SSP1-2.6, (b) SSP2-4.5, (c) SSP3-7.0 and (d) medium-confidence SSP5-8.5 scenarios 2	

Figure 116	State-wide rail lengths (km) by type exposed to inundation over time at different exceedance frequencies (from right to left: 1 day/year (annual), 3.6 days/year (1%), 36.5 days/year (10%), and 182.5 days/year (50%) exceedance) associated with (a) under medium-confidence SSP5-8.5 and (b) low-confidence SSP5-8.5 scenarios	
Figure 117	Bar plots of the 10 estuaries most exposed to inundation (defined in terms of rail lengths) in 2150 at different exceedance frequencies under (a) SSP1-2.6, (b) SSP2-4.5, (c) SSP3-7.0 and (d) medium-confidence SSP5-8.5 scenarios	
Figure 118	State-wide airports by type exposed to inundation over time at different exceedance frequencies (from right to left: 1 day/year (annual), 3.6 days/year (1%), 36.5 days/year (10%), and 182.5 days/year (50%) exceedance) under (a) medium-confidence SSP5-8.5 and (b) low-confidence SSP5-8.5 scenarios	37
Figure 119	State-wide runway lengths (km) exposed to inundation over time at different exceedance frequencies under (a) medium-confidence SSP5-8.5 and (b) low-confidence SSP5-8.5 scenario	S
Figure 120	State-wide Aboriginal cultural heritage sites exposed to inundation over time at different exceedance frequencies under (a) medium-confidence SSP5-8.5 and (b) low-confidence SSP5-8.5 scenarios	
Figure 121	State-wide lengths (km) of electricity transmission lines, by type exposed to inundation over time at different exceedance frequencies (from right to left: 1 day/year (annual), 3.6 days/year (1%), 36.5 days/year (10%), and 182.5 days/year (50%) exceedance) under (a) medium-confidence SSP5-8.5 and (b) low confidence SSP5-8.5 scenarios	/-
Figure 122	State-wide critical infrastructure assets, by category, exposed to inundation over time at different exceedance frequencies (from right to left: 1 day/year (annual), 3.6 days/year (1%), 36.5 days/year (10%), and 182.5 days/year (50%) exceedance) under (a) medium-confidence SSP5-8.5 and (b) low-confidence SSP5-8.5 scenarios	

## List of shortened forms

**AEP** annual exceedance probability

AHD Australian Height Datum

**AOA** Area of analysis

AR6 IPCC Sixth Assessment Report (IPCC 2023)

**AWRC** Australian Water Resources Code

**DEM** Digital elevation model

**ECDF** Empirical cumulative density function

**ENSO** El Niño Southern Oscillation

**EVA** Extreme value analysis

**GIS** Geographic information system

**ICOLLs** Intermittently closed-open lakes and lagoons

**IPCC** Intergovernmental Panel on Climate Change

MSL Mean sea level

NGI Non-gauged ICOLLs

**SLR** Sea level rise

**SSP** Shared socioeconomic pathway

**SWL** Still water level

**TWL** Total water level

## **Executive summary**

#### Context

This second state-wide assessment of coastal erosion and inundation hazard-exposure in New South Wales builds on the first conducted in 2018. It examines current and future exposure to coastal erosion, coastal overwash, and estuarine inundation hazards. As sea levels rise, the impacts of these hazards will intensify, increasing risks to services for communities, infrastructure, heritage and ecosystems in both coastal and estuarine environments.

Since 2018, the Intergovernmental Panel on Climate Change (IPCC) has released 2 key reports – the 2019 special report *The ocean and cryosphere in a changing climate* (IPCC 2012) and the IPCC's Sixth Assessment Report (AR6) (IPCC 2023) – that provide refined sea level rise (SLR) projections, including upper-end possibilities crucial for stakeholders managing long-term infrastructure investments. During this period, the NSW Government has advanced its data inventory, incorporating state-wide high-resolution seabed mapping, marine LiDAR and nearshore wave modelling. These improvements have enhanced the state's capability in coastal and estuarine hazard projections.

This report delivers the most comprehensive assessment of impacts from key coastal hazards. It employs consistent methods for modelling and mapping hazards, enabling the identification of geographic differences in exposure and informing risk-reduction efforts and adaptation strategies across the state.

#### Climate scenarios

This report assesses both current and future exposure to coastal erosion, coastal overwash and estuarine inundation hazards under several shared socioeconomic pathways (SSPs). IPCC AR6 has raised the upper projections of potential SLR for the coming decades and centuries, highlighting the need to consider all potential SLR projections when assessing coastal and estuarine hazards.

To provide a full picture of potential impacts, this report focuses on medium-confidence SSP1-2.6, SSP2-4.5 and SSP3-7.0 scenarios as the primary low, medium and high emission storylines for future climate projections, representing a broad range of potential futures from low to high emissions. This assessment also offers insights into medium-confidence SSP5-8.5 and low-confidence SSP5-8.5 as very high emission scenarios/storylines. This approach ensures alignment with state-wide, national and global best practices for SLR impact modelling and supports consistent, robust decision-making frameworks across NSW.

Overall, SLR remains inherently uncertain, with each scenario leading to significantly different outcomes for communities, infrastructure and ecosystems. By examining a comprehensive range of scenarios, this report ensures that decision-makers can plan for likely outcomes while also preparing for less probable, yet more severe, impacts. This

approach supports the development of flexible, adaptive strategies that limit vulnerabilities and enhance long-term resilience.

#### **Approach**

This assessment uses a baseline year of 2020 and evaluates the implications of SLR under multiple climate change scenarios at 10-year intervals up to 2150. The method applies a probabilistic framework to model coastal erosion, coastal overwash and estuarine inundation, thus supporting dynamic adaptive pathways.

Coastal erosion was modelled using a sediment volume-based response framework that simulates storm-driven erosion, beach fluctuations, sediment budget imbalances and long-term impacts of SLR. The model integrates historical satellite data and probability distributions for key factors, capturing erosion trends across 758 beach sectors, including 32 bay/estuary beaches. The modelling covers approximately 90% of NSW's sandy shorelines and provides spatial erosion extents.

Coastal overwash combines tide, storm surge, wave runup, and future SLR impacts. Modelling was performed along approximately 800 km of sandy coastline using high-resolution LiDAR data of backbeach levels to assess overwash likelihood. Locations susceptible to future overwash were determined using Monte Carlo methods, combining present-day extreme water levels with SLR distributions aligned with IPCC projections.

Estuarine inundation was assessed using tide gauge data and water surface fitting and probability methods, focusing on frequently occurring tidal maxima (for example, 1 day/year (annual) exceedance). For ungauged estuaries, data from nearby similar estuaries were used as proxies, while exceedance distributions for intermittently closed–open lakes and lagoons were averaged and scaled using berm heights. Future water levels incorporated SLR projections and, where available, resulting changes in tidal dynamics.

Exposure to these hazards was quantified where appropriate (coastal erosion and estuarine inundation only), by overlaying modelled hazard extents with spatial data on assets such as buildings, roads, critical infrastructure and cultural heritage sites. This provided projections of impacted areas, infrastructure and assets under different climate scenarios, supporting risk-based planning and adaptation strategies.

## **Key findings**

This assessment highlights that as sea levels rise, the impacts of coastal and estuarine hazards in NSW will become increasingly widespread over time, affecting communities and infrastructure. The results also reveal that the initially gradual increase in impacts may provide a critical window of opportunity to prioritise adaptive strategy actions and mitigation measures.

#### Coastal erosion

The landward reach of potential erosion hazards is projected to increase steadily over time, with larger extents under higher SLR scenarios and extreme storm conditions. Under higher SLR scenarios (for example, SSP3-7.0), the rate of erosion is projected to

accelerate, particularly between 2080 and 2150. Currently, approximately 660 buildings and 1,920 addresses are exposed to erosion at a 1% annual exceedance probability. By 2150, this is projected to increase to approximately 7,500 buildings and 22,820 addresses under a low emissions scenario (SSP1-2.6), and to 17,740 buildings and 48,400 addresses under a high emissions scenario (SSP3-7.0). Roads, paths and other infrastructure will also see increasing exposure.

#### Coastal overwash

Currently, approximately 6% (51 km) of NSW's sandy coastline is at risk of likely coastal overwash and backbeach inundation during 1% annual exceedance probability wave and water level conditions, mainly in areas with low backbeach terrain or built structures. While risk increases under all SLR scenarios, the growth in overwash hazard is moderate due to natural defences like dunes and cliffs. By 2150, the likely overwash length is projected to increase to 82 km under a low emissions scenario (SSP1-2.6) and to 124 km under a high emissions scenario (SSP3-7.0).

#### **Estuarine inundation**

The extent of inundation around estuary foreshores is projected to grow over time, with higher SLR scenarios resulting in greater impacts. Currently, approximately 3,345 buildings, 7,120 addresses, 355 km of roads and 2 km of railways are projected to be impacted by estuarine inundation at one day per year frequency. By 2050, 6,900 to 8,750 buildings and 14,400 to 18,000 addresses could face inundation (1 day/year) under low (SSP1-2.6) and high (SSP3-7.0) emissions scenarios, respectively. Under these two scenarios, exposure rises, respectively, to 50,700 to 86,700 buildings and 111,500 to 204,100 addresses by 2100, and to 145,300 to 213,000 buildings and 359,400 to 540,700 addresses by 2150. Roads, railways and other infrastructure will also see increased exposure.

## Limitations and assumptions

This assessment focuses on the impacts of SLR under various climate scenarios, excluding potential changes in wind patterns, storm tracks and other factors that influence coastal hazards. Present-day wave and tide conditions were assumed to continue into the future and simplified modelling approaches were used to assess SLR impacts across broad spatial and temporal scales.

#### Coastal erosion

Beach sectors were modelled using reduced-complexity approaches. Localised variability within sectors may not be fully captured, and interactions between erosion and inundation under high SLR scenarios may differ from forecasts. Modelling excludes bedrock areas, and erodible backshore materials were simplified, with detailed local studies needed for greater resolution.

#### Coastal overwash

Coastal overwash modelling combined tide, storm surge, wave runup and SLR, but assumed no changes in backbeach elevations over time. Wave runup was based on validated formulas, yet real-world variability in beach slopes could result in higher runup under extreme conditions.

#### **Estuarine inundation**

The broad-scale approach relied on tide gauge data and assumed that observed water levels at gauges translate directly to foreshore areas, which may vary due to local topography or flood mitigation structures. SLR-induced tidal changes were only considered in estuaries where detailed modelling was already available and were assumed to be static in others.

#### General assumptions

The lack of state-wide data on floor levels in buildings required an assumption that floors were at ground level, potentially overestimating exposure, particularly in flood-prone areas. LiDAR data provided a 5 m horizontal resolution and 0.3 m vertical accuracy; however, changes in landforms or infrastructure since data collection may affect accuracy.

For the exposure assessment, all asset and infrastructure data are based on current information, meaning future exposure results consider only existing assets and infrastructure, and do not account for potential future developments in hazard areas. Regarding buildings exposure, structures without an assigned address were excluded to reduce false positives, although secondary structures (for example, sheds, water tanks and carports) at locations with an assigned address remain in the dataset. Several building classes (for example, residential and commercial) were considered, so the building exposure results presented do not represent a single building class only.

## 1. Introduction

#### 1.1 Context

This report presents an updated state-wide assessment of exposure to coastal erosion, coastal overwash, and estuarine inundation for New South Wales (NSW). This assessment aims to provide a broad-scale overview of the potential threats to NSW coastal and estuarine settlements and communities from hazards associated with erosion and inundation. Previous assessments have indicated that considerable development along the NSW coast is already exposed to coastal erosion and inundation hazards, and projected sea level rise (SLR) is expected to substantially increase this exposure over time (OEH 2017, 2018; Kinsela et al. 2017; Hanslow et al. 2018).

Recent east coast lows in NSW have illustrated the severity of these threats to beachfront development (Harley et al. 2017; Mortlock et al. 2017), while emerging research has begun documenting the increasing frequency of nuisance inundation events in urban estuarine settings, showing that the early effects of SLR are both observable and measurable in NSW (Hague et al. 2020, 2022; Hanslow et al. 2019, 2023).

The Australian National Coastal Risk Assessment identified NSW as having the highest exposure to SLR of any Australian state (DCC 2009; Cechet et al. 2011). This exposure was confirmed by the NSW second-pass assessments of coastal erosion (OEH 2017; Kinsela et al. 2017) and estuarine inundation (OEH 2018; Hanslow et al. 2018). These assessments demonstrated that, while both open coast erosion and inundation are major concerns, the greatest increases in exposure due to SLR are associated with the inundation of low-lying developments adjacent to estuaries.

The first NSW state-wide assessment of future coastal erosion impacts associated with climate change by OEH (2017) and Kinsela et al. (2017) overlaid modelled coastal erosion hazard extents with spatial asset data to determine the impact of climate change across the state. This study identified approximately 1,200 property lots (2,300 total addresses) as potentially exposed to coastal erosion at present, rising to around 3,100 lots (5,200 total addresses) by 2050, and 4,800 lots (8,200 total addresses) by 2100; and about 70 km of NSW roadways as exposed to coastal erosion at present, increasing to 196 km by 2050 and 311 km by 2100. Importantly, Kinsela et al. (2017) concluded that the site-specific data on sediment availability and local seabed topography were crucial to reducing uncertainty in the projections of coastal evolution as SLRs. Later, Kinsela et al. (2022) further analysed the potential responses of a sediment compartment to climate change in the Illawarra region, highlighting the importance of detailed seabed data for future coastal erosion modelling across NSW.

The NSW state-wide estuarine inundation assessment (Hanslow et al. 2018; OEH 2018) identified 23,653 and 50,744 properties as potentially exposed to tidal inundation under 0.5 m and 1 m of SLR, respectively. Allowing for storm surge, the number of properties at risk was predicted to increase to potentially 51,557 and 74,746 under

0.5 m and 1 m of SLR, respectively. SLR inundation was also found likely to significantly impact low-lying infrastructure, with approximately 3,458 km of roads potentially subject to inundation under 1.5 m of SLR. While local roads and tracks comprise the majority of this exposure, some arterial and primary roads were also found to be impacted under the higher SLR scenarios. A similar amount of power infrastructure was potentially exposed, as electricity lines are typically paired with roadways. Using these exposure assessments, the NSW Treasury's intergenerational report estimated the potential impacts of SLR at between \$850 million and \$1.3 billion (real 2019–20 dollars) annually by 2061 (Wood et al. 2021).

Since these earlier hazard/exposure assessments were undertaken, two separate reports by the Intergovernmental Panel on Climate Change (IPCC) have provided updated SLR projections. These include the special report on "The ocean and cryosphere in a changing climate" in 2019 (IPCC 2022) and the IPCC Working Group I's Sixth Assessment Report (AR6) in 2021 (IPCC 2023). These reports offer improved projections for future SLR and, for the first time, provide more detailed information on upper-end possibilities, essential for holistic risk management, especially for stakeholders with low risk tolerance, such as those involved in coastal safety planning for cities and long-term investment in critical infrastructure (IPCC 2022).

In addition to the updated IPCC SLR projections, the NSW Government has made considerable progress in providing more rigorous data to improve coastal hazard modelling. These data have been collected with the specific aim of enhancing our understanding of coastal and estuarine hazards and their associated risks, and informing coastal management programs to address these risks. This includes the delivery of <a href="state-wide high-resolution seabed mapping">state-wide high-resolution seabed mapping</a>, including <a href="state-wide marine">state-wide marine</a> <a href="LiDAR">LiDAR</a> and <a href="seabed morphological classification">seabed mapping</a>, including <a href="state-wide marine">state-wide marine</a> <a href="LiDAR">LiDAR</a> and <a href="seabed morphological classification">seabed mapping</a>, including <a href="state-wide marine">state-wide marine</a> <a href="mailto:LiDAR">LiDAR</a> and <a href="seabed morphological classification">seabed mapping</a>, including <a href="state-wide marine">state-wide marine</a> <a href="mailto:LiDAR">LiDAR</a> and <a href="seabed morphological classification">seabed morphological classification</a> (see Linklater et al. 2023), as well as improved <a href="mailto:state-wide marine">state-wide marine</a> <a href="mailto:state-wide marine

Two satellite-derived shoreline datasets have recently become available for NSW beaches (Bishop-Taylor et al. 2021; Vos et al. 2019a, 2019b). These datasets use satellite imagery spanning the past 3 decades and provide improved state-wide data for understanding recent trends in beach behaviour.

#### 1.2 Aim

The aim of this assessment is to examine current and potential future exposure to coastal erosion, coastal overwash, and estuarine inundation in NSW, as well as to provide the hazard-exposure information in a suitable form for decision-makers and regional planners to broadly identify the coastal adaptation measures required to manage future exposure and increase community resilience to SLR hazards.

The assessment includes modelling and mapping of coastal hazard extents and quantification of risk exposure on a state-wide basis using consistent methods. Understanding the geographic distribution of coastal hazard exposure provides information to guide regional prioritisation of actions needed to manage risk and

improve resilience. It also provides an initial screening tool for prioritising more detailed coastal hazard studies to further quantify the risk and test specified adaptation scenarios.

#### 1.3 Outline

This assessment begins in Chapter 2 with a brief overview of the NSW coast and the processes that contribute to coastal erosion and inundation hazards. The chapter also provides context for the methods chosen to quantify coastal hazard exposure. Chapter 3 describes the methods used to model and map coastal hazards and to quantify both current and potential future exposure. (A more detailed presentation of the methods for a technical audience is provided in <a href="Appendix A: Methods">Appendix A: Methods</a>) The results of the hazard exposure assessment are presented in Chapter 4 with sections for each hazard considered: coastal erosion, coastal overwash, and estuarine inundation. The report concludes in Chapter 5 with a discussion of the results over different timeframes and an outline of the limitations of the assessment.

# Regional description and coastal hazards in NSW

### 2.1 Regional description

#### Geomorphic setting

The NSW coast stretches for approximately 2,065 km and includes around 1,038 km of sandy shorelines; the remaining open coastline consists of rocky cliffs or headlands and estuarine entrances (Short 2006, 2007). Successive rock cliffs or headlands are joined by sandy beach-barrier systems which may include one or more estuaries or coastal lakes (Chapman et al. 1982). The open coast is exposed to the predominant southeast swell and experiences a moderate to high energy, yet highly variable, wave regime (Short and Trenaman 1992).

On the coast south of Sydney, the beaches are predominantly pocket beaches, isolated by rocky headlands with little alongshore sand exchange between compartments. In the north of the state, beaches tend to be longer and have higher rates of alongshore sand movement, with sand moving from compartment to compartment, predominantly from south to north. Beaches are typically backed by high dunes that provide some protection against storm surges and wave inundation but experience episodic erosion, which can threaten existing beachfront development.

Beach-barrier systems along the NSW coast vary significantly in geomorphic character (Short 2006) and have been categorised into several barrier types, including prograded, stationary, receded and those characterised by episodic dune migration (Thom 1984). Variations in barrier type correspond to coastal sediment budgets and coastal responses following the post-glacial marine transgression. Underlying variations in coastal boundary slope play an important role in beach-barrier response to SLR and explain some of the variability in beach-barrier types across NSW (Cowell et al. 2003; Cowell and Kinsela 2018).

There are 184 recognised estuaries along the NSW coast. These vary significantly in shape and size, ranging from large coastal bays and drowned river valleys to major coastal river systems, large coastal lakes, and numerous smaller intermittently open coastal lakes and lagoons (ICOLLs) (Roy et al. 2001). These estuaries support various habitat types and species that are highly valued by local communities.

In many estuaries, considerable development is located on the low-lying land immediately adjacent to the foreshores, much of which is prone to occasional inundation caused by storms, floods, high ocean levels and prevailing entrance conditions. To reduce flood risk, estuary entrances are often managed with permanent structures (breakwaters and training walls) or, in the case of smaller lakes, with artificial openings to control or lower water levels.

This study used the Australian sediment compartments framework (Thom et al. 2018; Short 2020), which provides a useful organisational structure for capturing the regionally linked coastal geomorphology and processes along the NSW coast. The NSW coast features 9 primary and 47 secondary sediment compartments. The primary compartments are, from north to south, North Coast (nsw01), Northern Rivers (nsw02), Mid-North Coast (nsw03), Port Stephens (nsw04), Central Coast (nsw05), Sydney (nsw06), Illawarra (nsw07), Shoalhaven (nsw08) and South Coast (nsw09). The primary compartments are defined by large landforms such as prominent headlands and rivers, or major changes in coastline orientation. Secondary compartments are defined by sediment movement on the shoreface within and between beaches, particularly relevant to coastal erosion hazards. Further information on sediment compartments and their application in coastal hazard analysis can be found at CoastAdapt.

#### Wave and water level regime

The NSW ocean-wave climate is moderate to high energy by global standards, with long-term deep-water wave buoy records indicating a mean significant wave height and period of 1.6 m and 8 s in the central NSW region (Short and Trenaman 1992). Most wave energy originates from the south to southeast (Lord and Kulmar 2000), influencing beach alignment and driving northward littoral drift, especially on beaches in the north of the state. The wave climate is occasionally interrupted (approximately 5% of the time) by storm events, with offshore wave heights exceeding 3 m and reaching up to 8–10 m (Lord and Kulmar 2000).

The wave climate exhibits mild seasonality (that is, yearly variability), with winter energetic southeast waves from mid-latitude cyclones and wave activity from the northeast more prominent during summer due to tropical cyclones and local sea breezes (Morim et al. 2016). East coast lows generating in the central Tasman Sea impact the entire region, particularly during autumn and winter (Short and Trenaman 1992; Shand et al. 2011).

The wave climate also changes over longer periods of 2 to 7 years due to the El Niño Southern Oscillation (ENSO). During El Niño phases, there is less wave energy and fewer storms. Conversely, La Niña phases bring increased wave energy and more storms. Additionally, ENSO influences wave direction, shifting it from a more southerly direction during El Niño to a more easterly direction during La Niña (Phinn and Hastings 1995; Barnard et al. 2015; Harley et al. 2011; Davies et al. 2017).

Along the NSW coast, tides are microtidal and semi-diurnal with significant diurnal inequality. The highest astronomical tide at Fort Denison on the central NSW coast is 2.1 m above the lowest astronomical tide, with a mean spring range of 1.2 m and a mean neap range of 0.8 m (AHO 2023). The tide range increases along the NSW coast by around 0.2 m from south to north (MHL 2012, 2018). The influence of the lunar nodal cycle (18.61 years) on the NSW coast is relatively small (Haigh et al. 2011).

In addition to astronomical tides, various other processes contribute to fluctuations in water levels along the NSW coast (Hanslow et al. 2023). These tidal anomalies, generally less than 1 m in range, can vary significantly in duration (e.g. Modra and Hesse

2011; Viola et al. 2021, 2024a, 2024b). Influences include background variations in mean sea level caused by long-period ocean seiches (Folland et al. 1999) and incoming Rossby waves (Holbrook et al. 2011), which affect the East Australian Current over timescales associated with ENSO, the Pacific Decadal Oscillation, and the Interdecadal Pacific Oscillation.

Short-term phenomena also play a role in sea level variability, often resulting from a combination of wind setup, barometric pressure changes, and coastal trapped waves (e.g. Modra and Hesse 2011; Callaghan et al. 2017). While storm surges are typically smaller than those on many other global coastlines, they can still elevate water levels by more than 0.5 m above normal tidal levels (e.g. PWD 1990; You et al. 2012; Callaghan et al. 2017; MHL 2018), with durations ranging from several hours to days depending on storm characteristics. Coastal trapped waves, which frequently contribute to tidal anomalies along the NSW coast (Viola et al. 2024a; Maiwa et al. 2010; Woodham et al. 2013), usually range from 0.2 to 0.3 m in height but can reach up to 0.5 m (MHL 2015), with typical periods of 7 to 10 days. These longer-period events can propagate into large coastal lakes (McPherson et al. 2013), sometimes causing even low tide levels to exceed normal high tide levels (MHL 2015). Additional variability in sea level may also result from steric effects linked to the East Australian Current (MHL 2018).

#### Sea level rise

White et al. (2014) examined ocean tide gauge records from around Australia and found that sea level trends around the country are closely linked to ENSO, with the strongest influence on northern and western coasts. After adjusting for ENSO, glacial isostatic adjustment and air pressure, Australian mean sea level trends closely align with global mean trends from 1966 to 2009, showing an increase in the rate of rise in the early 1990s. White et al. found the Australian average rate of relative SLR between 1966 and 2009 to be  $2.1 \pm 0.2$  mm per year, increasing to  $3.1 \pm 0.6$  mm per year from 1993 to 2009.

At the NSW baseline sea level monitoring SEAFRAME station at Port Kembla, mean sea level has been rising at a rate of approximately 3.7 mm per year since 1991 (to 2023) (BOM 2024) (see Figure 1), resulting in a total increase of roughly 12.2 cm over the monitoring period. This is similar to the rate of  $3.4 \pm 1.2$  mm per year reported by Peng et al. (2022), but higher than the rate reported by Watson (2020). Off the NSW coast, the rate of SLR peaks at a latitude of about  $35^{\circ}$ S in the Tasman Sea, consistent with the spin-up of the South Pacific subtropical gyre due to increased wind stress curl (Roemmich et al. 2007; Church et al. 2012). Along the NSW coast, tide gauge data over the corresponding timeframe indicate a lower rate of rise, suggesting a gradient in sea level trends between the Tasman Sea and the coast, which is explained by increased strength and southward flow of the East Australian Current (Hill et al. 2008, 2011; Church et al. 2012; Deng et al. 2011), and contributions from glacial isostatic adjustment (Zhang et al. 2017).

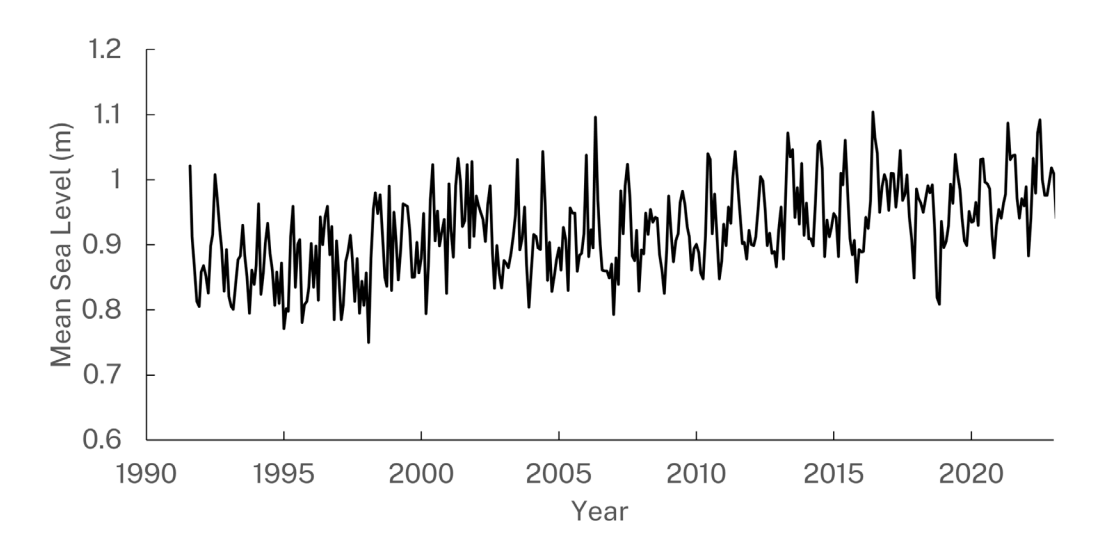


Figure 1 Measured mean sea level at the Port Kembla baseline sea level monitoring station from 1991 to 2023

Note the data for 1991 covers only part of the year. Source: BOM (n.d.).

Shared socioeconomic pathways (SSPs) are scenarios that explore potential global futures based on socioeconomic trends and their interactions with climate change mitigation and adaptation efforts. Developed within the IPCC framework, SSPs describe 5 distinct pathways, each representing a different trajectory of societal and environmental development. These pathways are paired with greenhouse gas concentration trajectories to model climate outcomes, including SLR projections, by linking socioeconomic trends to emissions, global warming, and associated impacts such as thermal expansion and ice sheet melt, providing a comprehensive basis for assessing future risks and adaptation strategies. These SSPs include:

- SSP1 (Sustainability taking the green road): A sustainable development pathway characterised by low inequality, green technology adoption, and efforts to achieve environmental sustainability, leading to low emissions.
- 2. SSP2 (Middle of the road): A pathway where historical trends continue, with moderate challenges to both mitigation and adaptation, resulting in emissions and socioeconomic trends similar to those observed today.
- 3. SSP3 (Regional rivalry a rocky road): A world marked by regionalisation, nationalism and limited international cooperation, leading to slow economic growth, high population levels and high emissions.
- 4. SSP4 (Inequality a road divided): A future where inequality within and between countries is pronounced, with well-resourced, high-emitting industrial sectors alongside vulnerable, resource-scarce communities.
- 5. SSP5 (Fossil-fuelled development taking the highway): A pathway driven by rapid economic growth and heavy reliance on fossil fuels, prioritising material consumption and technological innovation over environmental sustainability, resulting in very high emissions.

Typically, there are numerical extensions to these scenarios (for example, SSP1-2.6, SSP3-7.0) that link the SSPs to specific greenhouse gas concentration trajectories. These combinations help represent both socioeconomic and climate dimensions, creating a more integrated scenario framework. For example, SSP1-2.6 combines the sustainable development pathway of SSP1 with a low emissions scenario (reaching a radiative forcing of 2.6 W/m<sup>2</sup> by 2100), projecting warming of between 1.3 and 2.4°C and limited SLR (during 2081–2100). SSP2-4.5 reflects a medium emissions pathway (reaching a radiative forcing of 4.5 W/m<sup>2</sup> by 2100) with warming of between 2.1 and 3.5°C (during 2081–2100), while SSP3-7.0 represents a high emissions trajectory (reaching a radiative forcing of 7.0 W/m<sup>2</sup> by 2100) with between 2.8 and 4.6°C warming (during 2081–2100). For convenience, this report refers to the scenarios SSP1-2.6, SSP2-4.5 and SSP3-7.0 as low, medium and high emissions scenarios/storylines, respectively. At the extreme, SSP5-8.5 pairs fossil-fuel-driven development (reaching a radiative forcing of 8.5 W/m<sup>2</sup> by 2100) with severe warming of between 3.3 and 5.7°C (2081–2100 range), leading to significant SLR projections (IPCC 2023). This is referred to as a very high emissions scenario/storyline.

Future SLR along the NSW coast is projected to be slightly above (0–10%) the global average (Church et al. 2014). Model projections for SLR along the NSW coast are available from the NSS SLR projection tool (Fox-Kemper et al. 2023; Garner et al. 2022), which is based on modelling conducted for the IPCC AR6. At Port Kembla, this modelling suggests likely (17th–83rd percentile range) increases in sea level of 0.23–0.56 m (SSP1-2.6), 0.37–0.73 m (SSP2-4.5), 0.50–0.91 m (SSP3-7.0) and 0.59–1.04 m (SSP5-8.5) by 2100, relative to a 1995–2014 baseline. Equivalent ranges by 2150 are 0.33–0.93 m (SSP1-2.6), 0.58–1.29 m (SSP2-4.5), 0.83–1.65 m (SSP3-7.0) and 0.94–1.92 m (SSP5-8.5). Projections are slightly higher in the northern parts of the state, as shown in Table 1.

Table 1 The likely ranges (17th–83rd percentile range) of sea level rise projection in metres under SSP1-2.6 and SSP3-7.0 scenarios at Yamba, Port Kembla and Eden

Location	2050 SSP1-2.6	2050 SSP3-7.0	2100 SSP1-2.6	2100 SSP3-7.0	2150 SSP1-2.6	2150 SSP3-7.0
Yamba	0.14-0.27	0.17-0.30	0.31-0.65	0.55-0.97	0.45-1.07	0.90-1.77
Port Kembla	0.11-0.24	0.16-0.28	0.23-0.56	0.50-0.91	0.33-0.93	0.83-1.65
Eden	0.11-0.25	0.15-0.28	0.22-0.57	0.51-0.92	0.31-0.93	0.85-1.67

Note: The full range can be accessed using the NASA SLR projection tool.

These likely range projections do not include ice-sheet-related processes which are characterised by deep uncertainty. To account for these processes, the IPCC (2023) provides low-confidence modelling explained in a low-likelihood, high-impact storyline, designed for stakeholders with low risk tolerance who may need to consider possibilities beyond the 'likely range'. In this storyline, the IPCC suggests mean SLR at Port Kembla, as indicated by the 95th percentile of the low-confidence AR6 modelling

associated with SSP5-8.5 (incorporating ice-sheet processes), could reach as high as approximately 2.3 m by 2100 and 5.4 m by 2150. In the longer term, the IPCC highlights that sea level is committed to rise for centuries to millennia due to continuing deep ocean warming and ice-sheet melt.

Increased mean sea levels contribute directly to an increase in extreme water levels and the frequency of inundation events. The special report *The ocean and cryosphere in a changing climate* (IPCC 2022) concludes that even small to moderate changes in mean sea level could lead to hundred- to thousand-fold increases in the frequency of inundation events. For example, what is currently a 1-in-100-year event is likely to occur once or even multiple times per year at many locations globally in the future.

#### 2.2 Coastal hazards

#### **Erosion hazards**

Coastal erosion involves the temporary or permanent loss of sedimentary foreshore land due to ocean and estuarine processes, primarily waves and elevated sea levels. At timescales relevant to hazard management (hours to seasons) and future risk planning (years to centuries), erodible sedimentary foreshore along the NSW coast may be composed of:

- loose and mobile sand (beach and dunes)
- vegetated sand and soils of varying structure
- consolidated or weakly cemented sand and soils (indurated sand or coffee rock, beach rock)
- weakly lithified or weathered older rocks (for example, conglomerates, mudstones).

The presence of harder bedrock or artificial structures engineered to withstand ocean processes (to a particular design level) within the foreshore substrate may impede or restrict coastal erosion. The magnitude and frequency of coastal erosion at any location may vary depending on the coastal geomorphology, sediment availability and exposure to ocean conditions (that is, the driving processes).

Coastal storms that generate large waves, elevated sea levels (storm surge) and strong winds are the most visible drivers of coastal erosion. A storm erosion event may result from a single storm (Harley et al. 2017) or a series of consecutive (clustered) storms occurring over weeks to months (Dissanayake et al. 2015; Davies et al. 2017). Other drivers of coastal erosion include climate cycles (such as ENSO) that influence ocean wave climates (Barnard et al. 2015; Mortlock and Goodwin 2016), altering sandy shoreline alignment (beach rotation) and sand bypassing around headlands to downdrift beaches (Harley et al. 2011; Goodwin et al. 2013; da Silva et al. 2021). Depending on the scale, intensity and persistence of ocean drivers, erosion may affect extensive sections of the coast or be confined to specific beaches or even sectors of beaches.

Beach recovery following storms and during more favourable climate patterns may take weeks to years, with complete recovery taking up to a decade in extreme cases (Thom and Hall 1991). This has been captured in a 50-year beach survey record from Bengello

Beach (Moruya) in NSW (<u>Figure 2</u>), where no long-term trend of change (that is, erosion or accretion) is evident, but fluctuations in beach volume occur annually (seasonal fluctuation) and between years and decades. Because beach recovery is driven by nearshore wave processes (Phillips et al. 2017, 2019), climate patterns and the intensity and clustering of subsequent storms (e.g. Davies et al. 2017) will all influence beach recovery after severe erosion events.

Some beaches have been eroding or accreting for hundreds or even thousands of years, gradually adjusting to the local balance of coastal geomorphology, sediment availability and ocean processes (Kinsela et al. 2016a; Oliver et al. 2020), while other beaches have remained relatively stable. In all cases, beach fluctuation (that is, temporary erosion and accretion) due to storms and climate cycles (<u>Figure 2</u>) has occurred around the mean trend of eroding, accreting or stable shoreline behaviour.

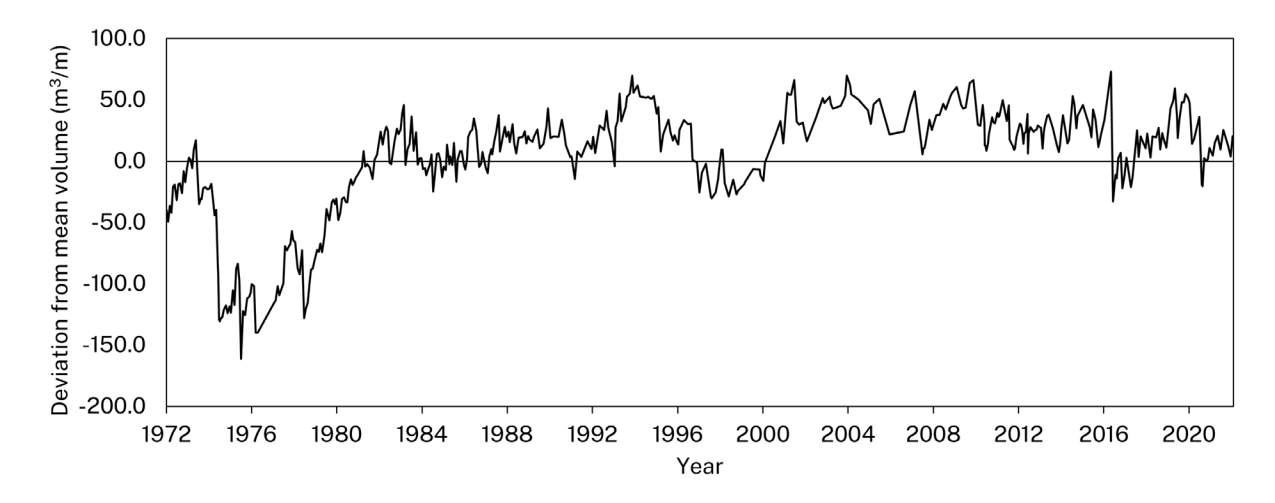


Figure 2 The 50-year record (1972–2022) of sand volume in the beach–foredune system at Bengello Beach (Moruya) showing a fluctuation phase exceeding 200 m<sup>3</sup>/m

Note: The full beach recovery after severe erosion in the early 1970s took almost a decade. Source: McLean et al. (2023).

Global climate change-induced SLR is now altering the balance between geomorphology, coastal processes and sediment availability (that is, the sediment budget) for all NSW beaches. This could drive a new phase of coastal erosion on beaches that have been historically stable (or slowly accreting) and exacerbate erosion on beaches that have been historically receding. The nature of such changes will depend on the magnitude and rate of SLR and the morphodynamic response of beach systems. The projected acceleration of SLR during this century could also lead to tipping-point changes if morphodynamic stability thresholds are exceeded.

Summarising the above, coastal erosion hazards can be separated into 2 principal components for the purpose of modelling (Figure 3):

- 1. beach fluctuation (temporary, although recovery may take several years)
- 2. shoreline recession (cumulative over timescales of decades to centuries).



Figure 3 Fluctuating beach erosion caused by severe storm events in (a) an undeveloped setting at Cronulla and (b) a developed setting at Wamberal, compared with sustained shoreline recession in (c) a natural setting at Woody Bay and (d) a developed setting at Old Bar. Photos: M Kinsela

Beach fluctuation encompasses all *temporary variations* in the beach–dune sediment volume (and coupled shoreline position) over timescales spanning days to years. It includes erosion events due to coastal storms (including rip cells) and climate cyclicity that influences storminess, beach alignment and sediment availability from the nearshore and alongshore (for example, headland sand bypassing). For beach fluctuation, the focus of modelling is the *range of fluctuation* in beach–dune volume (and shoreline position) that could occur during any year of the forecast period, including the final year.

Shoreline recession includes all *cumulative changes* in the beach–dune sediment volume (and coupled shoreline position) sustained over timescales of decades to centuries, regardless of beach fluctuation cycles. It includes any underlying or mean-trend erosion signals that may result from various drivers contributing to a sediment budget deficit, potentially including SLR. For shoreline recession (change), the focus of modelling is the *rate of change* in beach volume (and shoreline position) that could occur by the end of the forecast period.

The present-day erosion hazard zone includes only the beach fluctuation component, which reflects the potential range of temporary variations in the beach–dune volume and shoreline position that may persist for months to years. <u>Figure 4</u> illustrates this in cross-section, showing the present beach fluctuation zone as a sediment volume comprising the beach and foredune. Erosion is typically measured in cubic metres of

sand per metre of shoreline (m³/m) above the mean sea level (MSL). The distance of erosion corresponding to the sediment volume is usually measured landward from the shoreline (MSL) or the beach berm, which is often around 2 m Australian Height Datum (AHD) on NSW beaches.

The magnitude of beach fluctuation in any given year, present or future, may be expressed as a probability distribution, with a higher likelihood of modest erosion and a lower likelihood of severe erosion. This is illustrated for a present scenario in <a href="Figure 4">Figure 4</a>, showing a 50% likelihood that the beach will be eroded, and a 1% likelihood that the foredune will be significantly eroded. Importantly, the actual extents of these erosion zones will vary between beaches, depending on local coastal geomorphology and exposure to wave energy.

As sea level rises, beaches are generally expected to retreat (Nicholls and Cazenave 2010). However, the degree to which individual beaches will be affected and the rate of response is complex and will depend on the local coastal geomorphology (for example, dune height and volume, beach gradient, surf zone and shoreface profiles), exposure to wave energy, and the local sediment budget balance that may be evident in the historical shoreline behaviour (that is, stationary, accreting, receding). Prior state-wide coastal erosion hazard mapping (Kinsela et al. 2017; OEH 2018) found that exposure will increase across all regions of the NSW coastline during this century, though the extent of exposure will vary between regions and individual beaches.

The future coastal erosion hazard zone includes both beach fluctuation and recession components, representing the cumulative change in beach–dune volume by that point in time due to any underlying sediment budget imbalance and SLR. This is shown for 2070 and 2150 scenarios in <a href="Figure 4">Figure 4</a>, demonstrating the increasing influence of cumulative change for longer forecasts as SLR becomes a more dominant factor. For future forecasts, the coastal erosion potential from the combined fluctuation and cumulative components can also be expressed in terms of the reach of erosion for different probability levels.

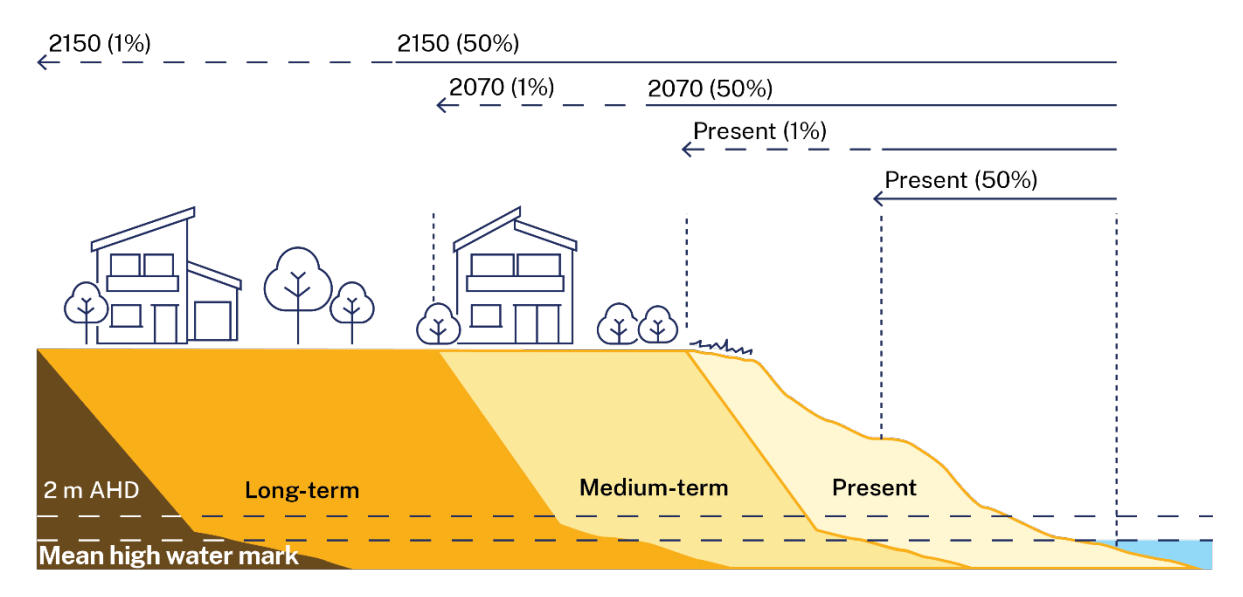


Figure 4 The coastal erosion hazard zones include the beach fluctuation extent (the only component for present scenarios) as well as cumulative erosion (shoreline recession) for future forecasts. The total potential erosion extent for each scenario spans a range of distances tied to probability levels. Example years and associated probabilities shown include present (1% and 50%), 2070 (1% and 50%), and 2150 (1% and 50%)

#### Coastal overwash

During storms, several physical processes may combine to raise ocean and coastal water levels, resulting in the inundation of beach infrastructure and potential overwash of coastal dunes. These processes include astronomical tides, storm surge and wave runup. The relatively steep nature of the NSW continental shelf, combined with the moderate- to high-energy wave climate, means that wave runup on this coast is the primary contributor to coastal overwash (order of several metres: Morris et al. 2016), whereas storm surge contributions are relatively modest (typically less than 0.4 m: Viola et al. 2021). In addition, wave runup magnitudes can be highly variable due to alongshore variations in wave exposure and spatio-temporal changes in beach steepness (e.g. Nielsen and Hanslow 1991).



Figure 5 Surveyed debris line on Maroubra Beach (Sydney NSW) on 7 June 2016 showing inundation elevations (m AHD) following the June 2016 east coast low

An example of the elevation reached by wave runup during storms is shown in <u>Figure 5</u>. Here, the elevation of the marine debris line was plotted along Maroubra Beach in the eastern suburbs of Sydney, collected using real-time kinematic surveying techniques immediately after the June 2016 storm. The debris line elevation varied significantly

alongshore and reached a maximum elevation of around 7.45 m AHD in the central part of the beach. Maximum still water level (SWL) (tide and surge) measured within Sydney Harbour for this event was 1.29 m AHD on 5 June 2016 at 20:15 hours, which includes a peak tidal residual (storm surge) of 0.2 m (Louis et al. 2016), suggesting a contribution from wave runup (above SWL) of over 6 m.

While total water levels from the combined effects of tides, surge and wave runup can be large (several metres), much of the NSW coast is characterised by relatively high dunes (Doyle and Woodroffe 2023; Doyle et al. 2024), which provide a natural defence against coastal overwash and inundation (Hanslow et al. 2016, 2018; Morris et al. 2016; McInnes et al. 2016; Short 1988). Although a state-wide assessment of coastal overwash in NSW has not been undertaken prior to the current study, reports of such inundation during major storm events to date have generally been limited to specific settings. These include:

- entrances to ICOLLs and low-lying areas landwards and adjacent to entrances
- surf clubs and low-lying car parks
- southern corners of beaches where dune heights are lower
- locations where dunes are degraded.





Figure 6 Damage resulting from overwash following the June 2016 East Coast Low at
(a) the Clan Motel adjacent to Terrigal Lagoon and (b) the surf club roller doors
at Terrigal Beach. Photos: DCCEEW

Some examples of overwash and associated inundation on the NSW coast are shown in <u>Figure 6</u>. Here we show damage following the June 2016 east coast low to the Clan Motel adjacent to Terrigal Lagoon (<u>Figure 6(a)</u>) and the surf club roller doors at Terrigal Beach (Figure 6(b)).

Given the evidence of coastal overwash from recent storms in NSW, it is now pertinent to apply a consistent state-wide approach to identify areas of current and potential future overwash risk.

#### Estuarine inundation hazards

Water levels within estuaries differ from those in the ocean due to various factors related to the shape and geomorphology of the estuary. These include tidal lag, tidal distortion, elevation of half-tide levels (tidal pumping) and variations in fortnightly tides (NSW Govt 1992). The tidal range in estuaries is affected by factors such as inertia related to acceleration and deceleration of the tidal flow; amplification associated with the decrease of the width and depth (convergence) of the estuary; dampening of the

tide due to bottom friction; and its partial reflection at abrupt changes in bathymetry (Dyer 1997; McDowell and O'Connor 1977; Savenije 2005; Prandle 2009; van Rijn 2010).

These processes result in fundamentally different tidal behaviours across estuaries (Hanslow et al. 2018; Du et al. 2018; Hughes et al. 2019). Some estuaries experience tidal amplification, while others are characterised by tidal attenuation, and some have a combination of both behaviours. In drowned river valley estuaries, the estuary geometry generally shallows and narrows in a landward direction, promoting tidal amplification and increasing tide range and height for considerable distances inland (Hanslow et al. 2018; NSW Govt 1992). Within tidal rivers, river entrance shoals contribute to initial tidal attenuation, followed by mild amplification before dampening occurs at fluvial gravel and sand bars around the estuary head (Hanslow et al. 2018; NSW Govt 1992). Tidal lakes are characterised by significant attenuation of the tidal range due to frictional effects in the entrance channel, with tide ranges in these systems reduced to as little as 10% of the offshore tide range (Hanslow et al. 2018; NSW Govt 1992). In these lakes, tidal pumping can significantly amplify the magnitude of the fortnightly tide (McLean and Hinwood 2011). Smaller lake systems are usually characterised by ICOLLs. When open, these ICOLLs often function like tidal lakes. When closed, they fill gradually, with water levels influenced by inflows and evaporation. In these systems, maximum water levels are generally controlled by the beach berm height, which varies with beach slope and exposure to waves (Hanslow et al. 2000; Haines 2006; Weir et al. 2006).

Significant development adjacent to NSW estuaries is often low-lying and thus vulnerable to SLR (Hanslow et al. 2018; OEH 2018). There are several towns along the NSW coast where tidal inundation (otherwise known as sunny day flooding or nuisance inundation) already occurs in urban streets during higher tides (Hague et al. 2020, 2022; Hanslow et al. 2019, 2023). Locations identified thus far include Tweed Heads, Fingal, Brunswick Heads, Ballina, Ballina West, Yamba, Coffs Harbour, North Shore, Camden Haven, Dunbogan, Manning Point, Tuncurry, Tea Gardens, Lemon Tree Passage, Bobs Farm, Tighes Hill, Carrington, Maryville, Marks Point, Swansea, Davistown, Empire Bay, Woy Woy, Spencer, Ettalong, Bobbin Head, Mona Vale, Haberfield, Tempe, Marrickville, Botany, Wooli Creek, Sylvania, Greenwell Point, Sussex Inlet, Corrigans Beach, Narooma, Bermagui and Merimbula. In most localities, this inundation originates through ingress of tidal water into stormwater systems and subsequently floods low-lying streets and gutters. Some examples of this are shown in Figure 7. Inundation occurs when tidal levels exceed the elevation of low-lying streets. While these inundation events currently result in minor, short-lived flooding of roads, paths and driveways, they suggest more widespread and significant impacts in the future as sea levels continue to rise (Hanslow et al. 2019).



Figure 7 Examples of tidal inundation (otherwise known as sunny day or nuisance flooding) in urban streets of (a) Marks Point, 13 May 2015, (b) Tea Gardens, 4 January 2018, (c) Woy Woy, 3 January 2018, and (d) Swansea, 2 January 2018. Photos: D Hanslow

At the initial street threshold, tidal inundation effects are highly localised and short in duration (typically up to an hour) but they become longer and more widespread during higher/deeper events. When tidal levels exceed street thresholds by 0.2 to 0.3 m, multiple streets are typically affected, and local businesses may be impacted for several hours over consecutive days (Hanslow et al. 2019).

Analyses by Hague et al. (2020, 2022) and Hanslow et al. (2019, 2023) indicate that while the frequency of these inundation events varies, it has increased significantly over recent decades due to SLR. This is shown in <u>Figure 8</u>, which plots the annual counts of days and total annual duration in hours, respectively, of street flooding in Sydney, using data from Fort Denison and the nuisance inundation threshold (1 m AHD) identified by Hanslow et al. (2019) and Hague et al. (2020).

Hanslow et al. (2019) point out that, in some locations, chronic inundation has necessitated adaptation measures, such as modifying stormwater outlets to limit ingress of tidal waters during higher tides. Such measures have been implemented in Carrington and Maryville on the Hunter River, Marks Point (now removed) and Swansea in Lake Macquarie, and Haberfield in Sydney (Hanslow et al. 2019, 2023).

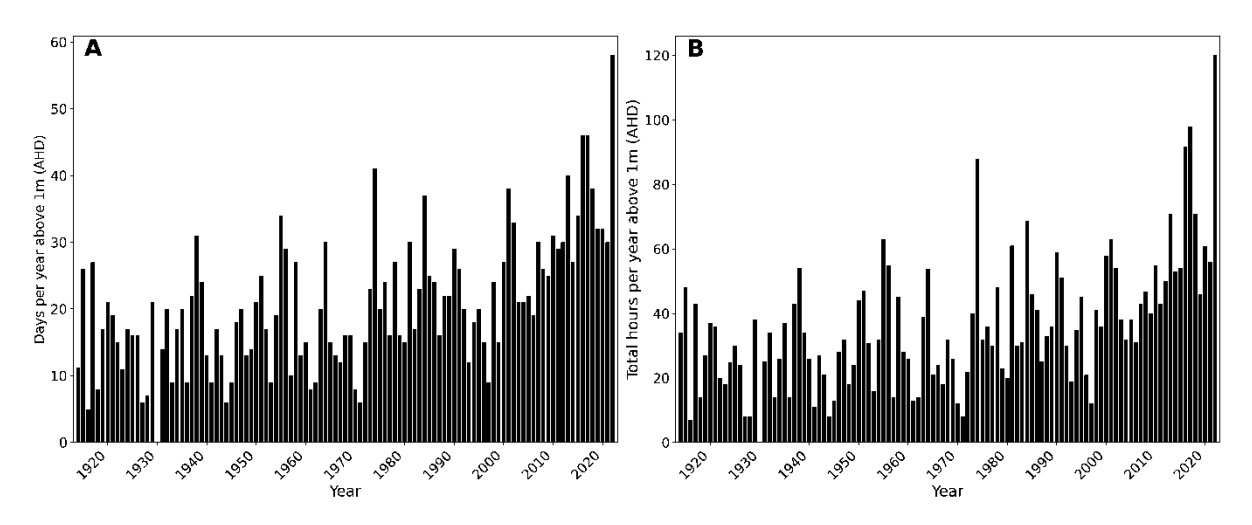


Figure 8 Plots of (a) days per year and (b) total annual duration (hours) of nuisance street inundation (above 1 m AHD) in Sydney, 1914–2022

As discussed by Sweet and Park (2014), the distribution of coastal water levels typically exhibits a highly nonlinear pattern characterised by increasing rates of inundation as water levels transition from the 'tail' towards the mean. The level of coastal infrastructure within this distribution is critical to determining the frequency of inundation. Sweet and Park describe this transition as a tipping point for coastal overwash impacts as sea levels rise.

Given that water levels and tide ranges in estuaries differ significantly from those in the ocean, the sensitivity of estuaries to SLR will vary depending on their typology and boundary conditions. In general, estuaries with restricted entrances and currently attenuated tides (such as tidal lakes and river estuaries) are likely to be the most sensitive to SLR impacts, because they have the potential to become more hydrodynamically efficient as sea levels rise. Analysis of water levels within Lake Macquarie (Australia's most exposed estuary) by Hanslow et al. (2023) suggests that this estuary could experience double the number of inundation days for a given amount of SLR compared to open coast locations. Many NSW coastal lakes are also experiencing ongoing entrance scour from entrance training works (e.g. Nielsen and Gordon 2008), leading to increasing tide ranges and higher rates of high water levels than expected from SLR alone (Hart et al. 2017; Palmer et al. 2022).

Idealised modelling of estuaries with restricted entrances indicates that they are likely to experience increases in tide range under future SLR scenarios, in the assumed absence of any morphological response, meaning local rates of high tide inundation within these estuaries may exceed those in open coast settings (Khojasteh et al. 2020, 2021, 2023). Conversely, in drowned river valley estuaries, which currently experience tidal amplification, SLR may result in less amplified tidal ranges (Khojasteh et al. 2020, 2021).

# 3. Methods

This assessment examined both current and potential future exposure to coastal erosion and inundation. This chapter is a high-level overview of methods used for the assessment, with the full technical details presented in <u>Appendix A: Methods</u>. The sea level rise (SLR) projections, baseline for the projections, scenarios, and the approach to managing uncertainty were common to the assessment of all three coastal hazards and are described in the first 4 sections of the chapter. The methods for assessing coastal erosion, coastal overwash, and estuarine inundation are described separately in the next 3 sections of the chapter. The final section describes the method to estimate the area of erosion and inundation and associated number of assets potentially impacted by these hazards along the NSW coast.

## 3.1 Sea level rise projections

Methods for assessing potential future exposure to coastal erosion, coastal overwash, and estuarine inundation were based on SLR projections from modelling undertaken for the Sixth Assessment Report (AR6) of the Intergovernmental Panel on Climate Change (IPCC) (Fox-Kemper et al. 2021). These projections were used in combination with available geomorphology data to further model coastal hazards for NSW. SLR projections for gauges along the NSW coast were accessed from the NASA SLR projection tool (Kopp et al. 2023), which is based on modelling conducted for the IPCC AR6 (Figure 9).

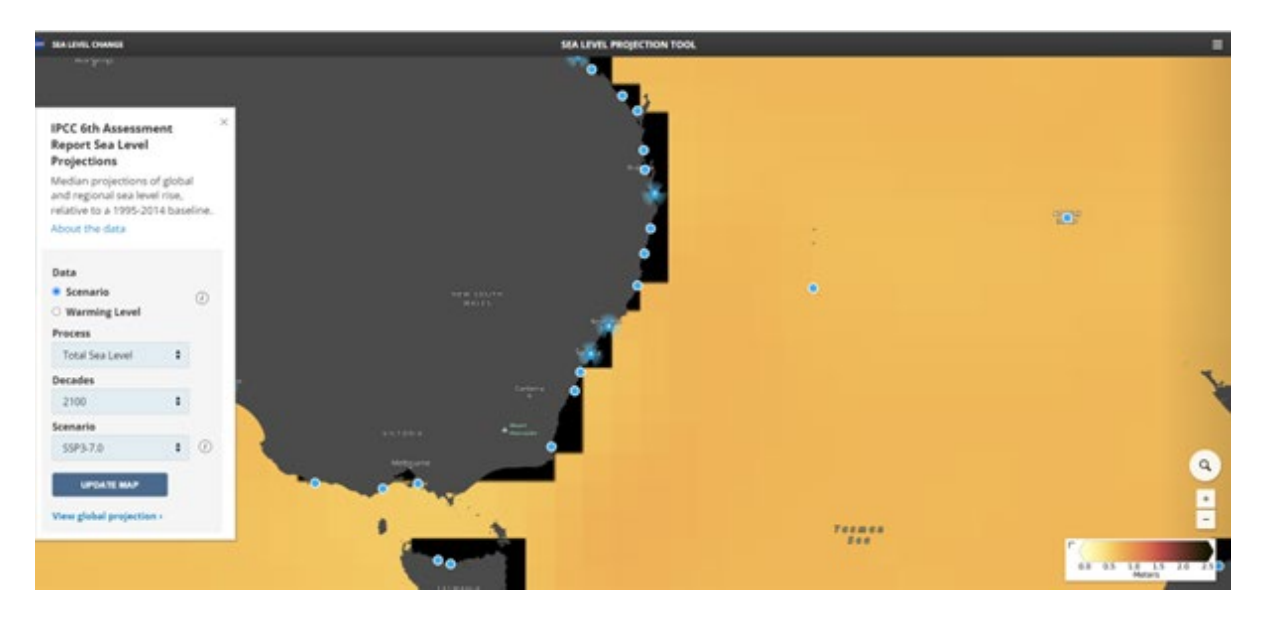


Figure 9 Screenshot of the NASA sea level projection tool

For current exposure, the study referenced to the year 2020 (baseline) and examined the implications of SLR at 10-year (decadal) intervals beyond this date, extending out to 2150. This approach is primarily based on the available SLR projections, but the decadal interval can also facilitate decision-making in the context of uncertain futures using a dynamic adaptive pathways approach (Haasnoot et al. 2013). The longer-term

projections to 2150, combined with a range of climate change scenarios, enable full consideration of risks relevant to projected growth and planning for any existing and new coastal development. The available data include quantile values (5%, 17%, 50%, 83%, 95%) of the likelihood of projected SLR at decadal intervals up to 2150. However, as outlined in Section 2.1 (Sea level rise), SLR is virtually certain to continue beyond 2150, which may need to be considered in policy development.

## 3.2 Baseline for the projections

The year 2020 was chosen as the reference baseline to optimise the use of the extensive measured water level and beach morphology data available in NSW and to align with the IPCC AR6 SLR data. Projected SLR from the IPCC AR6 data, originally referenced to the 1995–2014 period, was adjusted to 2020 by subtracting the modelled rise between 1995–2014 and 2020. This ensured that only SLR occurring after 2020 was considered in the analysis. To maintain consistency across hazard assessments and to align with the most recent and comprehensive data available, results from coastal erosion, coastal overwash and estuarine inundation were all referenced to 2020 as the current condition. This approach supports comparative analysis across hazards and ensures the findings remain relevant for decision-making and long-term planning.

Fundamental differences in modelling approaches, as well as limitations in data coverage and availability, necessitated tailored referencing methods for each hazard type. A brief description of how the baseline was selected and implemented for coastal erosion, coastal overwash and estuarine inundation is provided below, with detailed explanations in the following sections.

For erosion modelling, projected erosion volumes were applied to sector-averaged profiles behind a baseline shoreline derived from the 'most accreted' shoreline observed across all available LiDAR datasets (2007–2022). This approach represents an accreted beach state and ensures the modelling captures the maximum potential sediment volume available for erosion. Modelled erosion incorporates SLR from 2020 onwards.

For the inundation from coastal overwash analysis, the baseline sea level was calculated using water level records from 1990 to 2020. This timeframe was selected to ensure consistency across the limited number of gauges with long-term, overlapping datasets. Data were detrended to establish a 2020 reference still water level (SWL). Modelled total water levels responsible for coastal overwash includes SLR from 2020 onwards.

For the estuarine inundation analysis, the baseline sea level was determined using all available water level records up to July 2022. These records were detrended to establish water levels in 2020. This approach accounts for variability in gauge coverage across estuarine locations, where records often span 20–30 years but are shorter in some cases. Modelled inundation incorporates SLR from 2020 onwards.

### 3.3 Use of scenarios

Scenarios spanning a broad range of possible climate futures are presented in this report, with medium-confidence projections for the SSP1-2.6, SSP2-4.5 and SSP3-7.0

scenarios presented as the primary storylines for coastal hazards in NSW. SSP1-2.6 envisions a sustainable development future with significant emissions reductions; SSP2-4.5 reflects moderate challenges to mitigation and adaptation under continued historical trends; and SSP3-7.0 reflects a high-emissions scenario driven by limited international cooperation and regional rivalries.

Additionally, this assessment considered medium-confidence SSP5-8.5 and low-confidence SSP5-8.5 as high-impact scenarios, representing a fossil-fuel-driven future characterised by rapid economic growth, high emissions and severe climate outcomes. This is to help quantify potential SLR impacts for decision-makers that have low risk tolerance. The low-confidence projections integrate information from the structured expert judgement study by Bamber et al. (2019) for both the Greenland and Antarctic ice sheets, as well as results from a simulation study that incorporates marine ice-cliff instability in the Antarctic (DeConto et al. 2021).

This overarching approach aligns with state-wide, national and global best practices for SLR modelling, ensuring consistency in decision-making frameworks across NSW. Given the inherent uncertainty of SLR, different scenarios result in vastly different exposure levels for communities, infrastructure and ecosystems. By examining a wide range of scenarios, this assessment enables decision-makers to account for varying levels of risk, ensuring strategies are resilient to both likely impacts and less probable but more severe impacts. This approach supports the development of adaptive management solutions to address long-term uncertainties and mitigate vulnerabilities for critical assets and communities.

# 3.4 Approach to uncertainty

There is considerable uncertainty associated with assessing current and projected future hazards related to coastal erosion and inundation. This uncertainty arises from multiple sources and is typically categorised into two classes (Der Kiureghian and Ditlevsen 2009):

- aleatory uncertainty, which refers to inherent variability in natural processes (for example, in storm occurrence),
- epistemic uncertainty, which stems from a lack of knowledge, such as uncertainty regarding future sea level change.

Uncertainty is unavoidable in both inundation and coastal erosion modelling and forecasting due to incomplete knowledge about current processes (including, for example, water levels, beach response to storms or sea level change, and the intrinsic limitations of hydrodynamic and beach and shoreline response models), as well as the potential range of future forcing conditions.

To account for uncertainty in each of the SLR scenarios, a probabilistic approach was used to communicate future hazards in the context of the uncertainty space to support informed and transparent decision-making. By adopting this approach, this assessment aimed to explicitly communicate the likelihood (or probability) and potential

consequences of coastal hazards, allowing for risk assessment that takes uncertainty into account.

Understanding coastal risk requires assessment of both the likelihood of coastal hazards and their potential consequences. Available data were used in combination with SLR projections to model and map the potential likelihood of hazards associated with coastal inundation and erosion. The potential consequences were examined in the context of existing infrastructure and other assets. A probability distribution was fitted through the sets of quantile data to account for SLR uncertainty. Further information on the method for quantile fitting is presented in Appendix A: Methods.

### 3.5 Coastal erosion methods

#### Overview

Coastal erosion was modelled using a sediment volume-based response framework that simulates storm-driven erosion, beach fluctuations, and long-term impacts of SLR using a Monte Carlo simulation framework. The model integrates historical satellite data and probability distributions for key factors, capturing erosion trends across 758 beach sectors, including 32 bay/estuary beaches. The modelling covered approximately 90% of NSW's sandy shorelines and provided probability distributions of beach erosion volume, shoreline change and spatial erosion extent, for present and future scenarios.

Components of erosion considered in the model include beach fluctuation caused by storms and climate variability (scaled by local exposure to wave energy); historical trends in beach behaviour attributed to sediment budget imbalances; and the response to SLR, including the redistribution of sand from beaches and dunes to adjacent estuaries and the coastal seabed. Modelled beach erosion volumes were mapped as total erosion distances from present-day beach shorelines using high-resolution coastal terrain data. Hazard mapping and exposure statistics are provided for selected probability of exceedance levels (50%, 10%, 1% and 0.1%).

#### Data

The erosion modelling approach takes advantage of recent advances in coverage, resolution, frequency and availability of data for coastal geomorphology and ocean processes for NSW to provide the most detailed assessment of coastal erosion potential for the NSW coastline to date. Many datasets have been acquired and developed since the previous state-wide coastal erosion hazard assessment (Kinsela et al. 2017; OEH 2018). For example, high-resolution mapping of the coastal seabed, analysis of historical beach change trends from satellite observations, and local-scale nearshore wave modelling are all critical inputs to the coastal erosion modelling approach. Appendix B: Datasets lists the datasets used in this study.

### **Approach**

This section provides context for the drivers and components of coastal erosion considered in the modelling. The coastal erosion modelling approach builds on the previous state-wide coastal erosion exposure assessment (Kinsela et al. 2017;

OEH 2018) to provide a state-wide assessment of NSW open coast beaches. Select case studies for wave-dominated beaches in semi-enclosed bays and estuaries were also completed. The behaviour of beaches within estuaries and bays is complex, with locally varying wave exposure and estuarine sediment dynamics that may be beyond the scope of the modelling approach (Vila-Concejo et al. 2020; Fellowes et al. 2021). Hence, modelling erosion in such settings should be taken as a first-pass estimate, and more detailed site-specific studies are required to evaluate their sediment budgets comprehensively.

The method requires that backshore geomorphology landward of modelled beaches must fully or partially comprise unconsolidated or erodible sediment (Kinsela et al. 2016b, 2017). The NSW coastal quaternary geology mapping and the Smartline coastal geomorphology datasets (Appendix B: Datasets) were used to identify beaches with erodible backshore geomorphology for inclusion. Beaches with entirely non-erodible backshore geomorphology (for example, bedrock cliffs or other non-erodible substrates behind the beach) were excluded. For beaches with erodible backshore geomorphology which are protected by seawalls or other artificial structures, the natural response of the beach (assuming no protection) was modelled. As such, it is recommended that coastal erosion hazard mapping be interpreted in conjunction with data on existing coastal protection structures, where available or appropriate. Doing so ensures a more accurate understanding of the actual exposure to erosion hazards, as areas identified as susceptible to erosion may, in practice, be shielded by engineered defences.

Based on the above considerations such as the presence of erodible sediment, coastal erosion modelling was carried out for 336 open coast NSW beaches, modelled as 726 individual beach sectors (Appendix C: Beaches modelled). An additional 32 ocean-influenced bay/estuary beaches located within the entrances of Port Stephens (2), Broken Bay (3), Bate Bay (2), Jervis Bay (7), Batemans Bay (11) and Twofold Bay (7), exposed to ocean wave processes, were also considered as case studies, bringing the total number of modelled beaches to 368, across 758 individual sectors.

# Probabilistic modelling framework

Simulating coastal erosion over decades to centuries involves considerable uncertainty, which must be captured within the modelling process to communicate the full spectrum of potential responses in model forecasts (Cowell et al. 2006; French et al. 2016). Sources of uncertainty include (but are not limited to) historical observations of beach change and trends, present and future influences on local sediment budgets, the nature of and possible changes to coastal wave climates, and the modelling methods employed.

The coastal erosion modelling follows a probabilistic approach to manage these uncertainties, using a Monte Carlo simulation framework incorporating a reduced complexity model, and historical observations of beach change to estimate the potential extent of erosion for each scenario and each beach sector, as well as the distribution of probabilities across that extent (Cowell et al. 2006; Kinsela et al. 2017).

For each beach sector, scenario and forecast year, the probability distribution of potential coastal change was generated from 2 million Monte Carlo simulations, and the projected coastal change corresponding to selected probability of exceedance levels (namely, 50%, 10%, 1%, 0.1%) was mapped. This probabilistic approach allows for the full uncertainty space to be considered as the relative likelihood of erosion exposure for each scenario.

The Monte Carlo simulation method is commonly used in coastal modelling and allows for managing uncertainties in the drivers of coastal erosion and the modelled responses by evaluating probabilities across potential outcomes for each scenario (Cowell et al. 2006; Kinsela et al. 2017) using millions of Monte Carlo simulations across each beach sector. Information on the reduced complexity model and the probabilistic approach to erosion modelling are detailed further in Appendix A: Methods. Figure 10 conceptually shows the coastal erosion model which predicts beach erosion sediment volume (V) and converts it to erosion distance (R) using high-resolution topography data for each beach sector. Present scenarios consider the range of beach fluctuation while the future forecasts also consider cumulative volume change that causes permanent shoreline recession.

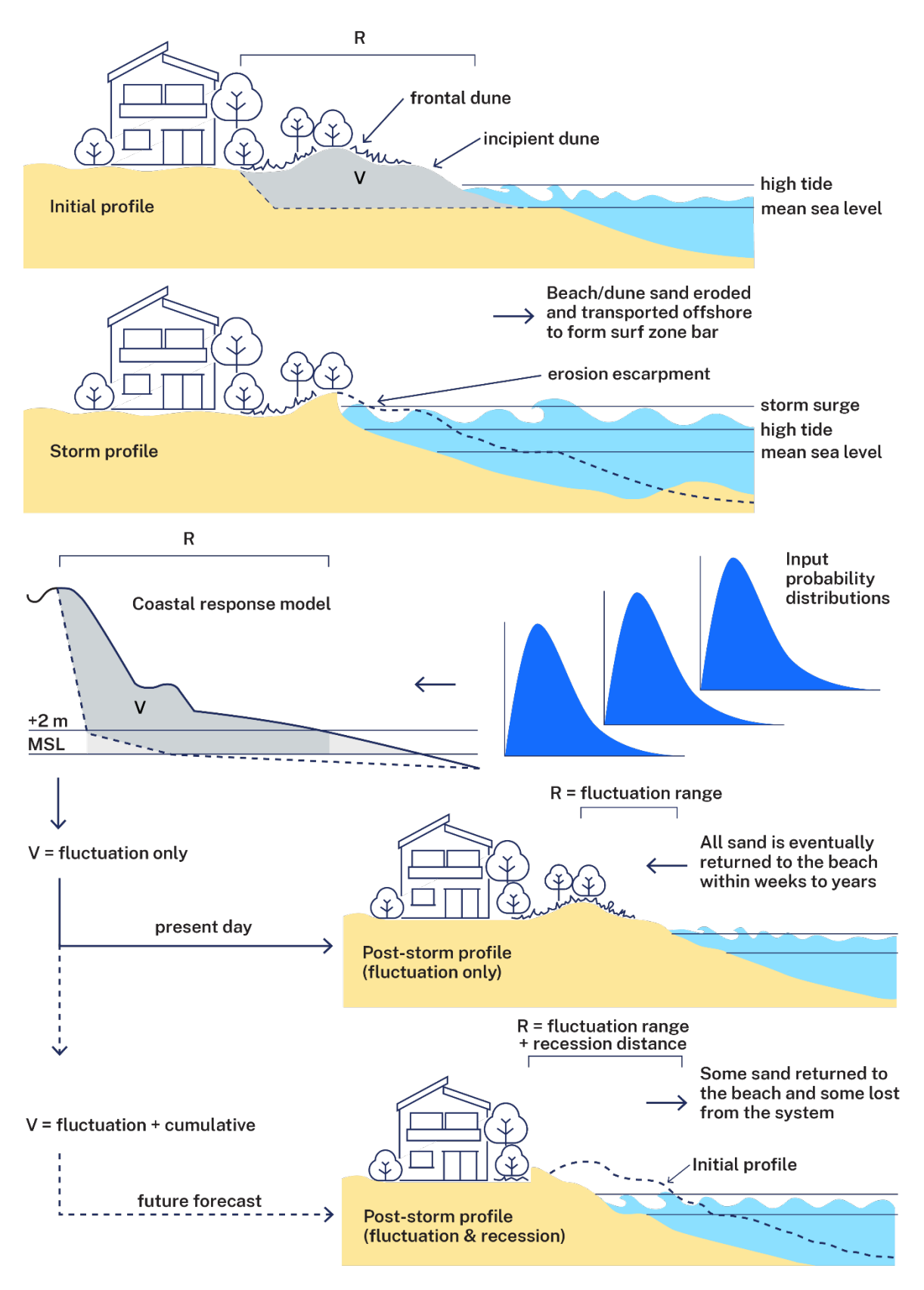


Figure 10 Conceptual diagram of the coastal erosion model used to predict the sediment volume (V) of coastal erosion, converted to the erosion distance (R) using local topography data

Source: Adapted from OEH (2017) and Kinsela et al. (2017).

### Coastal geomorphology

The unique geomorphology of the coastal sediment system forming each NSW beach, both above (beach and dunes) and below (surf zone and shoreface) the water, plays a strong role in how the beach responds to ocean drivers of coastal erosion. The coastal geomorphology includes the form (surface shape and elevation) and composition (sediment, rocks, biological structures) of the coastal system.

Within the scope of modelling coastal erosion into unconsolidated or weakly consolidated coastal sedimentary landforms (beaches, dunes and sand barriers), the distribution and volume of sediment within the coastal system that is erodible and potentially transportable must be known to evaluate the sediment redistribution under different scenarios. Further information on how the onshore and offshore geomorphology of each beach sector was factored into the erosion modelling is contained in Appendix A: Methods.

#### Ocean drivers of coastal erosion

Wave climate, storm surge and SLR are the key oceanic drivers of coastal erosion considered in this assessment. For wave climate, wave runup on beaches saturates the sand and provides the energy to destabilise beach and dune sand, which is then transported offshore by surf-zone currents. Storm surge refers to the temporary rise of coastal sea levels during storm conditions that enable waves to reach further across the beach face, attack and erode sub-aerial parts of the beach and dune system, and overwash low-lying backbeaches (Holman 1986; Nielsen and Hanslow 1991; Atkinson et al. 2017). SLR may influence coastal erosion by advancing the reach of wave attack and altering sediment distribution between coastal geomorphic features (such as the shoreface, beach, dunes and estuaries). In the absence of NSW regional projections of wave climate out to 2150, changing wave climate has not been incorporated into the model. Further information on these drivers and the modelling methods used to account for them are detailed in Appendix A: Methods.

### Modelled components of coastal erosion

Components of coastal erosion including beach fluctuation, sediment budget imbalance and the response to SLR are accounted for in the coastal erosion modelling. Key drivers of beach fluctuation include storm erosion, beach rotation and headland sand bypassing. Sediment budget imbalance can arise from geomorphology of the surrounding coastline, the stabilisation of sediment distribution from sea level change throughout the Holocene, and human coastal interventions such as river entrance training. The influence of sediment budget imbalance on shoreline change trends was investigated using decades of satellite mapping of the shoreline.

The response to SLR refers to gradual long-term sediment-volume loss and shoreline recession of beaches, which is caused by increased water depth and reduced wave-driven transport of sediment at the seabed. This can result in sand transported offshore during storms not fully returning to replenish the beach during calm conditions as it may

have previously. Further information on how components of coastal erosion are accounted for in the modelling are detailed further in Appendix A: Methods.

#### Mapping

Coastal erosion hazard mapping and exposure statistics were prepared for selected exceedance probability levels (50%, 10%, 1%, 0.1%) for the present (2020) and for each of the SSP scenarios considered for forecast years at decadal increments from 2030 to 2150. The mapping dataset comprises the 726 open coast and 32 bay/estuary beach sectors modelled. The individual hazard areas for each beach sector were merged within each primary sediment compartment, resulting in output dataset variants for each compartment. The coastal erosion mapping should be viewed in conjunction with the state-wide bedrock mapping layer for context on beaches that do contain unconsolidated or erodible sediment.

The modelled coastal erosion hazard areas represent the potential extent of erosion for each sea level (SSP) scenario and forecast year, and were mapped for selected exceedance probability levels (50%, 10%, 1% and 0.1%). For example, in Figure 11 the central sector of Wooli Beach shows the total potential erosion hazard zones mapped at different exceedance probability level shoreline positions for the present and future scenarios, depicting the feasible range of coastal erosion for each scenario and shoreline positions corresponding to selected exceedance probabilities.



Figure 11 Coastal erosion mapping for Wooli Beach showing the modelled potential erosion extent at present (2020) and for the SSP3-7.0 scenario in 2090

The present-day (2020) erosion hazard zones include only the beach fluctuation component, which reflects the potential range of temporary variations in the beach—

dune volume and shoreline position that may persist for months to years (<u>Appendix A: Methods</u>). The erosion hazard zones for future projections include beach fluctuation and the shoreline recession and storm or cyclical erosion impact components of coastal erosion, capturing the total beach–dune volume and shoreline position change.

For SSPs 1-2.6, 2-4.5, 3-7.0 and 5-8.5, where beach barriers are predicted to be entirely eroded through to backbarrier estuaries, land areas on the landward side of the estuaries have not been mapped as exposed. This is because the behaviour of coastal sand barriers following breaching or total destruction is complex and beyond the scope of the modelling approach. Foreshore areas on the landward sides of estuaries may be exposed to coastal erosion hazards in such cases, depending on the extent of barrier breaching and overall barrier behaviour alongshore.

For SSP5-8.5 (low-confidence), foreshore areas landward of estuaries that become exposed to ocean processes following barrier breaching are considered exposed, given much higher SLR that would at the least expose such areas to ocean inundation and otherwise enable rapid shoreline transgression. Coastal erosion and estuarine inundation mapping for the relevant SSP scenarios and forecast years should therefore be viewed together, to provide an indicative understanding of compounding erosion and inundation hazards where the present-day coastal morphology may be significantly modified by ocean processes.

### 3.6 Coastal overwash methods

### **Approach**

For the first time in NSW, this study identifies locations of sandy coastline likely to experience coastal overwash due to the combined effects of astronomical tides, storm surge, wave runup and future SLR. State-wide analyses have been undertaken using high-resolution 100-m spaced transects, covering more than 800 km of sandy coastline. Overwash of rocky environments along headlands is excluded from the analyses, as the complex overwash dynamics in these settings require detailed modelling approaches that are not practical on a state-wide level.

Conceptually, coastal overwash occurs when coastal total water level (TWL) exceeds the local backbeach elevation (for example, a dune crest) as shown in <u>Figure 12</u>. This study used coastal *TWL* defined by Serafin et al. (2017) as the addition of still water level (*SWL*) to wave runup (*R*):

TWL = SWL + R

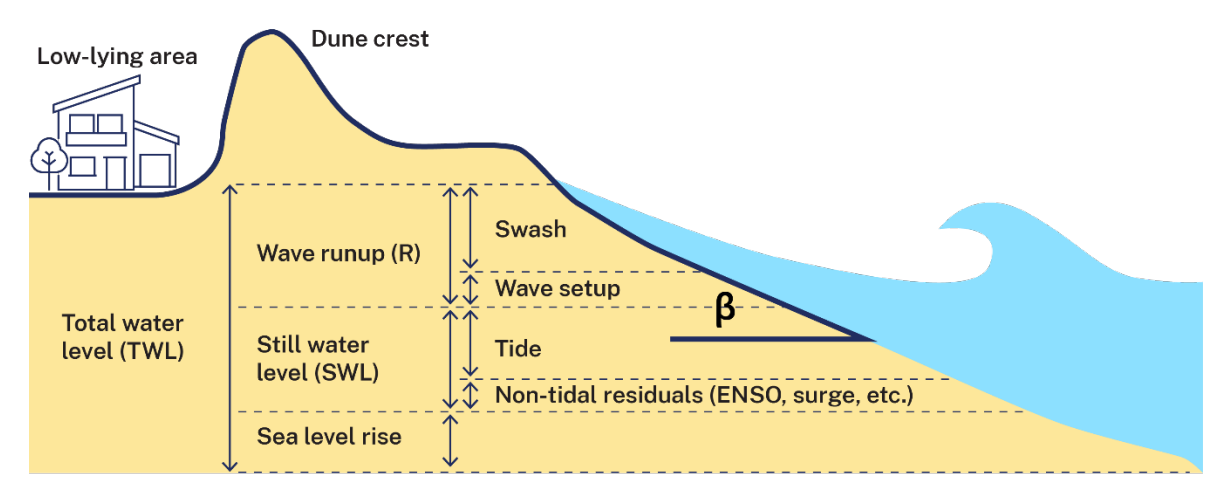


Figure 12 Diagram showing total water level components that contribute to coastal overwash

 $\beta$  = angle of foreshore beach slope; ENSO = El Niño Southern Oscillation.

SWL accounts for variations caused by factors such as astronomical tides and non-tidal residuals (that is, storm surge, coastal trapped waves, El Niño / La Niña effects, Eastern Australian Current, and so on), and can be obtained from ocean tide gauges. Wave runup (R) – the vertical excursion of waves at the shoreline – includes time-averaged (wave setup) and oscillating components of the water line (swash). Runup levels are typically estimated using empirical parametrisations that are forced with wave data and a representative foreshore beach slope  $(\beta)$  (Figure 12). In the future, TWLs will be amplified by rising sea levels (SLR):

$$TWL = SWL + R + SLR$$

Future SLR (as outlined in <u>Section 2.1 (Sea level rise)</u>) will result in increasing TWL which, over time, will result in increasing frequency of overwash in locations subject to inundation now, as well as in new locations that will need to be identified. To identify these locations, this study assessed the current and future likelihood of coastal overwash across a high-resolution spatial domain along the NSW coast. The method employed is summarised in Figure 13 and detailed in the following sections.

Briefly, simulations of historical (1990–2020) TWL at around 8,650 100-m spaced transects were calculated using tide gauges, a novel nearshore wave transformation tool (NSW nearshore wave tool), and site-specific probabilistic beach slope distributions. Probabilistic time series of historical TWL were generated using extreme value analysis (EVA). TWL magnitudes (with confidence bands) for different probability levels were compared to local backbeach inundation thresholds (for example, dune crest, seawall crest) to identify the likelihood of current overwash. Results are summarised in a simple traffic-light approach (cyan meaning likely overwash, green potential overwash, and blue unlikely overwash). Future overwash likelihoods were incorporated into the analysis using probability distributions of SLR, following a Monte Carlo approach.

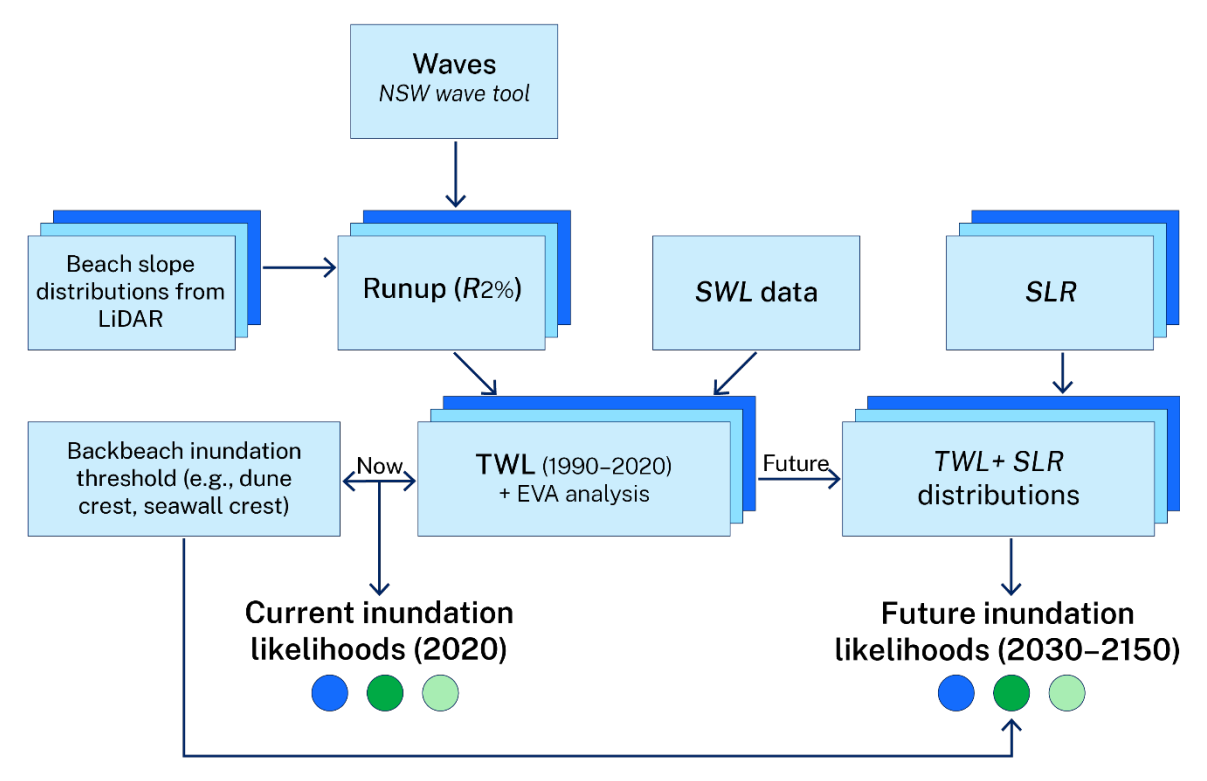


Figure 13 Coastal overwash hazard methodology at the transect scale (100-m spaced transects)

#### Current inundation likelihoods

#### Historical total water level time series

Total water level time series (TWL = SWL + R) were calculated over the 1990–2020 period using data from ocean tide gauges and the Atkinson et al. (2017) runup formula (Appendix D). To provide a broad range of probable historical total water levels, runup time series (R) were calculated 1,000 times (n) using ensemble members from randomly generated beach slope distributions (Appendix A: Methods). This resulted in 1,000 TWL time series – per transect – that reflect the local to regional variability in TWL from varying beach slopes and wave conditions in NSW. A sensitivity analysis to determine the adequate number of ensembles (n) is presented in Appendix E: Coastal overwash ensembles. Briefly, this analysis showed that using more ensemble members (n > 1,000) resulted in no improved modelling accuracy, while less than 1,000 members resulted in under-sampling issues.

#### Extreme value analysis

EVA of historical TWL was performed to determine expected TWL magnitudes for different annual exceedance probability (AEP) levels. Following existing EVA assessments of deepwater wave data in NSW (e.g. Shand et al. 2011), generalised extreme value distributions were fitted to yearly TWL maxima. EVA was repeated 1,000 times (n) per transect, providing TWL magnitudes for different AEPs (1%, 5%, 20%, 100%) and confidence bands, which were obtained empirically from the associated ensemble members.

#### Backbeach inundation thresholds

Conceptually, coastal overwash and inundation occurs when TWLs exceed a local backbeach inundation threshold (such as a dune crest, as shown in Figure 12). Selecting appropriate thresholds is essential to determine the likelihoods of coastal overwash. Each transect was first classified into 1 of 4 backbeach archetypes describing the feature located behind the active beach and the position of the backbeach inundation threshold. This includes dunes, ICOLLs, cliffs and structures classified using LiDAR data (further detailed in Appendix A: Methods). It was pragmatically assumed that the elevation of these thresholds remains unchanged over time, which represents a potential limitation of the approach. The potential future evolution of these systems, particularly for dunes and berms at lagoon entrances, is beyond the scope of this analysis.

#### Overwash likelihoods – traffic-light approach

To determine coastal overwash likelihoods, TWL exceedance levels for different AEP levels (for example, 1% AEP) were compared with local backbeach inundation thresholds (for example, a dune crest) and classified into 1 of 3 likelihoods. In this classification:

- the upper limit of the likely TWL range (83rd percentile) defines instances of likely overwash
- less likely to extreme TWL range (83rd to 99th percentile) defines potential overwash
- less likely extreme TWL occurrences (99th percentile) mark the limit where overwash likelihoods shift from potential to unlikely.

<u>Figure 14</u>(a) and (b) illustrates this classification for a 1% AEP TWL distribution. Here, the elevation of some local backbeach inundation threshold compared with TWL distribution falls between the 83rd and 99th percentiles of the 1% AEP TWL distribution, suggesting that this transect is currently experiencing potential overwash.

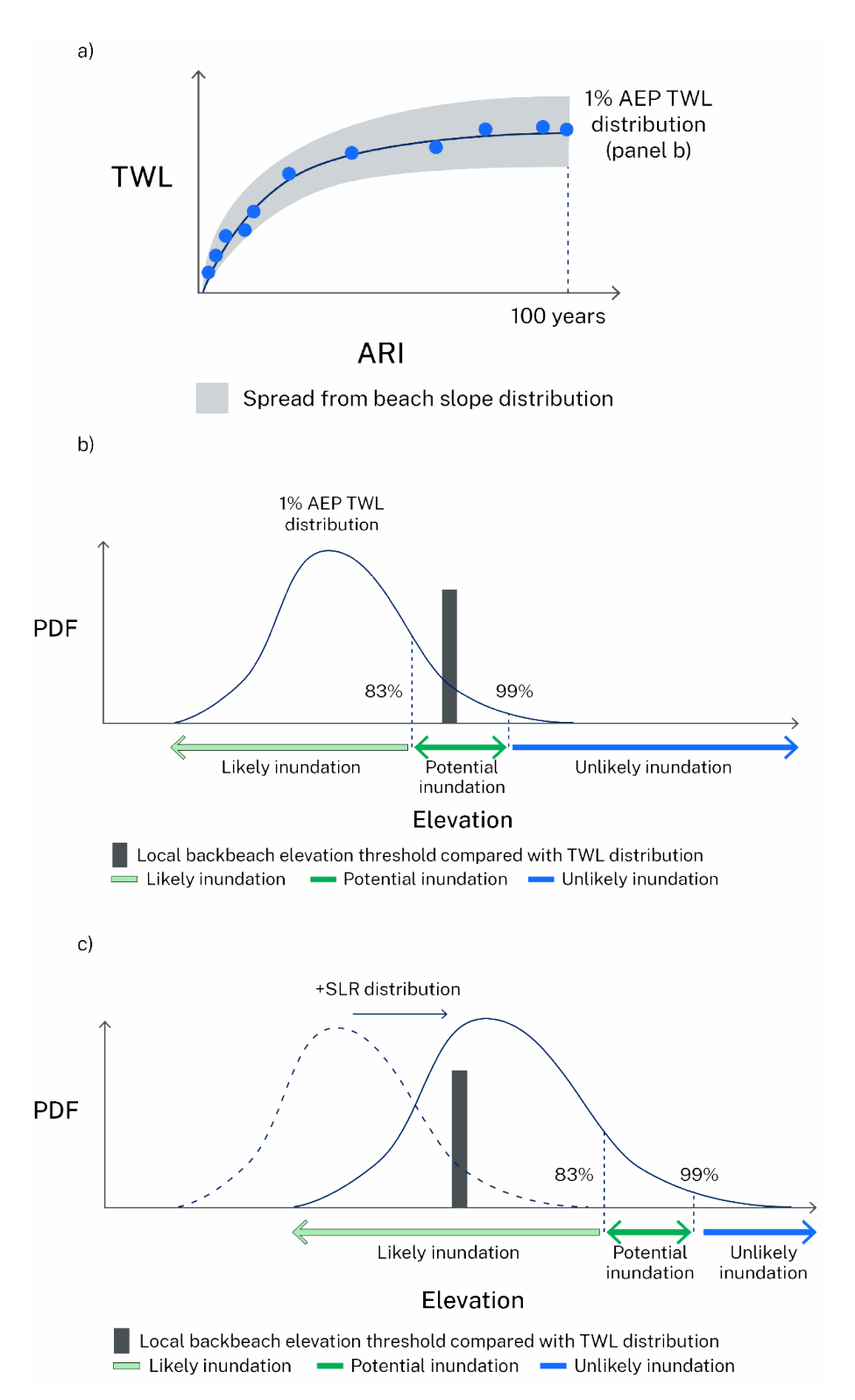


Figure 14 Diagram describing the transect-based overwash likelihood scale (shown as inundation) used in this study. (a) Extreme value analysis (EVA) of total water level (TWL) time series using block maxima (1990–2020). The distribution of the 1% annual exceedance probability (AEP) (100-year) TWL is used in (b) to define the overwash impacts based on percentiles and local backbeach inundation thresholds. (c) The method is repeated for future scenarios, where SLR distributions are now added to the original TWL distribution on a Monte-Carlo basis

#### Data

This assessment incorporated several datasets into the modelling approach for coastal overwash. The NSW sandy coastline was discretised into 100-m shore-normal transects along plan view shorelines representative of the mean high-water line (Smartline dataset, Hazelwood 2009). In total, 8,649 *major* transects were generated, covering 546 open coast sandy beaches. Additionally, a higher resolution 10-m spaced *minor* transect dataset was generated for higher-resolution beach slope calculations using LiDAR datasets.

Historical SWL datasets were obtained from Viola et al. (2021) for 5 ocean tide gauges. Data from 1990 to 2020 were selected due to data gaps before 1990 and adjusted to 2020 such that long-term trends were removed. Each 100-m spaced transect was assigned to the nearest tidal gauge location. Beach slope distributions were derived from available LiDAR topographic datasets to calculate probabilistic runup (*R*) contributions to TWL. Beach slopes were estimated from cross-shore profiles using linear regression of the profile data between the berm crest (around 2 m AHD: Kinsela et al. 2017) and mean sea level (around 0 m AHD) (that is, the foreshore slope).

To account for nearshore wave modifications and the sheltering effects of headlands, a novel high-resolution nearshore wave tool (NSW nearshore wave tool) was employed to transfer offshore wave data to the 10-m contour, every 250 m of coastline. This tool is based on a WAVEWATCHIII model forced by ERA5 wind fields (Hersbach et al. 2020). Calibration of the model was performed against existing offshore wave buoy data and more recent yearly deployments of inshore wave data from SOFAR Spotter buoys spanning more than 10 locations across NSW (Kinsela et al. 2024). Further information on the datasets and the rationale for using them are detailed in Appendix A: Methods.

### Runup model selection

Numerous wave runup formulas for sandy coastlines have been developed over the past few decades (da Silva et al. 2020). These formulas typically estimate the elevation exceeded by 2% of the waves over some period, typically one hour ( $R_{2\%}$ ) using deep water wave data ( $H_0$ ,  $L_0$ ) and the foreshore beach slope ( $\beta$ ). To evaluate the accuracy and applicability of several runup models using long-term average beach slopes derived from LiDAR, a regional scale dataset of storm runup debris line was used (Shoalhaven Heads to Newcastle) over 4 storm events between October 2014 and July 2020. Evaluation of 7 runup models was completed. The runup model proposed by Atkinson et al. (2017) was selected because it had the lowest root mean square error and bias. Further information on the runup model evaluation and selection is presented in Appendix A: Methods and Appendix D: Runup formula selection.

### Future overwash likelihoods

Estimating future coastal overwash likelihoods was performed similarly to present conditions. Distributions of historical extreme value TWL (for example, Figure 14(b)) were combined with SLR distributions (n = 1,000 ensemble members), following a Monte Carlo type approach (Figure 14(c)) and compared with backbeach inundation thresholds.

In the previous example, a transect classified as having *potential overwash* would experience *likely overwash* impacts in the future. Underlying assumptions of this approach include wave and SWL stationarity (that is, no change to the wave climate, storm surge and tide range due to climate change and SLR), as well as unchanged backbeach elevation.

### Results and mapping

Analyses were performed at the state-wide level (8,649 transects) for present (1990 to 2020) and future (2030 to 2150) conditions, considering several scenarios at decadal timeframes. Initially a state-wide picture of current overwash likelihoods, followed by regional (that is, primary sediment compartments: see <a href="Section 2.1">Section 2.1</a> 'Geomorphic setting'; Thom et al. 2018) and local-scale examples, are provided. Then, similar results are presented for future conditions.

Coastal overwash is a temporary process potentially driving localised coastal inundation adjacent to areas of overtopping. As such, it is not appropriate to map areas of coastal inundation using a static 'bathtub' approach, as is commonly performed in tide-only inundation studies. This first-pass study provides mapping output with the location of 100-m spaced transects and corresponding overwash likelihood only, highlighting locations that are likely experiencing coastal overwash both now and into the future.

### 3.7 Estuarine inundation methods

### Hazard overview

Previous studies have shown that extensive development adjacent to NSW estuaries is exposed to potential inundation as sea levels rise (OEH 2018; Hanslow et al. 2018; Section 2.2 'Some examples of overwash and associated inundation on the NSW coast are shown in Figure 6. Here we show damage following the June 2016 east coast low to the Clan Motel adjacent to Terrigal Lagoon (Figure 6(a)) and the surf club roller doors at Terrigal Beach (Figure 6(b)).

Given the evidence of coastal overwash from recent storms in NSW, it is now pertinent to apply a consistent state-wide approach to identify areas of current and potential future overwash risk.

Estuarine inundation hazards'). These sites are mostly located in the lower reaches of estuaries (Hanslow et al. 2019).

The approach is focused on addressing the chronic aspects of estuarine inundation, examining water levels at annual exceedance levels and below. Effects of rainfall-related flooding were removed, as more detailed modelling is required to assess the effects of SLR on flood-related processes (that is, they cannot simply be combined because changes in sea level will affect flood wave propagation further upstream).

# **Approach**

This study adopts an intermediate complexity approach to modelling and mapping water levels within estuaries. It is based primarily on the use of measured data from

individual tide gauges and uses a water surface fitting method which allows for variation in water levels both between and within individual estuaries. The method improves on simple 'bathtub' approaches used in previous national assessments but is less complex than hydrodynamic modelling for each estuary. To improve communication of current inundation frequency, this study adopted a daily water level exceedance approach, rather than relying on astronomic tidal planes as used in the previous NSW state-wide estuary tidal inundation exposure assessment (OEH 2018; Hanslow et al. 2018).

Daily maximum frequency distributions derived from water-level gauge data for 96 estuaries (MHL 2019) were used to represent current estuarine water levels. In ungauged estuaries, data from similar nearby estuaries were used, while for ICOLLs, an averaged exceedance distribution was applied, scaled according to measured berm elevation.

Potential future water levels were calculated at decadal intervals for each SLR scenario by adding SLR randomly sampled from each of the log normal distributions outlined in <a href="Appendix A: Methods">Appendix A: Methods</a>. In estuaries with available hydrodynamic models, potential changes to high tides were considered, associated with changes to tide dynamics as sea levels rise.

The water surface fitting method used an interpolated water level surface created from the gauge data. These water level surfaces were overlaid on digital elevation models derived from high-resolution LiDAR elevation data. The resulting spatial model of inundation improves on the representation of current inundation hazard extent and allows for improved assessment of the inundation hazard associated with potential SLR.

#### Data

#### **Current water levels**

The estuarine inundation modelling used tide gauge data and the best available data for each estuary catchment for terrain and elevation. Water levels across 96 NSW estuaries were recorded at approximately 213 gauge locations within the tidally influenced parts of the estuaries (MHL 2019; Appendix F: NSW estuarine tidal water level gauges). This includes data from 8 tide gauges that are considered fully representative of the ocean tides along the NSW coast including Coffs Harbour, Crowdy Head, Shoal Bay, Patonga, Sydney, Jervis Bay, Ulladulla and Eden (Table 9).

Linear detrending was applied to water level data to remove the effects of SLR and ensure water levels are adjusted to be representative of 2020, while still retaining interannual variability in the data. Water levels in the upstream reaches of many estuaries are often influenced by terrestrial floods, which can have considerable impacts, even at an annual recurrence interval basis. To remove these effects, a threshold method following Palmer et al. (2024) which defines flood event thresholds and removes flood events from the time series was implemented. Further information on the data used and post-processing methods applied are detailed in Appendix A: Methods.

Post-processed records were then used to calculate a set of empirical cumulative density functions (ECDFs) of daily maximum water levels. Exceedance statistics were extracted from these ECDFs, for current water levels for 4 frequencies: 1 day/year (annually exceeded), 3.6 days/year (~1% of days exceeded), 36.5 days/year (~10% of days exceeded), and 182.5 days/year (~50% of days exceeded). Water levels vary by estuary type and Figure 15 provides some examples of this variation. Drowned river valley estuaries, such as the Hawkesbury River, exhibit tidal amplification. Tidal lake estuaries, represented by Lake Macquarie, exhibit significant tidal attenuation. Riverine estuaries, such as the Tweed River, show initial tidal attenuation followed by amplification, while ICOLLs such as Lake Wollumboola exhibit a broader range of water levels owing to elevated berm levels.

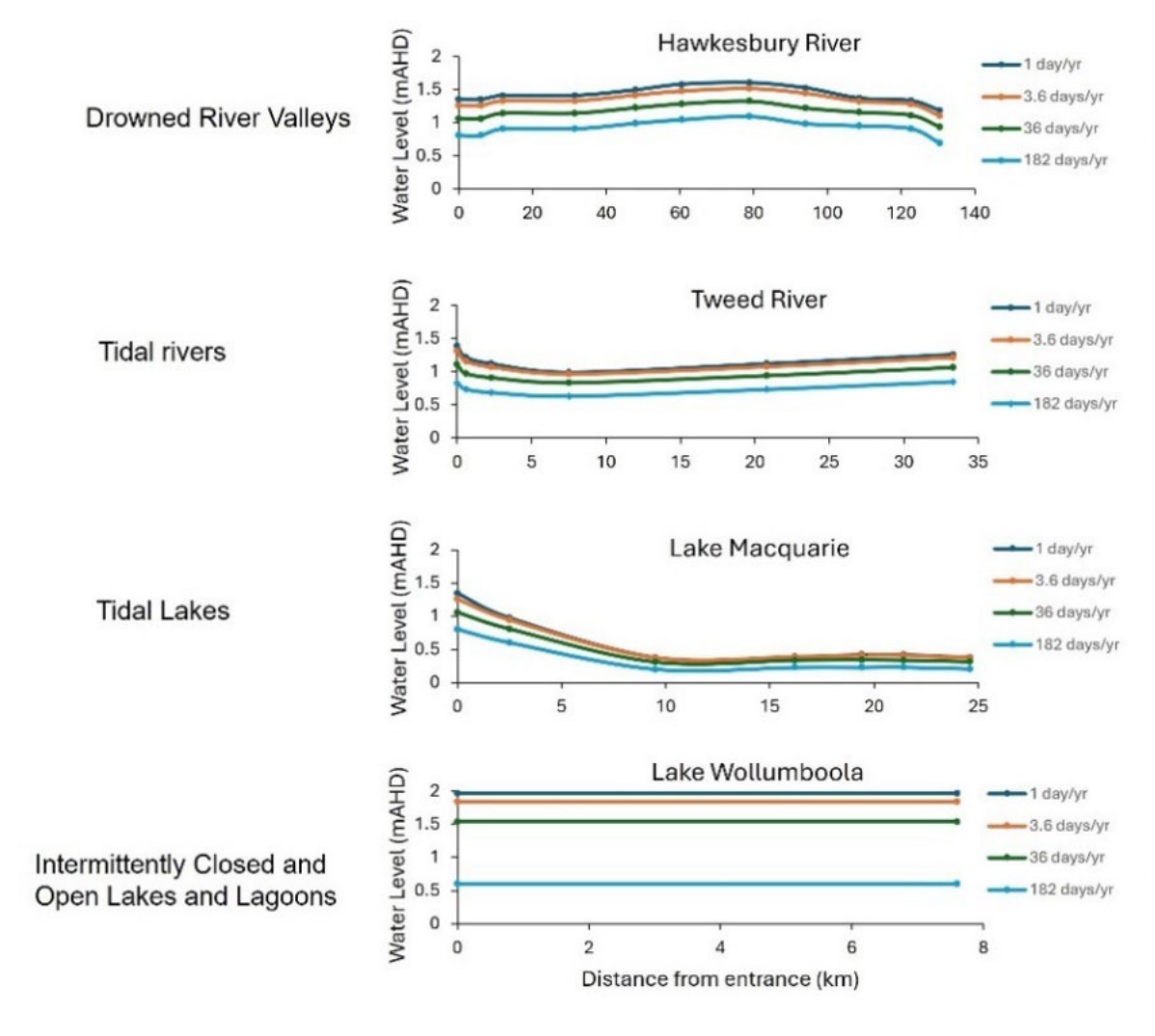


Figure 15 Examples of water levels representing different annual exceedance frequencies and how tidal amplification and attenuation can vary with distance from estuary entrance and in different estuary types

Nearby gauged estuaries of the same type (excluding non-gauged ICOLLs, referred to as NGIs) were selected as proxies for the 13 NSW estuaries without water level gauge data. Virtual gauge locations were chosen in each, based on the scaled distance from

the estuary entrance of the gauges in the proxy estuary, with the appropriate ECDF assigned to each. The extraction of exceedance statistics then proceeded as for gauged estuaries.

For NGIs, a method similar to that used in the first NSW state-wide estuary tidal inundation exposure assessment (OEH 2018) was implemented. In this case, generic non-dimensional ECDFs were determined using water level records from all ICOLLs with gauge data. These non-dimensional ECDFs were then scaled for each NGI using the maximum berm height as the maximum water level. Berm heights for each NGI were obtained from available LiDAR and survey data. As with other non-gauged estuaries, virtual gauge locations were chosen within each NGI to enable mapping of the exceedance levels.

All these data were compiled into a state-wide water level information database for use in the geographic information system (GIS) water surface modelling.

#### Future water levels

As outlined in <u>Section 3.4</u>, probability distributions are used to account for uncertainty in SLR for each scenario and timeframe. To obtain water level ECDFs for each future scenario and timeframe, the probability distributions were randomly sampled and added to current water level records. In addition, to account for potential changes in the tidal dynamics under SLR, an amplification/dampening factor (see below) was applied for the 12 modelled estuaries.

### Potential changes to tides

To accommodate potential future changes to tides (amplification, dampening, or a mix of both), detailed hydrodynamic modelling for selected estuaries was used. The primary aim was to formulate a factor that considers the interaction of SLR and tidal processes within different estuary types. This amplification/dampening factor uses positive values denoting a rise in maximum water levels and negative values denoting a reduction in maximum water levels under an SLR scenario.

A set of pre-existing calibrated hydrodynamic models was used for 12 estuaries in NSW to explore the potential impacts of various SLR scenarios on their longitudinal maximum water levels. A list of these models together with the references related to the model creation and calibration and their state-wide geographical distribution are presented in <u>Table 10</u>. Further information on how the hydrodynamic models were incorporated to formulate an amplification/dampening factor is also in <u>Appendix A: Methods</u>.

### Mapping

To map the extent of inundation within the NSW estuaries, a GIS-based model was developed, consisting of 2 main parts: the water surface model and the inundation model. This model uses QGIS (QGIS Development Team 2023) and Arc Desktop geoprocessing and spatial analysis functions (ESRI 2021). A flow chart outlining the structure of the estuarine inundation mapping model is shown in Figure 16.

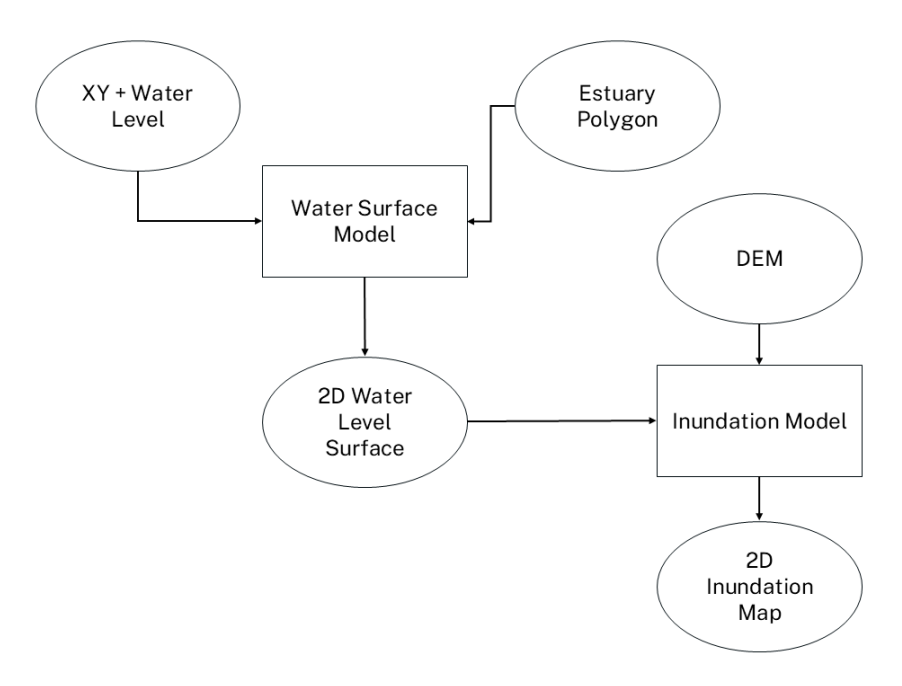


Figure 16 Flow chart showing simplified structure of the GIS-based estuarine inundation model

#### Water surface model

The GIS-based water surface model was used to generate an estuary wide 2-dimensional (2D) water level surface (WLS) analogously to the method outlined in Foulsham et al. (2012). In this study, the water levels are based on frequency of occurrence rather than harmonic tidal planes. For a given estuary, the water level information was extracted from the water level information database, which includes both ocean tide and estuary gauge water levels, as well as the tidal limit locations. Further information on the WLS model is detailed in Appendix A: Methods.

#### **Inundation model**

The WLS created using the water surface model was then used as one of the inputs to the GIS-based inundation model which estimates the spatial extent of estuarine inundation for a given estuary. A digital elevation model (DEM) of the estuary catchment is compiled from available data and constrained to elevations below 10 m AHD (Appendix A: Methods). The WLS was then spatially joined to the DEM, and the inundation status was calculated by assessing whether the WLS height is higher or lower than the elevation at each data point, producing a raw estuarine inundation polygon layer. Non-connected low-lying areas of inundation are differentiated from connected areas, although infrastructure may connect non-connected areas in reality. There were no state-wide data available to identify drainage connectivity. This process results in 2 polygon layers for each model run, the primary (connected) and isolated inundation polygon layers.

The final map layer outputs include 2 polygon layers of inundation extent associated with current and potential future scenarios (1 day/year (annual), 3.6 days/year (1%), 36 days/year (10%), and 182 days/year (50%)) at decadal intervals from 2020 to 2150 for

each SSP. The exception is low-confidence SSP5-8.5, where only the 2 lower inundation frequencies (36 days/year (10%) and 182 days/year (50%)) were mapped for the latter years, owing to limitations in the DEMs.

### 3.8 Exposure

### Approach to generating exposure statistics

To estimate the numbers and area of assets potentially impacted by inundation and erosion along the NSW coast, GIS processing in Python and in ArcGIS version 10.8.2 (ESRI 2021) was used to overlay and intersect generated hazard layers with existing asset layers. For each estuary and beach, counts, areas and lengths of assets exposed to inundation and erosion were generated by overlaying and intersecting hazard polygons with raster and polygon asset layers. Exposure to inundation and erosion can be examined as totals for NSW and by beach or estuary. Methods for calculating counts and areas vary according to asset type, which are detailed in Appendix A: Methods.

For erosion hazards, the hazard areas extend landward from the baseline beach berm position (adopted as the 2 m AHD position) for an accreted beach state, up to the inland extent of erosion predicted for each SLR scenario. Each combination of forecast horizon, SLR scenario and probability level produces a unique hazard area reflecting future shoreline changes due to coastal erosion.

For estuarine inundation hazards, 4 series of statistics are reported for the intersecting inundation hazard and asset features for each estuary and SLR scenario. These statistics represent combined primary and isolated estuarine inundation extents for inundation that would be exceeded under the following conditions: 182.5 days/year (50%), 36.5 days/year (10%), 3.6 days/year (1%) and 1 day/year (annual).

#### Data

Data for building footprints, transport infrastructure, Aboriginal heritage assets and critical infrastructure were incorporated into the exposure analysis. Building footprints were acquired from the *Geoscape buildings* product (Geoscape Australia 2023), a commercial dataset updated quarterly. Buildings include single residences, multidwelling complexes, non-residential structures, garages, and any other outbuildings with a footprint larger than 9  $\text{m}^2$ . Where the exposure of a building to either estuarine inundation or coastal erosion was less than 5  $\text{m}^2$ , it was classed as nuisance exposure and was excluded from building and address counts.

Road and rail segments are vector data sourced from the Transport Theme of the NSW Government <u>Spatial collaboration portal</u>. The statistics generated for transport infrastructure exposure to hazard extents include the lengths of road and rail segments, counts of airports, and lengths of runways.

Statistics on the number of Aboriginal cultural heritage sites were obtained from the Aboriginal heritage information system (OEH n.d.), which is a point dataset.

Statistics on critical infrastructure were derived from vector data available on the NSW Government *Spatial collaboration portal*. Critical infrastructure statistics were

generated for school and university facilities; hospitals; correctional centre and courthouse facilities; and emergency services assets, including police, fire and State Emergency Services stations.

All asset data are based solely on current information. When considering future timeframes, the results reflect exposure to only the currently known assets. No provision is made for future assets that may be built or established within the hazard areas.

# 4. Results

Results are presented for the medium-confidence scenarios SSP1-2.6, SSP2-4.5 and SSP3-7.0 as primary storylines representing low emission, medium emission and high emission pathways, respectively, for future climate projections. To provide a complete picture of potential sea level rise (SLR) impacts for decision-makers and stakeholders with low risk tolerance, findings for medium-confidence SSP5-8.5 and low-confidence SSP5-8.5 scenarios representing very high emission pathways are also included, with more detailed information provided in <u>Appendix G</u> for coastal erosion, <u>Appendix H</u> for coastal overwash, and <u>Appendix I</u> for estuarine inundation. By examining this comprehensive range of scenarios, decision-makers can account for varying levels of risk, ensuring that management strategies are resilient not only to more likely outcomes but also to less probable, yet more severe, impacts. This approach supports the development of flexible, adaptive management solutions that address long-term uncertainties and help mitigate the vulnerability of communities, key assets and ecosystems.

For each future SLR scenario and each decade, the hazard modelling was repeated with different input values, leading to a distribution of hazard projections within the combined range of uncertainty. The hazard projections distribution can be presented as either a probability density function or an empirical cumulative density function. Key hazard projections of interest were extracted and can be expressed as percentiles of the ECDF, cumulative probabilities, or probabilities of exceedance. For example, the 90th percentile of the ECDF of hazard projections can be interpreted as a (cumulative) probability that 90% of the hazard projections were less than that value. It is also true that 10% of the hazard projections exceeded that value, which can be expressed as the 10% probability of exceedance (or exceedance probability).

### 4.1 Coastal erosion

### **Erosion potential**

Coastal erosion hazards were investigated for 336 open coast beaches in NSW, modelled as 726 individual beach sectors, representing 90% of the state's sandy shorelines (Figure 17). Additionally, 32 beaches located in estuaries and bays that are directly exposed to ocean wave processes were also modelled as a separate case study, bringing the total number of beaches modelled to 368, comprising 758 individual beach sectors (see Table 18 for present-day exposure statistics).

Each modelled beach sector is characterised by distinct onshore and offshore geomorphology, underlying trends evident in historical data, exposure to wave processes and storm impacts, and response to SLR (<u>Appendix A.3 Coastal erosion methods</u>). The higher proportions of beaches not modelled in some compartments (<u>Figure 17</u>) reflect the large number of small, bedrock-backed pocket beaches in those compartments. The proportions of open coast beach shorelines by length that were modelled show that more than 75% in each compartment have potentially erodible

backshores, totalling 90% along the NSW's sandy coastline (<u>Figure 17</u>). While all NSW beaches may experience erosion, those with hard (non-erodible) backshore geomorphology that were not modelled may narrow and potentially disappear with SLR, although assessing this was beyond the scope of this study.

The modelled coastal erosion hazard areas represent the potential extent of erosion for each SSP scenario and projected year, and were mapped for selected probability of exceedance levels of the hazard projections distribution (50%, 10%, 1% and 0.1%), as shown in <u>Figure 11</u>. The erosion hazard distance is measured as the distance landward from the baseline of each beach sector, which represents the most accreted shoreline or berm position (2 m AHD contour). The erosion distance corresponds to the location of the crest of a slumped dune scarp following erosion (see <u>Appendix A: Methods</u>).

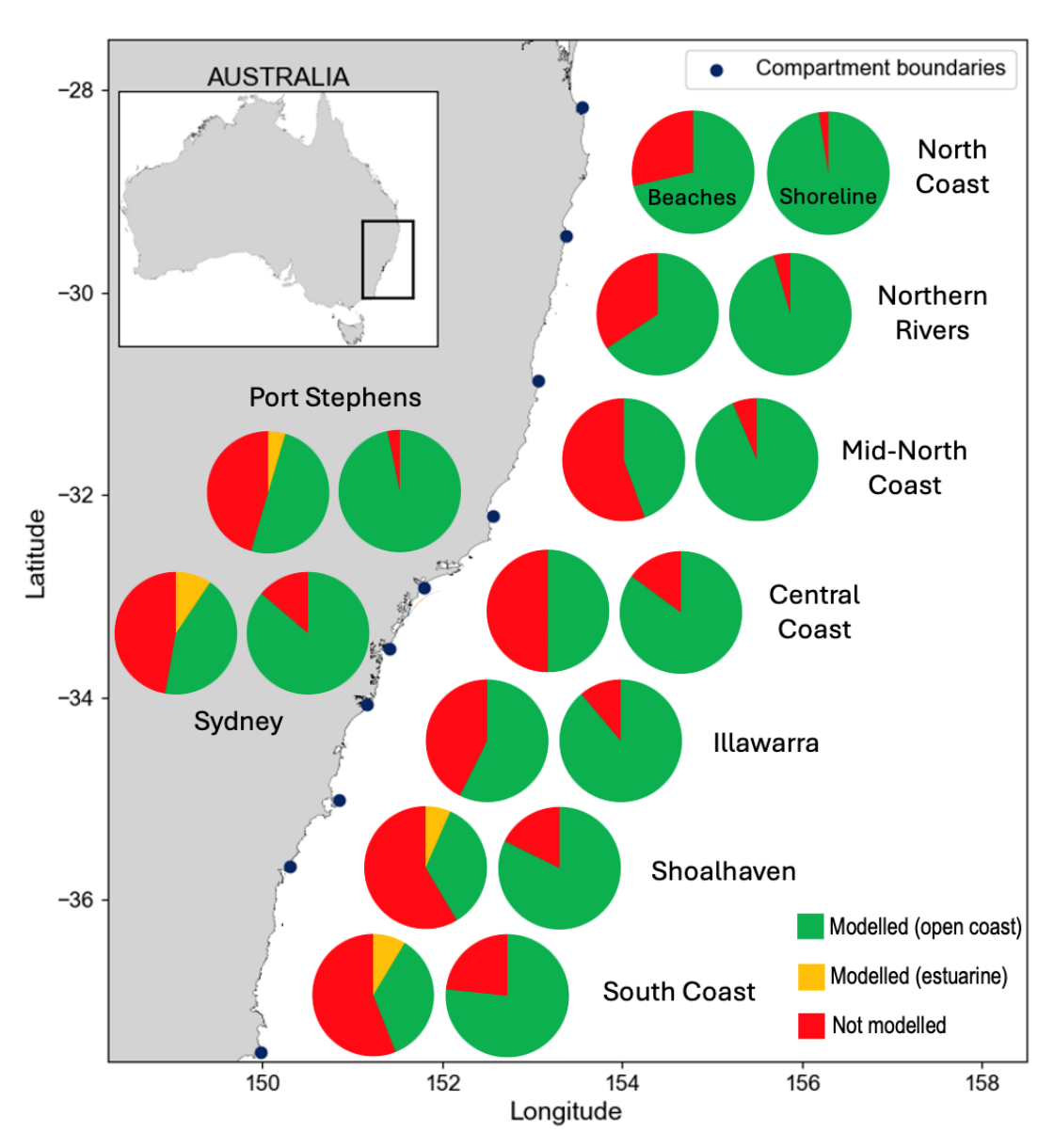


Figure 17 Proportion of open coast and bay/estuarine beaches (by count) and beach shorelines (by length) for which erosion modelling was carried out in each compartment

Erosion distances for all modelled open coast beach sectors within each primary compartment at the 1% exceedance probability level of the hazard projections distribution under the SSP3-7.0 scenario are shown as box plots for the present (2020, Figure 18(a)) and for 2050 (Figure 18(b)), 2100 (Figure 18(c)) and 2150 (Figure 18(d)). Present median erosion distances were 60–65 m, with upper ranges extending to 80–90 m. For future forecasts, modelled erosion distances increased over time due to rising sea levels under all scenarios, as seen for SSP3-7.0 in 2050, 2100 and 2150. In all cases, the increase in modelled erosion during the latter third of forecasts (2100–2150) was greater than in earlier periods, due to the increased influence of SLR on coastal sediment systems. This is evident in the relative change in erosion distances from 2100 to 2150 when compared with the change from 2050 to 2100. This indicates that based on the SSP scenarios considered, the reach of coastal erosion hazards will continue to advance, potentially at increasing rates.

The modelled erosion distances for each forecast year also vary between the SSP scenarios due to different SLR projections (<u>Appendix A.2 Sea level rise</u>), as shown in box plots for all modelled beach sectors within each compartment at the 1% exceedance probability level in 2100 for medium-confidence SSP1-2.6, SSP2-4.5, SSP3-7.0 scenarios (Figure 19).

Figure 18 and Figure 19 summarise the differences in erosion hazard distances between and within compartments, reflecting the distinct coastal geomorphology of the regions and individual beaches. Although a detailed analysis of these relationships is beyond the scope of this study, it is evident, for example, that regions characterised by expansive low-lying coastal sediment plains and gently sloping coastal profiles (such as compartments nsw01, nsw02 and nsw03) have a greater likelihood of larger erosion distances than regions with greater bedrock presence in the coastal zone and steeper coastal profiles. However, the overlap in the full percentile ranges and outliers between regions emphasises the diversity of coastal geomorphology and exposure to coastal erosion at a local scale, highlighting the importance of accounting for site-specific factors in modelling the coastal responses to projected SLR.

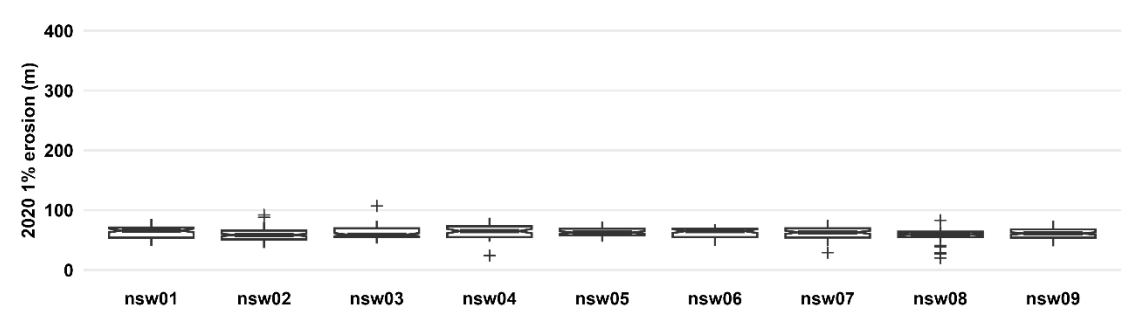
The increased number of outliers for forecasts with higher SLR (that is, later forecast years or higher emissions scenarios, or both) suggests that, at some point, the barrier-dunes of many beach sectors, which developed during the prolonged and comparatively stable Holocene period, may be entirely overwhelmed or breached by erosion, exposing low-lying backbarrier plains to ocean processes. In such cases, shoreline recession may proceed much more rapidly. The complexities of modelling such cases at the scale of this study are discussed in Section 5.2: Coastal erosion. Despite these complexities, the outlier erosion distances indicate the potential magnitude difference in coastal response following the (majority) breaching of a barrier-dune.

Due to the limitations in modelling bay and estuary beaches (for example, simplified treatment of sediment dynamics and exclusion of overtopping and estuarine inundation), these areas have been excluded from the exposure assessment presented below. As such, the statistics and figures reported for infrastructure and heritage sites exposed to coastal erosion do not capture potential impacts in bay and estuary settings.

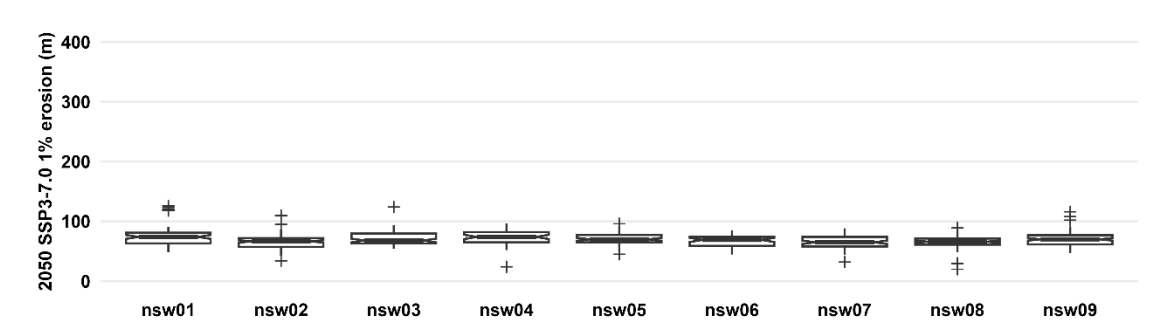
Further, exposure to coastal erosion is also based on the assumption that no engineered coastal protection is in place, meaning the exposure results represent a scenario of natural shoreline response without any control or prevention.

An approximately 2.5 km contour from the shoreline was used to clip all asset inputs for the coastal erosion exposure statistics assessment. Regarding buildings exposure, structures without an assigned address were excluded to reduce false positives, though secondary structures (for example, sheds, water tanks, carports) at locations with an assigned address remain in the dataset. Because several building categories (for example, residential, commercial, recreational, community use) were considered, the building exposure results presented do not represent major residential buildings only. Further, for the buildings exposure analysis, only buildings projected to experience more than 5 m² of erosion were included in the results. Other building exposure assessment approaches may select and utilise available data differently and for distinct purposes, leading to varying outcomes depending on their filtering processes, underlying assumptions, specific focus, and other methodological or contextual factors.

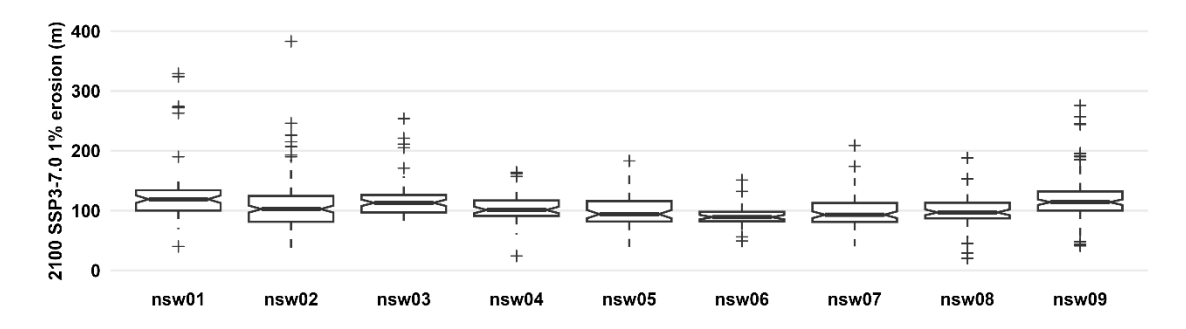












d.

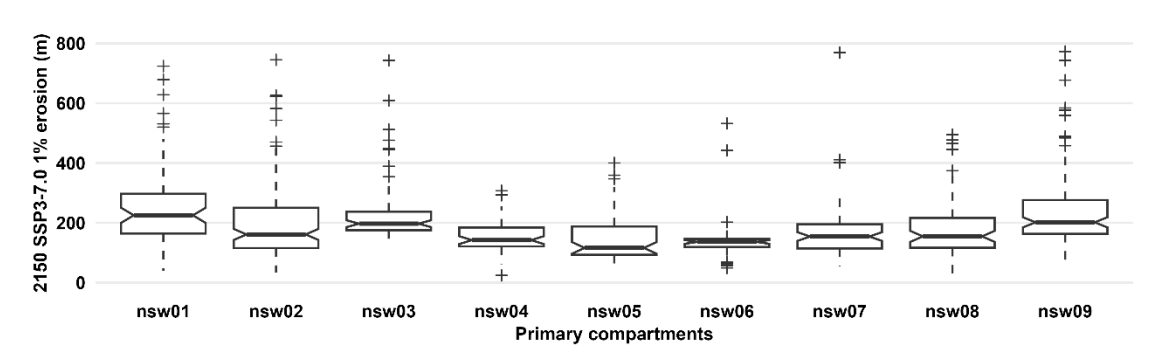
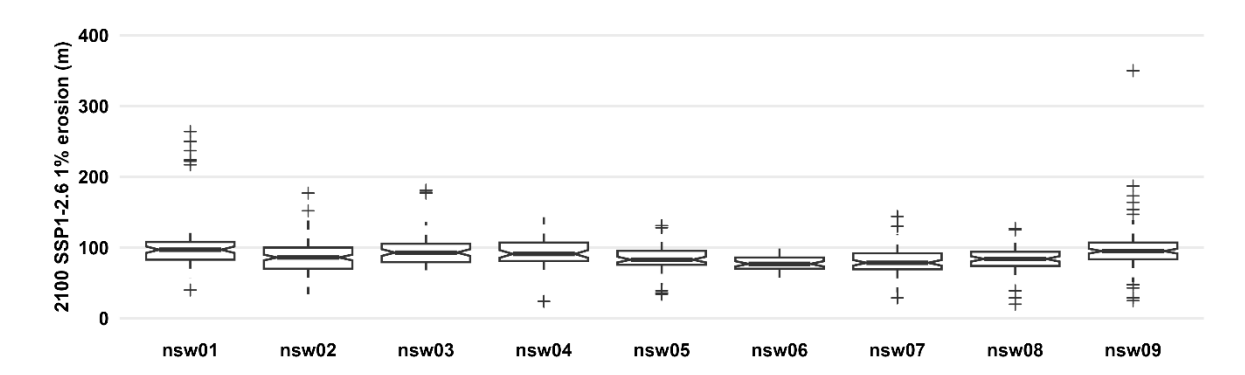


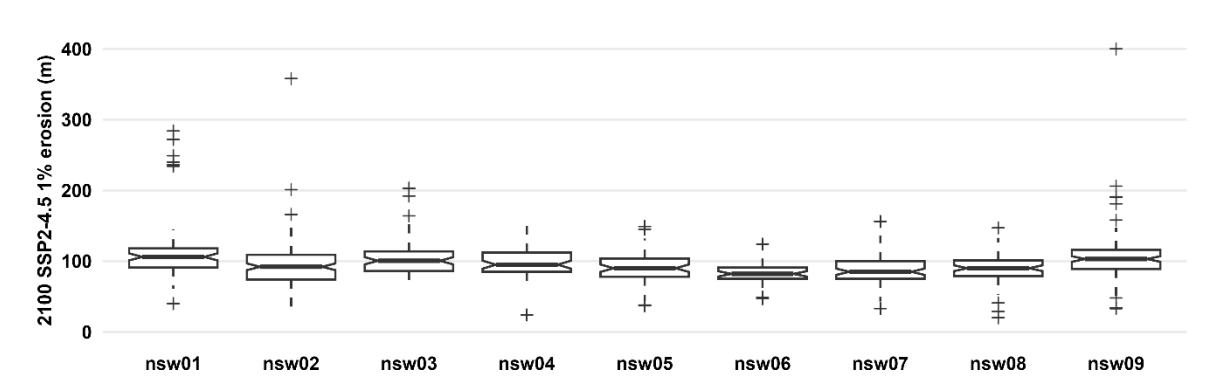
Figure 18 Box plots summarising the modelled shoreline erosion distances in each primary sediment compartment at the 1% exceedance probability level at (a) present (2020) conditions, and for SSP3-7.0 sea level scenario at (b) 2050, (c) 2100 and (d) 2150

Note: The y-axis scales differ and may have been limited for illustrative clarity.

a.



b.



c.

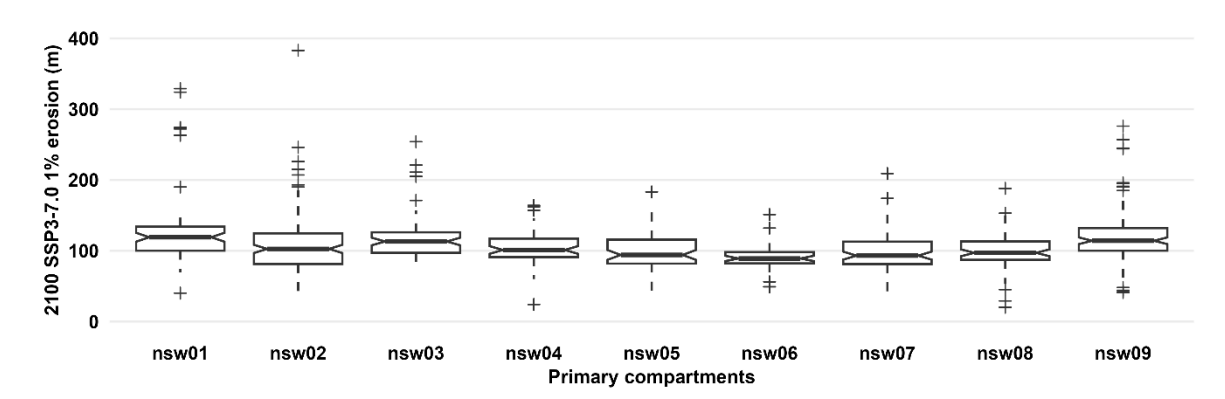


Figure 19 Box plots summarising modelled shoreline erosion distances at the 1% exceedance probability level at 2100 for the (a) SSP1-2.6, (b) SSP2-4.5, and (c) SSP3-7.0 scenarios

Note: The y-axis scales may have been limited for illustrative clarity.

# Buildings exposed to erosion

On a state-wide basis, the results indicate that approximately 660 buildings and 1,920 addresses are currently exposed to coastal erosion (for 1% AEP storm erosion volume). At a 1% exceedance probability in the hazard projections distribution, exposure increases to approximately 910 buildings and 2,600 addresses by 2050 under the low emissions pathway (SSP1-2.6), 940 buildings and 2,700 addresses by 2050 under the

medium emissions pathway (SSP2-4.5), and 960 buildings and 2,750 addresses by 2050 under the high emissions pathway (SSP3-7.0), as depicted in Figure 20 and Figure 21.

By 2100, exposure (at 1% exceedance probability in the hazard projections distribution) further increases to around 2,460 buildings and 6,550 addresses under the low emissions pathway (SSP1-2.6), 3,100 buildings and 9,050 addresses under the medium emissions pathway (SSP2-4.5), and 4,530 buildings and 12,420 addresses under the high emissions pathway (SSP3-7.0). By 2150, exposure (at 1% exceedance probability) rises again to around 7,500 buildings and 22,820 addresses under the low emissions pathway (SSP1-2.6), 10,710 buildings and 32,000 addresses under the medium emissions pathway (SSP2-4.5), and 17,740 buildings and 48,400 addresses under the high emissions pathway (SSP3-7.0), as illustrated in Figure 20 and Figure 21.

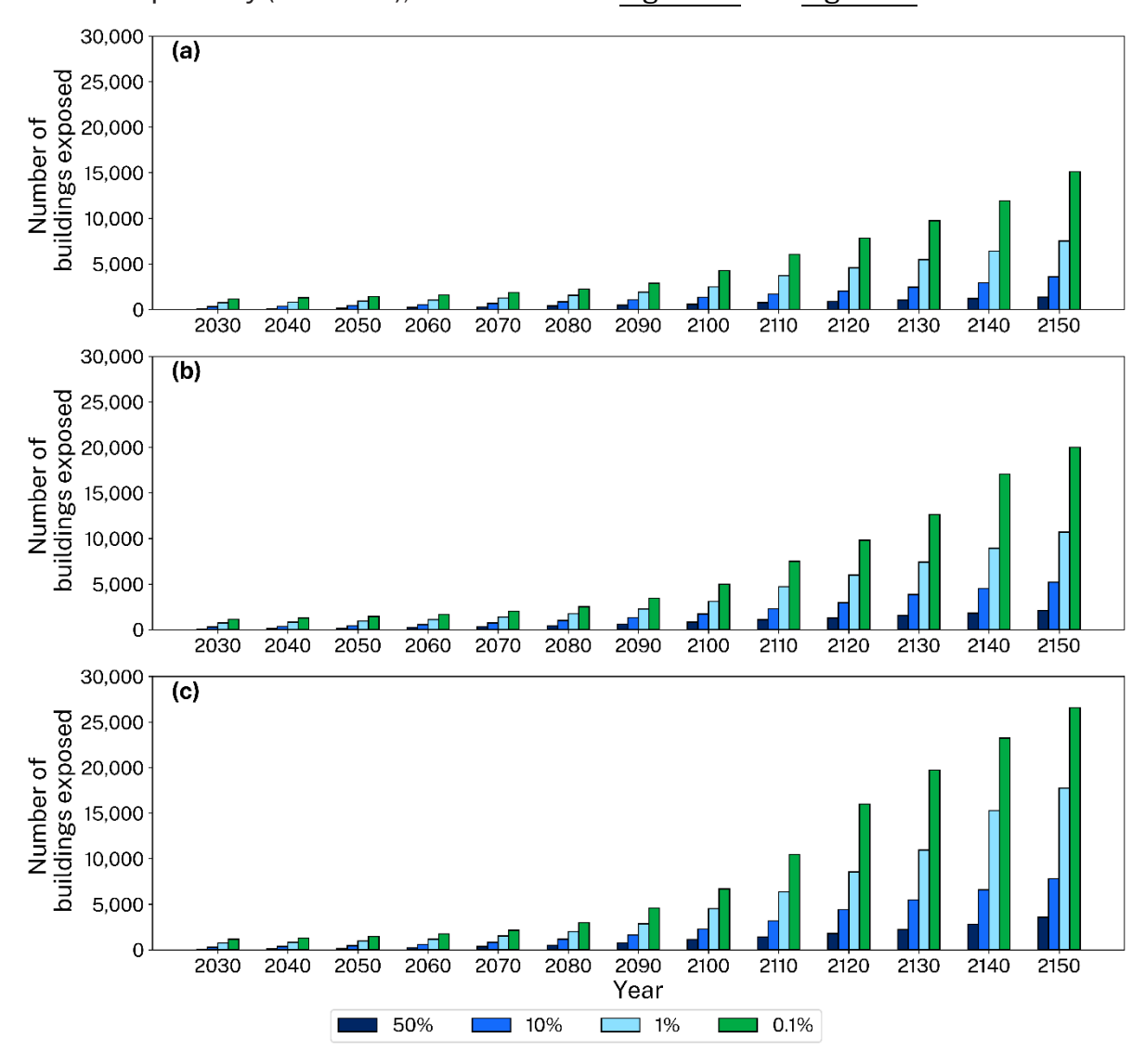


Figure 20 State-wide counts of building exposure to coastal erosion at different exceedance probability levels (0.1%, 1%, 10%, and 50%), from 2030 to 2150 under (a) SSP1-2.6, (b) SSP2-4.5 and (c) SSP3-7.0

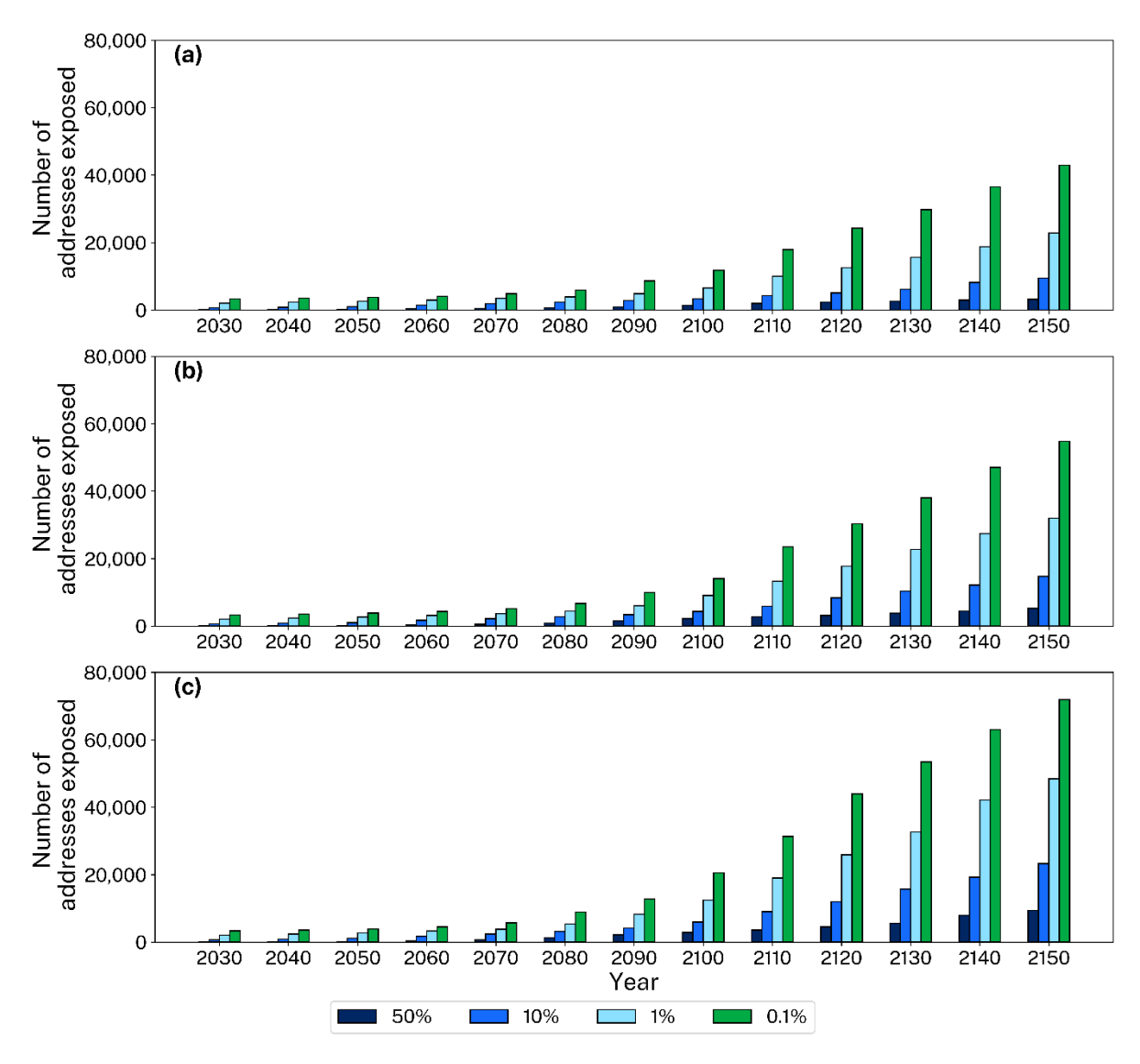


Figure 21 State-wide counts of address exposure to coastal erosion at different exceedance probability levels (0.1%, 1%, 10%, and 50%), from 2030 to 2150, under (a) SSP1-2.6, (b) SSP2-4.5 and (c) SSP3-7.0

### Transport infrastructure

#### Roads and paths

Plots of the lengths of roads and paths exposed to coastal erosion are shown in Figure 22 (roads) and Figure 23 (paths). On a state-wide basis, the results indicate that around 22 km of roads and 35 km of paths are currently exposed to coastal erosion (for the 1% AEP storm erosion volume) (Table 18). This exposure is projected to increase to approximately 32 km of roads and 42 km of paths at a 1% probability of exceedance level in the hazard projections distribution by 2050, 88 km of roads and 66 km of paths by 2100, and 247 km of roads and 111 km of paths by 2150 under the low emissions pathway (SSP1-2.6).

Under the medium emissions pathway (SSP2-4.5), exposure (at 1% exceedance probability) rises to around 34 km of roads and 42 km of paths by 2050, 112 km of roads and 75 km of paths by 2100, and 321 km of roads and 128 km of paths by 2150.

Finally, under the high emissions pathway (SSP3-7.0), exposure (at 1% exceedance probability) increases to approximately 34 km of roads and 43 km of paths by 2050, 155 km of roads and 87 km of paths by 2100, and 458 km of roads and 150 km of paths by 2150.

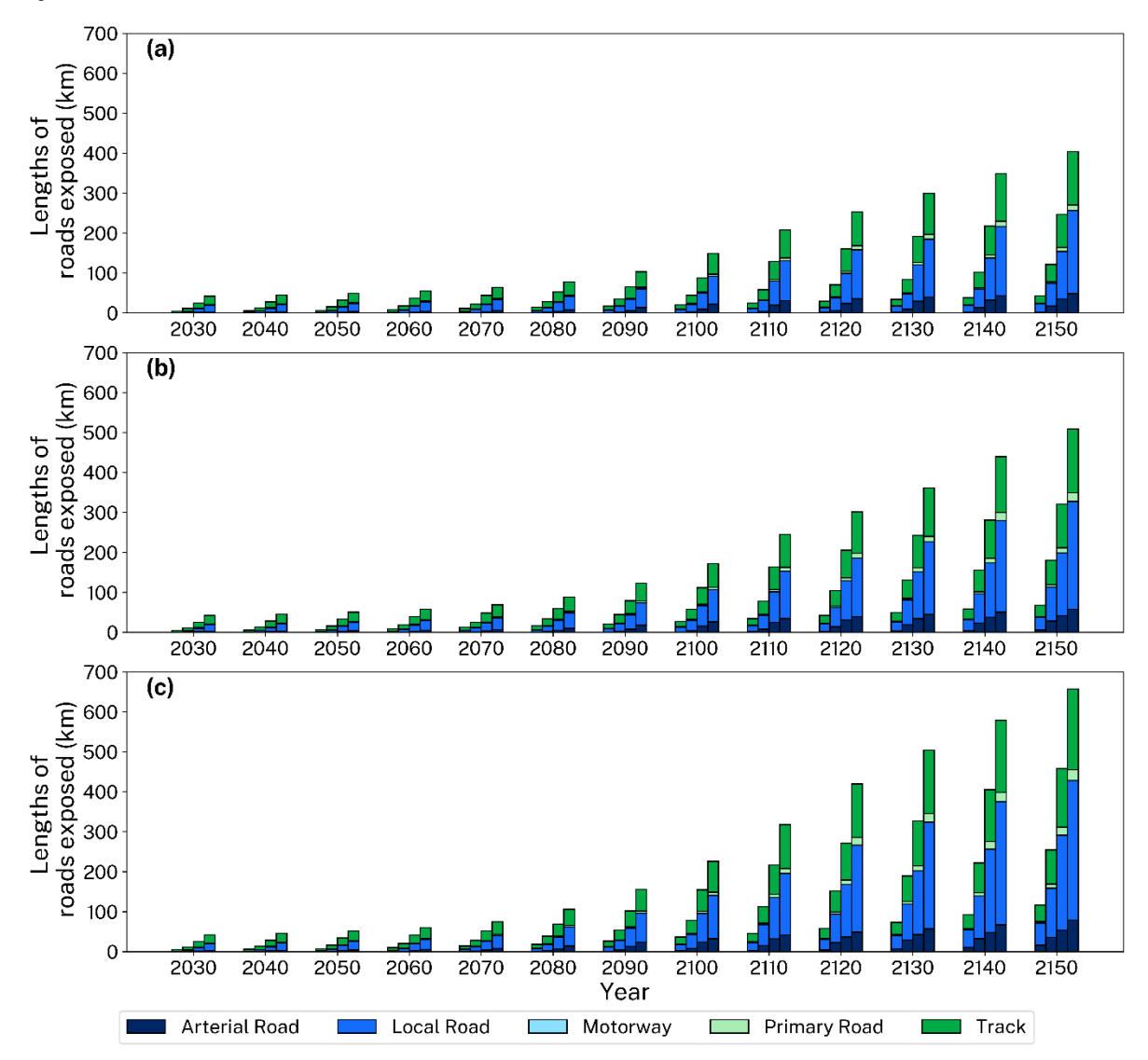


Figure 22 State-wide exposure of road lengths (km) by type to coastal erosion at different exceedance probability levels (from right to left: 0.1%, 1%, 10% and 50%), from 2030 to 2150, under (a) SSP1-2.6, (b) SSP2-4.5 and (c) SSP3-7.0

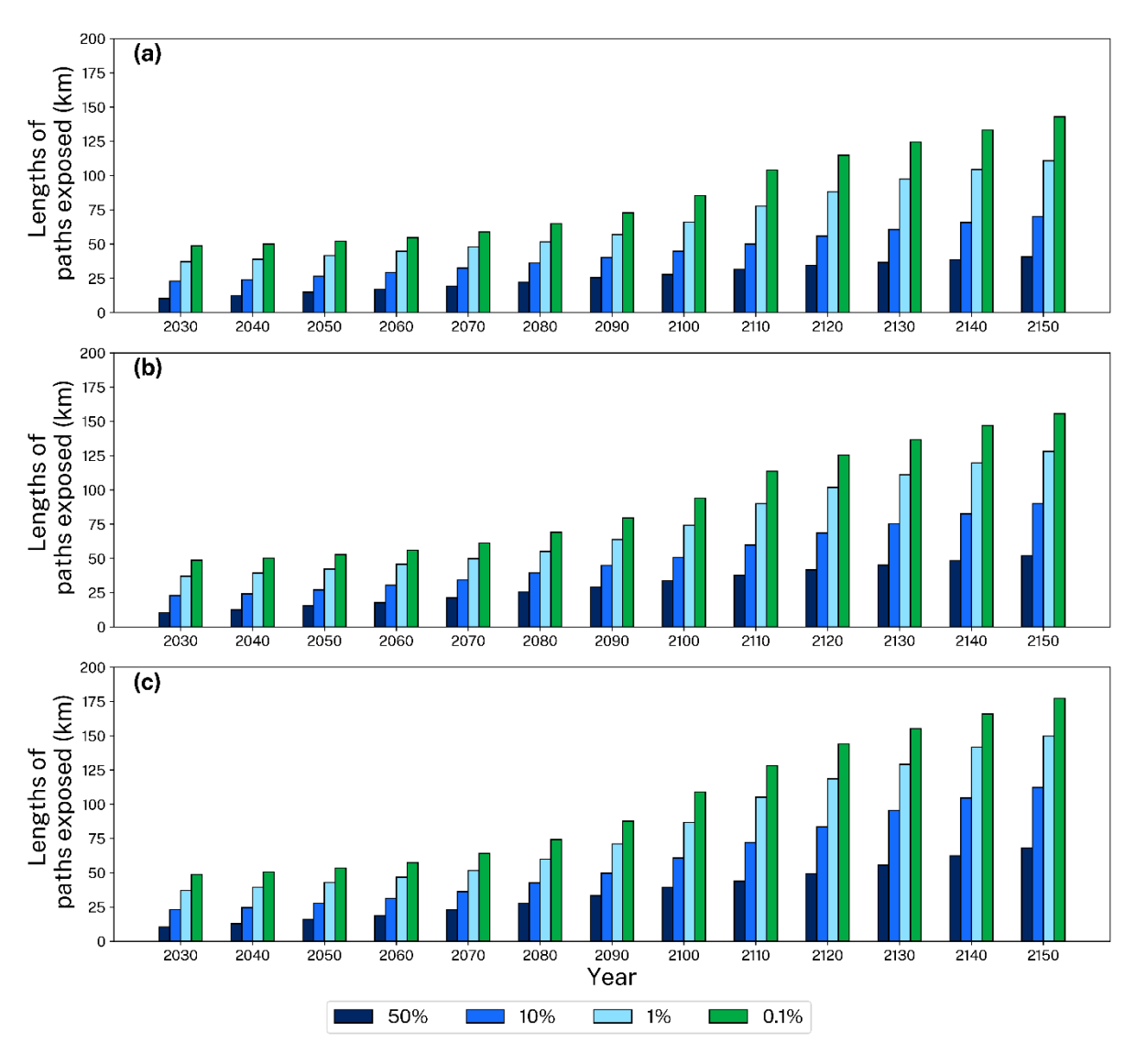


Figure 23 State-wide exposure of path lengths (km) to coastal erosion at different exceedance probability levels (0.1%, 1%, 10%, and 50%), from 2030 to 2150, under (a) SSP1-2.6, (b) SSP2-4.5 and (c) SSP3-7.0

### Rail

A plot of the lengths of rail exposed to erosion is shown in <u>Figure 24</u>. On a state-wide basis, the results indicate that less than 1 km of rail lines are currently exposed to erosion for the 1% AEP storm erosion volume (<u>Table 18</u>). At a 1% exceedance probability level in the hazard projections distribution, this exposure remains minimal for the next 50–60 years but is projected to rise to around 1 km by 2100 and 2.7 km by 2150 under the low emissions pathway (SSP1-2.6), to 1 km by 2100 and 3.3 km by 2150 under the medium emissions pathway (SSP2-4.5), and to 1.4 km by 2100 and 4 km by 2150 under the high emissions pathway (SSP3-7.0).

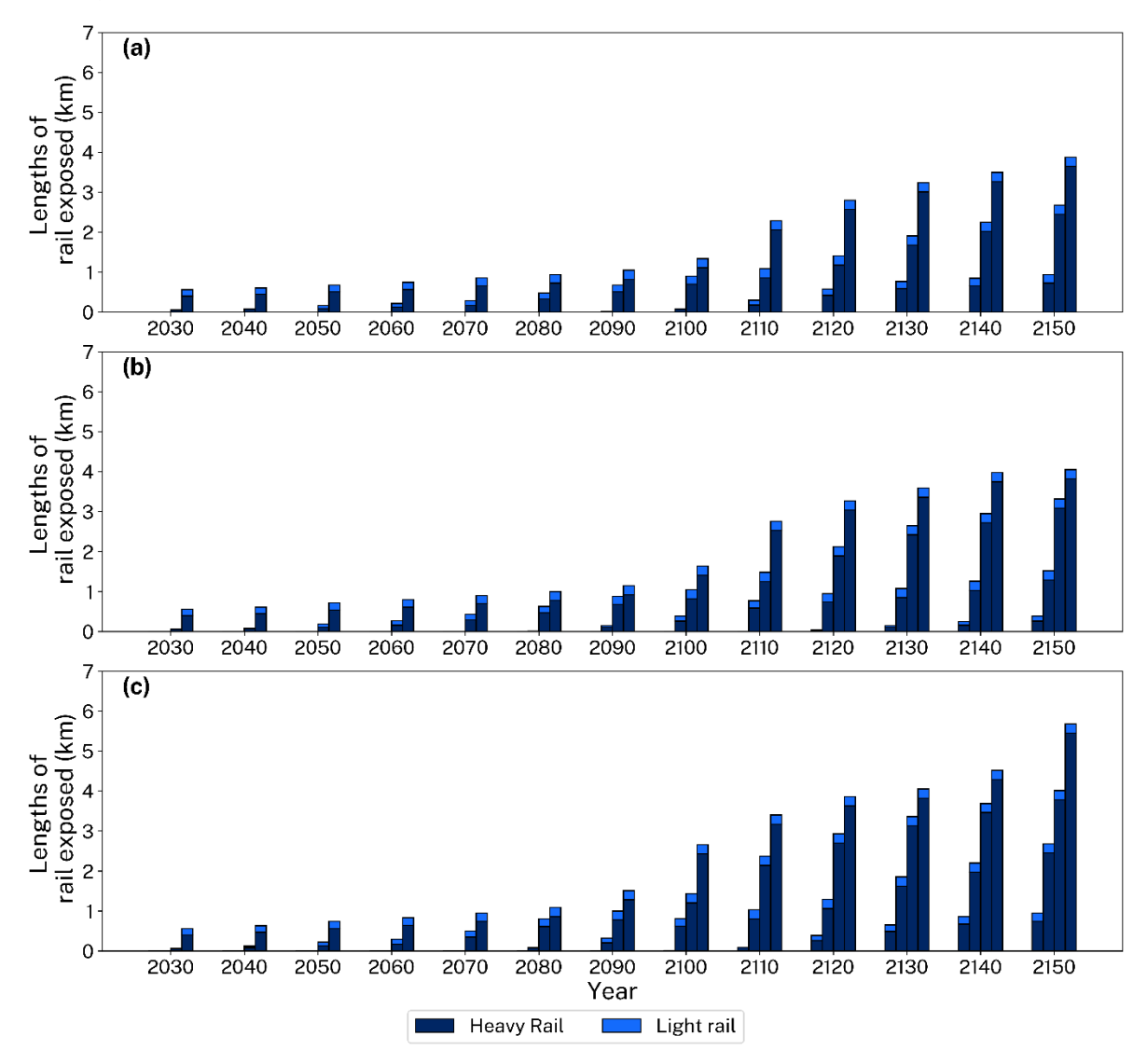


Figure 24 State-wide exposure of rail lengths (km) by type to coastal erosion at different exceedance probability levels (from right to left: 0.1%, 1%, 10% and 50%), from 2030 to 2150, under (a) SSP1-2.6, (b) SSP2-4.5 and (c) SSP3-7.0

## Airport and runways

Plots of the number of airports and lengths of runways exposed to coastal erosion are shown in <u>Figure 25</u> (airports) and <u>Figure 26</u> (runways). As evident from these figures, no airports or runways are currently exposed to erosion (<u>Table 18</u>), and minimal exposure is projected in the coming century. For instance, at a 1% exceedance probability level in the hazard projections distribution, by 2150, it is estimated that no airport and almost no (around 50 m for SSP2-4.5) lengths of runways will be exposed to erosion under the low and medium emission pathways (SSP1-2.6 and SSP2-4.5). The exposure (at 1% probability) is projected to be one heliport and 2 km of runways by 2150 under the high emissions pathway (SSP3-7.0).

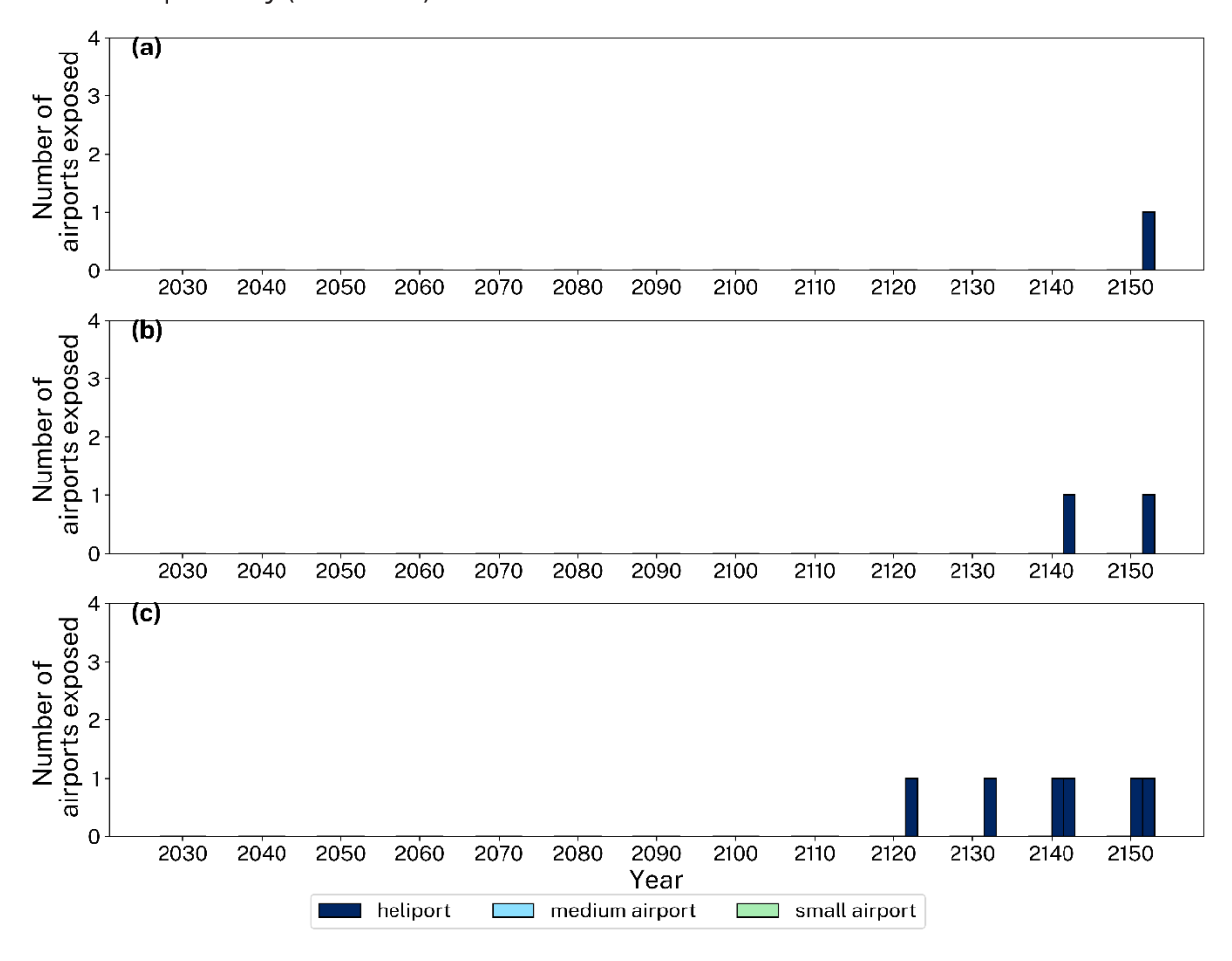


Figure 25 State-wide exposure of airports by type to coastal erosion at different exceedance probability levels (from right to left: 0.1%, 1%, 10% and 50%), from 2030 to 2150, under (a) SSP1-2.6, (b) SSP2-4.5 and (c) SSP3-7.0

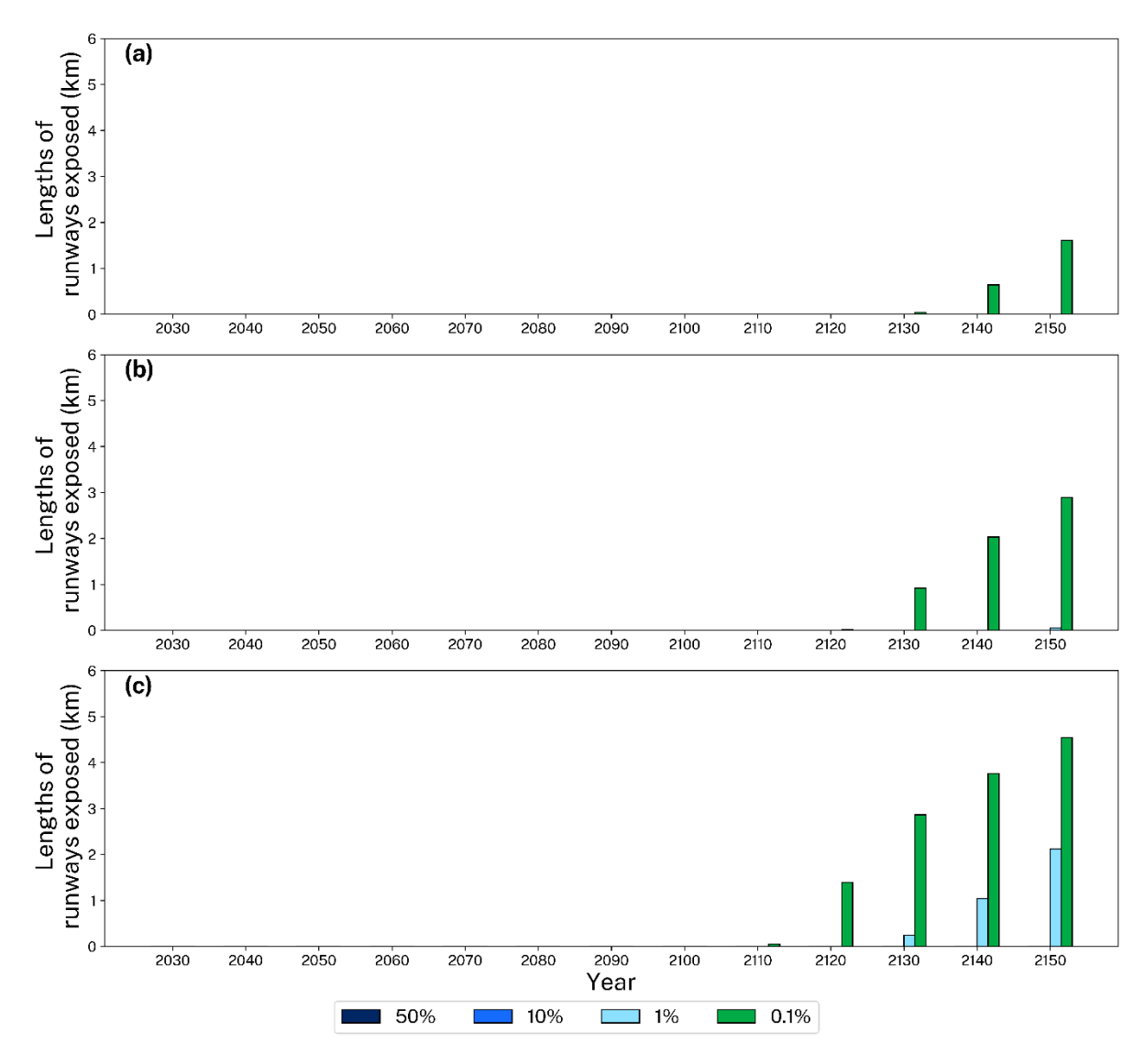


Figure 26 State-wide exposure of runway lengths (km) to coastal erosion at different exceedance probability levels (0.1%, 1%, 10%, and 50%), from 2030 to 2150, under (a) SSP1-2.6, (b) SSP2-4.5 and (c) SSP3-7.0

# Aboriginal cultural heritage assets

A plot of the total number of currently identified Aboriginal cultural heritage sites exposed to coastal erosion is shown in <u>Figure 27</u>. On a state-wide basis, the results indicate that 288 sites are currently exposed to erosion for the 1% AEP storm erosion volume (<u>Table 18</u>). At a 1% exceedance probability level in the hazard projections distribution, this exposure is projected to increase to approximately 319 sites by 2050, 475 sites by 2100, and 695 sites by 2150 under the low emissions pathway (SSP1-2.6). For the same exceedance probability level under the medium emissions pathway (SSP2-4.5), exposure increases to around 323 sites by 2050, 509 sites by 2100, and 786 sites by 2150. Under the high emissions pathway (SSP3-7.0), exposure increases to around 325 sites by 2050, 570 sites by 2100, and 927 sites by 2150.

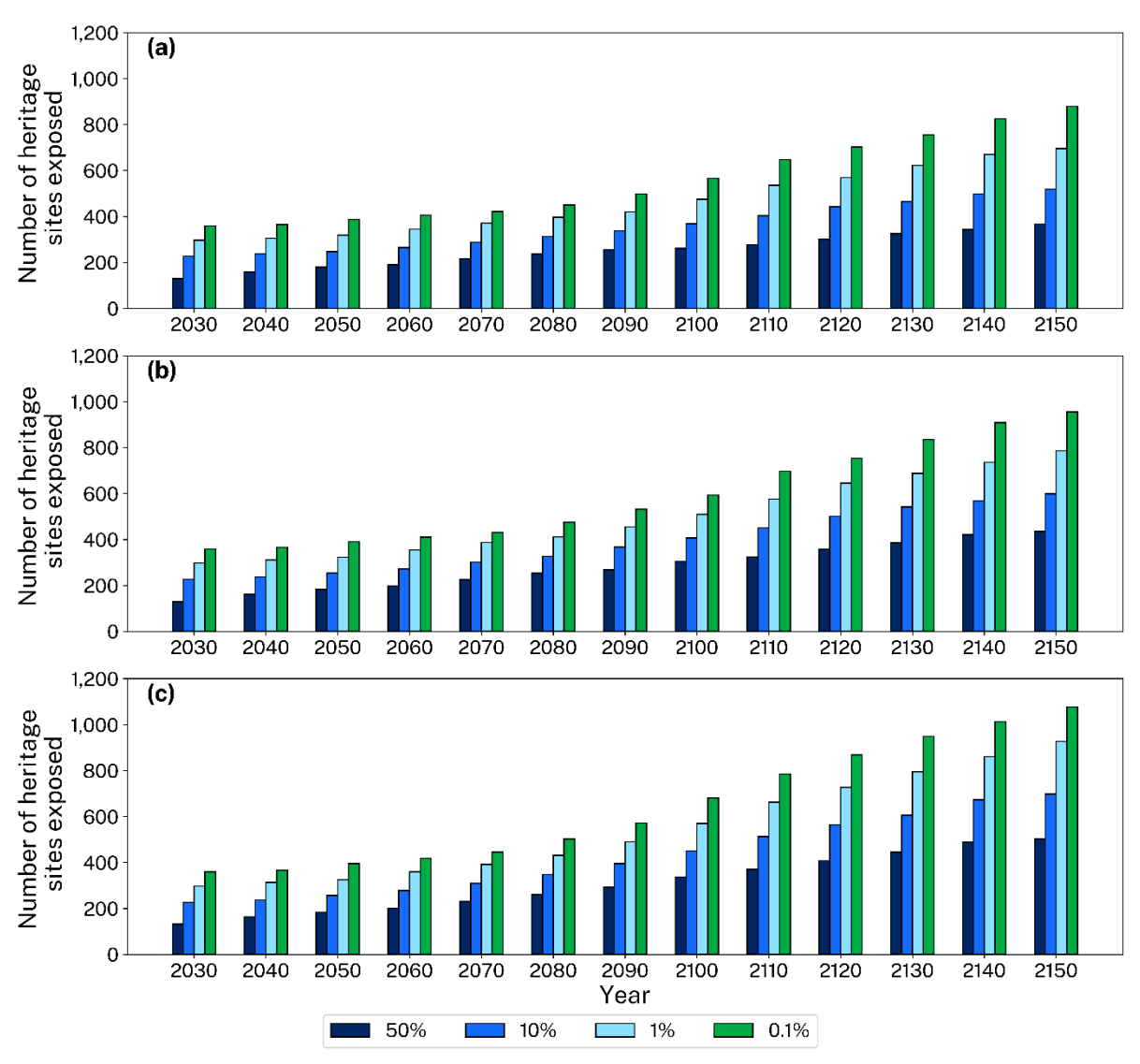


Figure 27 State-wide exposure of currently identified Aboriginal cultural heritage sites to coastal erosion at different exceedance probability levels (0.1%, 1%, 10% and 50%), from 2030 to 2150, under (a) SSP1-2.6, (b) SSP2-4.5 and (c) SSP3-7.0

## Critical infrastructure

## **Electricity transmission lines**

The combined length of overhead and underground electricity transmission lines currently exposed to coastal erosion (for 1% AEP storm erosion volume) is around 14 km (<u>Table 18</u>). At a 1% exceedance probability level in the hazard projections distribution, this exposure is estimated to increase to approximately 20 km by 2050, 56 km by 2100, and 208 km by 2150 under the low emissions pathway (SSP1-2.6) (<u>Figure 28(a)</u>). Under the medium emissions pathway (SSP2-4.5), the length of exposed powerlines increases to approximately 20 km by 2050, 74 km by 2100, and 297 km by 2150 (<u>Figure 28(b)</u>). Under the high emissions pathway (SSP3-7.0), the length of exposed powerlines increases to around 21 km by 2050, 113 km by 2100, and 477 km by 2150 at a 1% exceedance probability level (Figure 28(c)).

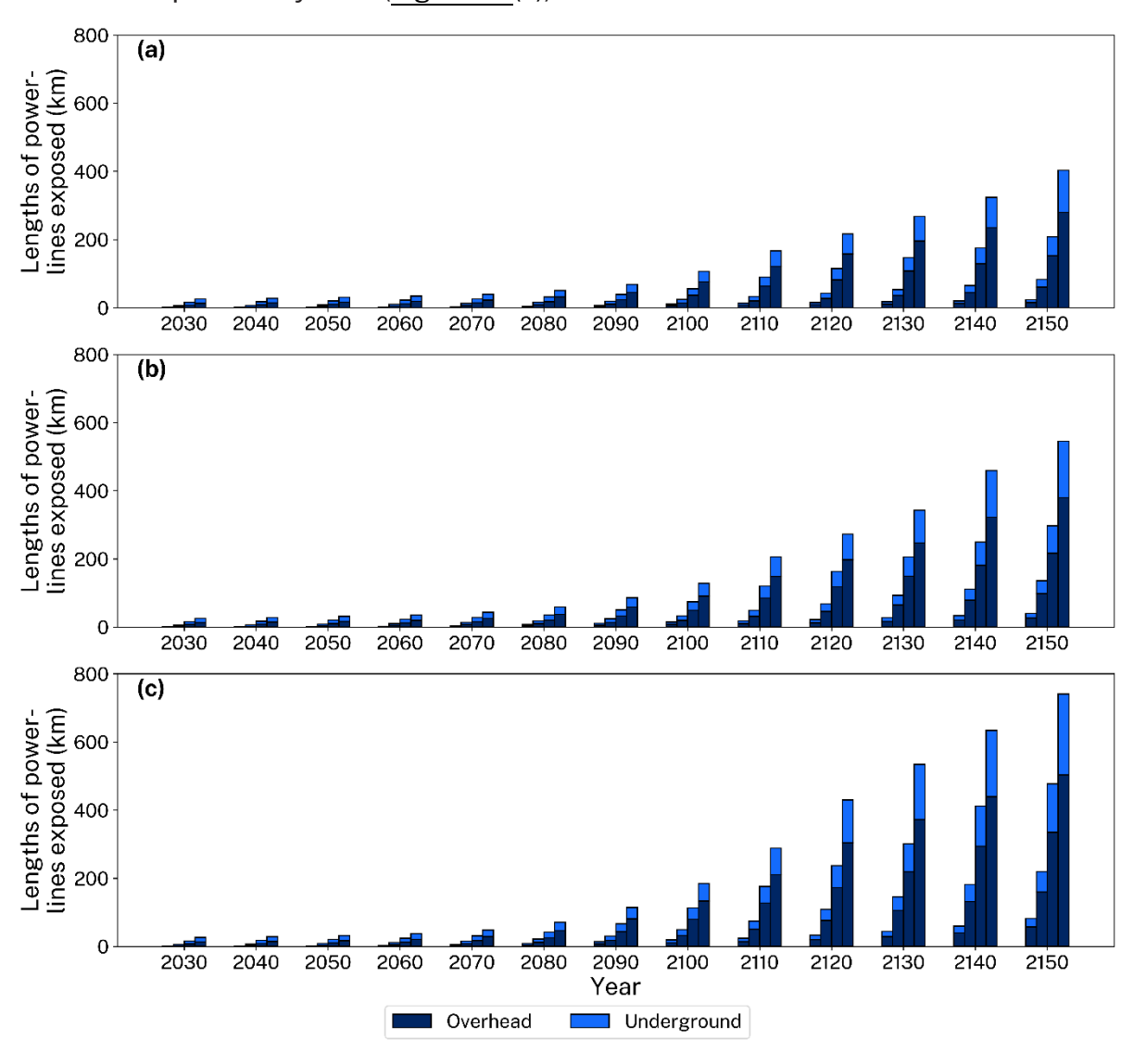


Figure 28 State-wide exposure of power lines (km) by type to coastal erosion at different exceedance probability levels (from right to left: 0.1%, 1%, 10%, and 50%), from 2030 to 2150, under (a) SSP1-2.6, (b) SSP2-4.5 and (c) SSP3-7.0

### Critical infrastructure sites

Critical infrastructure sites include emergency services, schools and universities, correctional facilities and courthouses, and hospitals. Currently, there are no critical infrastructure sites exposed to coastal erosion on a state-wide basis (<u>Table 18</u>). The total number of exposed critical infrastructure sites (at 1% exceedance probability level in the hazard projections distribution) is projected to increase to 3 by 2100 and 4 by 2150 under the low emissions pathway (SSP1-2.6) (<u>Figure 29(a)</u>). For the same exceedance probability level, under the medium emissions pathway (SSP2-4.5), the number of exposed sites increases to 3 by 2100 and 4 by 2150 (<u>Figure 29(b)</u>). Under the high emissions pathway (SSP3-7.0), the number of exposed sites rises to 3 by 2100 and 6 by 2150 (Figure 29(c)).

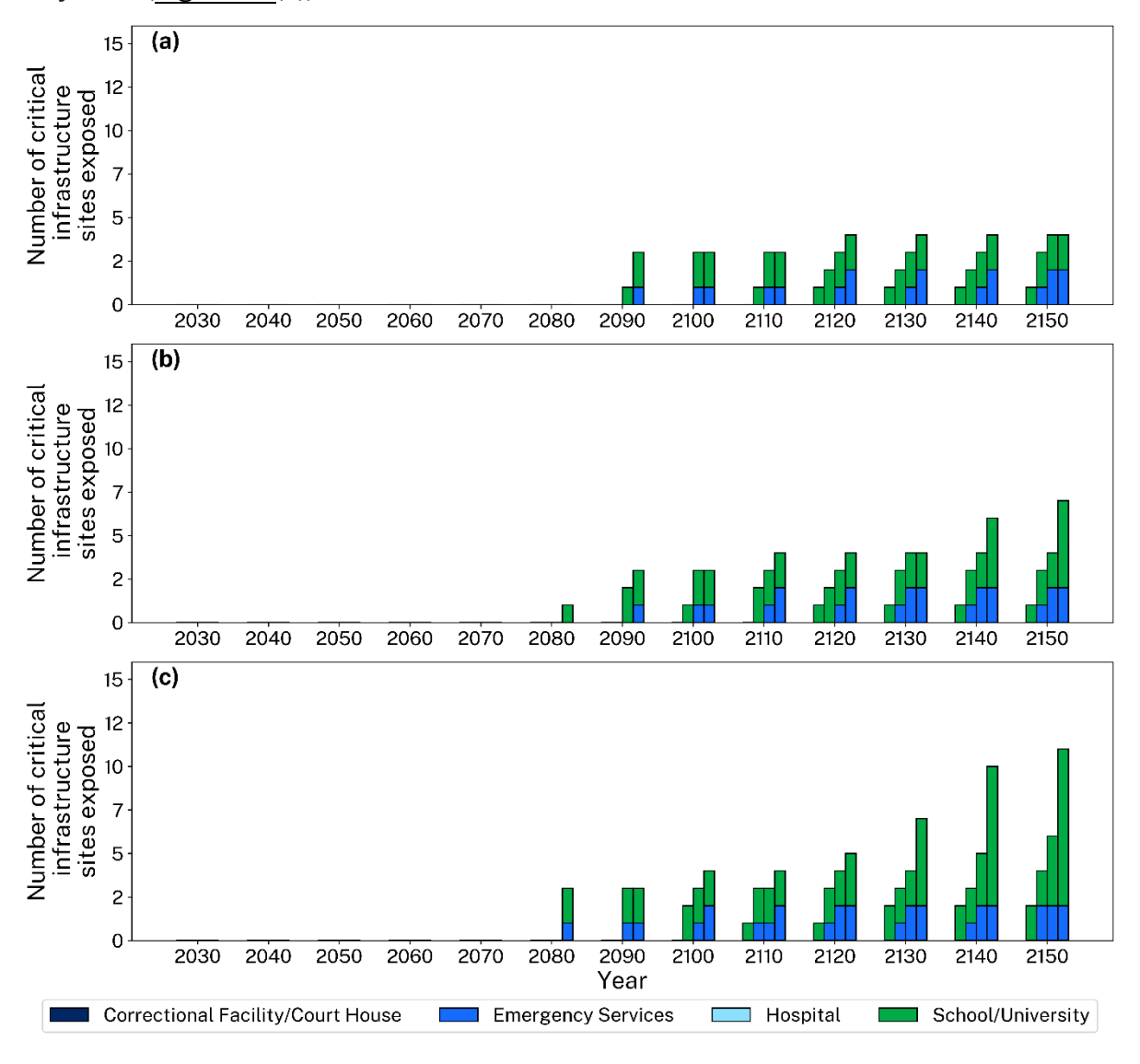


Figure 29 State-wide exposure of critical infrastructure by type to coastal erosion at different exceedance probability levels (from right to left: 0.1%, 1%, 10%, and 50%), from 2030 to 2150, under (a) SSP1-2.6, (b) SSP2-4.5 and (c) SSP3-7.0

# Beaches in bays and estuaries

A selection of 32 bay/estuary beaches particularly exposed to ocean wave processes were modelled to demonstrate that coastal erosion hazards also occur in estuary and bay settings and will increase with SLR. The modelling of bay/estuary beaches considered only fluctuating erosion caused by storms and the translation component of potential beach response to SLR (Appendix A: Beach fluctuation). Such beaches are typically connected to adjacent flood-tide deltas and tidal inlets, which influence their sediment dynamics. Hence, modelling erosion in such settings should be taken as a first-pass estimate, and more detailed site-specific studies are required to comprehensively evaluate their sediment budgets and dynamics.

The modelling for bay/estuary beaches did not account for overwash of the often low barrier-dunes, nor the impacts of estuarine inundation, both of which could enable and exacerbate coastal erosion. The coastal erosion forecasts for bay/estuary beaches should therefore be considered minimum projections and viewed in the context of the inundation hazards assessed in this study.

<u>Figure 30</u> shows a box plot of erosion distances for all modelled bay/estuary beach sectors at a 1% exceedance probability level in the hazard projections distribution for the present (2020) and for 2050, 2100 and 2150 under the high SSP3-7.0 sea level scenario. The analysis shows that, while the modelled erosion distances are lower than those for open coast beaches (<u>Figure 18</u>), the median erosion distance for bay/estuary beaches at 2100 is projected to double relative to a very severe erosion event today, and to triple by 2150. The increase for bay/estuary beaches more susceptible to erosion than the median case is greater again. These minimum projections for the bay/estuary case study beaches indicate that exposure to coastal erosion hazards will not be limited to open coast NSW beaches but will also affect sheltered bay and estuary settings.

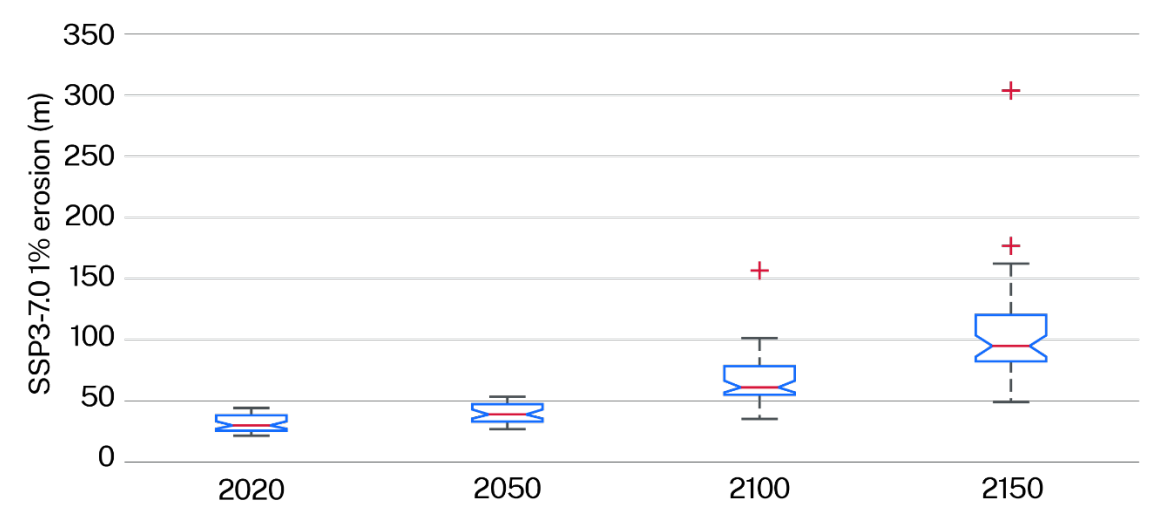


Figure 30 Box plot summarising the modelled shoreline erosion distances for bay/estuary beaches at a 1% exceedance probability level at present (2020), and for the SSP3-7.0 sea level scenario at 2050, 2100 and 2150

## Very high emissions scenarios and comparative insights

This section offers high-level insights into coastal erosion exposure in NSW for the high-impact scenarios (that is, medium-confidence SSP5-8.5 and low-confidence SSP5-8.5). It also draws exemplary comparisons across all SSP scenarios, including SSP1-2.6, SSP2-4.5 and SSP3-7.0, to illustrate how emissions trajectories may shape future risks. By exploring these scenarios, this assessment highlights the challenges posed by higher emissions and identifies hazards and opportunities for proactive mitigation and adaptation to reduce long-term exposure. Exemplary results are presented here for exposure of buildings, roads, critical infrastructure and heritage sites at a 1% exceedance probability level in the hazard projections distribution. The results of exposure for all assets and infrastructure under very high emission scenarios are provided in Appendix G.

## Buildings exposure across SSP scenarios

Currently, approximately 660 buildings are exposed to coastal erosion. By 2080, clear differences among scenarios become apparent (<u>Figure 31</u>(a)). By 2080, exposure increases to 1,560 buildings under SSP1-2.6, 1,750 buildings under SSP2-4.5, and 2,000 buildings under SSP3-7.0. High-emissions scenarios show greater increases in exposure with time, reaching 2,240 buildings by 2080 under medium-confidence SSP5-8.5 and 5,410 buildings by 2080 under low-confidence SSP5-8.5.

By 2150, exposure increases further across all SSPs (<u>Figure 31</u>(a)), to 7,500 buildings under SSP1-2.6, 10,710 buildings under SSP2-4.5 and 17,740 buildings under SSP3-7.0. Under medium-confidence SSP5-8.5, exposure increases to 22,120 buildings, and under low-confidence SSP5-8.5 to 97,970 buildings, representing a 2.1-fold and 9.1-fold increase compared to SSP2-4.5, respectively. These trends highlight the accelerating exposure under very high emissions pathways.

## Critical infrastructure exposure across SSP scenarios

Exposure of critical infrastructure to coastal erosion is currently negligible state-wide, with no identified exposure in 2020. By 2080, SSP1-2.6, SSP2-4.5 and SSP3-7.0 continue to show no exposure at a 1% exceedance probability level in the hazard projections distribution, while medium-confidence SSP5-8.5 has an exposure of one critical infrastructure asset. Low-confidence SSP5-8.5 is projected to have an exposure of 3 assets by 2080 (Figure 31(b)).

By 2150, exposure under SSP1-2.6 and SSP2-4.5 increases to 4 critical infrastructure assets. SSP3-7.0 shows greater increase to exposure with 6 assets, and under medium-confidence SSP5-8.5 exposure increases to 9 assets. Low-confidence SSP5-8.5 exhibits the highest growth, reaching 71 exposed critical infrastructure assets by 2150 (Figure 31(b)). Given the high cost and importance of critical infrastructure, it is likely that no level of exposure is acceptable, so results from the very high emissions scenarios may provide a sound basis for decision-making.

## Heritage site exposure across SSP scenarios

At present, 288 currently identified Aboriginal cultural heritage sites are exposed to coastal erosion (<u>Figure 31</u>(c)). By 2080, exposure increases to 396 sites under SSP1-2.6, 411 sites under SSP2-4.5 and 431 sites under SSP3-7.0. Under medium-confidence SSP5-8.5, exposure increases to 451 sites, and under low-confidence SSP5-8.5 to 597 sites. By 2150, exposure grows to 695 sites under SSP1-2.6, 786 sites under SSP2-4.5 and 927 sites under SSP3-7.0; and exposure reaches 1,000 sites under medium-confidence SSP5-8.5 and 2,254 sites under low-confidence SSP5-8.5.

### Road exposure across SSP scenarios

Currently, road exposure to coastal erosion stands at 22 km state-wide (<u>Figure 31</u>a). By 2080, exposure increases to 53 km under SSP1-2.6, 59 km under SSP2-4.5 and 69 km under SSP3-7.0. Under medium-confidence SSP5-8.5, 76 km of road is exposed. Low-confidence SSP5-8.5 has the largest road exposure by 2080, reaching 177 km. By 2150, road exposure reaches 247 km under SSP1-2.6, 321 km under SSP2-4.5, and 458 km under SSP3-7.0. Under medium-confidence SSP5-8.5, road exposure reaches 558 km, and under low-confidence SSP5-8.5 it reaches 2,417 km.

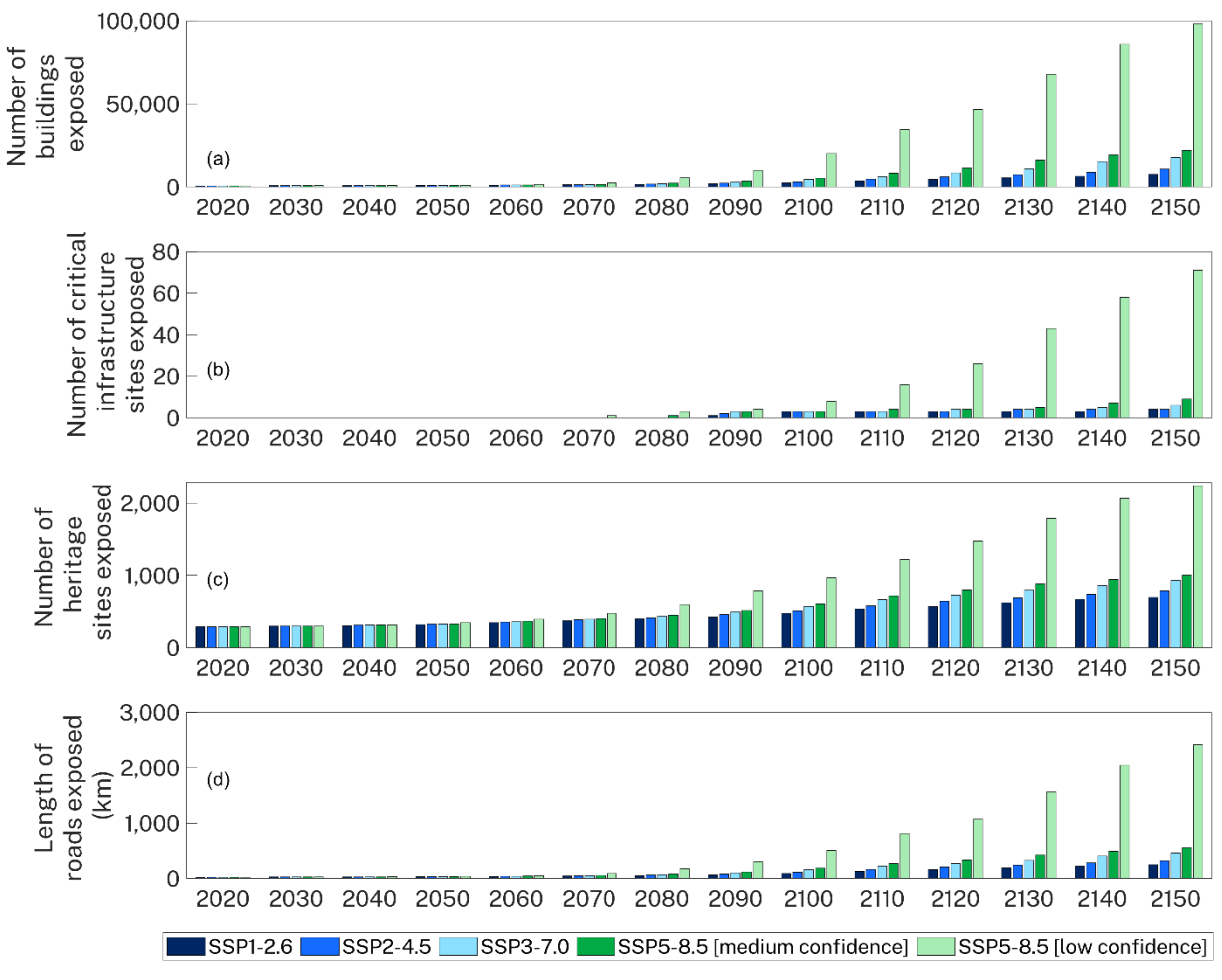


Figure 31 State-wide exposure of (a) buildings, (b) critical infrastructure, (c) heritage sites and (d) roads (km) to coastal erosion at 1% exceedance probability, from present (2020) to 2150, under SSP1-2.6, SSP2-4.5, SSP3-7.0, medium-confidence SSP5-8.5 and low-confidence SSP5-8.5

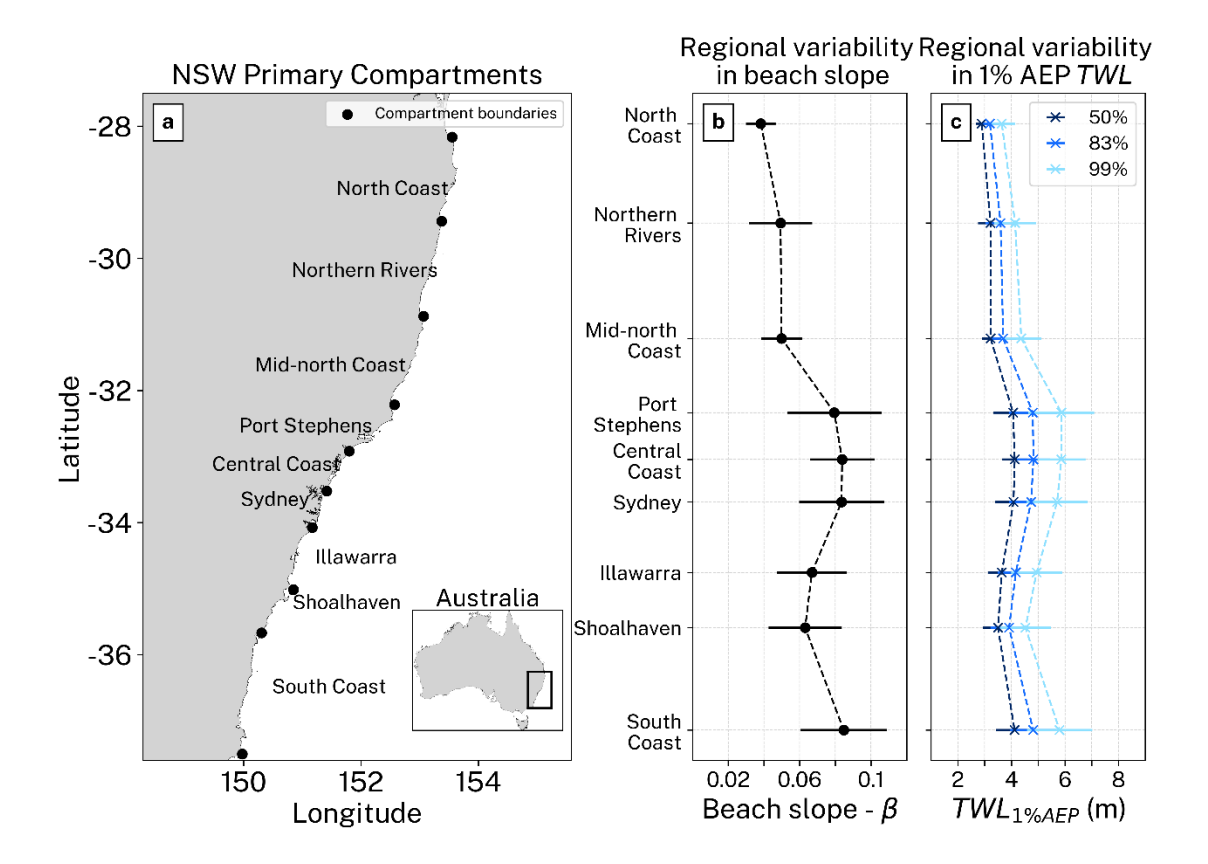
## Summary

This assessment highlights that coastal erosion exposure is projected to increase across all SSPs in NSW, with the rate of exposure varying across timeframes and emissions pathways. While coastal erosion exposure will inevitably increase over time, the degree of increase will depend on actual climate conditions in the future. Proactive measures such as reducing emissions and following lower emissions pathways, improving land-use planning, and investing in resilient infrastructure can help manage exposure growth and minimise long-term vulnerabilities.

## 4.2 Coastal overwash

## Overview of modelling input

<u>Figure 32</u>(a) shows the NSW coastline and the boundaries of the state's primary sediment compartments. Regional variability in beach slopes (β) and 1% AEP for total water level (TWL) (that is, a nominal design value) by primary compartment are shown in panels (b) and (c), respectively. Increasing beach slope magnitudes are evident towards southern NSW, mirrored by the magnitude of 1% AEP TWL for different percentiles of the hazard projections distribution (50%, 83% and 99%). Primary compartments located in the north of NSW (North Coast to Mid-north Coast) are characterised by gentle slopes (β is around 0.03), while steeper beaches are more prevalent in the south (Port Stephens to South Coast, β is around 0.08–0.1) (for example, due to variation in grain size). The TWL magnitudes for 1% AEP vary from 3 m to 5 m AHD in the north and from 4 m to approximately 7 m AHD in southern compartments, depending on the percentile level. Overall, these analyses suggest that low-lying areas up to around 7 m AHD are potentially overwashed during extreme storms (1% AEP TWL).



Key: Horizontal lines denote standard deviation around the mean. AEP = annual exceedance probability; TWL = total water level.

Figure 32 Overview of modelling data input by primary sediment compartment, showing

(a) geographical setting of the NSW region and boundaries of primary sediment compartments, (b) regional variability in beach slope by primary compartment and (c) regional variability in percentiles of the modelled distribution of 1% AEP total water levels

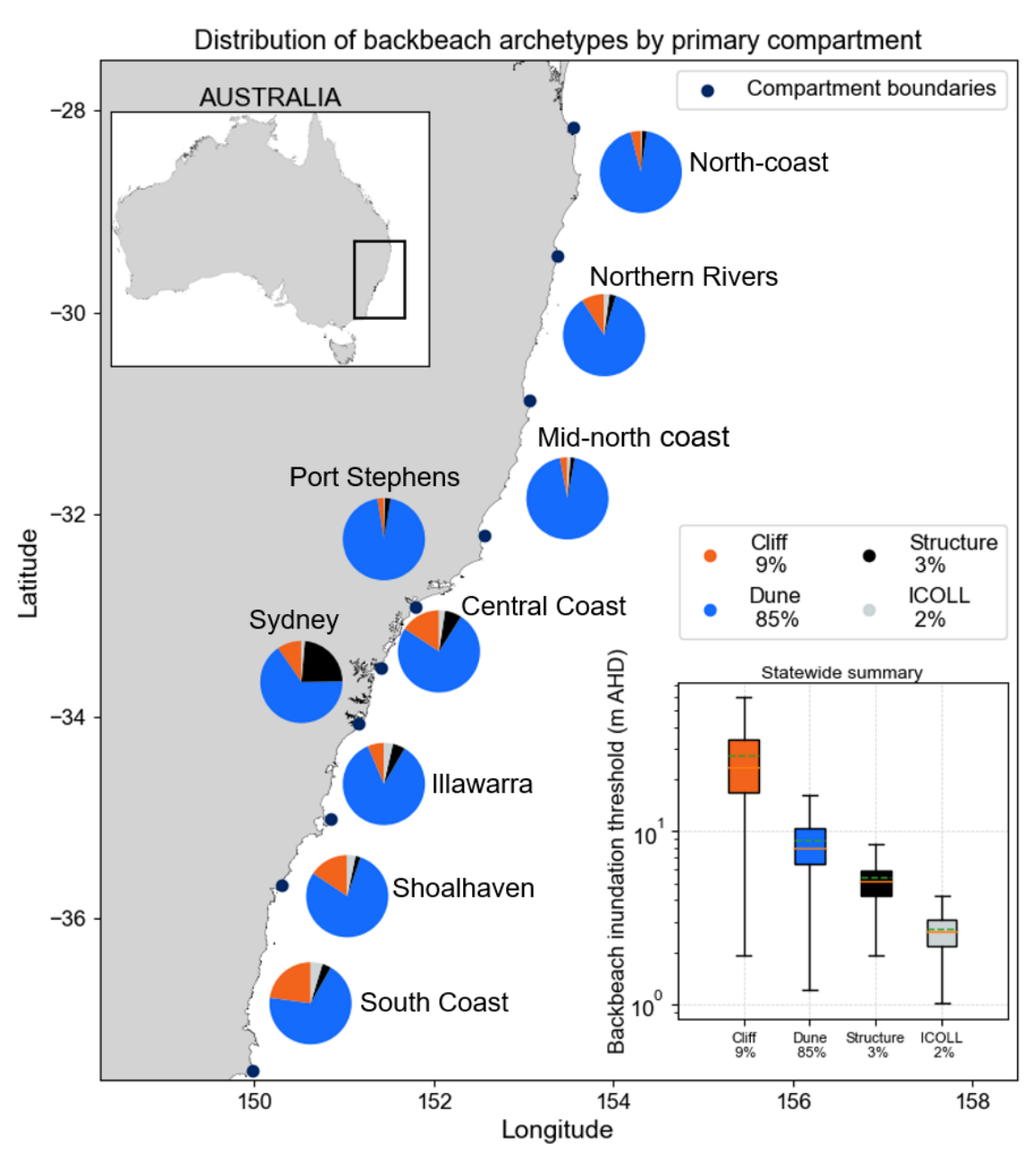


Figure 33 Distribution of backbeach archetypes by primary sediment compartment, with inset showing state-wide distribution of backbeach overwash thresholds for different archetypes

Figure 33 shows the state-wide spatial distribution within primary sediment compartments of backbeach archetypes, including dune, cliff, structure and intermittently open coastal lakes and lagoons (ICOLLs). Overall, dunes are the most prevalent backbeach archetype in NSW (85% of transects, 738 km of sandy coastline), followed by cliffs (9%, 79 km), structures (3%, 30 km) and ICOLLs (2%, 18 km). The spatial distribution of these archetypes varies along the NSW coast, with dunes being more prevalent in northern regions and cliffs more common in southern compartments. Structures are predominantly located in the Sydney region, with fewer found in northern compartments (less than 5% of the compartment's transects) compared to the Central Coast, Illawarra, Shoalhaven and South Coast (more than 5%). ICOLLs are present

across all primary compartments but represent a minority (less than 5% per compartment) of the NSW open coast.

The likelihood of inundation due to coastal overwash largely depends on the selected backbeach inundation thresholds across these coastal archetypes (<u>Table 7</u>). The inset panel in the lower right of <u>Figure 33</u> shows state-wide distributions of backbeach inundation thresholds by coastal archetype. Higher elevations are associated with cliff tops (average 27.7 m AHD, std deviation = 16.1 m), followed by dune crests (average 8.8 m AHD, std deviation = 3.4 m), structure crests (average 5.4 m AHD, std deviation = 2.1 m), and berm heights at ICOLLs (average 2.7 m AHD, std deviation = 0.8 m). Comparing these elevations with 1% AEP TWL (3 m to 7 m AHD, <u>Figure 32</u>(c)) suggests that structures, ICOLLs and lower dunes are currently experiencing, and will continue to experience, overwash of the backbeach locations into the future.

## Current coastal overwash likelihoods

### State-wide overview

<u>Figure 34</u> summarises the current (2020) likelihood of coastal overwash at the state-wide level and by coastal archetype for a nominal 1% AEP TWL. Most of the NSW sandy coastlines fall into the *unlikely inundation (overwash)* category (89%, 773 km of coastline), followed by *potential inundation (overwash)* category (5%, 41 km of coastline) and *likely inundation (overwash)* category (6%, 51 km of coastline). Similarly, overwash likelihoods by coastal archetype indicate that most high dunes and cliff environments do not experience inundation at present, largely because their higher elevations provide a buffer against coastal overwash. However, around 3% of the state's dunes currently experience likely overwash. The remaining transects currently exposed to coastal overwash hazards fall into the structure and ICOLL archetypes, with around 32% and 91% of them experiencing likely inundation, respectively.

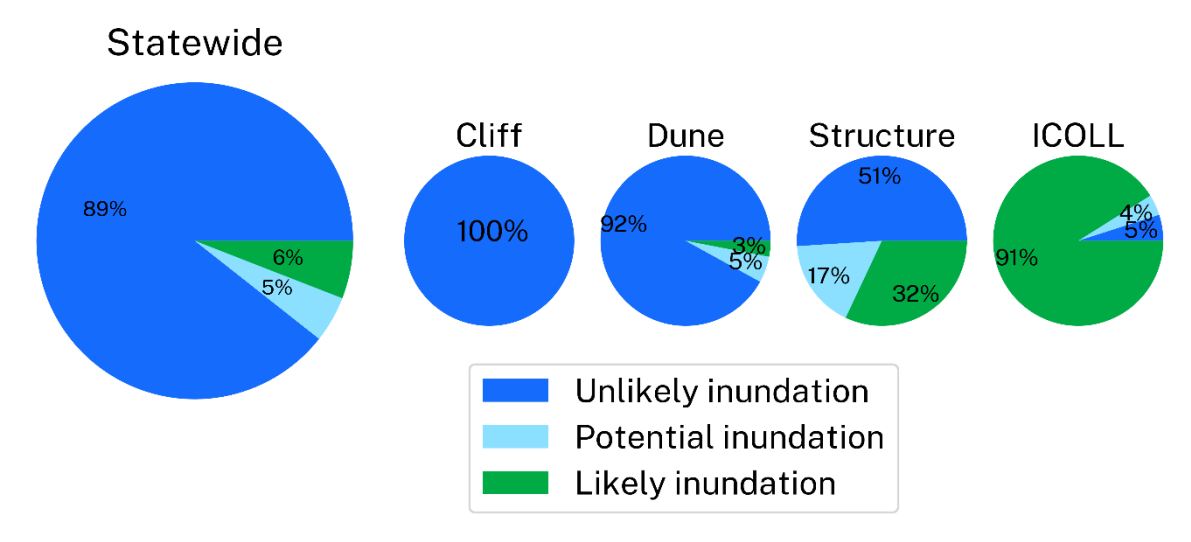


Figure 34 Current (2020) coastal overwash (shown as inundation) likelihoods for total water level distributions at 1% annual exceedance probability, at the state-wide level and by coastal archetype

The overall variation in elevation for each overwash class is shown in <u>Figure 35</u>, which presents the variation in predicted overwash elevation in the overview of modelling input above; portions of coastline at 7 m AHD (or lower) are currently classified as potential or likely inundation.

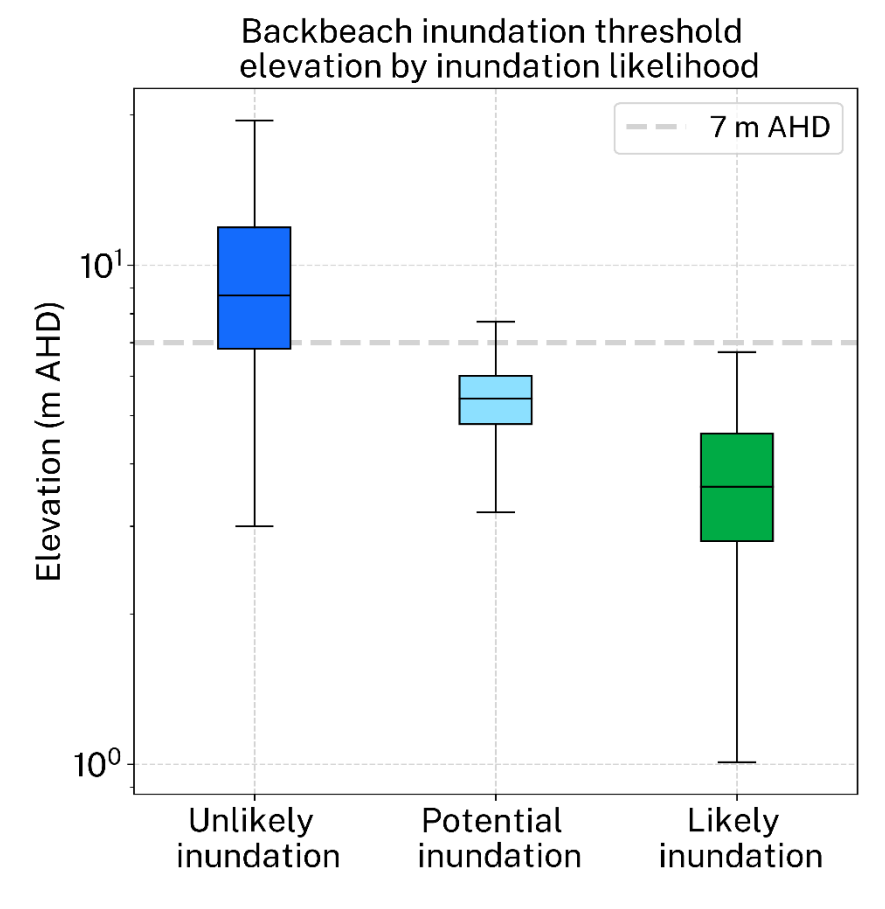


Figure 35 Distribution of backbeach overwash thresholds clustered by overwash (shown as inundation) likelihood at 1% annual exceedance probability

Figure 36 and Table 2 summarise current coastal overwash likelihoods at the state-wide level (panel a) and by coastal archetype (panel b). These results indicate the proportion of sandy coastlines that experience overwash likelihoods for different TWL AEPs. Results show that 2% to 6% of the coastlines experience likely coastal overwash for a 1% to 100% AEP TWL. Focusing on results by coastal archetype, Figure 36(b) shows that structures and ICOLLs exhibit more variability in coastal overwash likelihoods for different AEP TWL, with approximately 4% to 33% and 64% to 91% experiencing likely overwash for 1% to 100% AEP TWL, respectively. This implies that 4% of structure profiles and 64% of ICOLL profiles experience overwash every year (on average). Conversely, most cliffs and dunes fall into the unlikely overwash category, irrespective of the TWL AEP forcing. For the remainder of this section, the results and analyses focus on the nominal 1% AEP TWL magnitude.

Table 2 State-wide distribution (% of coastline) of current overwash likelihoods for several annual exceedance probability (AEP) levels of total water level

Overwash likelihood	100% AEP	20% AEP	5% AEP	1% AEP
Likely	2%	4%	5%	6%
Potential	2%	4%	4%	5%
Unlikely	96%	92%	91%	89%

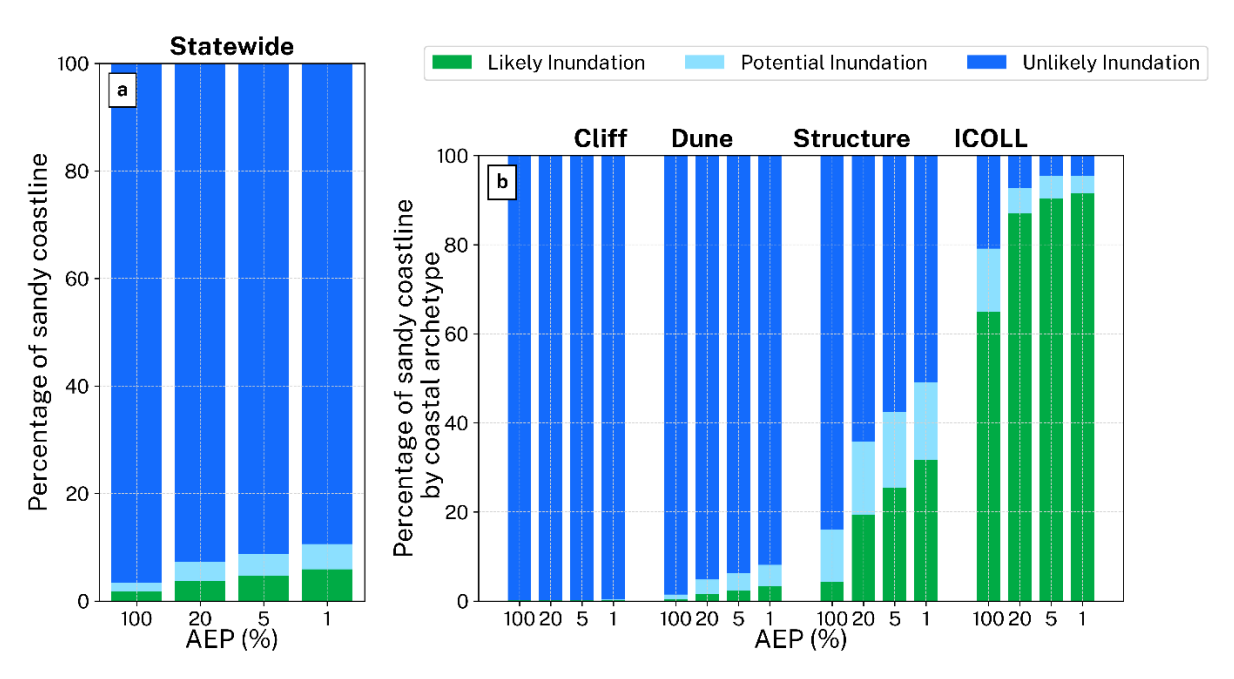


Figure 36 Current (2020) coastal overwash (shown as inundation) likelihoods at (a) statewide level and (b) by coastal archetype for 100%, 20%, 5% and 1% AEP

## Regional variability

<u>Figure 37</u> shows coastal overwash likelihoods for a nominal 1% AEP TWL by primary sediment compartment. Similar to the state-wide analyses, these results indicate that for more than 75% of transects, overwash is unlikely, particularly on the North Coast, Northern Rivers and Mid-north Coast compartments. Increased overwash likelihoods are observed from Port Stephens to the south, with at least 8% of the compartment transects (maximum of 14% of transects) currently experiencing likely overwash for a 1% AEP TWL.

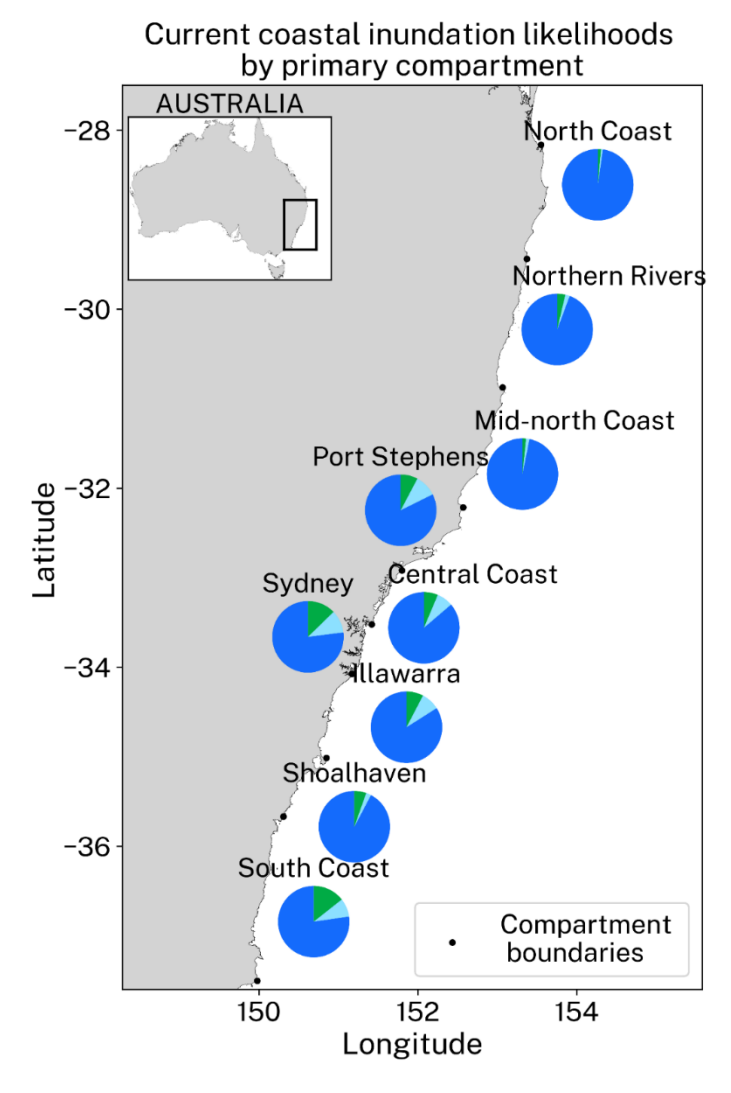


Figure 37 Regional variability of current (2020) coastal overwash (shown as inundation) likelihoods by primary compartment

Note: The legend (colours) in Figure 36 applies to this figure.

## Local scale example: Wamberal-Terrigal Beach

Wamberal–Terrigal beach on the NSW Central Coast provides an example of inundation from coastal overwash at the local beach scale. Wamberal–Terrigal beach is divided into 26 discrete 100-m spaced transects (<u>Figure 38(a)</u>). Most (17) of these transects are backed by natural and modified dunes; 4 transects at Terrigal beach are backed by coastal structures and 2 are backed by ICOLLs (Wamberal and Terrigal lagoons); and higher cliff environments are present in 2 transects south of Terrigal Lagoon entrance.

#### a. Backbeach archetype b. Classification inundation likelihoods 2020 20.0 Terrigal 17.5 Lagoon 15.0 Elevation (m AHD) Wambera 12.5 10.0 7.5 5.0 2.5 0 5 10 15 20 25 c. Mapping output 2020 Transect number (south to north) Key Cliff Dune **ICOLL** Vambera Structure agoon Unlikely inundation

Figure 38 Local scale example of 83rd and 99th percentiles of the distribution for current 1% annual exceedance probability (AEP) of total water level (TWL) and classed as overwash (shown as inundation) likelihoods at Wamberal-Terrigal Beach transects by (a) backbeach archetype, (b) different overwash likelihoods (based on elevations), and (c) mapping of current overwash likelihoods

Potential inundation Likely inundation Inundation threshold

99%, 1% AEP TWL

83%, 1% AEP TWL

0

Kilometres

The elevation of backbeach overwash thresholds along Wamberal–Terrigal Beach is shown in Figure 38(b), along with the predicted alongshore elevation of the 1% AEP TWL for two percentiles of the distribution of modelled TWLs: 83% and 99%. Using the probabilistic likelihood classification defined in Appendix A: Methods (see Table 8), the hazard (that is, total water level, TWL) and degree of exposure (backbeach overwash thresholds) determine the current overwash likelihood classes along the beach (Figure 38(c)). Most dunes and cliff transects have likelihood classifications of unlikely overwash, largely because their higher inundation thresholds provide a buffer against coastal overwash. Conversely, the ICOLLs and the sea wall structure at the southern end of the beach are susceptible to overwash for present-day conditions (that is, likely overwash). These locations are already known to experience inundation from coastal overwash during major storm events, as occurred in Terrigal Lagoon (Figure 39 panels a and c) and at Terrigal Beach (Figure 39 panels b and d) following the June 2016 east coast low.

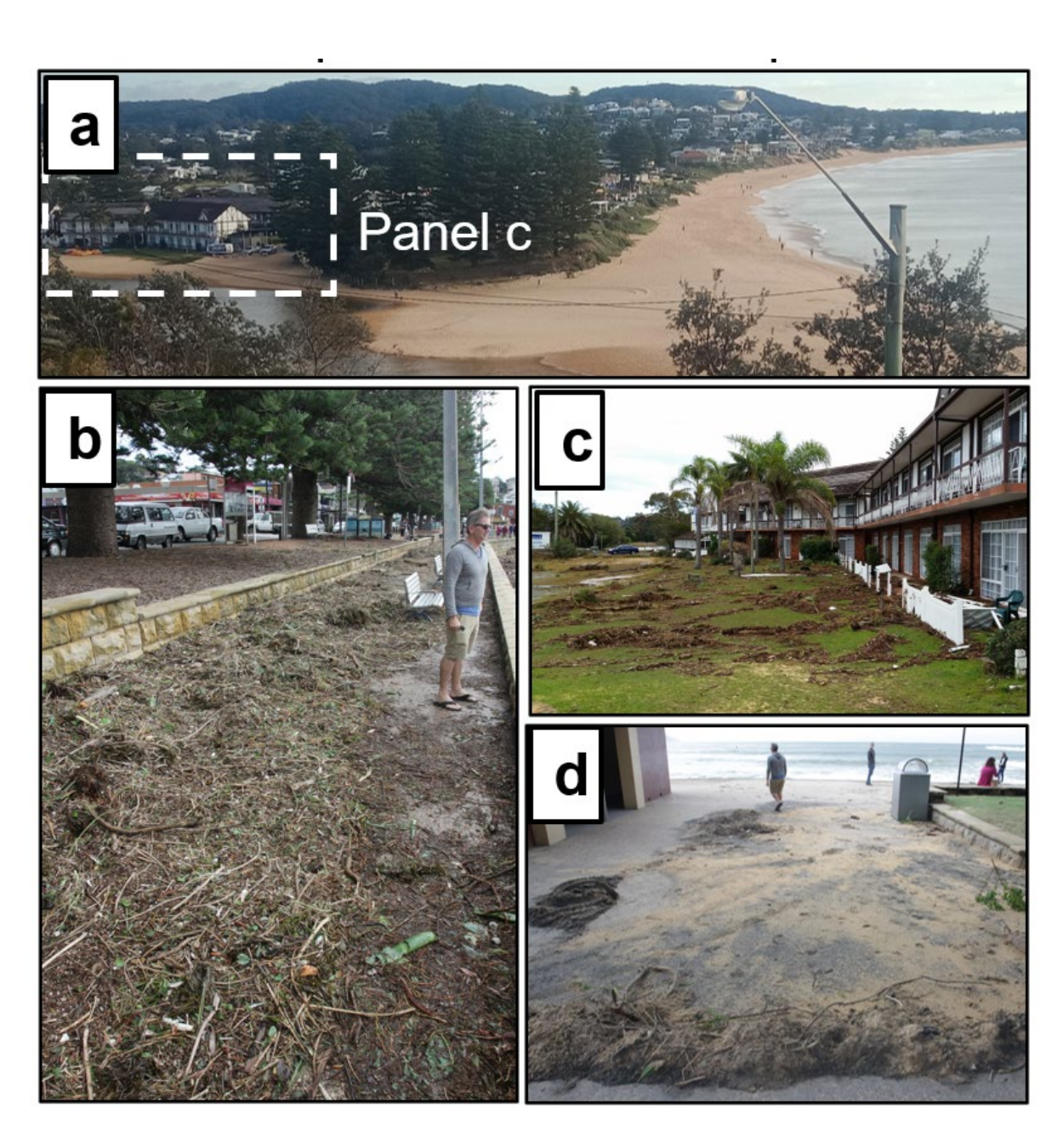


Figure 39 Coastal overwash and inundation event in Terrigal Beach and Lagoon after the June 2016 east coast low. Panels a (photo: Chris Drummond) and c show photos of Terrigal Lagoon (photo: DCCEEW), and panels b and d depict coastal structures in South Terrigal (photo: DCCEEW)

## Future coastal overwash likelihoods

### State-wide overview

Similar to the results shown for current state-wide likelihoods (<u>Figure 34</u>), this section presents the decadal evolution (2020 to 2150) of coastal overwash and inundation likelihoods for SSP1-2.6, SSP2-4.5 and SSP3-7.0 scenarios for present-day 1% AEP TWL plus SLR forcing. Further analyses and interpretation of results focus on the *likely overwash* category. Broadly, results for the 3 scenarios indicate only minor (< 1%) increases in impacts before 2050.

For the SSP1-2.6 scenario, <u>Figure 40</u>(a) shows an increase in sandy coastline exposure to likely overwash, from 6% (51 km of coastline) of the state's transects at present to 9% (82 km of coastline) by 2150. Similarly, for the SSP2-4.5 scenario, <u>Figure 40</u>(b) indicates increases in sandy coastline exposure to likely overwash, from 6% (51 km of coastline) of the state's transects at present to 12% (100 km of coastline) by 2150. For the SSP3-7.0 scenario, <u>Figure 40</u>(c) shows that sandy coastline exposure to likely overwash increases from 9% (81 km of coastline) in 2100 to 14% (124 km of coastline) in 2150.

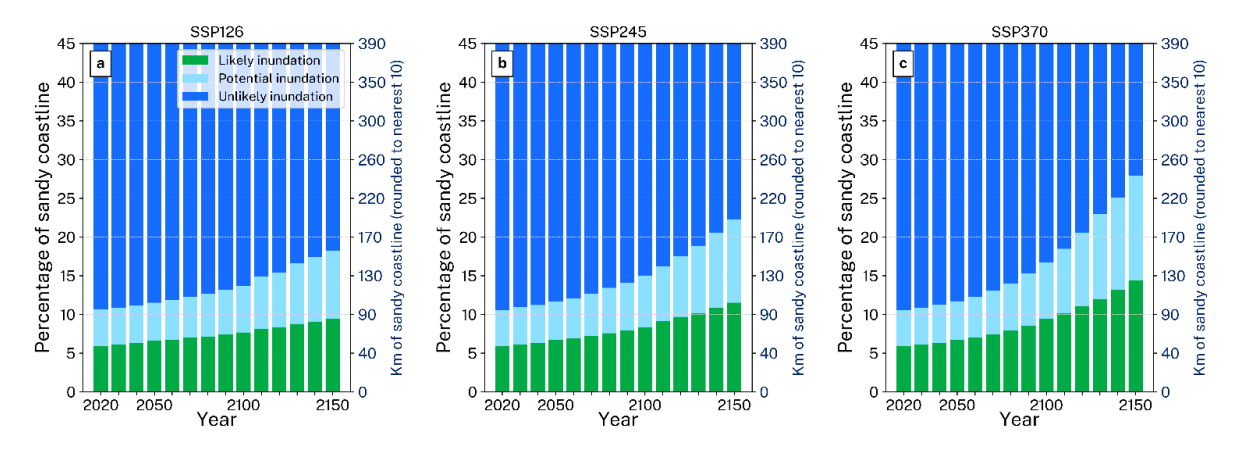


Figure 40 Decadal evolution (2020 to 2150) of coastal overwash (shown as inundation) likelihoods considering present 1% annual exceedance probability of total water level distributions plus SLR, showing results for (a) low emissions (SSP1-2.6) SLR, (b) medium emissions (SSP2-4.5), and (c) high emissions (SSP3-7.0) SLR scenarios

Note: Percentage of sandy coastline is limited to 45% to facilitate visualisation of the results.

## Future likelihoods by sediment compartment

The percentage of transects (by primary sediment compartment) experiencing likely overwash by 2020, 2040, 2070, 2100 and 2150 are shown for SSP1-2.6 (Figure 41(a)), SSP2-4.5 (Figure 41(b)) and SSP3-7.0 (Figure 41(c)) scenarios at current 1% AEP TWL plus SLR forcing. Results show lower percentages of sandy shoreline exposure in northern compartments, with increased overwash risk from the Central Coast to the south. Similar to the state-wide analysis, these results indicate only small increases between current (2020) and mid-century (2040 to 2070) conditions. Significant increases in likely coastal overwash start from around 2100. This is particularly true for the Port Stephens, Central Coast, Sydney and South Coast compartments. Lower impacts are projected for the SSP1-2.6 and SSP2-4.5 scenarios, while SSP3-7.0 conditions show a nearly 2-fold increase (from 2020 to 2150) in transects subjected to likely overwash from the Central Coast to the south.

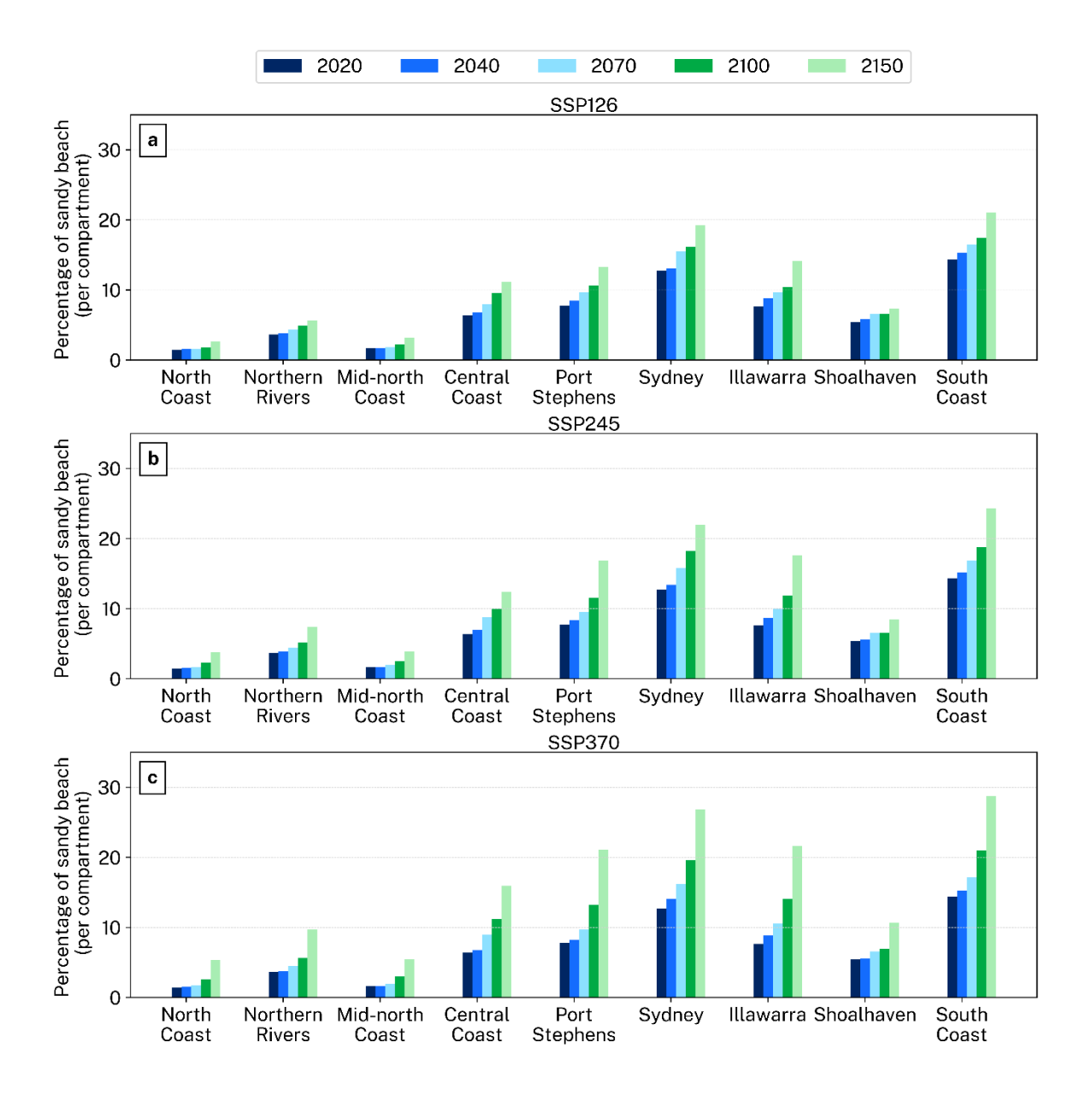


Figure 41 Future evolution of sandy coastline exposure to *likely* overwash by primary compartment (1% AEP TWL plus SLR) under (a) SSP1-2.6, (b) SSP2-4.5, and (c) SSP3-7.0 scenarios for the years 2020, 2040, 2070, 2100 and 2150

## Future likelihoods by coastal archetype

The evolution of likely overwash exposure was investigated for different coastal archetypes. Based on the fundamental assumption of unchanged backbeach overwash thresholds in the future, the results indicate varying levels of exposure to inundation from coastal overwash depending on the coastal setting. Notably, coastal structures – which are assumed to remain unchanged in the future – show the largest increase in coastal overwash likelihoods. These results highlight that the extent of sandy coastline backed by structures experiencing likely overwash will increase by 14% under SSP1-2.6 (Figure 42(a)), 21% under SSP2-4.5 (Figure 42(b)), and 28% under SSP3-7.0 by 2150 (Figure 42(c)). In contrast, likelihoods are negligible for sandy coastline backed by cliffs, while dune crest overwash may increase to 7% (SSP1-2.6), 9% (SSP2-4.5) and 12%

(SSP3-7.0) of the sandy coastline backed with dunes by 2150, compared to 3% at present (Figure 34). Berm heights across ICOLL settings are also likely to continue experiencing overwash in the future, although the future evolution of these features as sea levels rise is complex and will likely result in varying inundation thresholds.

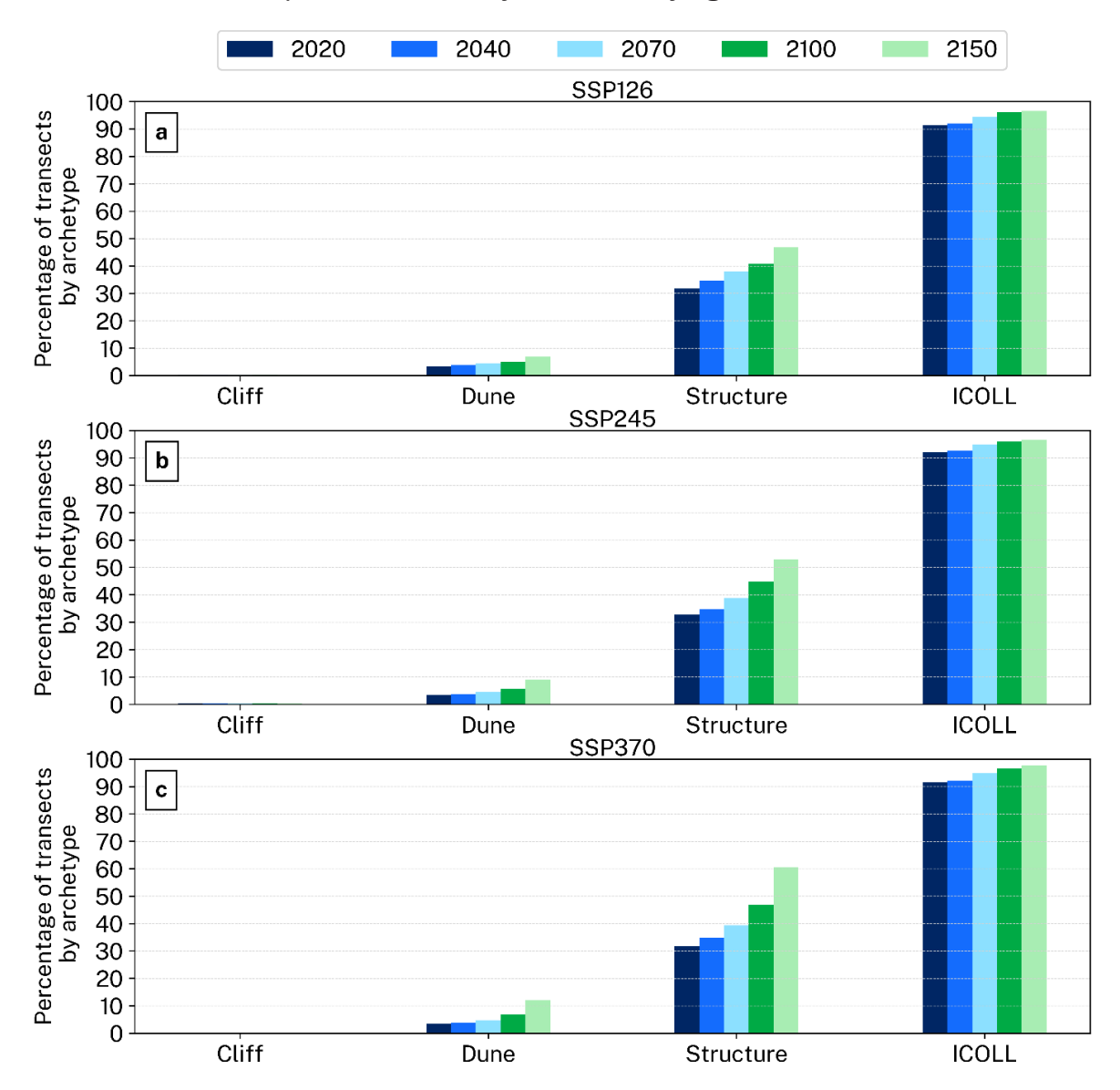


Figure 42 Future evolution of exposure to *likely* overwash by coastal backbeach archetype (1% AEP TWL plus SLR) under (a) SSP1-2.6, (b) SSP2-4.5 and (c) SSP3-7.0 SLR scenarios for the years 2020, 2040, 2070, 2100 and 2150

# Very high emissions scenarios and comparative insights

This section provides high-level insights into the implications of very high emissions scenarios (medium-confidence SSP5-8.5 and low-confidence SSP5-8.5) for *likely overwash* of open coast locations (from coastal overwash of backbeach locations) in NSW. A summary of coastal overwash statistics for all SSP scenarios and inundation likelihoods is included in Appendix H.

Comparisons are drawn across all SSP scenarios, including SSP1-2.6, SSP2-4.5 and SSP3-7.0, to demonstrate how varying emissions trajectories influence future inundation risks from coastal overwash (Figure 43). By examining these scenarios, this assessment identifies the challenges posed by increasing sea levels and highlights opportunities for adaptation and mitigation to reduce long-term impacts. Exemplary results are presented for the percentage of coastline likely overwashed (Figure 43(a)) and the corresponding kilometres (Figure 43(b)) under present-day 1% AEP TWL conditions plus SLR.

Under present-day 1% AEP wave and water level conditions, approximately 6% of the NSW sandy coastline (51 km) is currently at risk, representing the baseline exposure (<u>Figure 43</u>). By 2050, the sandy coastline exposure to likely overwash increases modestly across all SSPs, reaching 7% (57 km) under SSP1-2.6, 7% (58 km) under SSP2-4.5 and SSP3-7.0, 7% (58 km) under medium-confidence SSP5-8.5, and 7% (60 km) under low-confidence SSP5-8.5.

By 2100, however, the increased exposure to likely inundation varies more widely across the scenarios (<u>Figure 43</u>). The sandy coastline exposed to likely overwash rises to 8% (66 km) under SSP1-2.6, 8% (72 km) under SSP2-4.5, 9% (81 km) under SSP3-7.0, but increases further to 10% (87 km) under medium-confidence SSP5-8.5 and 13% (110 km) under low-confidence SSP5-8.5.

By 2150, disparities between SSPs are likely to become most pronounced (<u>Figure 43</u>). Likely overwash exposure reaches 9% (82 km) of the sandy coastline under SSP1-2.6, 12% (100 km) under SSP2-4.5, and 14% (124 km) under SSP3-7.0. Exposure under medium-confidence SSP5-8.5 grows to 16% (141 km), while low-confidence SSP5-8.5 is likely to see a much larger increase to 44% (377 km).

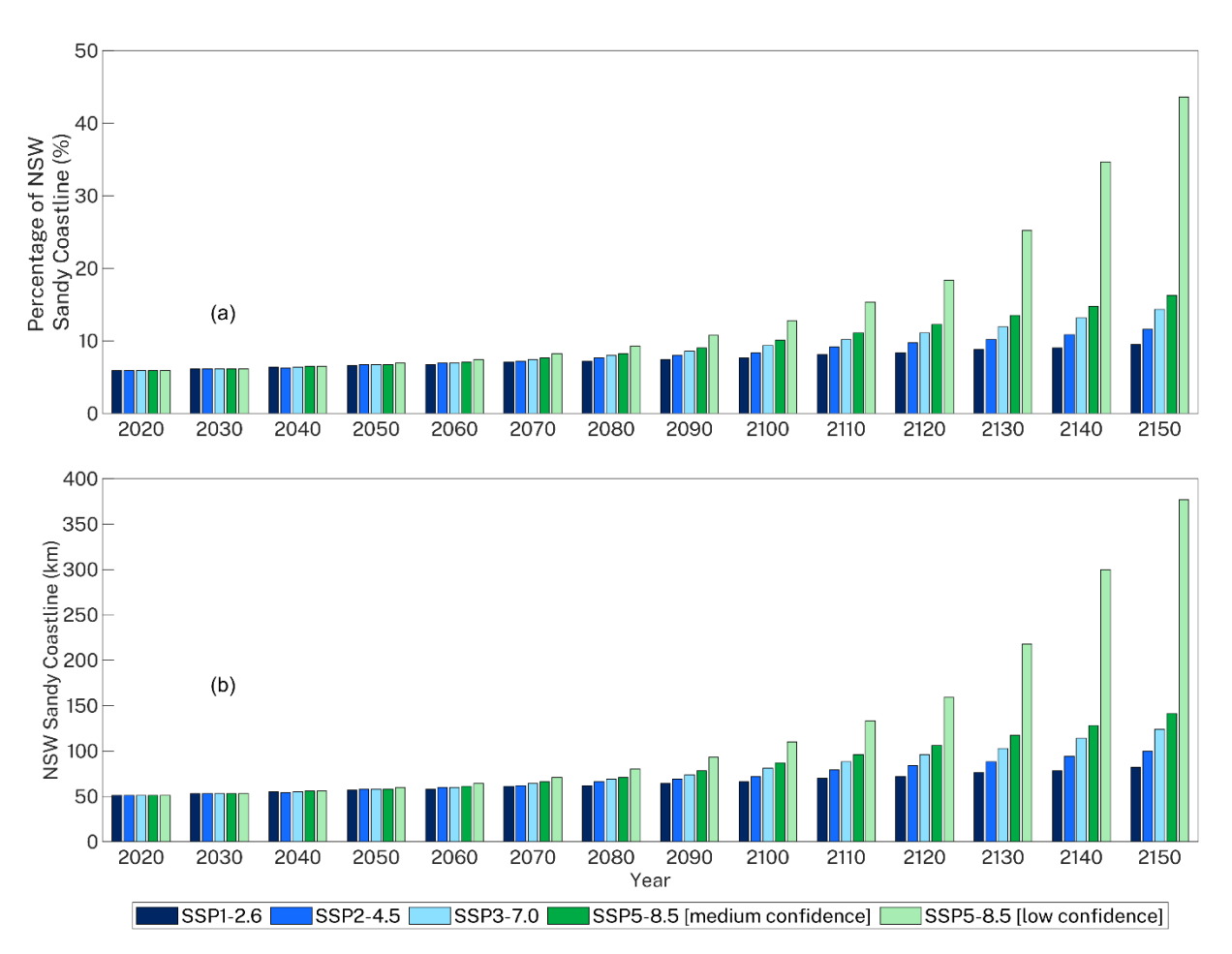


Figure 43 State-wide (a) percentage (%) and (b) kilometres of sandy coastline experiencing likely coastal overwash at 1% annual exceedance probability associated with SSP1-2.6, SSP2-4.5, SSP3-7.0, medium-confidence SSP5-8.5 and low-confidence SSP5-8.5 scenarios

Overall, coastal overwash is projected to occur more in locations with low backbeach terrain, particularly around the entrances of ICOLLs, and in locations characterised by built structures (such as sea walls). Overwash likelihood is highest from Port Stephens southwards, where these settings are more prevalent. Exposure to inundation from coastal overwash is less likely on the far North Coast.

# **Summary**

The results show that following lower emissions pathways offers comparatively more controlled increases in coastal overwash exposure, providing valuable time for adaptive planning and mitigation. For example, by 2100, the likely overwash exposure under SSP1-2.6 is 8% (66 km) of the state's sandy coastline, compared to 13% (110 km) under low-confidence SSP5-8.5. This contrast highlights the benefits of reducing emissions and building adaptive capacity to safeguard communities and critical infrastructure.

While coastal overwash likelihood is expected to increase over time, there is a window of opportunity to take action, particularly over the next few decades where there is minimal increase in overwash hazards.

## 4.3 Estuarine inundation

## State-wide results

As outlined in Appendix A.5: <u>Approach</u>, this study generated map layers for 4 water-level exceedance scenarios for every estuary in NSW under current conditions (2020) and at decadal intervals out to 2150 for the assessed SLR scenarios. In this section, for estuarine inundation hazard, the extracted exceedance probabilities are discussed in terms of their equivalent annual frequencies. For example, the 50%, 10%, 1% and 0.27% (annual) exceedance probabilities are equivalent to exceedance inundation frequencies of 182.5 days/year, 36.5 days/year, 3.6 days/year and 1 day/year, respectively. For each time step and scenario, the exposure of existing property and infrastructure to potential estuarine inundation is quantified (see <u>Table 20</u> for present-day exposure statistics). For each inundation scenario, connected areas and isolated areas (that is, areas which are lower than the mapped water surface but separated from the estuarine water body by more than 5 m) are mapped separately.

An example of the state-wide mapping output is shown in <u>Figure 44</u>, showing the northern, central and southern sections of coastline. This figure displays the current mapped extent of NSW estuaries, along with the extent of inundation at the 1 day per year exceedance level in 2050, 2100 and 2150 under the SSP3-7.0 scenario.



Figure 44 Map of the northern (left), central (centre) and southern (right) sections of NSW coastline showing the current mapped extent of NSW estuaries along with the extent of inundation at 1 day per year exceedance level in 2020, 2050, 2100 and 2150 under SSP3-7.0 scenario

Source: The base map uses data from Earthstar Geographics, the New Zealand National Institute of Water and Atmospheric Research (NIWA), Geosciences Australia, ESRI, GEBCO, Garmin, and NaturalVue.

## Area inundated

As sea levels rise over time, the total state-wide area of inundation associated with each scenario gradually increases. The total state-wide area of inundation associated with each scenario is presented in <u>Figure 45(a)</u> (SSP1-2.6), <u>Figure 45(b)</u> (SSP2-4.5) and Figure 45(c) (SSP3-7.0).

The total state-wide area of estuary foreshore inundation (1 day/year) increases from 770 km² in 2020 to 1,080 km² in 2050, 1,890 km² in 2100, and 2,920 km² in 2150 under a low emissions pathway (SSP1-2.6). Under the medium emissions pathway (SSP2-4.5), the total state-wide area of inundation (1 day/year) rises to around 1,120 km² in 2050, 2,045 km² in 2100, and 3,170 km² in 2150. Finally, under a high emissions pathway (SSP3-7.0), the total state-wide area increases to about 1,160 km² in 2050, 2,290 km² in 2100, and 3,480 km² in 2150.

The 10 estuaries with the greatest increases in inundated area by 2150 for each climate change scenario based on annual recurrence frequency are shown in <u>Figure 46</u>(a) (SSP1-2.6), <u>Figure 46</u>(b) (SSP2-4.5), and <u>Figure 46</u>(c) (SSP3-7.0). These 10 estuaries include the Clarence River, Richmond River, Macleay River, Hastings River, Manning River, Tweed River, Shoalhaven River, Wallis Lake and Myall River. The largest increases occur in the larger coastal rivers, which are characterised by extensive low-lying floodplain areas (for example, the Clarence and Richmond Rivers).

For the exposure assessment to estuarine inundation, a 10-m elevation contour was used to clip all asset inputs for the estuarine inundation exposure statistics. Regarding buildings exposure, structures without an assigned address were excluded to reduce false positives, though secondary structures (for example, sheds, water tanks, carports) at locations with an assigned address remain in the dataset. Because several building categories (for example, residential, commercial, recreational, community use) were considered, the buildings exposure results do not represent major residential buildings only. Further, for the buildings exposure analysis, only buildings projected to experience more than 5 m² of estuarine inundation were included in the results. Other buildings exposure assessment approaches may select and utilise available data differently and for distinct purposes, leading to varying outcomes depending on their filtering processes, underlying assumptions, specific focus, and other methodological or contextual factors.

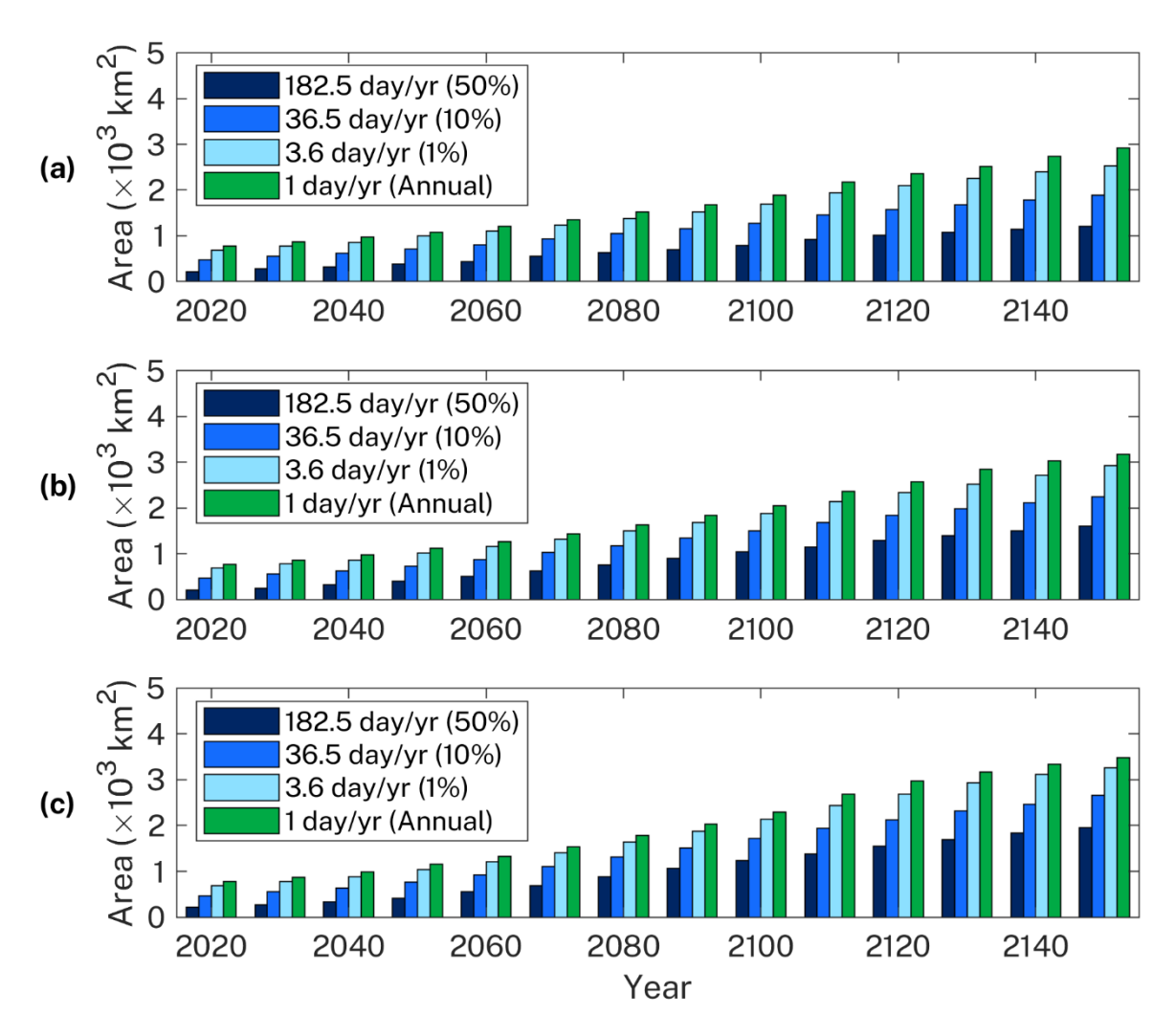


Figure 45 State-wide estuarine inundation area increasing over time (2020 to 2150) for each exceedance inundation frequency under (a) SSP1-2.6, (b) SSP2-4.5 and (c) SSP3-7.0 scenarios

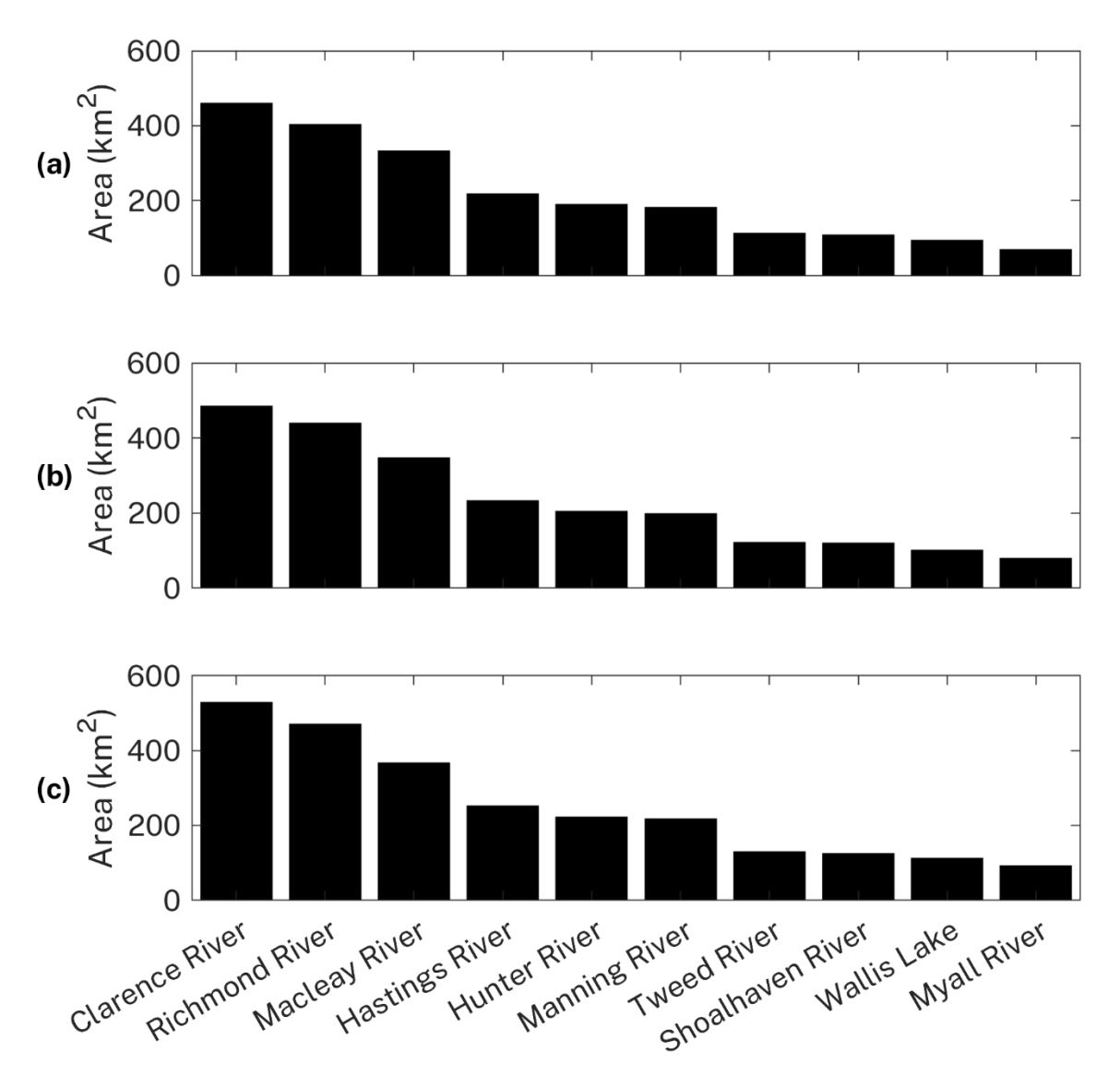


Figure 46 Estuaries with the greatest increases in inundated area on an annual frequency (1 day/year) by 2150 under (a) SSP1-2.6, (b) SSP2-4.5, and (c) SSP3-7.0

# Buildings exposed to inundation

On a state-wide basis, the results indicate approximately 3,345 buildings are currently exposed to estuarine inundation occurring at one day per year frequency (<u>Table 20</u>). It is possible that many of these structures have raised floor levels and are thus adapted to the current frequency of inundation. For the same inundation frequency, exposure is projected to increase to around 6,900 buildings by 2050, 50,700 buildings by 2100, and 145,300 buildings by 2150 under the low emissions pathway scenario (SSP1-2.6, <u>Figure 47(a)</u>). Under the medium emissions pathway (SSP2-4.5, <u>Figure 47(b)</u>) and high emissions pathway (SSP3-7.0, <u>Figure 47(c)</u>) scenarios, exposure rises to, respectively, 7,400 and 8,750 buildings by 2050, 64,900 and 86,700 buildings by 2100, and 177,400 and 213,000 buildings by 2150.

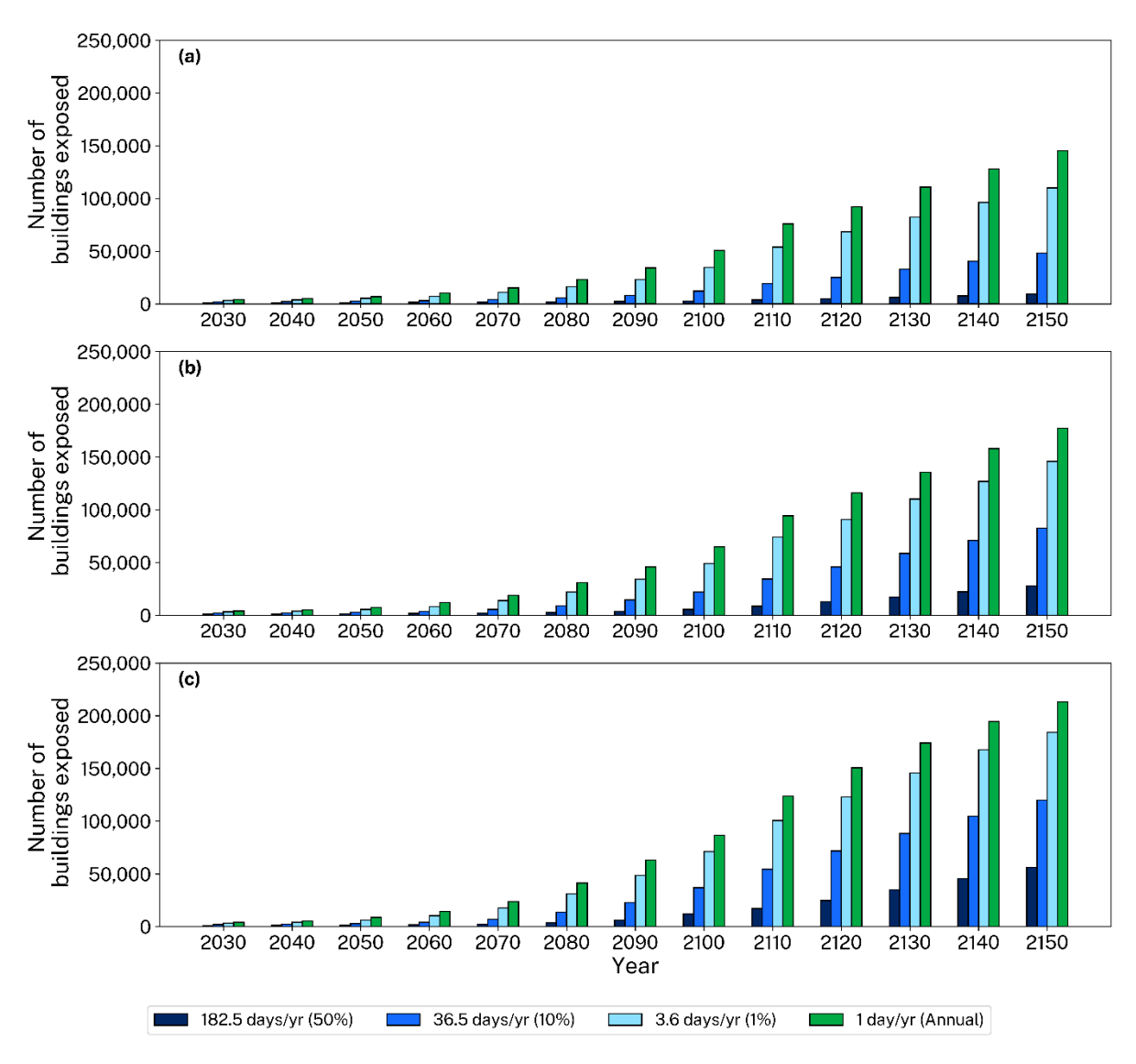


Figure 47 State-wide building counts exposed at different exceedance inundation frequencies, from 2030 to 2150, under (a) SSP1-2.6, (b) SSP2-4.5, and (c) SSP3-7.0

In terms of total addresses, the results indicate that approximately 7,120 addresses are currently exposed to estuarine inundation at one day per year frequency (<u>Table 20</u>). This exposure is projected to increase to around 14,400 addresses by 2050, 111,500 by 2100, and 359,400 by 2150 under SSP1-2.6 (<u>Figure 48(a)</u>). Under SSP2-4.5 (<u>Figure 48(b)</u>) and SSP3-7.0 (<u>Figure 48(c)</u>), exposure rises to, respectively, 15,400 and 18,000 addresses by 2050, 143,900 and 204,100 by 2100, and 447,700 and 540,700 by 2150. Many of these addresses are unlikely to be directly inundated as they include multistorey buildings, although ground-level and sub-ground-level infrastructure (for example, access and common areas, garages) may still be impacted at these addresses.

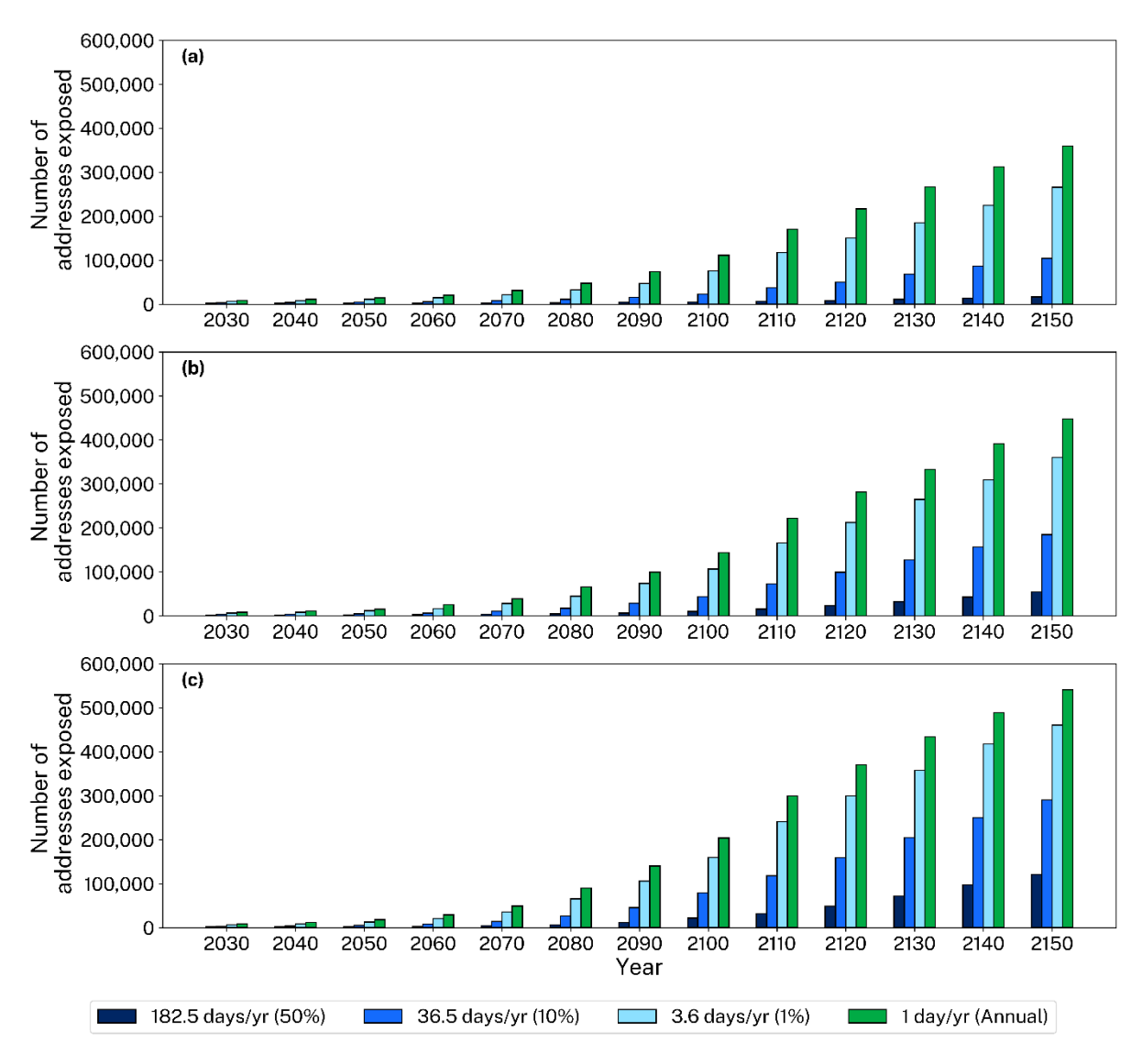


Figure 48 State-wide address counts exposed at different exceedance inundation frequencies, from 2030 to 2150, under (a) SSP1-2.6, (b) SSP2-4.5, and (c) SSP3-7.0

# Transport infrastructure

## Roads and paths

On a state-wide basis, the results indicate that approximately 355 km of roads currently experience inundation at one day per year frequency (<u>Table 20</u>). This exposure is projected to increase to around 620 km by 2050, 2,100 km by 2100, and 4,780 km by 2150 under the low emissions pathway (SSP1-2.6, <u>Figure 49(a)</u>); 670 km by 2050, 2,490 km by 2100, and 5,600 km by 2150 under the medium emissions pathway (SSP2-4.5, <u>Figure 49(b)</u>); and 710 km by 2050, 3,110 km by 2100, and 6,620 km by 2150 under the high emissions pathway (SSP3-7.0, Figure 49(c)).

The results also indicate that the length of paths currently exposed state-wide is 32 km (<u>Table 20</u>). Under the SSP1-2.6 scenario, this increases to 57 km by 2050, 214 km by 2100, and 450 km by 2150 (<u>Figure 50(a)</u>). Under the SSP2-4.5 scenario, this exposure is

projected to rise to 60 km by 2050, 255 km by 2100, and 513 km by 2150 (<u>Figure 50(b)</u>). Under the SSP3-7.0 scenario, the results indicate that 66 km of paths are exposed by 2050, 316 km by 2100, and 580 km by 2150 (Figure 50(c)).

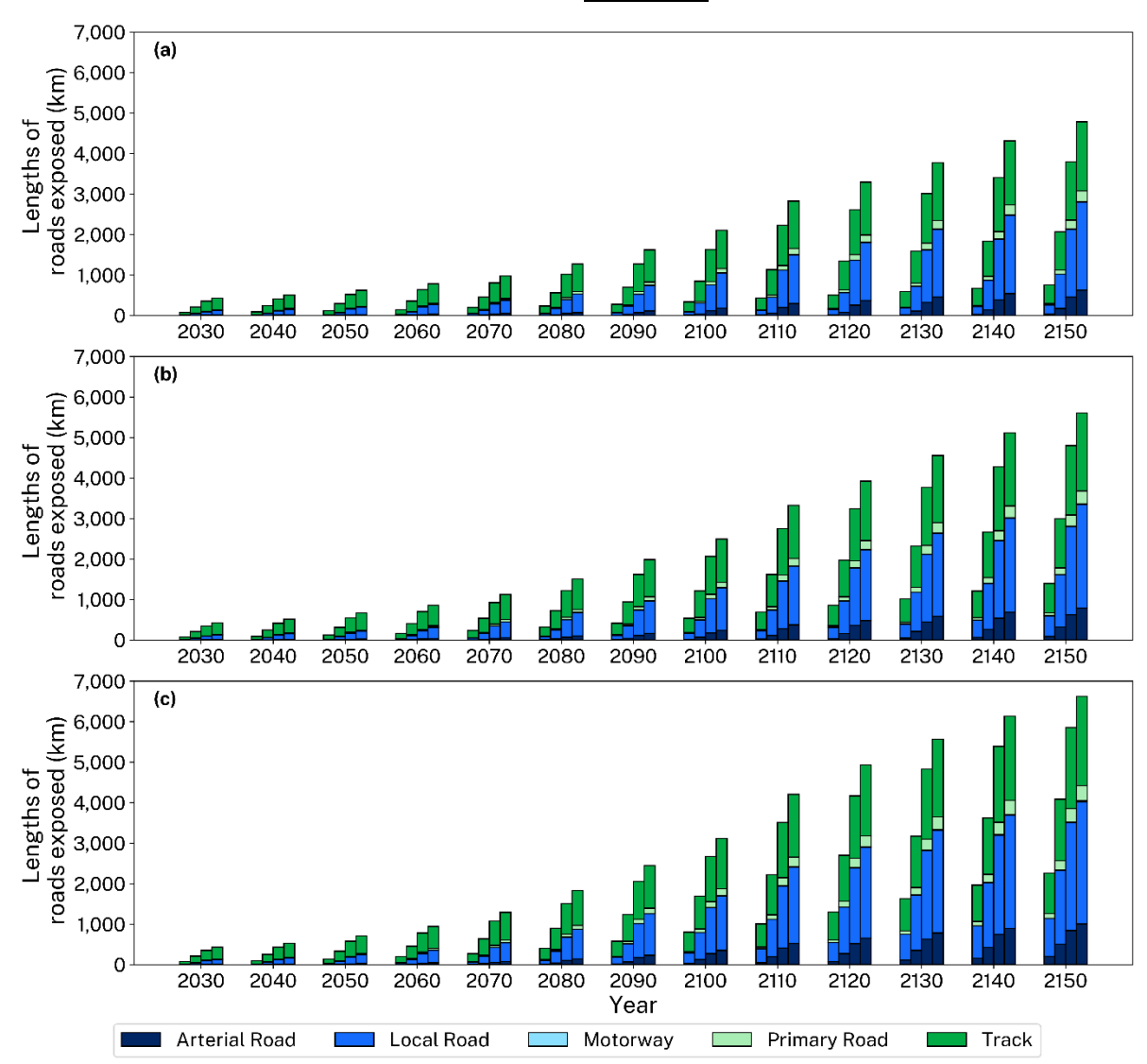


Figure 49 State-wide road lengths (km) by type exposed at different exceedance inundation frequencies (from right to left: 1 day/year (annual), 3.6 days/year (1%), 36.5 days/year (10%) and 182.5 days/year (50%)), from 2030 to 2150, under (a) SSP1-2.6, (b) SSP2-4.5 and (c) SSP3-7.0

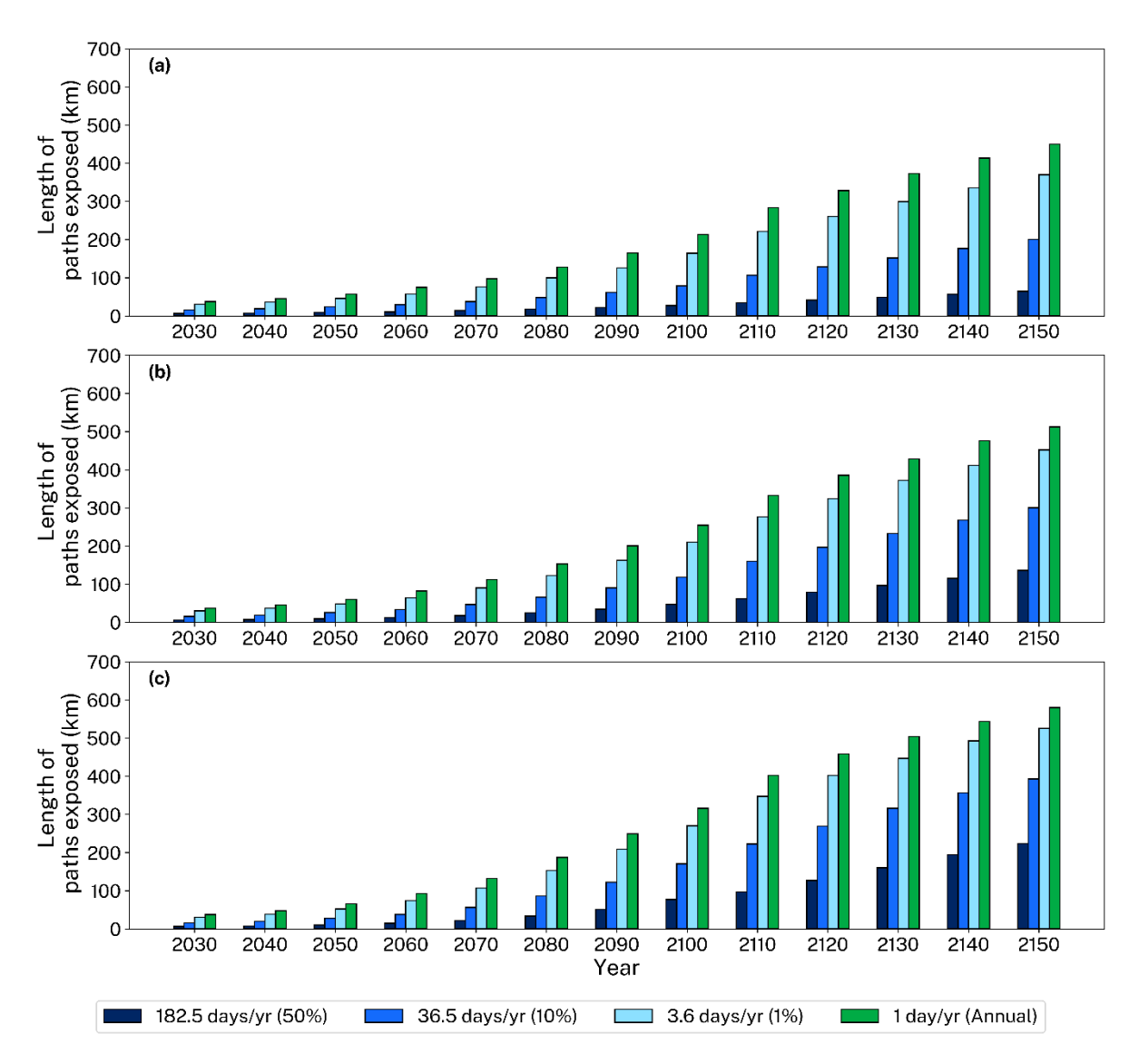


Figure 50 State-wide path lengths (km) exposed at different exceedance inundation frequencies, from 2030 to 2150, under (a) SSP1-2.6, (b) SSP2-4.5 and (c) SSP3-7.0

## Rail

On a state-wide basis, the results indicate that approximately 2 km of rail lines (both heavy and light rail) currently experience inundation at one day per year frequency (<u>Table 20</u>). For the same inundation frequency, this exposure is projected to rise to around 7 km by 2050, 38 km by 2100, and 159 km by 2150 under the low emissions pathway (SSP1-2.6, <u>Figure 51(a)</u>); 7 km by 2050, 49 km by 2100, and 207 km by 2150 under the medium emissions pathway (SSP2-4.5, <u>Figure 51(b)</u>); and 8 km by 2050, 75 km by 2100, and 272 km by 2150 under the high emissions pathway (SSP3-7.0, <u>Figure 51(c)</u>).

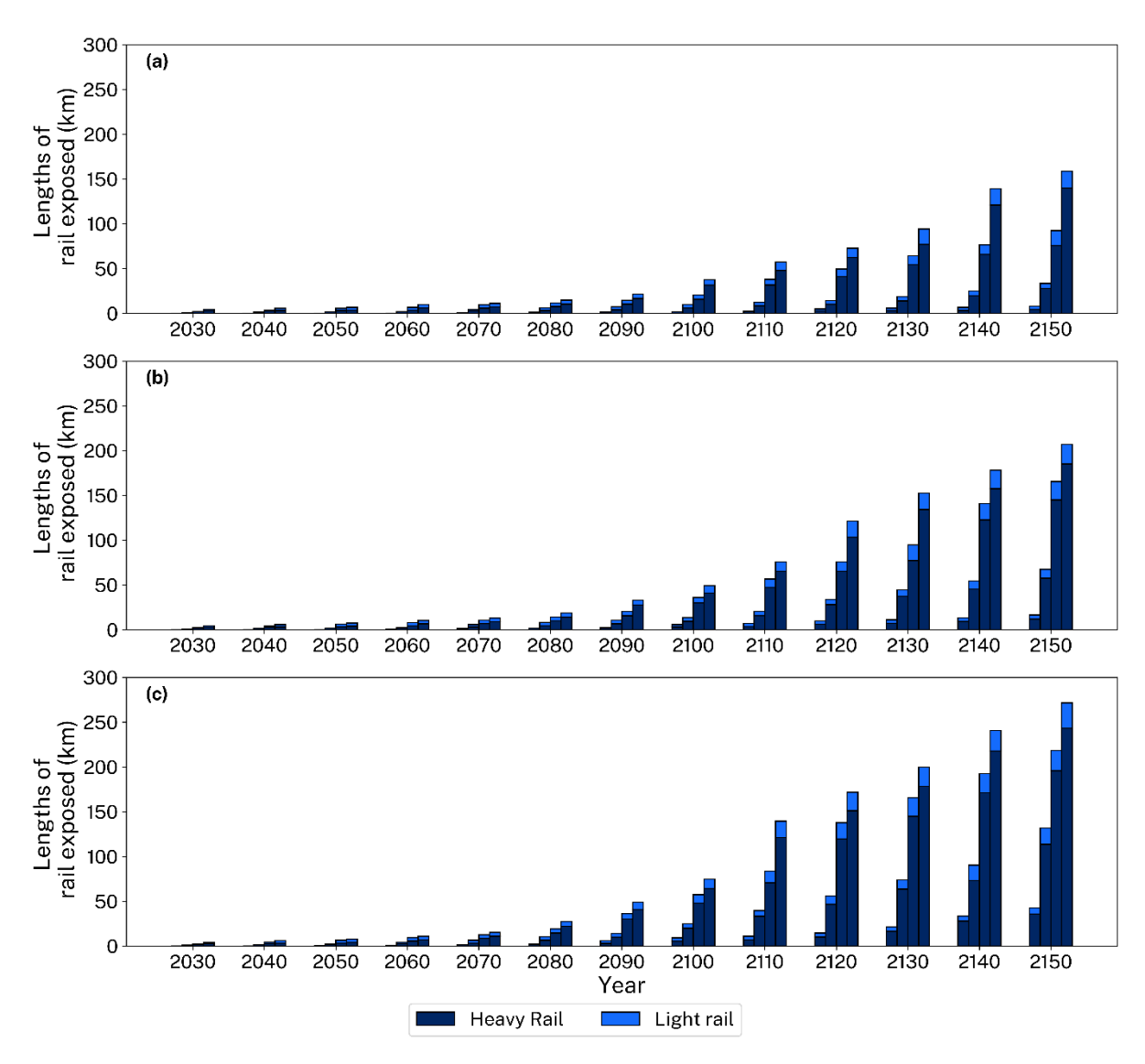


Figure 51 State-wide rail lengths (km) by type exposed over time (2030 to 2150) at different exceedance inundation frequencies (from right to left: 1 day/year (annual), 3.6 days/year (1%), 36.5 days/year (10%), and 182.5 days/year (50%) exceedance) associated with (a) SSP1-2.6, (b) SSP2-4.5 and (c) SSP3-7.0

## Airports and runways

There is currently one small airport (in Macleay) exposed to estuarine inundation in NSW and a state-wide total of 3.5 km of exposed runway (<u>Table 20</u>). The number of exposed airports is projected to remain at one by 2050, and increase to 6 by 2100, and to 16 by 2150 under SSP1-2.6 (<u>Figure 52(a)</u>). Under the SSP2-4.5 scenario, the number of exposed airports remains at one by 2050, and increases to 8 by 2100, and to 18 by 2150 (<u>Figure 52(b)</u>). Under SSP3-7.0, this number is estimated to remain at one by 2050, and to rise to 9 by 2100, and to 20 by 2150 (<u>Figure 52(c)</u>).

There are currently 3.5 km of runways state-wide that are exposed to inundation at one day per year frequency (<u>Table 20</u>). For the same inundation frequency, the length of exposed runway is projected to increase to 6 km by 2050, 23 km by 2100, and 52 km by 2150 under SSP1-2.6 (<u>Figure 53(a)</u>). Under SSP2-4.5, exposed runway length rises to

6 km by 2050, 24 km by 2100, and 63 km by 2150 (<u>Figure 53(b)</u>). Under SSP3-7.0, the length of exposed runway increases to 6 km by 2050, 37 km by 2100, and 85 km by 2150 (Figure 53(c)).

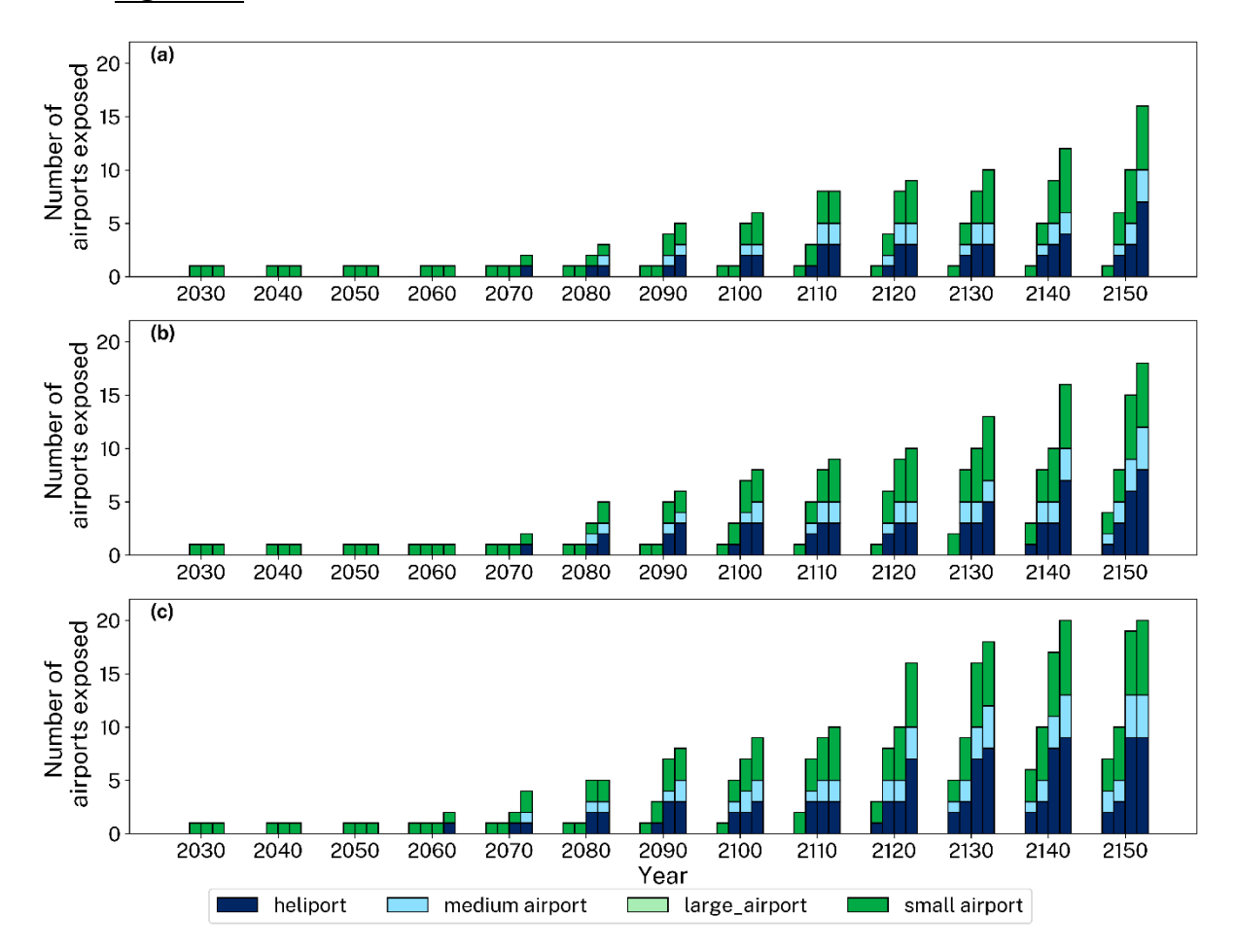


Figure 52 State-wide airports by type exposed over time (2030 to 2150) at different exceedance inundation frequencies (from right to left: 1 day/year (annual), 3.6 days/year (1%), 36.5 days/year (10%), and 182.5 days/year (50%) exceedance) associated with (a) SSP1-2.6, (b) SSP2-4.5 and (c) SSP3-7.0

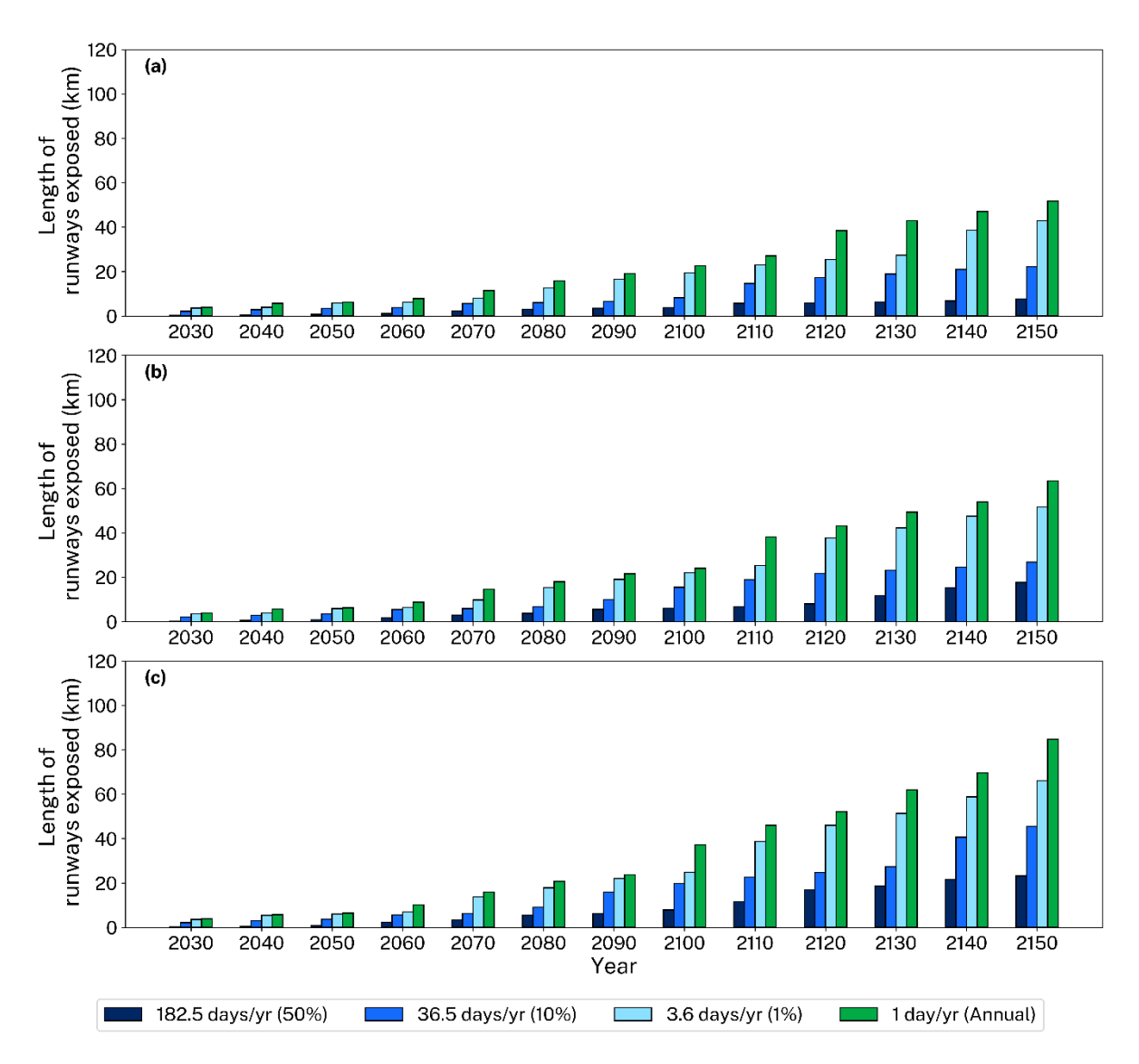


Figure 53 State-wide runway lengths (km) exposed at different exceedance inundation frequencies, from 2030 to 2150, under (a) SSP1-2.6, (b) SSP2-4.5 and (c) SSP3-7.0

# Aboriginal cultural heritage sites

The number of identified Aboriginal cultural heritage sites exposed to estuarine inundation (at 1 day/year frequency) on a state-wide basis is currently around 611 (<u>Table 20</u>). This number is projected to increase to 831 by 2050, 1,461 by 2100, and 2,596 by 2150 under SSP1-2.6 (<u>Figure 54(a)</u>). Under SSP2-4.5, the number of exposed heritage sites is estimated to rise to 865 by 2050, 1,621 by 2100, and 2,951 by 2150 (<u>Figure 54(b)</u>). Under SSP3-7.0, the number of exposed sites increases to 897 by 2050, 1,913 by 2100, and 3,408 by 2150 (Figure 54(c)).

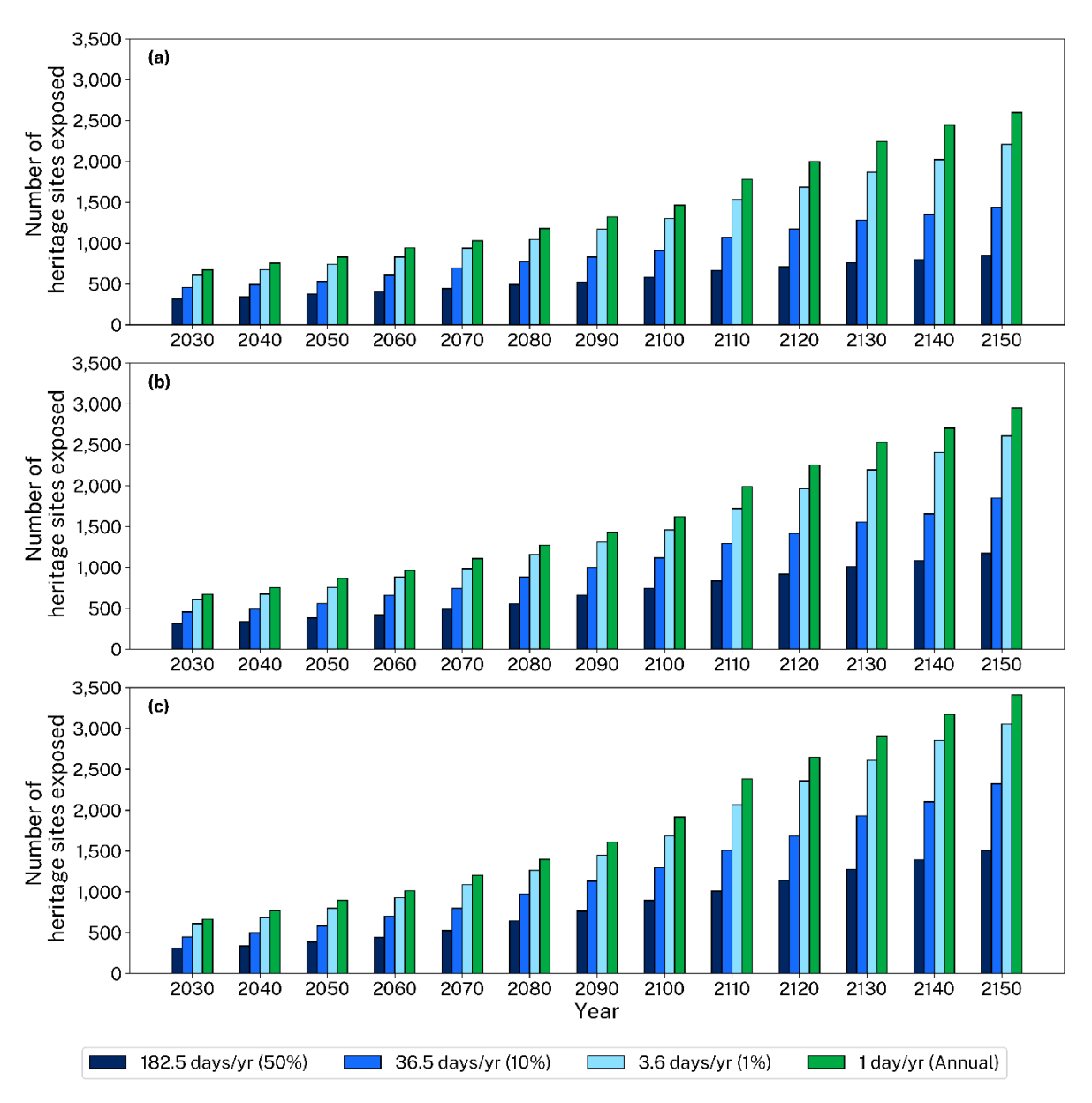


Figure 54 State-wide exposure of Aboriginal cultural heritage sites at different exceedance inundation frequencies, from 2030 to 2150, under (a) SSP1-2.6, (b) SSP2-4.5 and (c) SSP3-7.0

### Critical infrastructure

#### **Electricity transmission lines**

The length of exposed overhead and underground electricity transmission lines is currently around 395 km and 13 km, respectively, for inundation that would be exceeded annually (<u>Table 20</u>). For the one day/year exceedance inundation frequency, these numbers are projected to increase to approximately 625 km of overhead and 21 km of underground lines by 2050, 2,175 km of overhead and 115 km of underground lines by 2100, and 4,685 km of overhead and 405 km of underground lines by 2150 under SSP1-2.6 (<u>Figure 55(a)</u>); 660 km of overhead and 22 km of underground lines by 2050, 2,550 km of overhead and 145 km of underground lines by 2100, and 5,440 km of overhead and 495 km of underground lines by 2150 under SSP2-4.5 (Figure 55(b)); and

705 km of overhead and 23 km of underground lines by 2050, 3,100 km of overhead and 215 km of underground lines by 2100, and 6,405 km of overhead and 620 km of underground lines by 2150 under SSP3-7.0 (Figure 55(c)).

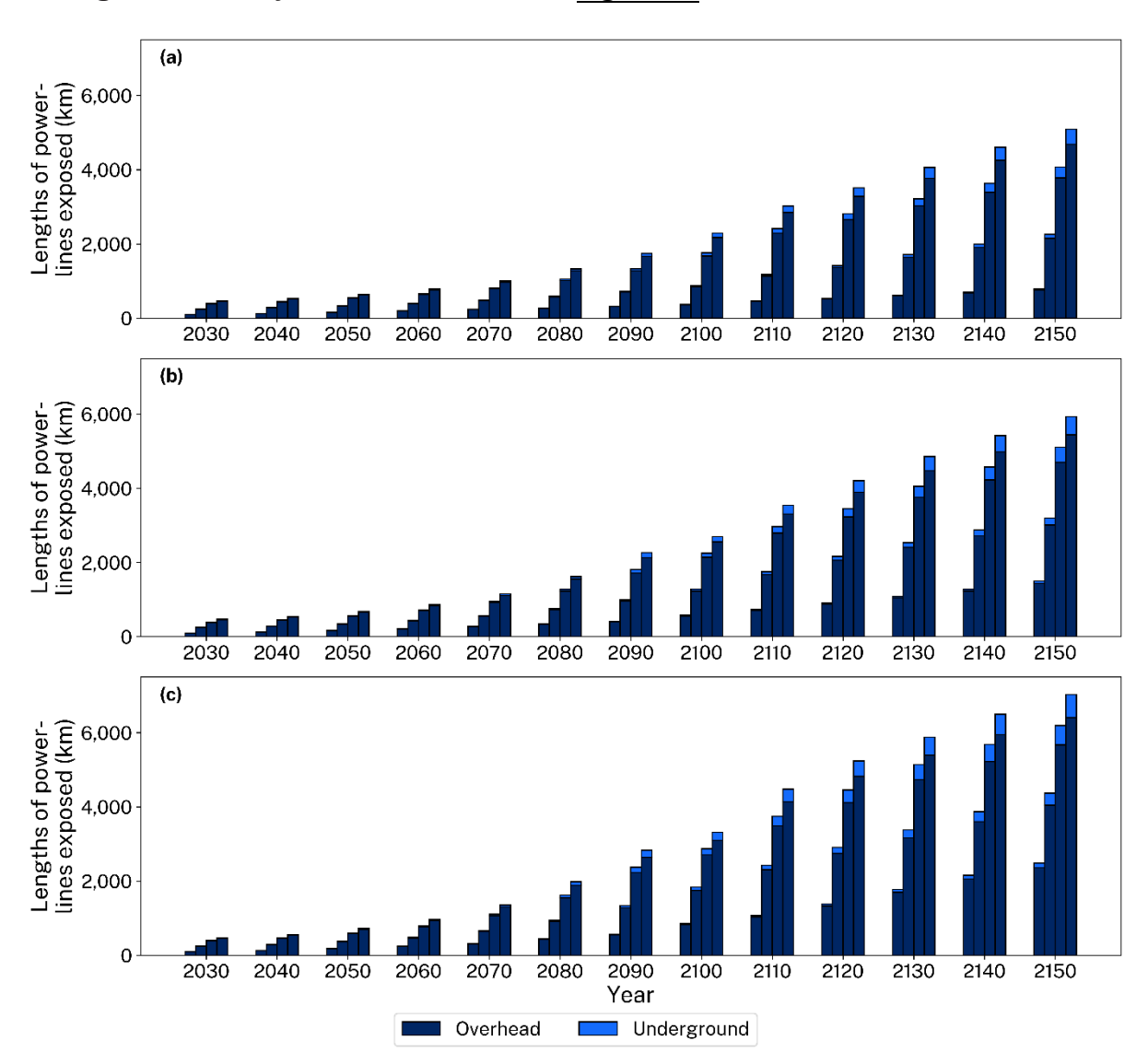


Figure 55 State-wide exposure of powerline length (km) by type over time (2030 to 2150) at different exceedance inundation frequencies (from right to left: 1 day/year (annual), 3.6 days/year (1%), 36.5 days/year (10%) and 182.5 days/year (50%) exceedance) associated with (a) SSP1-2.6, (b) SSP2-4.5 and (c) SSP3-7.0

#### Critical infrastructure sites

Critical infrastructure sites are categorised into emergency services, schools and universities, correctional facilities and courthouses, and hospitals. Currently, there are 2 exposed critical infrastructure sites on a state-wide basis, and these are in the emergency services category (<u>Table 20</u>). The total number of critical infrastructure sites exposed to inundation is projected to increase to 4 by 2050, 40 by 2100, and 142 by 2150 under SSP1-2.6 (<u>Figure 56a</u>); 4 by 2050, 55 by 2100, and 165 by 2150 under SSP2-4.5 (<u>Figure 56a</u>); and 6 by 2050, 72 by 2100, and 212 by 2150 under SSP3-7.0 (Figure 56c).

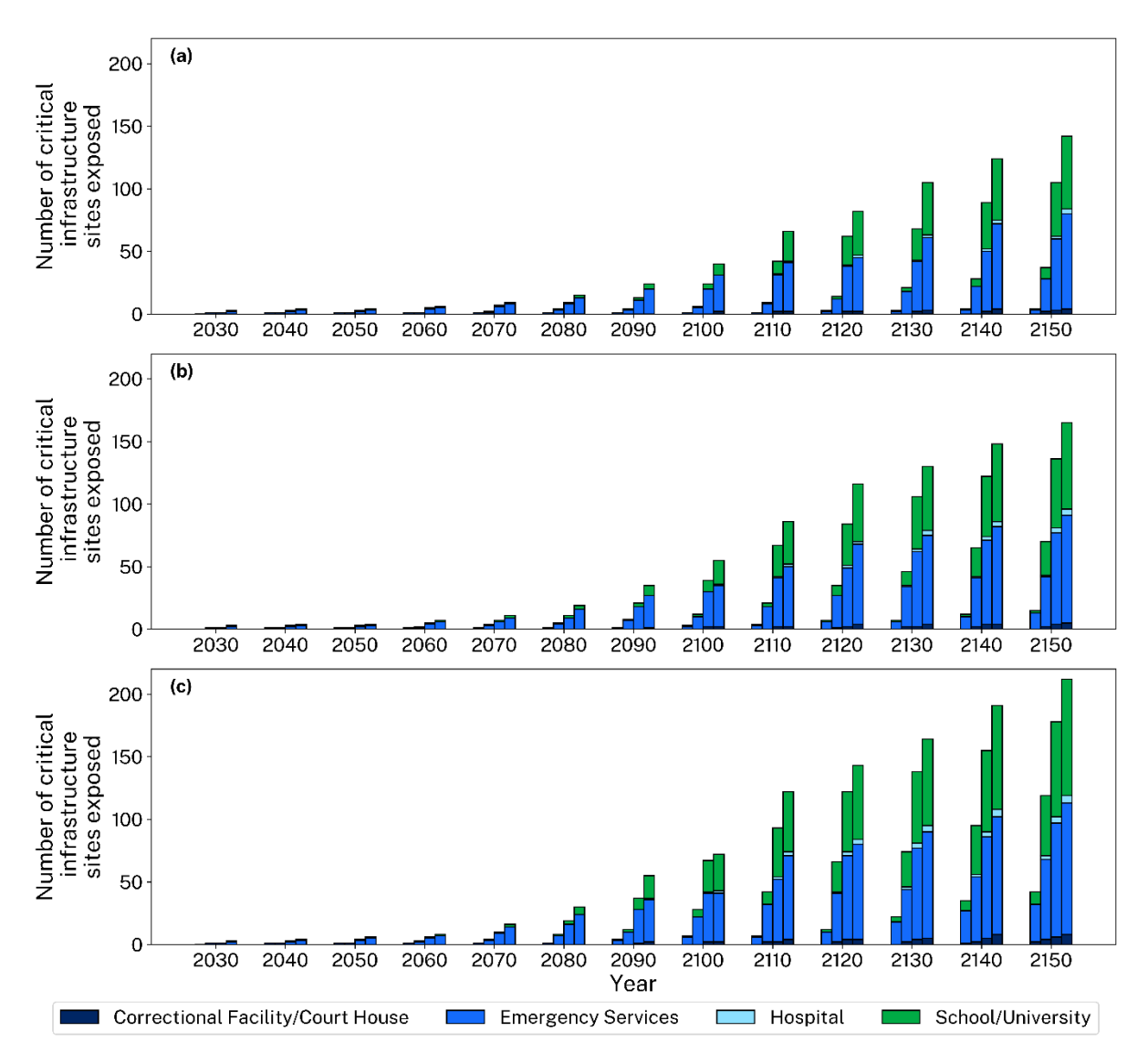


Figure 56 State-wide counts of critical infrastructure sites, by category, exposed over time (2030 to 2150) at different exceedance inundation frequencies (from right to left: 1 day/year (annual), 3.6 days/year (1%), 36.5 days/year (10%), and 182.5 days/year (50%) exceedance) under (a) SSP1-2.6, (b) SSP2-4.5 and (c) SSP3-7.0

# Very high emissions scenarios and comparative insights

This section provides an overview of estuarine inundation exposure to current conditions (2020) and projected exposures under all SSPs (SSP1-2.6, SSP2-4.5, SSP3-7.0, medium-confidence SSP5-8.5 and low-confidence SSP5-8.5) for a few selected future years. The analysis underscores how emissions trajectories shape the rate and extent of future exposure, with slower increases up to 2030 to 2040 and more pronounced growth thereafter. As examples, results for building exposure, critical infrastructure, heritage sites and road exposure are presented for 1 day/year exceedance inundation frequency. A comprehensive summary for all assets and infrastructure, as well as all scenarios and frequencies, is included in Appendix I.

#### Buildings exposure across SSP scenarios

Currently, approximately 3,345 buildings are exposed to estuarine inundation at a 1 day/year frequency. By 2030, exposure increases to 4,110 buildings under both SSP1-2.6 and SSP2-4.5 scenarios, and to 4,170 buildings under SSP3-7.0. Exposure under medium-confidence SSP5-8.5 rises to 4,260 buildings, and under low-confidence SSP5-8.5, to 4,370 buildings by 2030 (Figure 57(a)).

Under scenario SSP1-2.6, by 2050, exposure increases to 6,900 buildings; and under SSP2-4.5 and SSP3-7.0, to 7,400 and 8,750 buildings, respectively. Under medium-confidence SSP5-8.5, exposure rises to 9,110 buildings, while under low-confidence SSP5-8.5, exposure reaches 15,520 buildings by 2050. By 2080, exposure rises to 23,110 buildings under SSP1-2.6, to 30,980 buildings under SSP2-4.5, and 41,330 buildings under SSP3-7.0. By 2080, under medium-confidence SSP5-8.5, exposure rises to 48,910 buildings, while under low-confidence SSP5-8.5 it reaches 136,290 buildings (Figure 57(a)).

By 2100, exposure rises to 50,700 buildings under SSP1-2.6, 64,900 buildings under SSP2-4.5, and 86,700 buildings under SSP3-7.0. By 2100, under medium-confidence SSP5-8.5, exposure rises further to 103,150 buildings, while under low-confidence SSP5-8.5 it climbs to 240,420 buildings. By 2150, exposure reaches 145,300 buildings under SSP1-2.6, 177,400 buildings under SSP2-4.5, and 213,000 buildings under SSP3-7.0. Under medium-confidence SSP5-8.5, exposure climbs to 244,090 buildings by 2150 (Figure 57(a)).

#### Critical infrastructure exposure across SSP scenarios

Currently, exposure of critical infrastructure to estuarine inundation includes 2 assets in 2020. By 2030, exposure grows to 3 assets under each of SSP1-2.6, SSP2-4.5, SSP3-7.0, medium-confidence SSP5-8.5 and low-confidence SSP5-8.5. By 2050, exposure of critical infrastructure under SSP1-2.6 and SSP2-4.5 rises to 4 assets, while under SSP3-7.0 and medium-confidence SSP5-8.5 it grows to 6 assets. Under low-confidence SSP5-8.5, exposure increases further to 9 assets (Figure 57(b)).

By 2080, exposure rises to 15 assets under SSP1-2.6, 19 assets under SSP2-4.5, 30 assets under SSP3-7.0, and 39 assets under medium-confidence SSP5-8.5, while climbing to 126 assets under low-confidence SSP5-8.5. By 2100, exposure reaches

40 assets under SSP1-2.6, 55 assets under SSP2-4.5, 72 assets under SSP3-7.0 and 95 assets under medium-confidence SSP5-8.5, while rising even higher to 253 assets under low-confidence SSP5-8.5 (Figure 57(b)).

By 2150, exposure increases to 142 assets under SSP1-2.6, 165 assets under SSP2-4.5, 212 assets under SSP3-7.0, and 257 assets under medium-confidence SSP5-8.5 (<u>Figure 57(b)</u>). Given the high importance and costs associated with critical infrastructure, such as hospitals, any level of exposure demands careful consideration, with outcomes from high-impact scenarios likely offering essential guidance for planning and adaptation.

#### Aboriginal cultural heritage site exposure across SSP scenarios

Currently, 611 identified heritage sites are exposed to estuarine inundation at a 1 day/year exceedance frequency. By 2050, exposure of heritage sites increases to 831 under SSP1-2.6, 865 sites under SSP2-4.5, 897 sites under SSP3-7.0, 898 sites under medium-confidence SSP5-8.5, and 1,025 sites under low-confidence SSP5-8.5. By 2080, exposure rises to nearly 1,178 sites under SSP1-2.6, 1,273 sites under SSP2-4.5, 1,396 sites under SSP3-7.0, and 1,459 sites under medium-confidence SSP5-8.5, while under low-confidence SSP5-8.5, exposure rises further to 2,511 sites (Figure 57(c)).

By 2100, exposure reaches 1,461 sites under SSP1-2.6, 1,621 sites under SSP2-4.5, 1,913 sites under SSP3-7.0, and 2,115 sites under medium-confidence SSP5-8.5, while under low-confidence SSP5-8.5, it climbs to 3,745 sites. By 2150, exposure rises to approximately 2,596 sites under SSP1-2.6, 2,951 sites under SSP2-4.5, 3,408 sites under SSP3-7.0, and 3,766 sites under medium-confidence SSP5-8.5 (Figure 57(c)).

These results highlight the increasing risks to Aboriginal cultural heritage sites, underscoring the importance of prioritising lower emissions pathways and proactive adaptation strategies to preserve these invaluable sites.

#### Road exposure across SSP scenarios

Currently, exposure of roads to estuarine inundation is approximately 355 km statewide. By 2050, exposure increases to 620 km under SSP1-2.6, 670 km under SSP2-4.5, 710 km under SSP3-7.0 and 735 km under medium-confidence SSP5-8.5, while under low-confidence SSP5-8.5, it grows to 975 km (Figure 57(d)).

By 2080, exposure rises to 1,265 km under SSP1-2.6, 1,510 km under SSP2-4.5, 1,830 km under SSP3-7.0 and 2,055 km under medium-confidence SSP5-8.5, while under low-confidence SSP5-8.5 it climbs to 4,520 km. By 2100, exposure reaches 2,100 km under SSP1-2.6, 2,490 km under SSP2-4.5, 3,110 km under SSP3-7.0 and 3,535 km under medium-confidence SSP5-8.5, while climbing to 7,325 km under low-confidence SSP5-8.5. By 2150, exposure increases to 4,780 km under SSP1-2.6, 5,600 km under SSP2-4.5, 6,620 km under SSP3-7.0 and 7,410 km under medium-confidence SSP5-8.5 (Figure 57(d)).

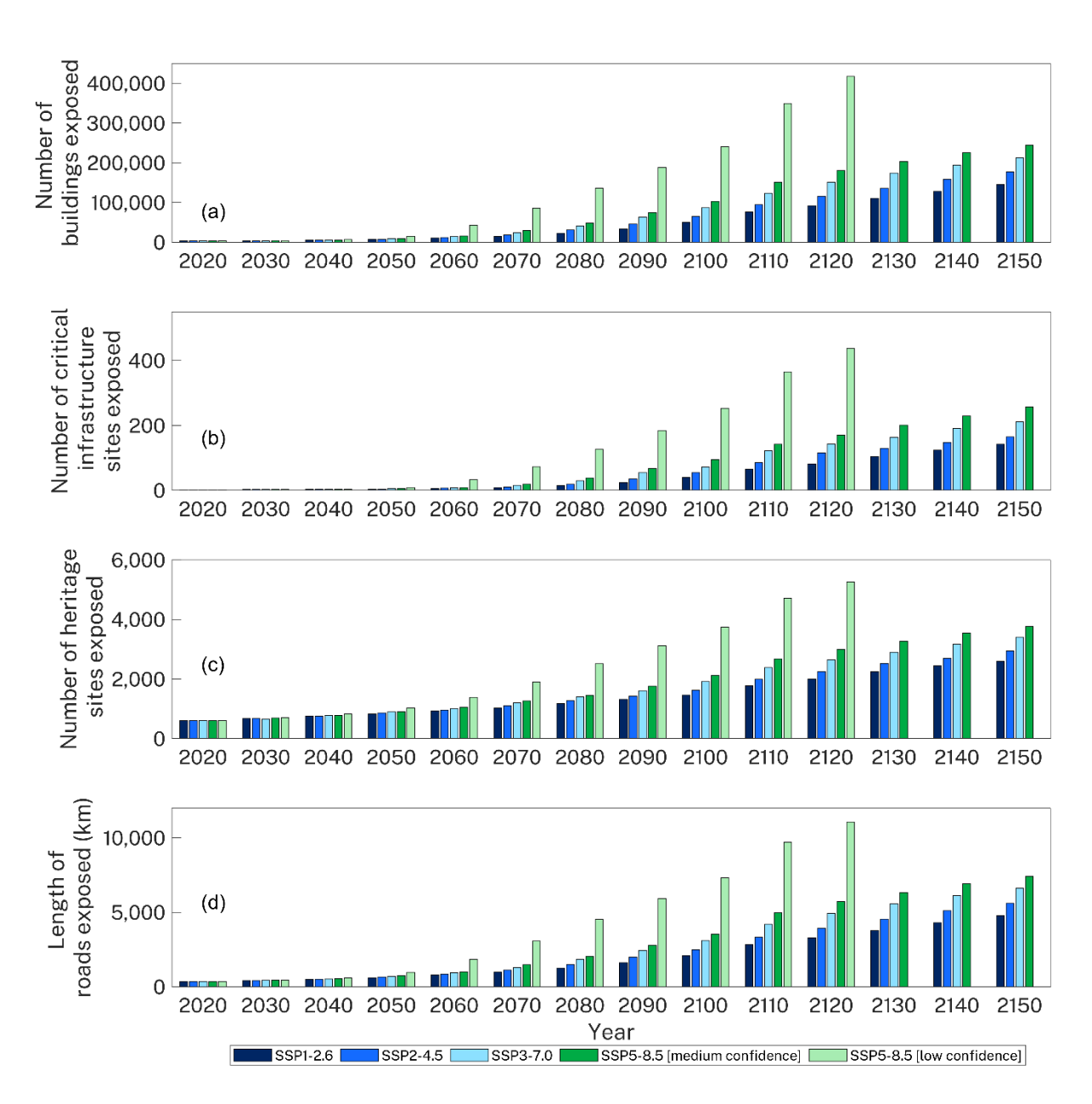


Figure 57 State-wide exposure over time (current (2020) to 2150) of (a) buildings, (b) critical infrastructure, (c) heritage sites and (d) roads (km) to estuarine inundation (at 1 day/year exceedance inundation frequency) associated with SSP1-2.6, SSP2-4.5, SSP3-7.0, medium-confidence SSP5-8.5 and low-confidence SSP5-8.5 scenarios

Note: Bar plots for 2130 to 2150 are not visualised for the low-confidence SSP5-8.5 scenario due to limitations of the digital elevation model.

# **Summary**

This assessment highlights the state's increasing exposure to estuarine inundation across all SSP scenarios. While future growth in exposure is inevitable, a focused effort on emissions reduction and resilience-building may offer a pathway to manage long-term vulnerabilities.

# 5. Key findings

# 5.1 Summary

Consistent with previous assessments, under accelerating sea level rise (SLR), the impacts of coastal erosion, coastal overwash, and estuarine inundation are projected to be both substantial and widespread, affecting coastal and estuarine communities, assets and infrastructure. This section summarises the results for each hazard.

#### Coastal erosion

The analysis of open coast NSW beaches revealed that approximately 90% of sandy beach shorelines form parts of beach systems that are fully or partially backed by erodible geomorphology, making them vulnerable to coastal erosion. The remaining 10% of sandy beach shorelines are entirely backed by non-erodible bedrock geology.

For coastal erosion, the extent of potential erosion hazards gradually increases over time, with larger erosion extents associated with higher SLR scenarios. This erosion is projected to impact increasing amounts of infrastructure over time.

It was found that, at present, approximately 660 buildings and 1,920 addresses along the NSW coastline are exposed to coastal erosion at a 1% annual exceedance probability (AEP) storm erosion volume. This exposure is projected to rise to around 7,500 buildings and 22,820 addresses by 2150 under the low emissions SLR scenario (SSP1-2.6), and to 17,740 buildings and 48,400 addresses by 2150 under the high emissions scenario (SSP3-7.0). Roads, paths and other infrastructure are also at risk of erosion hazards. Currently, around 22 km of roads and 35 km of paths are exposed to coastal erosion at a 1% AEP storm erosion volume. This exposure increases for roads and paths, respectively, under the low emissions scenario (SSP1-2.6) to 32 km and 42 km by 2050, 88 km and 66 km by 2100, and 247 km and 111 km by 2150; and under the high emissions scenario (SSP3-7.0) to 34 km and 43 km by 2050, 155 km and 87 km by 2100, and 458 km and 150 km by 2150.

#### Coastal overwash

Under current conditions, approximately 6% (51 km of coastline) of the NSW sandy coastlines are assessed as likely to experience coastal overwash during 1% AEP wave and water level conditions. The overwash occurs mostly in entrances to intermittently closed–open lakes and lagoons (ICOLLs) and sites characterised by structures (for example, sea walls).

With SLR, coastal overwash likelihood increases under all climate change scenarios. For a present-day 1% AEP event plus future SLR, the likely overwash increases by an additional 31 km of coastline by 2150 under the SSP1-2.6 scenario, and by an additional 73 km under the SSP3-7.0 scenario.

#### **Estuarine inundation**

As sea levels rise, the extent of inundation around estuarine foreshores is projected to increase, impacting property and infrastructure. The total state-wide area of inundation (at one day per year frequency) increases from approximately 770 km² in 2020 to 1,080 km² in 2050, and further to 1,890 km² in 2100, and 2,920 km² in 2150 under a low emissions scenario (SSP1-2.6). In contrast, under a high emissions scenario (SSP3-7.0), the total state-wide area exposed to inundation increases to around 1,160 km² in 2050, 2,290 km² in 2100, and 3,480 km² in 2150.

For estuarine inundation, the results highlight that, by 2050, approximately 6,900 buildings (14,400 addresses) may be exposed to inundation (1 day/year) under the low emissions scenario (SSP1-2.6), and 8,750 buildings (18,000 addresses) under the high emissions scenario (SSP3-7.0). This exposure is projected to rise by 2100 to between 50,700 buildings (111,500 addresses) and 86,700 buildings (204,100 addresses); and by 2150 to between 145,300 buildings (359,400 addresses) and 213,000 buildings (540,700 addresses) for the low and high emissions scenarios, respectively.

Significant lengths of roads, railways and other infrastructure are also at risk of estuarine inundation. By 2050, an estimated 620 km of roads and 7 km of rail may be exposed to inundation (1 day/year) under the low emissions scenario (SSP1-2.6), rising to 710 km of roads and 8 km of rail under the high emissions scenario (SSP3-7.0). By 2100, this increases to 2,100 km of roads and 38 km of rail under the low emissions scenario (SSP1-2.6), and 3,110 km of roads and 75 km of rail under the high emissions scenario (SSP3-7.0). By 2150, the exposure is projected to reach between 4,780 km of roads and 159 km of rail for the low emissions scenario, and 6,620 km of roads and 272 km of rail for the high emissions scenario.

## 5.2 Limitations

This assessment is underpinned by several assumptions and limitations related to the methods, available data and the state-wide scale of the study. While the consistency in methods provides for a solid overall understanding of risk exposure to coastal erosion, coastal overwash and estuarine inundation, as well as of geographic variability, the results can nevertheless be improved through more detailed local-scale investigations and studies. This section outlines key limitations.

#### Coastal erosion

A volume-based coastal erosion model was used to simulate changes in beach volume and associated shoreline distances in response to the combined influences of drivers of coastal change, both fluctuating (storms, climate cyclicity) and cumulative (sediment budget imbalance, SLR). The model was applied within a Monte Carlo framework to sample the range of uncertainty in each erosion component and so develop probability distributions of potential coastal change for each scenario. The model scenarios included present-day conditions (fluctuation only) and 5 climate change shared socioeconomic pathways with associated SLR at decadal increments from 2030 to 2150.

The spatial resolution of the erosion modelling at the beach-sector scale has ensured that alongshore variations in coastal geomorphology and gradients in coastal processes across sandy beaches and coastal embayments are quantified and included in the model results, and the complex geomorphology forming each sector is captured through spatial aggregation techniques. This means that predicted coastal erosion reflects the distinctive coastal geomorphology of each beach sector. However, subsector variability may be diluted by this approach, meaning that abrupt changes in erosion drivers or responses within a sector might not be fully accounted for.

The modelled coastal erosion for each beach sector and scenario reflects input probability distributions for each component of erosion, which represent the range of uncertainty or variability. The input distributions have been informed by the best available observation data in each case, as described in Appendix A: <a href="Modelled components of coastal erosion">Modelled components of coastal erosion</a>. However, the potential for changes in the coastal process–response system beyond the range of uncertainty captured by input probability distributions was not considered. For example, the model assumes no significant change in future wave climate that would alter the beach fluctuation probability distributions scaled for each beach sector.

Furthermore, site-specific underlying trends in historical coastal change, which usually reflect a local sediment budget imbalance, were derived from multi-decadal satellite observation data providing a consistent analysis for all NSW beaches. In the absence of more detailed site-specific analysis beyond the scope of this project, it has been assumed that these trends will be sustained into the future throughout the simulation scenarios. In some cases, trends observed in satellite data may be influenced by shorter timescale responses to multi-decadal climate variability or human interventions in coastal systems (for example, river entrance training), and underlying trends may change in the future beyond our current understanding.

The volume-based coastal erosion model, using sector-averaged geomorphology, provides a reasonable representation of shoreline change in response to sediment redistribution from combined storm impacts and cyclicity, underlying sediment budget imbalances and SLR. The method suits the well-developed beach and dune morphology, the moderate- to high-energy environment of the NSW coastline, and the scale of application. For upper range SLR scenarios, where existing coastal sand barriers may become entirely eroded, the subsequent response will depend on complex barrier dynamics, which are beyond the scope of this investigation. Realised coastal erosion and shoreline recession in such cases could be more severe or moderate compared to the forecasts presented here. However, the typically low terrain behind existing narrow barrier-dunes and surrounding backbarrier estuaries, which may be vulnerable to rapid transgression following barrier breaching, is identified by the combined erosion and inundation mapping for upper-range scenarios.

For settings and scenarios where sand barriers are predicted to be entirely eroded through to backbarrier estuaries, areas on the landward side of estuaries have not been mapped as exposed for medium-confidence SSP1-2.6, SSP2-4.5, SSP3-7.0 and SSP5-8.5 scenarios. These areas may still be exposed to coastal erosion hazards, depending

on the extent of barrier breaching and overall alongshore barrier behaviour. For the low-confidence SSP5-8.5, the foreshore areas landward of estuaries that become exposed to ocean processes following barrier breaching were mapped as exposed due to much higher SLR, which would likely lead to ocean inundation and shoreline transgression.

With increased SLR, and particularly rapid SLR, the potential for waves to overtop and wash over dunes increases, shifting the sediment sink for sand eroded from the beach and foredune by wave action from the shoreface to behind the barrier-dune system. In such cases, barrier roll-over may occur, where the landward migration of the coastal profile is more influenced by the backbarrier gradient rather than the shoreface gradient (Dean and Maurmeyer 1983). Some suggest that overtopping is not necessary for dune aggradation to keep pace with SLR, as dune destabilisation from wave attack may trigger transgression and increased delivery of sand from the eroding shoreface to dunes through wind processes (Davidson-Arnott 2005).

The direction of sand transport during SLR and shoreline transgression has been investigated through modelling for various settings, including southeast Australia (Aagaard and Sorensen 2012; Cowell et al. 1995; Roy et al. 1994; Wolinsky and Murray 2009). The direction is generally found to depend on the coastal profile gradient, with transport offshore for steeper slopes and onshore for gentler slopes. However, sensitivity to different elements of the coastal profile (for example, shoreface, beachface, coastal plain) varies with spatial–temporal scales. Over longer timescales and larger migrations, both the trajectory and rate of shoreline recession increasingly depend on the coastal plain gradient, diverging from predictions based on the beach or shoreface slope (Wolinsky and Murray 2009). Thus, in low-gradient settings, when barrier roll-over occurs, shoreline recession may exceed the model shown in Figure 68 (Dean and Maurmeyer 1983; Wolinsky and Murray 2009).

The coastal erosion modelling and mapping consider sedimentary coastal settings where the backshore substrate is presumed to be erodible. State-wide mapping of bedrock areas in the NSW coastal quaternary geology mapping dataset (see Appendix B: Datasets) was used to exclude areas known or considered to have non-erodible bedrock substrate. The resolution quality of the geology mapping means that detailed site-specific investigations may contradict the regional-scale substrate mapping used in this study. Backshore substrate may consist of variably resistant or erodible materials (Kinsela et al. 2016b, 2017), which are beyond the scope of this assessment.

For maximum context and transparency, coastal erosion hazard mapping should be viewed alongside state-wide bedrock mapping extent and corresponding estuarine inundation hazard mapping for each scenario (namely, present-day conditions or SSP/year). This ensures that the combined (and likely interacting) exposure to coastal erosion and inundation on low-lying coastal plains is fully considered.

Regarding exposure of buildings to erosion, structures without an assigned address were excluded to reduce false positives, although secondary structures (for example, sheds, water tanks, and carports) at locations with an assigned address remain in the dataset. Because several building categories (for example, residential, commercial) were considered, the exposure results do not represent a single building class only.

Exposure results may differ across (future) studies due to variations in data selection and processing, filtering methods, assumptions, focus, and other methodological or contextual factors.

#### Coastal overwash

For coastal overwash, this assessment modelled the combined effects of tide, storm surge, wave runup and future SLR, and compared the predicted total water level (TWL) to current backbeach elevation thresholds. No change in backbeach elevation over time was assumed, except at the entrances to ICOLLs, where berms were assumed to accrete with SLR. The study also adopted the present-day TWL for future projections under various SLR scenarios, assuming that the future wave climate and associated runup will be the same as the present-day condition.

Modelled wave runup was based on the assumption of linearity in beach slope, which may, in reality, be more complex. While the runup formulas have been validated using data from NSW beaches during several extreme storms, and variance in beach slopes has been allowed, more extreme runup is possible particularly if the actual beach slope during an event is steeper than assumed or if runup is channelled by surrounding morphology.

The approach only identifies overwash locations by comparing predicted total water levels to backbeach elevation thresholds for different events. More detailed overland flow modelling could be undertaken (for example, through the coastal management program) to determine the potential extent, depth and velocity of coastal inundation.

#### **Estuarine inundation**

For estuarine inundation, the adopted approach allows for variation in water levels between and along individual estuaries, but it remains a broadscale assessment. It does not replace the need for catchment flood or inundation studies specific to individual estuaries, or more detailed estuarine inundation assessments where appropriate. This study assumes that water levels measured at individual gauge locations are able to inundate adjacent areas of estuarine foreshore. The validity of this assumption likely varies with distance from the main water body, overland friction, and the available time at high tide for inundation to occur. Where adjacent low-lying areas are separated from the main water body by more than 5 m, these areas are separately classified as potentially inundated. In some cases, low-lying areas separated from estuarine water bodies by flood mitigation structures or tidal gates of less than 5 m wide may still be included in the inundation mapping, and these may need to be excluded separately through more detailed studies. However, these areas may still be impacted by either or both reduced drainage capacity and elevated groundwater levels.

At inland sites, the input water level data are affected by intermittent floods, sometimes lasting for several days. To limit these effects, the study applied a flood removal process, so that the assessment focused on more regular tidal and ocean driven inundation, but some flood influence may remain in the mapped inundation extents. For estuaries with detailed modelling available, potential changes in high water levels are

included as sea levels rise. However, for other estuaries, no changes in water level exceedances beyond those resulting from SLR or increases in berm height are assumed.

Inundation extents were mapped by overlaying water surfaces on digital elevation models derived from LiDAR data, which have a vertical accuracy of around 0.3 m. In some instances, landforms and infrastructure such as roads may have changed since the LiDAR data were collected, meaning the models may not fully reflect current conditions.

Regarding exposure, state-wide data on floor levels of buildings are absent, and thus building counts assume no raised floor levels. Buildings are likely to be raised in estuarine upstream areas that are prone to significant flooding, as a means of minimising flood impacts. While the results provide a robust representation of potential exposure, raised floor levels may result in reduced actual flood damage and other property-specific impacts.

Regarding exposure of buildings to estuarine inundation, structures without an assigned address were excluded to reduce false positives, although secondary structures (for example, sheds, water tanks, and carports) at locations with an assigned address remain in the dataset. Because several building categories (for example, residential, commercial) were considered, the exposure results do not represent a single building class only. Exposure results may differ across (future) studies due to variations in data selection and processing, filtering methods, assumptions, focus, and other methodological or contextual factors.

# Acknowledgements

Funding for this study was provided by the Disaster Risk Reduction Fund, which is jointly funded by the Australian and New South Wales governments and administered by the NSW Reconstruction Authority. In-kind support was also provided by the NSW Department of Climate Change, Energy, the Environment and Water, with funding from the Climate Change Fund. We express our gratitude to the University of Newcastle. We also extend our thanks to Manly Hydraulics Laboratory for providing the water level data, and to Baird Australia Pty Ltd for supplying nearshore wave modelling data.

The authors of the report are Mr David Hanslow, Dr Danial Khojasteh, Dr Michael Kinsela, Dr Rai Ibaceta, Dr Bradley Morris, Dr Penny Godwin, Dr Shivanesh Rao, and Dr Sara Shaeri Karimi.

Thanks to the members of the Project Reference Group for their peer review of the methodology, and to Dr Tracey MacDonald, Dr Jocelyn Dela-Cruz, Dr Michael Hughes, Dr Marc Daley, and Mr Bruce Coates for their peer review of the report. We also thank Dr Michelle Linklater for her help producing and quality-controlling several data layers. We also thank our two external reviewers for their time and for providing valuable feedback that improved this report.

# References

Aagaard T and Sørensen P (2012) 'Coastal profile response to sea level rise: a process-based approach', *Earth Surface Processes and Landforms*, 37(3):354–362, doi:10.1002/esp.2271.

AHO (Australian Hydrographic Office) (2023) <u>Australian nation tide tables</u>, *Australian Hydrographic Publication 11*, AHO, Department of Defence, Australian Government.

Anthony EJ and Aagaard T (2020) 'The lower shoreface: morphodynamics and sediment connectivity with the upper shoreface and beach', *Earth-Science Reviews*, 210:103334, doi:10.1016/j.earscirev.2020.103334.

Atkinson AL, Power HE, Moura T, Hammond T, Callaghan DP and Baldock TE (2017) 'Assessment of runup predictions by empirical models on non-truncated beaches on the south-east Australian coast', *Coastal Engineering*, 119:15–31, doi:10.1016/j.coastaleng.2016.10.001.

Baird Australia (2024) <u>NSW nearshore wave tool: validation report</u>, Report prepared for the Department of Climate Change, Energy, the Environment and Water, NSW Government, Sydney.

Bamber JL, Oppenheimer M, Kopp RE, Aspinall WP and Cooke RM (2019) 'Ice sheet contributions to future sea-level rise from structured expert judgment', *Proceedings of the National Academy of Sciences*, 116(23):11195–11200, doi:10.1073/pnas.1817205116.

Barnard PL, Short AD, Harley MD, Splinter KD, Vitousek S, Turner IL, Allan J, Banno M, Bryan KR, Doria A and Hansen JE (2015) 'Coastal vulnerability across the Pacific dominated by El Niño/Southern Oscillation', *Nature Geoscience*, 8(10):801–807, doi:10.1038/ngeo2539.

Belgorodski N, Greiner M, Tolksdorf K, Schueller K (2022) <u>rriskDistributions: fitting</u> <u>distributions to given data or known quantiles</u>, R Package version 2.1.2. 2017, accessed December 2023.

Bishop-Taylor R, Nanson R, Sagar S and Lymburner L (2021) 'Mapping Australia's dynamic coastline at mean sea level using three decades of Landsat imagery', *Remote Sensing of Environment*, 267:112734, doi:10.1016/j.rse.2021.112734.

BOM (Bureau of Meteorology) (n.d.) <u>Monthly sea levels for Port Kembla</u>, accessed 20 March 2025.

BOM (2024) <u>Monthly data report – December 2023: Australian Baseline Sea Level Monitoring Array</u>, BOM, Australian Government.

Bruun P (1962) 'Sea-level rise as a cause of shore erosion', *Journal of the Waterways and Harbors division*, 88(1):117–130.

Callaghan DP, Nielsen P, Short A and Ranasinghe R (2008) 'Statistical simulation of wave climate and extreme beach erosion', *Coastal Engineering*, 55(5):375–390, doi:10.1016/j.coastaleng.2007.12.003.

Callaghan DP, Ranasinghe R and Roelvink D (2013) 'Probabilistic estimation of storm erosion using analytical, semi-empirical, and process-based storm erosion models', *Coastal Engineering*, 82:64–75, doi:10.1016/j.coastaleng.2013.08.007.

Callaghan DP, Couriel E, Hanslow D, Modra B, Fitzhenry M and Jacobs R (2017) 'Comparing extreme water levels using different techniques and impact of climate indices', in *Australasian coasts & ports 2017: working with nature*, Engineers Australia, PIANC Australia and Institute of Professional Engineers New Zealand, Barton, ACT.

Cechet B, Taylor P, Griffin C and Hazelwood M (2011) 'Australia's coastline: adapting to climate change', *AusGeo News* 101:13–21.

Chapman DM, Geary M, Roy PS and Thom BG (1982), Coastal evolution and coastal erosion in New South Wales, Coastal Council of NSW, Sydney.

Church JA, White NJ, Hunter JR and McInnes KL (2012) 'Sea level', in Poloczanska E, Hobday AJ and Richardson AJ (eds), *Marine climate change in Australia, impacts and adaptation responses, 2012 report card,* CSIRO, Cleveland, Qld.

Church JA, Clark PU, Cazenave A, Gregory JM, Jevrejeva S, Levermann A, Merrifield MA, Milne GA, Nerem RS, Nunn PD, Payne AJ, Pfeffer WT, Stammer D and Unnikrishnan AS (2014) 'Sea level change', in Intergovernmental Panel on Climate Change (IPCC), *Climate change 2013: the physical science basis*, Contribution of Working Group I to the Fifth Assessment Report of the IPCC, Prepared by TF Stocker, D Qin, G-K Plattner, M Tignor, SK Allen, J Boschung, A Nauels, Y Xia, V Bex and PM Midgley (eds), Cambridge University Press, doi:10.1017/CBO9781107415324.026.

Cowell PJ, Roy PS and Jones RA (1995) 'Simulation of large-scale coastal change using a morphological behaviour model', *Marine Geology*, 126:45–61, doi:10.1016/0025-3227(95)00065-7.

Cowell PJ, Stive MJF, Niedoroda AW, de Vriend HJ, Swift DJP, Kaminsky GM and Capobianco M (2003) 'The coastal-tract (part 1): a conceptual approach to aggregated modeling of low-order coastal change', *Journal of Coastal Research*, 19:812–827.

Cowell PJ, Thom BG, Jones RA, Everts CH and Simanovic D (2006) 'Management of uncertainty in predicting climate-change impacts on beaches', *Journal of Coastal Research*, 22(1):232–245, doi:10.2112/05A-0018.1.

Cowell PJ and Kinsela MA (2018) 'Shoreface controls on barrier evolution and shoreline change', in Moore LJ and Murray AB (eds) *Barrier dynamics and response to changing climate*, Springer International.

da Silva PG, Coco G, Garnier R and Klein AH (2020) 'On the prediction of runup, setup and swash on beaches', *Earth-Science Reviews*, 204:103148, doi:10.1016/j.earscirev.2020.103148.

da Silva AP, da Silva GV, Strauss D, Murray T, Woortmann LG, Taber J, Cartwright N and Tomlinson R (2021) 'Headland bypassing timescales: processes and driving forces', *Science of the Total Environment*, 793:148591, doi:10.1016/j.scitotenv.2021.148591.

Davidson-Arnott RG (2005) 'Conceptual model of the effects of sea level rise on sandy coasts', *Journal of Coastal Research*, 21(6):1166–1172, doi:10.2112/03-0051.1.

Davies G, Callaghan DP, Gravois U, Jiang W, Hanslow D, Nichol S and Baldock T (2017) 'Improved treatment of non-stationary conditions and uncertainties in probabilistic models of storm wave climate', *Coastal Engineering*, 127:1–19, doi:10.1016/j.coastaleng.2017.06.005.

DCC (Department of Climate Change) (2009) Climate change risks to Australia's coast: a first pass national assessment, DCC, Australian Government.

DCS Spatial Services (2020) Elevation data product specification and description – Source: airborne light detecting and ranging (LiDAR), Department of Customer Service, NSW Government.

Dean RG and Houston JR (2013), 'Recent sea level trends and accelerations: comparison of tide gauge and satellite results', *Coastal Engineering*, 75:4–9, doi:10.1016/j.coastaleng.2013.01.001.

Dean RG and Maurmeyer EM (1983) 'Models for beach profile response', in Komar PD (ed.), Hand-book of coastal processes and erosion, CRC Press, Boca Raton, FL.

DeConto RM, Pollard D, Alley RB, Velicogna I, Gasson E, Gomez N, Sadai S, Condron A, Gilford DM, Ashe EL and Kopp RE (2021) 'The Paris Climate Agreement and future sealevel rise from Antarctica', *Nature*, 593(7857):83–89, doi:10.1038/s41586-021-03427-0.

Deng X, Griffin DA, Ridgway K, Church JA, Featherstone WE, White NJ and Cahill M (2011) 'Satellite altimetry for geodetic, oceanographic, and climate studies in the Australian region', in Vignudelli S, Kostianoy A, Cipollini P and Benveniste J (eds), *Coastal Altimetry*, Springer, doi:10.1007/978-3-642-12796-0\_18.

Der Kiureghian A and Ditlevsen O (2009) 'Aleatory or epistemic? Does it matter?', Structural Safety, 31(2):105–112, doi:10.1016/j.strusafe.2008.06.020.

Dissanayake P, Brown J, Wisse P and Karunarathna H (2015) 'Comparison of storm cluster vs isolated event impacts on beach/dune morphodynamics', *Estuaries, Coasts and Shelf Science*, 164:301–312, doi:10.1016/j.ecss.2015.07.040.

Doyle TB and Woodroffe CD (2023) 'Modified foredune eco-morphology in southeast Australia', *Ocean & Coastal Management*, 240:106640, doi:10.1016/j.ocecoaman.2023.106640.

Doyle TB, Hesp PA and Woodroffe CD (2024) 'Foredune morphology: regional patterns and surfzone–beach–dune interactions along the New South Wales coast, Australia', *Earth Surface Processes and Landforms*, 49(10):3115–3138, doi:10.1002/esp.5879.

Du J, Shen J, Zhang YJ, Ye F, Liu Z, Wang Z, Wang YP, Yu X, Sisson M and Wang HV (2018) 'Tidal response to sea-level rise in different types of estuaries: the importance of length, bathymetry, and geometry', *Geophysical Research Letters*, 45(1):227–235, doi:10.1002/2017GL075963.

Dyer KR (1997) Estuaries: a physical introduction, Wiley and Sons, 1997.

ESRI (Environmental Systems Research Institute) (2021), *ArcGIS Desktop*, version 10.8.2 [geographic information system app], support.esri.com/en/, accessed 2023–2024.

Eysink WD (1990) 'Morphologic response of tidal basins to changes', *Coastal Engineering Proceedings*1(2):1948–1961, doi:10.9753/icce.v22.%p.

Fellowes TE, Vila-Concejo A, Gallop SL, Schosberg R, de Staercke V and Largier JL (2021) 'Decadal shoreline erosion and recovery of beaches in modified and natural estuaries', *Geomorphology*, 390:107884, doi:10.1016/j.geomorph.2021.107884.

FitzGerald DM, Fenster MS, Argow BA and Buynevich IV (2008) 'Coastal impacts due to sea-level rise', *Annual Review of Earth and Planetary Sciences*, 36:601–647, doi:10.1146/annurev.earth.35.031306.140139.

Folland CK, Parker DE, Colman AW and Washington R (1999) 'Large scale modes of ocean surface temperature since the late nineteenth century', in Navarra A (ed), *Beyond El Niño: decadal and interdecadal climate variability*, Springer, doi:10.1007/978-3-642-58369-8\_4.

Foulsham E, Morris B and Hanslow D (2012) 'Considering tidal modification when mapping inundation hazard in NSW estuaries' [conference presentation], 21st NSW Coastal Conference, Kiama, NSW.

Fox-Kemper B, Hewitt HT, Xiao C, Aðalgeirsdóttir G, Drijfhout SS, Edwards TL, Golledge NR, Hemer M, Kopp RE, Krinner G, Mix A, Notz D, Nowicki S, Nurhati IS, Ruiz L, Sallée J-B, Slangen ABA and Yu Y (2023) 'Ocean, cryosphere and sea level change', in Intergovernmental Panel on Climate Change (IPCC), *Climate change 2021: the physical science basis*, Contribution of Working Group I to the Sixth Assessment Report of the IPCC, Prepared by V Masson-Delmotte, P Zhai, A Pirani, SL Connors, C Péan, S Berger, N Caud, Y Chen, L Goldfarb, MI Gomis, M Huang, K Leitzell, E Lonnoy, JBR Matthews, TK Maycock, T Waterfield, O Yelekçi, R Yu, and B Zhou (eds), Cambridge University Press, doi:10.1017/9781009157896.011.

French J, Payo A, Murray B, Orford J, Eliot M and Cowell P (2016) 'Appropriate complexity for the prediction of coastal and estuarine geomorphic behaviour at decadal to centennial scales', *Geomorphology*, 256:3–16, doi:10.1016/j.geomorph.2015.10.005.

Garner G, Hermans TH, Kopp R, Slangen A, Edwards T, Levermann A, Nowicki S, Palmer MD, Smith C, Fox-Kemper B and Hewitt H (2022) *IPCC AR6 WGI sea level projections*, [data set], World Data Center for Climate Change, doi:10.26050/WDCC/AR6.IPCC-DDC\_AR6\_Sup\_SLPr.

Geoscape Australia (2023), *Geoscape buildings*, version 3.1 [data set], accessed up to 18 December 2023.

Goodwin ID, Freeman R and Blackmore K (2013) 'An insight into headland sand bypassing and wave climate variability from shoreface bathymetric change at Byron Bay, New South Wales, Australia', *Marine Geology*, 341:29–45, doi:10.1016/j.margeo.2013.05.005.

Gordon AD (1987) 'Beach fluctuations and shoreline change: NSW', in Eighth Australasian conference on coastal and ocean engineering, 1987: preprints of papersInstitution of Engineers, Australia, Barton, ACT.

Haasnoot M, Kwakkel JH, Walker WE and Ter Maat J (2013) 'Dynamic adaptive policy pathways: a method for crafting robust decisions for a deeply uncertain world', *Global Environmental Change*, 23(2):485–498, doi:10.1016/j.gloenvcha.2012.12.006.

Hague BS, McGregor S, Murphy BF, Reef R and Jones DA (2020) 'Sea level rise driving increasingly predictable coastal inundation in Sydney, Australia', *Earth's Future*, 8(9):e2020EF001607, doi:10.1029/2020EF001607.

Hague BS, Jones DA, Jakob D, McGregor S and Reef R (2022) 'Australian coastal flooding trends and forcing factors', *Earth's Future*, 10(2):e2021EF002483, doi:10.1029/2021EF002483.

Haines PE (2006), <u>Physical and chemical behaviour and management of intermittently closed and open lakes and lagoons (ICOLLs) in NSW</u> [PhD thesis], Griffith University, doi:10.25904/1912/3646.

Hallermeier RJ (1980) 'A profile zonation for seasonal sand beaches from wave climate', *Coastal Engineering*, 4:253–277, doi:10.1016/0378-3839(80)90022-8.

Hanslow DJ, Davis GA, You BZ-J and Zastaway J (2000) <u>'Berm height at coastal lagoon entrances in NSW'</u> [conference presentation], *10th NSW Coastal Conference*, Yamba, NSW.

Hanslow DJ, Dela-Cruz J, Morris BD, Kinsela MA, Foulsham E, Linklater M and Pritchard TR (2016) 'Regional scale coastal mapping to underpin strategic land use planning in southeast Australia', *Journal of Coastal Research*, 75(sp1):987–991, doi:10.2112/SI75-198.1.

Hanslow DJ, Morris BD, Foulsham E and Kinsela MA (2018) 'A regional scale approach to assessing current and potential future exposure to tidal inundation in different types of estuaries', *Scientific Reports*, 8(1):7065, doi:10.1038/s41598-018-25410-y.

Hanslow DJ, Fitzhenry MG, Power HE, Kinsela MA and Hughes MG (January 2019) 'Rising tides: tidal inundation in southeast Australian estuaries' [conference presentation], Australasian Coasts & Ports 2019 Conference, Hobart, Tasmania.

Hanslow DJ, Fitzhenry MG, Hughes MG, Kinsela MA and Power HE (2023) 'Sea level rise and the increasing frequency of inundation in Australia's most exposed estuary', *Regional Environmental Change*, 23:146, doi:10.1007/s10113-023-02138-8.

Haigh ID, Eliot M, Pattiaratchi C (2011) 'Global influences of the 18.61-year nodal cycle and 8.85-year cycle of lunar perigee on high tidal levels', *Journal of Geophysical Research: Oceans*, 116(C6), doi:10.1029/2010JC006645.

Harley MD, Turner IL, Short AD and Ranasinghe R (2011) 'A re-evaluation of coastal embayment rotation: the dominance of cross-shore versus alongshore sediment transport processes, Collaroy-Narrabeen Beach, southeast Australia', *Journal of Geophysical Research: Earth Surface*, 116(F4):F04033, doi:10.1029/2011JF001989.

Harley MD, Turner IL, Kinsela MA, Middleton JH, Mumford PJ, Splinter KD, Phillips MS, Simmons JA, Hanslow DJ and Short AD (2017) 'Extreme coastal erosion enhanced by anomalous extratropical storm wave direction', *Scientific Reports*, 7(1):6033, doi:10.1038/s41598-017-05792-1.

Hart RM, Power H E and Hanslow D J (2017) 'Tidal dynamics and oscillations within coastal lakes', in *Australasian coasts & ports 2017: working with nature*, Engineers Australia, PIANC Australia and Institute of Professional Engineers New Zealand, Barton, ACT.

Hazelwood M (2009) <u>Geomorphology smartline geopackage</u> [data set], Geoscience Australia, researchdata.edu.au, accessed 2023–2024.

Hedges TS and Mase H (2004) 'Modified Hunt's equation incorporating wave setup', *Journal of Waterway, Port, Coastal, and Ocean Engineering*, 130(3):109–113, doi:10.1061/(ASCE)0733-950X(2004)130:3(109).

Hersbach H, Bell B, Berrisford P, Hirahara S, Horányi A, Muñoz-Sabater J, Nicolas J, Peubey C, Radu R, Schepers D and Simmons A (2020) 'The ERA5 global reanalysis', *Quarterly Journal of the Royal Meteorological Society*, 146(730):1999–2049, doi:10.1002/qj.3803.

Hill KL, Rintoul SR, Coleman R and Ridgway KR (2008) 'Wind-forced low frequency variability of the East Australian Current', *Geophysical Research Letters*, 35:L08602, doi:10.1029/2007GL032912.

Hill KL, Rintoul SR, Ridgway KR and Oke PR (2011) 'Decadal changes in the South Pacific western boundary current system revealed in observations and ocean state estimates', *Journal of Geophysical Research: Oceans*, 16(C1):C01009, doi:10.1029/2009JC005926.

Holbrook NJ, Goodwin ID, McGregor S, Molina E and Power SB (2011) 'ENSO to multidecadal time scale changes in East Australian Current transports and Fort Denison sea level: oceanic Rossby waves as the connecting mechanism', *Deep Sea Research Part II: Topical Studies in Oceanography*, 58(5):547–558, doi:10.1016/j.dsr2.2010.06.007.

Holman RA (1986) 'Extreme value statistics for wave run-up on a natural beach', *Coastal Engineering*, 9(6):527–544, doi:10.1016/0378-3839(86)90002-5.

Hughes MG, Rogers K and Li W (2019) 'Saline wetland extents and tidal inundation regimes on a micro-tidal coast, New South Wales, Australia', *Estuarine, Coastal and Shelf Science*, 227:106297, doi:10.1016/j.ecss.2019.106297.

ICSM (Intergovernmental Committee on Surveying and Mapping) (2021) <u>ELVIS – Elevation and depth – foundation spatial data</u> [data set], accessed 18 December 2023.

IPCC (Intergovernmental Panel on Climate Change) (2022) *The ocean and cryosphere in a changing climate*, IPCC special report prepared by H-O Pörtner, DC Roberts, V Masson-Delmotte, P Zhai, M Tignor, E Poloczanska, K Mintenbeck, A Alegría, M Nicolai, A Okem, J Petzold, B Rama, NM Weyer (eds), Cambridge University Press, doi:10.1017/9781009157964.

IPCC (2023) Climate change 2021: the physical science basis, Contribution of Working Group I to the Sixth Assessment Report of the IPCC, Prepared by V Masson-Delmotte, P Zhai, A Pirani, SL Connors, C Péan, S Berger, N Caud, Y Chen, L Goldfarb, MI Gomis, M Huang, K Leitzell, E Lonnoy, JBR Matthews, TK Maycock, T Waterfield, O Yelekçi, R Yu and B Zhou (eds), Cambridge University Press, doi:10.1017/9781009157896.

Khojasteh D, Hottinger S, Felder S, De Cesare G, Heimhuber V, Hanslow DJ and Glamore W (2020) 'Estuarine tidal response to sea level rise: the significance of entrance restriction', *Estuarine, Coastal and Shelf Science*, 244:106941, doi:10.1016/j.ecss.2020.106941.

Khojasteh D, Glamore W, Heimhuber V and Felder S (2021) 'Sea level rise impacts on estuarine dynamics: a review', *Science of The Total Environment*, 780:146470, doi:10.1016/j.scitotenv.2021.146470.

Khojasteh D, Felder S, Heimhuber V and Glamore W (2023) 'A global assessment of estuarine tidal response to sea level rise', *Science of The Total Environment*, 894:165011, doi:10.1016/j.scitotenv.2023.165011.

Kinsela MA, Daley MJA and Cowell PJ (2016a) 'Origins of Holocene coastal strandplains in Southeast Australia: shoreface sand supply driven by disequilibrium morphology', *Marine Geology*, 374:14–30, doi:10.1016/j.margeo.2016.01.010.

Kinsela MA, Morris BD, Daley MJA and Hanslow DJ (2016b) 'A flexible approach to forecasting coastline change on wave-dominated beaches', *Journal of Coastal Research*, 75(sp1):952–956, doi:10.2112/SI75-191.1.

Kinsela MA, Morris BD, Linklater M and Hanslow DJ (2017) 'Second-pass assessment of potential exposure to shoreline change in New South Wales, Australia, using a sediment compartments framework', *Journal of Marine Science and Engineering*, 5(4):61–101, doi:10.3390/jmse5040061.

Kinsela MA, Hanslow DJ, Carvalho RC, Linklater M, Ingleton TC, Morris BD, Allen KM, Sutherland MD and Woodroffe CD (2022) 'Mapping the shoreface of coastal sediment compartments to improve shoreline change forecasts in New South Wales, Australia', *Estuaries and Coasts*, 45:1143–1169, doi:10.1007/s12237-020-00756-7.

Kinsela MA, Morris BD, Ingleton TC, Doyle TB, Sutherland MD, Doszpot NE, Miller JJ, Holtznagel SF, Harley MD and Hanslow DJ (2024) 'Nearshore wave buoy data from southeastern Australia for coastal research and management', *Scientific Data*, 11:190, doi:10.1038/s41597-023-02865-x.

Kopp RE, Garner GG, Hermans TH, Jha S, Kumar P, Slangen ABA, Turilli M, Edwards TL, Gregory JM, Koubbe G, Levermann A, Merzky A, Nowicki S, Palmer MD and Smith C (2023) 'The Framework for Assessing Changes To Sea-level (FACTS) v1.0-rc: a platform for characterizing parametric and structural uncertainty in future global, relative, and extreme sea-level change', *EGUsphere*, doi:10.5194/egusphere-2023-14.

Linklater M, Ingleton TC, Kinsela MA, Morris BD, Allen KM, Sutherland MD and Hanslow DJ (2019) 'Techniques for classifying seabed morphology and composition on a

subtropical-temperate continental shelf', *Geosciences*, 9(3):141, doi:10.3390/geosciences9030141.

Linklater M, Morris BD and Hanslow DJ (2023) 'Classification of seabed landforms on continental and island shelves', *Frontiers in Marine Science*, 10:1258556, doi:10.3389/fmars.2023.1258556.

Lord D and Kulmar M (2000) 'The 1974 storms revisited: 25 years experience in ocean wave measurement along the south-east Australian coast', in Edge BL (ed) *Coastal Engineering 2000*, American Society of Civil Engineers, doi:10.1061/40549(276)44.

Louis S, Couriel E, Lewis G, Glatz M, Kulmar M, Golding J and Hanslow D (2016) 'NSW east coast low event – 3 to 7 June 2016 weather, wave and water level matters' [conference presentation], NSW Coastal Conference, Coffs Harbour, NSW.

Maiwa K, Masumoto Y and Yamagata T (2010) 'Characteristics of coastal trapped waves along the southern and eastern coasts of Australia', *Journal of Oceanography*, 66:243–258, doi:10.1007/s10872-010-0022-z.

McCarroll RJ, Masselink G, Valiente NG, Scott T, Wiggins M, Kirby J-A and Davidson M (2021) 'A rules-based shoreface translation and sediment budgeting tool for estimating coastal change: ShoreTrans', *Marine Geology*, 435:106466, doi:10.1016/j.margeo.2021.106466.

McDowell DM and O'Connor B A (1977) *Hydraulic behaviour of estuaries*, Macmillan, London.

McInnes KL, White CJ, Haigh ID, Hemer MA, Hoeke RK, Holbrook NJ, Kiem AS, Oliver ECJ, Ranasinghe R, Walsh KJE, Westra S and Cox R (2016) 'Natural hazards in Australia: sea level and coastal extremes', *Climatic Change*, 139(1):69–83, doi:10.1007/s10584-016-1647-8.

McLean EJ and Hinwood JB (2011) <u>'Spring tidal pumping'</u> [conference presentation], *34th IAHR World Congress*, Brisbane, Qld.

McLean R, Thom B, Shen J and Oliver T (2023) '50 years of beach–foredune change on the southeastern coast of Australia: Bengello Beach, Moruya, NSW, 1972–2022', *Geomorphology*, 439:108850, doi:10.1016/j.geomorph.2023.108850.

McPherson B, Young S, Modra B, Couriel E, You B, Hanslow D, Callaghan D, Baldock T and Nielsen P (2013) 'Penetration of tides and tidal anomalies in New South Wales estuaries', in Coasts & ports 2013: combining the 21st Australasian Coastal and Ocean Engineering Conference and the 14th Australasian Port and Harbour Conference, Engineers Australia, Barton, ACT.

MHL (Manly Hydraulics Laboratory) (2012) <u>OEH NSW tidal planes analysis: 1990–2010 harmonic analysis</u>, Report MHL2053, Report prepared for the NSW Office of Environment and Heritage, MHL, Manly Vale, NSW.

MHL (2015) <u>NSW ocean and river entrance tidal levels annual summary 2014–2015</u>, Report MHL2384, Report prepared for the NSW Office of Environment and Heritage, MHL, Manly Vale, NSW.

MHL (2018) <u>NSW extreme ocean water levels</u>, Report MHL2236, Report prepared for the NSW Office of Environment and Heritage, MHL, Manly Vale, NSW.

MHL (2019) <u>Review of NSW OEH automatic water level recorder network 2019</u>, Report MHL2546, Report prepared for the NSW Office of Environment and Heritage, MHL, Manly Vale, NSW.

Modra B and Hesse S (2011) 'NSW ocean water levels' [conference presentation], NSW Coastal Conference, Tweed Heads, NSW.

Morim J, Cartwright N, Etemad-Shahidi A, Strauss D and Hemer M (2016) 'Wave energy resource assessment along the Southeast coast of Australia on the basis of a 31-year hindcast', *Applied Energy*, 184:276–297, doi:10.1016/j.apenergy.2016.09.064.

Morris BD, Foulsham E, Laine R, Wiecek D and Hanslow D (2016) 'Evaluation of runup characteristics on the NSW coast', *Journal of Coastal Research*, 75(sp1:1187–1191, doi:10.2112/SI75-238.1.

Mortlock TR and Goodwin ID (2016) 'Impacts of enhanced central Pacific ENSO on wave climate and headland-bay beach morphology', *Continental Shelf Research*, 120:14–25, doi:10.1016/j.csr.2016.03.007.

Mortlock TR, Goodwin ID, McAneney JK and Roche K (2017) 'The June 2016 Australian east coast low: importance of wave direction for coastal erosion assessment', *Water*, 9(2):121, doi:10.3390/w9020121.

Nicholls RJ, Birkemeier WA and Lee GH (1998) 'Evaluation of depth of closure using data from Duck, NC, USA', *Marine Geology*, 148(3–4):179–201.

Nicholls RJ and Cazenave A (2010) 'Sea-level rise and its impact on coastal zones', *Science*, 328(5985):1517–1520, doi:10.1126/science.1185782.

Nielsen AF and Gordon AD (2008) 'The hydraulic stability of some large NSW estuaries', *Australian Journal of Civil Engineering*, 5(1):49–60, doi:10.1080/14488353.2008.11463937.

Nielsen AF, Lord DB and Poulos HG (1992) 'Dune stability considerations for building foundations', *Transactions of the Institute of Engineers, Australia: Civil Engineering* CE34(2):167–174.

Nielsen P and Hanslow DJ (1991) 'Wave runup distributions on natural beaches', *Journal of Coastal Research*, 7(4):1139–1152.

NSW Govt (New South Wales Government) (1992) Estuary management manual, NSW Government Printer, Sydney.

OEH (Office of Environment and Heritage) (n.d.) <u>Aboriginal heritage information system</u> [data set], environment.nsw.gov.au, accessed 2023–2024.

OEH (2013) Corporate spatial database [data set], OEH, NSW Government, Sydney, accessed 2023–2024.

OEH (2017) <u>Coastal erosion in New South Wales: state-wide exposure assessment</u>, OEH, NSW Government, Sydney.

OEH (2018) <u>NSW estuary tidal inundation exposure assessment</u>, OEH, NSW Government, Sydney.

Oliver TSN, Tamura T, Brooke BP, Short AD, Kinsela MA, Woodroffe CD and Thom BG (2020) 'Holocene evolution of the wave-dominated embayed Moruya coastline, southeastern Australia: sediment sources, transport rates and alongshore interconnectivity', *Quaternary Science Reviews*, 247:106566, doi:10.1016/j.quascirev.2020.106566.

Palmer K, Harris RM, Watson CS, Hunter JR and Power HE (2022) 'Coastal lake tidal range amplifies sea-level threat in Lake Macquarie, Australia', in *Australasian coasts & ports 2021: te oranga takutai, adapt and thrive*, New Zealand Coastal Society, Christchurch, NZ.

Palmer K, Watson CS, Power HE and Hunter JR (2024) 'Quantifying the estuary and sea level component contributions to changing high water levels', *Journal of Geophysical Research: Oceans*, 129(8):e2023JC020737, doi:10.1029/2023JC020737.

Peng F, Deng X and Cheng X (2022) 'Australian coastal sea level trends over 16 yr of reprocessed Jason altimeter 20-Hz data sets', *Journal of Geophysical Research: Oceans*, 127(3):e2021JC018145, doi:10.1029/2021JC018145.

Phillips MS, Harley MD, Turner IL, Splinter KD and Cox RJ (2017) 'Shoreline recovery on wave-dominated sandy coastlines: the role of sandbar morphodynamics and nearshore wave parameters' *Marine Geology*, 385:146–159, doi:10.1016/j.margeo.2017.01.005.

Phillips MS, Blenkinsopp CE, Splinter KD, Harley MD and Turner IL (2019) 'Modes of berm and beachface recovery following storm reset: observations using a continuously scanning lidar', *Journal of Geophysical Research: Earth Surface*, 124(3):720–736, doi:10.1029/2018JF004895.

Phinn SR and Hastings PA (1995) 'Southern oscillation influences on the Gold Coast's summer wave climate', *Journal of Coastal Research*, 11(3):946–958.

Power HE, Gharabaghi B, Bonakdari H, Robertson B, Atkinson AL and Baldock TE (2019) 'Prediction of wave runup on beaches using gene-expression programming and empirical relationships', *Coastal Engineering*, 144:47–61, doi:10.1016/j.coastaleng.2018.10.006.

Prandle D (2009) Estuaries, Cambridge University Press.

PWD (Public Works Department) (1990) Coastline management manual, NSW Government Printer, Sydney.

QGIS Development Team (2023) QGIS [geographic information system app], QGIS.org.

Roemmich D, Gilson J, Davis R, Sutton P, Wijffels S and Riser S (2007) 'Decadal spinup of the South Pacific subtropical gyre', *Journal of Physical Oceanography*, 37(2):162–173, doi:10.1175/JPO3004.1.

Rosati JD, Dean RG and Walton TL (2013) 'The modified Bruun Rule extended for landward transport', *Marine Geology*, 340(1):71–81, doi:10.1016/j.margeo.2013.04.018.

Roy PS, Cowell PJ, Ferland MA and Thom BG (1994) 'Wave dominated coasts', in Carter RWG and Woodroffe CD (eds), *Coastal evolution: late quaternary shoreline morphodynamics*, Cambridge University Press.

Roy PS, Williams RJ, Jones AR, Yassini I, Gibbs PJ, Coates B, West RJ, Scanes PR, Hudson JP and Nichol S (2001) 'Structure and function of south-east Australian estuaries', *Estuarine, Coastal and Shelf Science*, 53(3):351–384, doi:10.1006/ecss.2001.0796.

Savenije HHG (2005) Salinity and tides in alluvial estuaries, Elsevier.

Schneider L, Maher WA, Floyd J, Potts J, Batley GE and Gruber B (2016) 'Transport and fate of metal contamination in estuaries: using a model network to predict the contributions of physical and chemical factors', *Chemosphere*, 153:227–236, doi:10.1016/j.chemosphere.2016.03.019.

Serafin KA, Ruggiero P and Stockdon HF (2017) 'The relative contribution of waves, tides, and nontidal residuals to extreme total water levels on US West Coast sandy beaches', *Geophysical Research Letters*, 44(4):1839–1847, doi:10.1002/2016GL071020.

Shand TD, Goodwin IA, Mole MA, Carley JT, Browning S, Coghlan IR, Harley MD and Peirson WL (2011) *NSW coastal inundation hazard study: coastal storms and extreme waves*, University of New South Wales (UNSW) Water Research Laboratory Technical Report No 2010/16, UNSW Water Research Laboratory.

Shih FY and Wu YT (2004) 'Fast Euclidean distance transformation in two scans using a 3 × 3 neighborhood', *Computer Vision and Image Understanding*, 93(2):195–205, doi:10.1016/j.cviu.2003.09.004.

Short AD (1988) 'Areas of Australia's coast prone to sea-level inundation', in Pearman GI (ed), *Greenhouse: planning for climate change*, CSIRO Publishing, Victoria.

Short AD (2006) 'Australian beach systems – nature and distribution', *Journal of Coastal Research*, 22(1):11–27, doi:10.2112/05A-0002.1.

Short AD (2007) Beaches of the New South Wales Coast, Sydney University Press.

Short AD (2020) Australian coastal systems: beaches, barriers and sediment compartments, Springer Nature.

Short AD and Trenaman NL (1992) 'Wave climate of the Sydney region, an energetic and highly variable ocean wave regime', *Marine and Freshwater Research*, 43(4):765–791, doi:10.1071/MF9920765.

Stockdon HF, Holman RA, Howd PA and Sallenger Jr AH (2006) 'Empirical parameterization of setup, swash, and runup', *Coastal Engineering*, 53(7):573–588, doi:10.1016/j.coastaleng.2005.12.005.

Sweet WV and Park J (2014) 'From the extreme to the mean: acceleration and tipping points of coastal inundation from sea level rise', *Earth's Future*, 2(12):579–600, doi:10.1002/2014EF000272.

Thom BG (1984), 'Transgressive and regressive stratigraphies of coastal sand barriers in southeast Australia', *Marine Geology*, 56(1–4):137–158, doi:10.1016/0025-3227(84)90010-0.

Thom BG and Hall W (1991) 'Behavior of beach profiles during accretion and erosion dominated periods', Earth *Surface Processes and Landforms*, 16(2):113–127, doi:10.1002/esp.3290160203.

Thom BG, Eliot I, Eliot M, Harvey N, Rissik D, Sharples C, Short AD and Woodroffe CD (2018) 'National sediment compartment framework for Australian coastal management', *Ocean & Coastal Management*, 154:103–120, doi:10.1016/j.ocecoaman.2018.01.001.

Tukey JW (1977) Exploratory data analysis, Addison-Wesley, Reading.

Van Goor MA, Zitman TJ, Wang ZB and Stive MJF (2003) 'Impact of sea-level rise on the morphological equilibrium state of tidal inlets', *Marine Geology*, 202:211–227, doi:10.1016/S0025-3227(03)00262-7.

van Maanen B, Nicholls RJ, French JR, Barkwith A, Bonaldo D, Burningham H, Murray AB, Payo A, Sutherland J, Thornhill G, Townend IH, van der Wegen M and Walkden MJA (2016) 'Simulating mesoscale coastal evolution for decadal coastal management: a new framework integrating multiple, complementary modelling approaches', *Geomorphology*, 256:68–80, doi:10.1016/j.geomorph.2015.10.026.

van Rijn L (2010) *Tidal phenomena in the Scheldt Estuary*, Report prepared for Deltares, Project 1202016-000, Delft, Netherlands.

Vila-Concejo A, Gallop SL and Largier JL (2020) 'Sandy beaches in estuaries and bays', in Jackson DWT and Short AD (eds), Sandy beach morphodynamics, Elsevier, London.

Viola CNA, Verdon-Kidd DC, Hanslow DJ, Maddox S and Power HE (2021) 'Long-term dataset of tidal residuals in New South Wales, Australia', *Data*, 6(10):101, doi:10.3390/data6100101.

Viola CN, Verdon-Kidd DC and Power HE (2024a) 'Characterising continental shelf waves and their drivers for the southeast coast of Australia', *Ocean & Coastal Management*, 253:107145, doi:10.1016/j.ocecoaman.2024.107145.

Viola CN, Verdon-Kidd DC and Power HE (2024b) 'Spatially varying impacts of pacific and southern ocean climate modes on tidal residuals in New South Wales, Australia', *Estuarine, Coastal and Shelf Science*, 305:108869, doi:10.1016/j.ecss.2024.108869.

Vos K, Harley MD, Splinter KD, Simmons JA and Turner IL (2019a) 'Sub-annual to multi-decadal shoreline variability from publicly available satellite imagery', *Coastal Engineering*, 150:160–174, doi:10.1016/j.coastaleng.2019.04.004.

Vos K, Splinter KD, Harley MD, Simmons JA and Turner IL (2019b) 'CoastSat: a Google Earth Engine-enabled Python toolkit to extract shorelines from publicly available satellite imagery', Environmental Modelling and Software, 122:104528, doi:10.1016/j.envsoft.2019.104528.

Vos K, Harley MD, Splinter KD, Walker A and Turner IL (2020) 'Beach slopes from satellite-derived shorelines', *Geophysical Research Letters*, 47(14):e2020GL088365, doi:10.1029/2020GL088365.

Vousdoukas MI, Wziatek D and Almeida LP (2012) 'Coastal vulnerability assessment based on video wave run-up observations at a mesotidal, steep-sloped beach', *Ocean Dynamics*, 62(1):123–137, doi:10.1007/s10236-011-0480-x.

Watson PJ (2020) 'Updated mean sea-level analysis: Australia', *Journal of Coastal Research*, 36(5):915–931, doi:10.2112/JCOASTRES-D-20-00026.1.

Weir FM, Hughes MG and Baldock TE (2006) 'Beach face and berm morphodynamics fronting a coastal lagoon', *Geomorphology*, 82(3–4):331–346, doi:10.1016/j.geomorph.2006.05.015.

White NJ, Haigh ID, Church JA, Koen T, Watson CS, Pritchard TR, Watson PJ, Burgette RJ, McInnes KL, You ZJ and Zhang X (2014) 'Australian sea levels – trends, regional variability and influencing factors', *Earth-Science Reviews*, 136:155–174, doi:10.1016/j.earscirev.2014.05.011.

Wolinsky MA and Murray AB (2009) 'A unifying framework for shoreline migration: 2. Application to wave-dominated coasts', *Journal of Geophysical Research: Earth Surface*, 114(F1):F01009, doi:10.1029/2007JF000856.

Wood N, Beauman M and Adams P (2021) 'An indicative assessment of four key areas of climate risk for the 2021 NSW Intergenerational Report', Treasury Technical Research Paper Series TTRP 21-05, Treasury, NSW Government.

Woodham R, Brassington GB, Robertson R and Alves O (2013) 'Propagation characteristics of coastally trapped waves on the Australian continental shelf', *Journal of Geophysical Research: Oceans*, 118(9):4461–4473, doi:10.1002/jgrc.20317.

Wright LD and Short AD (1984) 'Morphodynamic variability of surf zones and beaches: a synthesis', *Marine Geology*, 56(1–4):93–118, doi:10.1016/0025-3227(84)90008-2.

You ZJ, Nielsen P, Hanslow DJ and Pritchard T (2012) 'Elevated water levels at trained river entrances on the east coast of Australia', *Coastal Engineering Proceedings* 33(1):currents.48, doi:10.9753/icce.v33.currents.48.

Zhang X, Church JA, Monselesan D and McInnes KL (2017) 'High resolution sea level projections for Australian coasts in the 21st century', *Geophysical Research Letters*, 44(16):8481–8491, doi:10.1002/2017GL074176.

# Appendix A: Methods

# A.1 Timeframes and approach to uncertainty

In this assessment, both current and potential future exposure to coastal erosion, coastal overwash, and estuarine inundation were examined. The study references to the year 2020 and examines the implications of SLR at decadal intervals beyond this date, extending out to 2150. This approach is primarily based on the available SLR projections, but the use of decadal intervals also facilitates decision-making in the context of uncertain futures using dynamic adaptive pathways approaches (Haasnoot et al. 2013). The longer-term projections to 2150, combined with a range of climate change scenarios, enable full consideration of risks relevant to projected population growth in existing communities and planning for any new coastal development. However, as outlined in Appendix A.2 Sea level rise, SLR is virtually certain to continue beyond 2150, and this may need to be considered separately in policy development.

The year 2020 was chosen as the reference baseline to optimise use of the extensive measured water level and beach morphology data available in NSW and to align with the IPCC AR6 SLR projections. Projected SLR from the IPCC AR6 data, originally referenced to the 1995–2014 period, was adjusted to 2020 by subtracting the modelled rise between 1995–2014 and 2020. This adjustment ensures that only SLR occurring after 2020 is considered in the analysis.

Fundamental differences in modelling approaches, as well as limitations in data coverage and availability, necessitated tailored methods for baseline referencing for each hazard type. A brief description of how the baseline was implemented for coastal erosion, coastal overwash, and estuarine inundation is provided below, with detailed explanations in the following sections.

For erosion modelling, projected erosion volumes were applied to sector-averaged profiles behind a baseline shoreline derived from the 'most accreted' shoreline observed across all available LiDAR datasets (2007–2022). This approach ensured the modelling captured the maximum potential sediment volume available for erosion, representing an accreted beach state. Modelled erosion incorporates SLR from 2020 onwards.

For the coastal overwash analysis, the baseline sea level was calculated using water level records from 1990 to 2020. This timeframe was selected to ensure consistency across the limited number of gauges with long-term, overlapping datasets. Data were detrended to establish a 2020 reference SWL. Modelled overwash includes SLR from 2020 onwards.

For the estuarine inundation analysis, the baseline sea level was determined using all available water level records up to July 2022. These records were detrended to represent water levels in 2020. This approach accounts for variability in gauge coverage across estuarine locations, where records often span 20–30 years but are shorter in some cases. Modelled inundation incorporates SLR from 2020 onwards.

Note that there is considerable uncertainty associated with assessing both current and potential future hazards related to coastal erosion, coastal overwash, and estuarine inundation. This uncertainty arises from multiple sources and is typically categorised into 2 classes (Der Kiureghian and Ditlevsen 2009):

- aleatory uncertainty, which refers to inherent variability in natural processes (for example, in storm occurrence)
- epistemic uncertainty, which stems from a lack of knowledge, such as uncertainty regarding potential future sea level.

Uncertainty is unavoidable in both inundation and coastal erosion modelling and forecasting due to incomplete knowledge about current processes – for example, water levels, beach response to storms or sea level change, and the intrinsic limitations of hydrodynamic and beach and shoreline response models – as well as the potential range of future forcing conditions.

To address these uncertainties, a probabilistic approach is used to communicate future hazards in the context of the uncertainty space to support informed and transparent decision-making. By adopting this approach, this assessment aims to explicitly communicate the likelihood (or probability) of coastal hazards, allowing for risk assessment that takes uncertainty into account.

Understanding coastal risk requires assessment of both the likelihood of coastal hazards and their potential consequences. Available data were used in combination with SLR projections to model and map the potential likelihood of hazards associated with coastal erosion, coastal overwash, and estuarine inundation. The potential consequences were examined in the context of exposed existing infrastructure and other assets.

### A.2 Sea level rise

The adopted SLR projections were from modelling undertaken for IPCC AR6 (Fox-Kemper et al. 2021). Specifically, sea level projections for tide gauges along the NSW coast were accessed from the <u>NASA SLR projection tool</u> (Kopp et al. 2023), which is itself based on modelling conducted for the IPCC AR6 (Figure 58).



Figure 58 Screenshot of the NASA sea level projection tool

This dataset includes both medium-confidence and low-confidence modelling (the latter including marine ice-cliff instability). For both sets of modelling, the available data include quantile values (5, 17, 50, 83, 95%) of the projected SLR at decadal intervals up to 2150. For the medium-confidence modelling, the data include several greenhouse gas emission and socioeconomic scenarios (namely, SSP1-1.9, SSP1-2.6, SSP2-4.5, SSP3-7.0, and SSP5-8.5).

Beyond the likely range, the IPCC provides low-confidence projections for high-impact scenarios (for example, SSP5-8.5 low-confidence scenario). This modelling helps quantify potential SLR projections and impacts for decision-makers and stakeholders with low risk tolerance. The low-confidence projections integrate information from the structured expert judgement study by Bamber et al. (2019) for both the Greenland and Antarctic ice sheets, as well as results from a simulation study that incorporates marine ice-cliff instability in the Antarctic (DeConto et al. 2021). The IPCC AR6 data are referenced to the period 1995–2014 and have been adjusted to 2020 for this study by subtracting the initial value (2020) in the modelled data – that is, the projected rise between 1995–2014 and 2020 is removed.

To provide a comprehensive understanding of potential SLR impacts, this assessment report focuses on medium-confidence scenarios SSP1-2.6, SSP2-4.5 and SSP3-7.0 as primary storylines representing lower emissions, medium emissions, and high emissions pathways for future climate projections. SSP1-2.6 envisions a sustainable development future with significant emissions reductions; SSP2-4.5 reflects moderate challenges to mitigation and adaptation under continued historical trends; and SSP3-7.0 represents a high-emissions scenario driven by limited international cooperation and regional

rivalries. Additionally, this assessment considers medium-confidence SSP5-8.5 and low-confidence SSP5-8.5 as very high emission scenarios, representing a fossil-fuel-driven future characterised by rapid economic growth, high emissions and severe climate outcomes.

This overarching approach aligns with state-wide, national and global best practices for SLR modelling, ensuring consistency in decision-making frameworks across NSW. Given the inherent uncertainty of SLR, different scenarios result in vastly different exposure levels for communities, infrastructure and ecosystems. By examining a wide range of scenarios, this assessment enables decision-makers to account for varying levels of risk, ensuring strategies are resilient to both likely and less probable, yet more severe, impacts. This comprehensive approach supports the development of flexible, adaptive management solutions to address long-term uncertainties and mitigate vulnerabilities in critical assets and communities.

To account for uncertainty in each of the SLR scenarios, a probability distribution was fitted through the sets of quantile data. This is undertaken using the quantile fitting statistical computing software called *rriskDistributions* (Belgorodski et al. 2022), created using the R package version 2.1.2. This package fits a wide range of continuous distributions to quantile data and identifies the best fit distributions by minimising plotting and convergence tolerance. To select a distribution for fitting to each of the sets of SLR quantiles, the best fit distributions were first identified at the Fort Denison tide gauge on the central NSW coast. This distribution was then fitted to each of the sets of quantile data (with equal weighting) for each timeframe, SSP and tide gauge. An example of the resultant set of normalised distributions covering the full range of possibilities for each time horizon up to 2150, for SSP3-7.0 at Fort Denison, is shown in Figure 59.

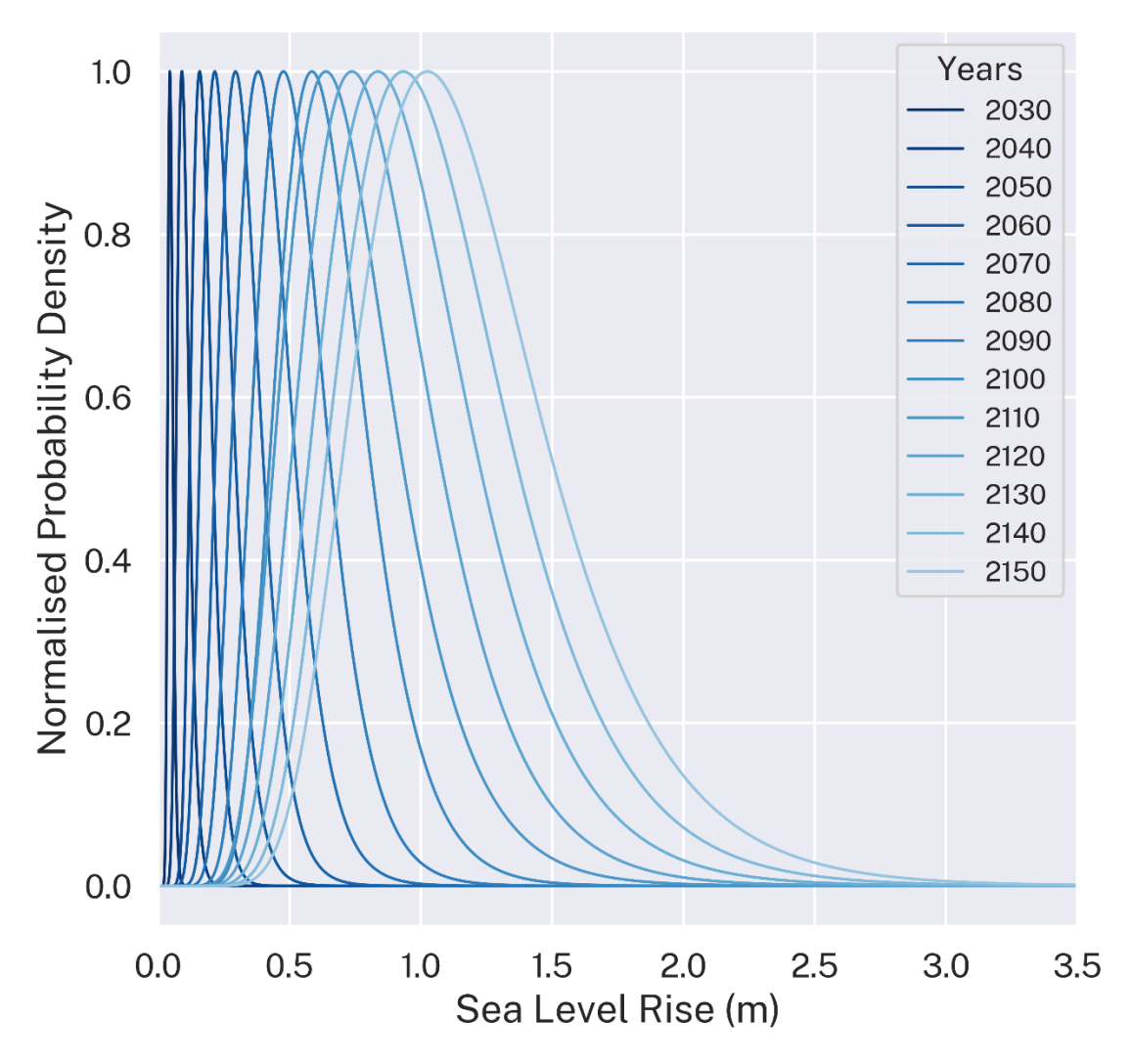


Figure 59 Log normal sea level rise distributions for each time horizon for SSP3-7.0 at Fort Denison

## A.3 Coastal erosion methods

#### Overview

Coastal erosion is modelled using a sediment-volume-based coastal response model, applied within a Monte Carlo simulation framework to generate probability distributions of beach erosion volume and shoreline change for present and future scenarios. Components of erosion considered in the model include beach fluctuation caused by storms and climate variability (scaled by local exposure to wave energy), historical trends in beach behaviour attributed to sediment budget imbalances, and the response to SLR, including the redistribution of sand from beaches and dunes to adjacent estuaries and the coastal seabed. Modelled beach erosion volumes are mapped as total erosion distances from present-day beach shorelines using high-resolution coastal terrain data. Hazard mapping and exposure statistics are provided for selected exceedance probability levels (50%, 10%, 1%, and 0.1%) extracted from the distribution of modelling outcomes.

#### Data

The erosion modelling approach takes advantage of recent advances in available data describing coastal geomorphology and ocean processes along the NSW coast. Many datasets have been acquired and developed since the previous state-wide coastal erosion hazard assessment (Kinsela et al. 2017; OEH 2018). For example, high-resolution mapping of the coastal seabed, consistent analysis of historical beach change trends from satellite observations, and local-scale nearshore wave modelling are all critical inputs to the coastal erosion modelling approach. Appendix B: Datasets lists the datasets used in this study, enabling the most detailed assessment of coastal erosion potential along the NSW coastline to date.

# **Approach**

The coastal erosion modelling approach builds on the previous state-wide coastal erosion exposure assessment (Kinsela et al. 2017; OEH 2018), taking particular advantage of recent advances in the coverage, resolution, frequency and availability of datasets describing the coastal geomorphology, historical behaviour and ocean processes of NSW beaches. This section outlines key aspects of the approach, providing context for later descriptions of the drivers and components of coastal erosion considered in the modelling.

#### Modelling scope

The spatial extent of the coastal erosion modelling and hazard exposure assessment covers the NSW coastline, with the scope primarily limited to open coast beaches, although selected wave-dominated beaches in semi-enclosed bays and estuaries were considered as a case study. The behaviour of beaches within estuaries and bays is complex, with locally varying wave exposure and estuarine sediment dynamics that may be beyond the scope of the open coast erosion modelling approach (Vila-Concejo et al. 2020; Fellowes et al. 2021). Hence, modelling erosion in such settings should be taken as a first-pass estimate, and more detailed site-specific studies are required to evaluate their sediment budgets comprehensively.

A second restriction on the erosion modelling scope was that the backshore geomorphology landward of the modelled beaches must fully or partially comprise unconsolidated or erodible sediment (Kinsela et al. 2016b, 2017). The NSW coastal quaternary geology mapping and the Smartline coastal geomorphology datasets (see Appendix B: Datasets) were used to identify beaches with erodible backshore geomorphology considered in the modelling.

Beaches with entirely non-erodible backshore geomorphology (such as bedrock cliffs or other non-erodible substrates behind the beach) were excluded. In such settings, the beach may be entirely removed by extreme storm impacts at present, re-forming when sand returns from the nearshore. That could involve partial or total temporary loss of the beach at present, and potentially permanent loss in the future due to SLR. Assessing the potential for future annihilation of such beaches was beyond the scope of the modelling.

For beaches with erodible backshore geomorphology but protected by seawalls or other artificial structures, the natural response of the beach (assuming no protection) was modelled. As such, it is recommended that coastal erosion hazard mapping be interpreted in conjunction with data on existing coastal protection structures (for example, seawalls), where available or appropriate. Doing so ensures a more accurate understanding of the actual exposure to erosion hazards, as areas identified as susceptible to erosion may, in practice, be shielded by engineered defences.

Based on the considerations above, coastal erosion modelling was carried out for 336 open coast NSW beaches, modelled as 726 individual beach sectors (<u>Appendix C: Beaches modelled</u>). An additional 32 ocean-influenced bay/estuary beaches located within the entrances of Port Stephens (2), Broken Bay (3), Bate Bay (2), Jervis Bay (7), Batemans Bay (11) and Twofold Bay (7), which are exposed to ocean wave processes, were also considered as case studies, bringing the total number of modelled beaches to 368, across 758 individual sectors.

The temporal scope of coastal erosion modelling included projections from present to 2150, at decadal increments, following the SLR projections (<u>Appendix A.2</u>) and consistent with the coastal overwash (<u>Appendix A.4</u>) and estuarine inundation (<u>Appendix A.5</u>) assessments.

### Reduced complexity model

The spatial and temporal scales of the coastal erosion modelling require an approach that is appropriately efficient to allow for millions of Monte Carlo simulations across hundreds of beach sectors, for decadal forecast horizons from present to 2150, and across 5 future SLR emissions pathways. The Monte Carlo simulation method allows for managing uncertainties in the drivers of coastal erosion and the modelled responses by evaluating probabilities across potential outcomes for each scenario (Cowell et al. 2006; Kinsela et al. 2017).

The method follows a reduced-complexity approach, where physical processes driving beach erosion are summarised into parameters that capture the resulting beach sediment-volume change. This approach is commonly used in large-scale and long-term coastal evolution modelling exercises, in which simulating the physical processes of coastal change at the desired scales is computationally infeasible and exceeds reasonable levels of confidence in our ability to accurately simulate sediment transport processes at longer timescales (Cowell et al. 2003; French et al. 2016; van Maanen et al. 2016).

The modelling is data-informed, with probability distributions for key parameters guided by historical observations of beach change at either the local scale (for example, historical mean-trend change captured by satellite shoreline change mapping) or regional scale (for example, probability distribution for storm-driven erosion on fully exposed NSW beaches). This ensures the model reflects historical fluctuations and cumulative beach volume and shoreline change signals. While that invokes an implicit assumption that historical trends in coastal change will persist into the future, long-term trends stemming from sediment budget imbalances are likely to influence future

coastal change, including the response to SLR. Any local- to regional-scale trends may moderate or enhance the predicted response to SLR.

<u>Figure 10</u> conceptually shows the modelled beach erosion sediment-volume (*V*), converted to an erosion distance (*R*) using high-resolution topography data for each beach sector modelled. Present scenarios consider the range of beach fluctuation while the future projections also consider cumulative volume change that causes permanent shoreline recession.

In present scenarios, only fluctuating erosion is considered, as sand eroded from beaches is deposited offshore in surf zone bars and on the upper shoreface and is expected to return to replenish the beach and foredune during calmer conditions. In future forecast scenarios, the addition of cumulative erosion components means that the reach of coastal erosion will progress landwards over time as eroded sand may be lost to sinks in the coastal sediment system, depending on the local sediment balance and response to SLR relative to any underlying trends in the system.

All model parameters contributing to fluctuating and cumulative erosion are expressed as sediment volumes per metre of shoreline (m³/m) along each beach sector. Any components that are observed or calculated as distances are converted to volumes using the local beach topography. This ensures that coastal change predictions reflect the accurate morphology of the beach and dunes in each sector, rather than assuming fixed and constant dune heights during erosion (Kinsela et al. 2017; McCarroll et al. 2021).

# Probabilistic modelling framework

Simulating coastal erosion over decades to centuries involves considerable uncertainty, which must be captured and managed within the modelling process to communicate the full spectrum of potential responses in model forecasts (Cowell et al. 2006; French et al. 2016). Sources of uncertainty include (but are not limited to) historical observations of beach change and analysis of trends; present and future influences on local sediment budgets; the nature of and possible changes to coastal wave climates; changing environmental drivers such as SLR; the aggregation and parametrisation of complex coastal geomorphology to a scale suitable for modelling; and the modelling methods employed.

To manage these uncertainties, the coastal erosion modelling follows a probabilistic approach, using a Monte Carlo simulation framework to estimate the potential extent of erosion for each scenario and each beach sector, as well as the distribution of probabilities across that extent (Cowell et al. 2006; Kinsela et al. 2017). For each beach sector, scenario and forecast year, the probability distribution of potential coastal change was generated from 2 million Monte Carlo simulations, and the projected coastal changes corresponding to selected exceedance probability levels (50%, 10%, 1%, 0.1%) were mapped. This probabilistic approach allows for the full uncertainty space to be considered and expressed as the relative likelihood of erosion exposure across the feasible range for each scenario.

# Coastal geomorphology

The unique geomorphology of the broader coastal sediment system forming each NSW beach, both above the water (beach and dunes) and below the water (surf zone and shoreface), plays a strong role in how the beach responds to ocean drivers of coastal erosion. The coastal geomorphology includes the form (surface shape and elevation) and composition (sediment, rocks, biological structures) of the coastal system. Within the scope of modelling coastal erosion into unconsolidated or weakly consolidated coastal sedimentary landforms (beaches, dunes and sand barriers), the distribution and volume of sediment within the coastal system that is erodible and potentially transportable must be known to evaluate the sediment redistribution under different scenarios.

#### Compartments, beaches and sectors

The modelling was carried out using the Australian sediment compartments framework (Thom et al. 2018; Short 2020) as an organisational structure for data analysis and model operation. The NSW coast features 9 primary and 47 secondary sediment compartments. These compartments provide a useful framework for arranging and executing the modelling and defining model parameters representing coastal erosion components at different space–time scales. The tertiary compartment and subcompartment classifications of Kinsela et al. (2017) were also used to identify sandy shorelines connected to estuary sediment sinks.

The Australian Beach Safety and Management Program beach numbering system for NSW beaches (Short 2007) was then used to identify individual beaches for modelling. According to this system, there are 721 NSW beaches that are either open coast or located within entrances of semi-enclosed bays or estuaries. These include some beaches within the entrances of Broken Bay, Port Hacking, Jervis Bay, Batemans Bay and Twofold Bay. As described in the modelling scope, ocean-influenced bay/estuary beaches were considered as a separate case study.

Beaches that are less than or equal to 900 m in alongshore length, based on the erosion modelling baselines, were modelled as one single sector. That is because short beaches do not typically feature strong shoreline curvature or alongshore gradients in morphology and processes, due to the limited space for such variations to evolve. Therefore, modelled beach change is expected to be similar along the length of the shoreline.

Beaches longer than 900 m alongshore were divided into 3 sectors – north (sector a), central (b) and south (c) – each of equivalent shoreline length. Some particularly long beaches featuring strong shoreline curvature at the southern ends were divided into 5 or 6 sectors, in which case, the initial southern third sector (c) was then divided into 3 (c, d, e) or 4 (c, d, e, f) sectors of equivalent length.

For this scale of modelling the sectors are a pragmatic method of considering alongshore gradients in the coastal geomorphology and ocean processes that may vary along longer beaches. For example, long beaches often have higher wave exposure and larger dunes at the northern end, with reduced wave exposure and lower morphology at

the southern end. Central sectors may exhibit more uniform alongshore characteristics compared to northern and southern ends, where headland-attached reef outcrops and estuary inlets also tend to occur.

All model components were defined and analysed at the beach sector scale, including:

- onshore beach-dune morphology and substrate
- offshore surf zone-shoreface morphology and sediment cover
- nearshore wave climate and shoreline exposure
- beach fluctuation due to storms and climate cyclicity
- underlying shoreline change due to sediment budget imbalance
- response to SLR.

The impacts of cumulative erosion components were shared along continuous shorelines (that is, sectors sharing the same beach number), reflecting sediment distribution along embayed beaches over longer timescales. In contrast, fluctuating erosion impacts were specific to each sector, reflecting alongshore variations in exposure to wave processes.

An example of an embayment with 2 beaches is at Wooli, where the long and continuous Wooli Beach (nsw073) was divided into 3 sectors for modelling, while Jones Beach (nsw074) was modelled as a single sector (<u>Figure 60</u>). Alongshore variation in the onshore and offshore coastal geomorphology throughout the Wooli embayment is used to demonstrate the features and application of the coastal erosion model through the subsequent model description, which was applied to all NSW beach sectors considered (Appendix C: Beaches modelled).

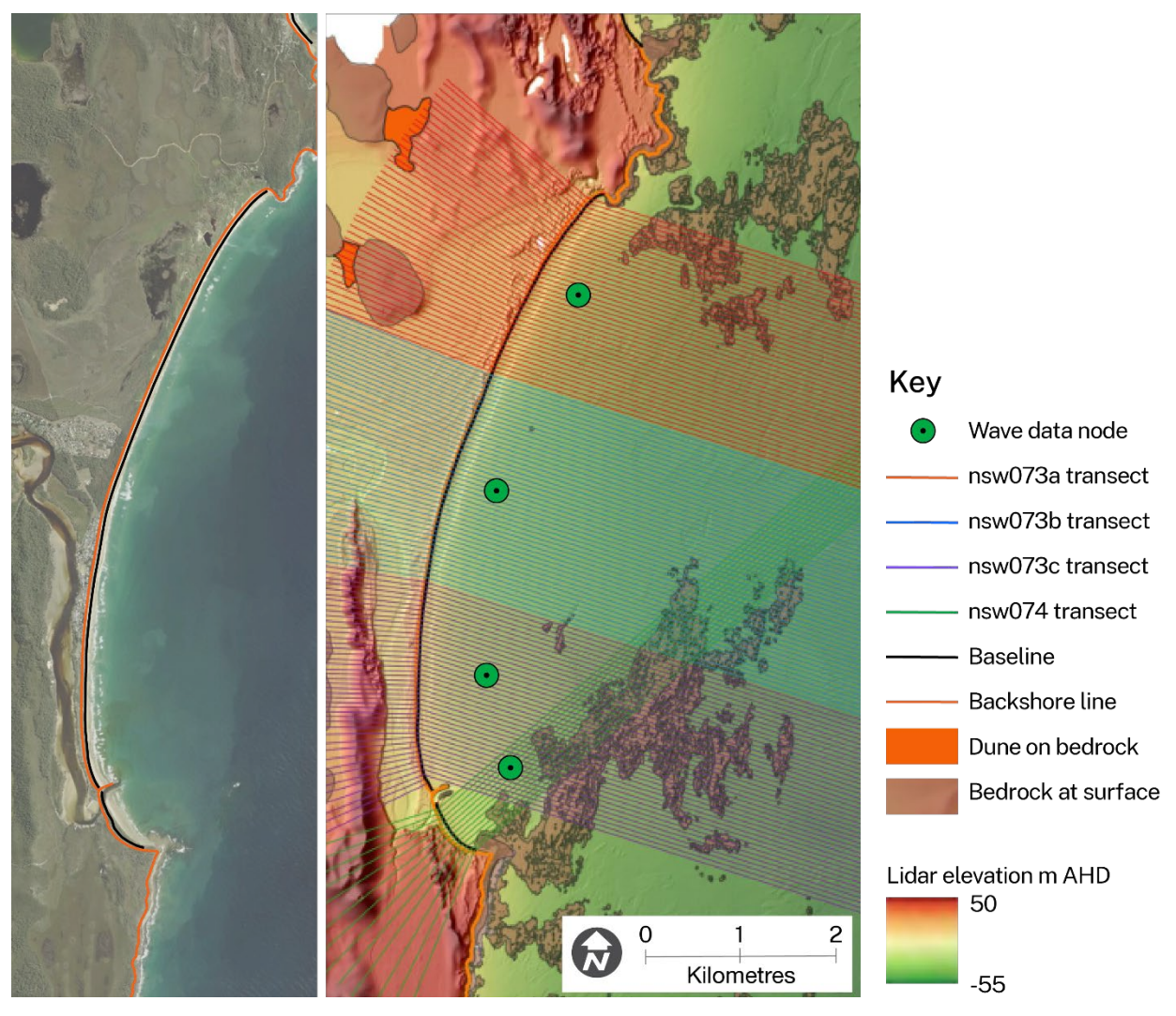


Figure 60 Example of onshore and offshore coastal geomorphology sampling design in Wooli embayment, showing division of Wooli Beach (nsw073) into 3 sectors, and the shorter Jones Beach (nsw074) as one sector, for erosion modelling, with wave data node (10 m water depth) for each sector also shown

## Onshore geomorphology

The complex 3-dimensional geomorphology of each beach, as shown by the LiDAR terrain data in <u>Figure 60</u>, was simplified, by alongshore-averaging, into 2-dimensional (2D) profiles for each sector (<u>Figure 61</u>), consistent with the reduced-complexity modelling methods. Coastal tract principles for spatially aggregated coastal modelling (Cowell et al. 2003) were applied to capture alongshore morphological variation within each beach sector.

The following spatial datasets were created for each modelled beach sector to represent the onshore geomorphology (Figure 60):

 a backshore line, which traces the back of the beach, where an incipient dune, a dune scarp toe, or the base of a seawall may be found (depending on the setting)

- an accreted baseline, which approximates the berm position as the 2 m AHD contour during the most accreted beach state (for each sector), captured in all available LiDAR data (Appendix B: Datasets)
- a set of sampling transects, oriented perpendicular to the shore and regularly spaced 50 m apart along the beach, from which morphology profiles were derived a sector-averaged onshore profile representing the average morphology from all sampling transects within each sector.

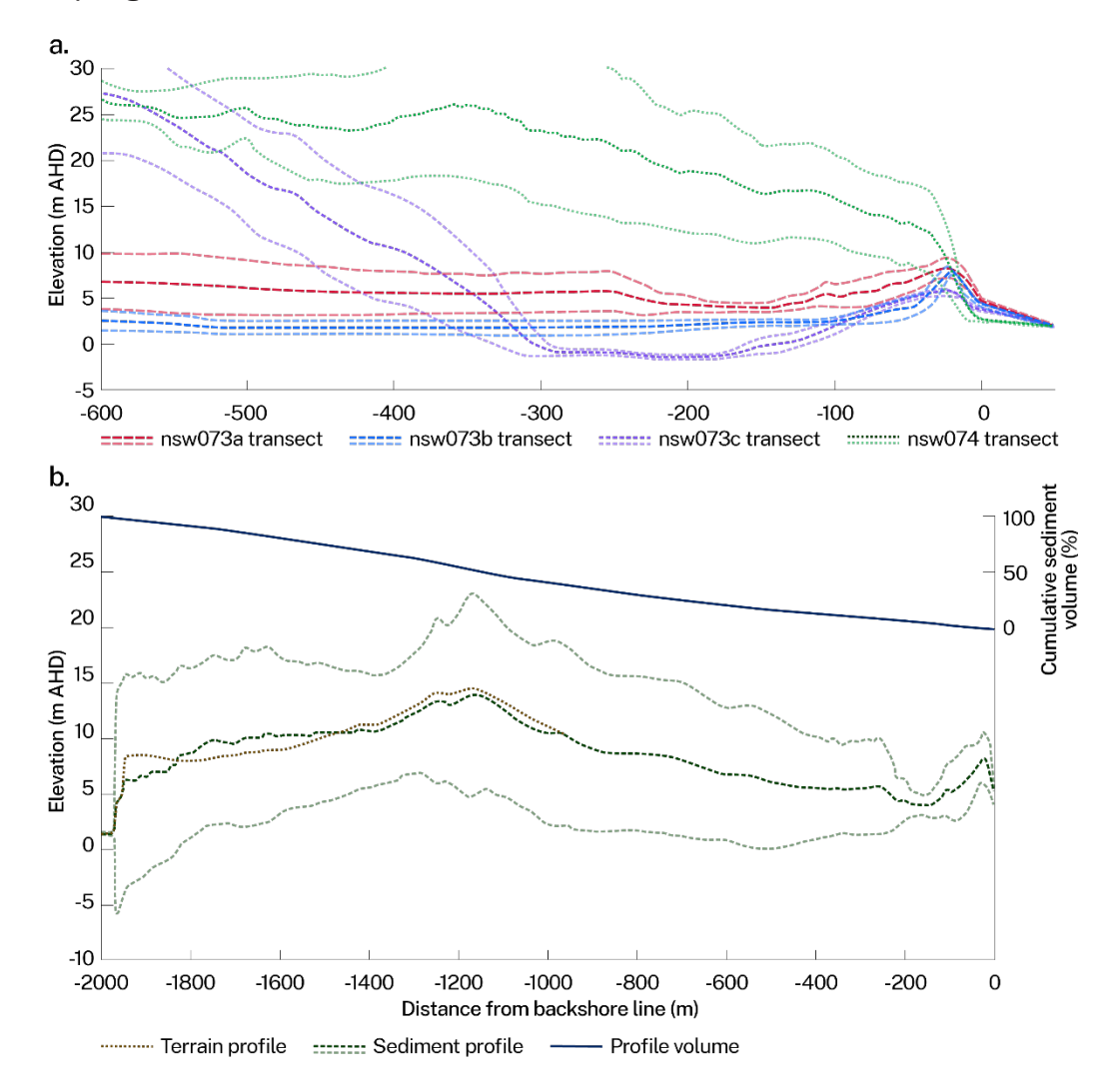


Figure 61 Example sector-average onshore profiles showing (a) the morphology of the 3
Wooli Beach sectors (nsw073a, nsw073b, nsw073c) and the Jones Beach
sector (nsw074) from the baseline to 600 m landward of the backshore line;
and (b) complete profile extending 2 km inland for sector nsw073a showing the
difference between the full terrain profile and sediment profile (bedrock
removed), and the cumulative sediment volume across the profile

The onshore topography used for erosion modelling was derived from 2018 and 2010–2014 LiDAR elevation datasets (<u>Appendix B: Datasets</u>). The 2018 dataset was prioritised due to its more recent collection and its seamless integration with the offshore bathymetry data. In areas where the 2018 data had narrower coverage, the 2010–2014 LiDAR data supplemented the analysis.

The onshore topography defines the sediment volume potentially available for erosion, depending on the modelled scenario. However, the backshore geomorphology may include materials that are considered non-erodible over the modelling timescales. In such cases, these areas can be excluded from the sediment volume definition. The *NSW Coastal quaternary geology mapping* dataset (Appendix B: Datasets) was used to identify and exclude topography that has been mapped as basement rock (bedrock) or bedrockmantling dunes (Figure 60) at the surface. This process generated terrain profiles that only reflect erodible land areas, and thus the erodible sediment volume of the beach and dunes (Figure 61).

The onshore morphology profile, representing the potentially erodible land area and sediment volume within each beach sector, was generated by sampling the onshore LiDAR mosaic (after basement rock and bedrock-mantling dunes were removed) along each transect landward of the backshore line. The set of sampled profiles within each beach sector were then averaged to generate a representative onshore morphology profile for each beach sector (Figure 61).

A hypothetical fully accreted beach was constructed for each sector by linear extrapolation between the backshore line and the baseline (accreted 2 m AHD contour). The backshore elevation was determined by sampling the onshore LiDAR mosaic along the backshore line. Using the fully accreted beach face addresses the fact that beach morphology captured by the 2018 LiDAR survey represents one point in time (and one beach state), and ensures the beach volume applied in modelling represents an accreted state for all sectors.

## Offshore geomorphology

A similar approach to the onshore geomorphology was applied to offshore geomorphology, simplifying it into 2D profile sections representing each sector, consistent with the reduced-complexity modelling methods. A set of transects regularly spaced 50 m apart alongshore was generated for each beach sector from which bathymetry profiles were derived (Figure 60). In this case, however, all sector profile sets for each continuous beach were aligned perpendicular to the average central shoreline orientation, to ensure that the sampled offshore morphology was representative of each sector.

The offshore geomorphology of NSW beaches may be complex, often comprising a variable mixture of sedimentary seabed and temperate rocky reefs, with the balance ranging from reef-dominated to sediment-dominated shorefaces even in adjacent settings (Linklater et al. 2019, 2023; Kinsela et al. 2022). This complexity poses challenges for modelling the potential response of the submerged beach system to SLR, which is a critical component of the future forecasts (Appendix A.3: Response to sea level rise).

Complex seabed geomorphology is evident within the Wooli embayment (<u>Figure 60</u>), for which <u>Figure 62</u> shows the modelling profiles for the northern (nsw074a) and southern (nsw074c) sectors, respectively. The seabed profiles include all seabed morphology and capture the reef outcrops, which rise above the surrounding sediment profiles that

represents the seabed in the absence of reefs. The shoreface is predominantly sandy in nsw074a whereas the interruption by rocky reefs is evident in the seabed sediment cover across the shoreface within nsw074c.

The model's approach for predicting the response of the submerged beach system is based on an assumption that sedimentary seabed areas may aggrade with SLR (Appendix A.3: Response to sea level rise), but this assumption is not valid for seabed affected by protruding reef outcrops. A pragmatic method for handling this complexity is to limit the modelled response of the offshore beach system (in terms of sediment volume redistribution) to only the sedimentary areas of seabed fronting each beach sector (Kinsela et al. 2022).

Bathymetry mosaics were created for each sediment compartment from the seamless 2018 coastal LiDAR dataset and all available multibeam echosounder surveys (Appendix B: Datasets). The NSW seabed landforms mapping analysis methods (Linklater et al. 2023) were used to identify all rocky reef areas within the mosaics. To address the geometric complexities of rocky reefs and capture surrounding scour areas where the sedimentary seabed surface is often disturbed, mapped reef areas were buffered by 25 m. These buffered reef areas were then used to erase reefs from the bathymetry mosaics, with the remaining gaps interpolated across using the triangular-irregular network approach followed by raster conversion.

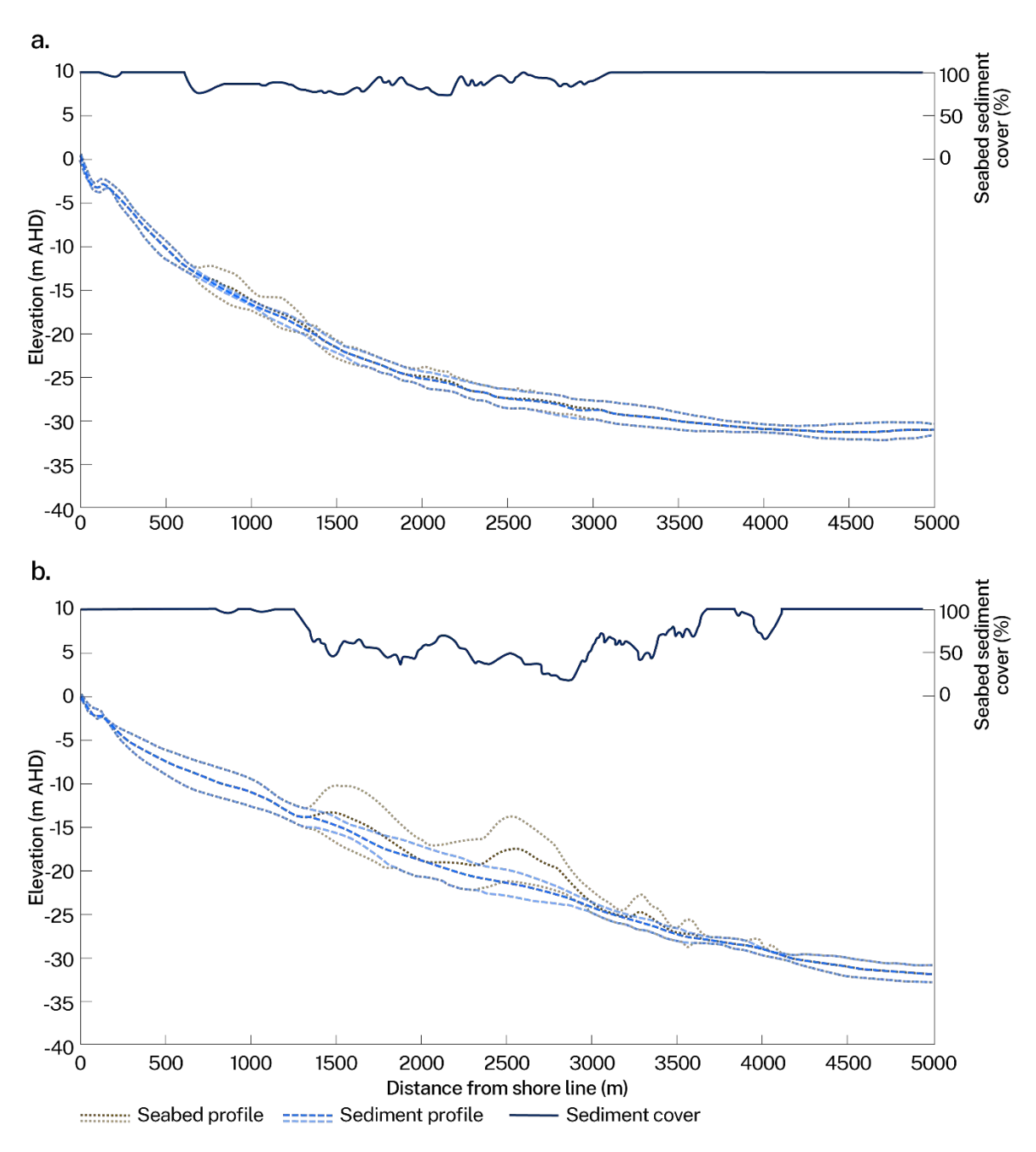


Figure 62 Examples of sector-averaged offshore profiles comparing (a) the average shoreface morphology in sector nsw074a and (b) nsw074c as shown in Figure 60

The result was a bathymetry mosaic set depicting the seabed as it would appear without rocky reefs. The offshore transect set for each beach sector was then used to sample that bathymetry mosaic at 5-m intervals to derive offshore bathymetry profiles. The profiles from each beach sector were then averaged to generate a representative offshore morphology profile for each sector (Figure 62).

The depth-based distribution of sediment and rocky reefs along each profile transect was sampled along each transect in each sector set using the seabed landforms mapping to identify and remove reef areas from the bathymetry mosaics. Thus, a seabed

response potential proportionate to the balance of sediment cover and rocky reef seabed across each sector shoreface was derived for each sector offshore profile.

## Ocean drivers of coastal erosion

## Wave climate

Wave runup on beaches saturates the sand and provides the energy to destabilise beach and dune sand, which is then transported offshore. The frequency–magnitude relationship of the fluctuation component of coastal erosion (<a href="Appendix A.3: Beach fluctuation">Appendix A.3: Beach fluctuation</a>), both now and in future, will vary with local exposure to regional wave climate. This exposure may be reduced by sheltering afforded by coastline orientation, shoreline curvature, headlands, built structures (such as inlet training walls), and offshore islands and reefs.

The local wave climate for each beach sector was analysed using long-term hindcast wave data from the *NSW nearshore wave transformation tool* version 2 (Baird Australia 2024). Continuous hourly nearshore (10 m water depth) wave data spanning 67 years (1957–2023) was generated at wave nodes nearest to the centre of each beach sector, capturing alongshore variation in wave exposure along continuous shorelines and between beaches. The local wave climate of a short beach (less than 900 m long) with only one sector was represented by wave data from one wave model node, while for a long beach (longer than 900 m), the wave nodes nearest to the centre of the northern, central and southern sectors were used. For particularly long beaches with strong curvature, 5 or 6 wave nodes were used, covering the additional sectors for the curved and typically more sheltered southern ends.

Standard descriptive statistics (mean, mode, median, minimum, maximum, standard deviation, and so on) were calculated for wave parameters across the long-term record for each beach sector to compare the local wave climates. Significant wave height (H<sub>s</sub>), spectral peak period (T<sub>p</sub>), and peak direction (D<sub>p</sub>) were key parameters available for the analysis. To characterise the extreme storm wave climate for each beach sector, the annual 12-hour exceedance significant wave height (H<sub>sx</sub>) and corresponding T<sub>p</sub> and D<sub>p</sub> values were calculated for each hindcast year, and subsequently the long-term means of those values calculated. These extreme wave parameters were used to scale the beach fluctuation relationship for each sector (Appendix A.3: Beach fluctuation) and to calculate the shoreface closure depth for the translation component of the response to SLR (Appendix A.3: Response to sea level rise).

## Storm surge

Storm surge refers to the temporary rise of coastal sea levels during storm conditions, caused by a combination of meteorological and oceanographic processes such as barometric setup (caused by low pressure), wind setup (caused by strong onshore winds), and wave setup (caused by large waves), each of which contributes to raising the coastal sea level above the predicted tide level for periods of hours to days. The elevated coastal sea levels, combined with large waves in the surf zone, enable wave runup processes to reach across the beach face to the dunes, allowing waves to attack

and erode sub-aerial parts of the beach and dune system (Holman 1986; Nielsen and Hanslow 1991; Atkinson et al. 2017). The processes modelled to assess the coastal overwash hazard (Appendix A.4 Overwash likelihoods) also drive coastal erosion.

Storm surge and wave runup processes are not explicitly simulated in the coastal erosion model as they exceed the appropriate scale for the modelling approach. Rather, the beach fluctuation probability distribution implicitly accounts for these processes as it captures the erosion outcome of combined waves and storm surge. This reflects the parameterisation approach for this scale of modelling, whereby coupled process–response behaviours are aggregated for model efficiency and to best reflect our actual understanding of medium- to long-term coastal change.

#### Sea level rise

SLR can drive coastal erosion by advancing the reach of wave attack and altering the balance of sediment distribution between coastal geomorphic features (for example, the shoreface, beach, dunes and estuaries) that are connected by the sediment system.

The climate change scenarios for SLR considered in coastal erosion modelling included SSP1-2.6, SSP2-4.5 and SSP3-7.0, consistent with coastal overwash (<u>Appendix A.4 Overwash</u> likelihoods) and estuarine inundation (<u>Appendix A.5 Estuarine inundation</u>) hazard analyses. The SLR projections for each scenario and forecast year were defined as log-normal probability distributions following the approach described in <u>Appendix A.2 Sea level rise</u>.

For each coastal erosion model simulation set for future projections (2030–2150), the SLR applied in each Monte Carlo model iteration was randomly sampled from the lognormal probability distribution corresponding to the future emissions scenario and forecast year. The modelled response of the coastal sediment system to SLR and its contribution to modelled coastal erosion and shoreline change are described in Appendix A.3: Hazard projections. Since the present-day scenarios (that is, 2020) were limited to the beach fluctuation component under current sea level conditions (Appendix A.3: Beach fluctuation), SLR was not included in these scenarios.

# Modelled components of coastal erosion

#### **Beach fluctuation**

All potential components of beach fluctuation are aggregated and described by a gamma probability distribution that reflects the feasible range and likelihood of temporary fluctuations in beach-dune sediment volume on exposed NSW beaches (Figure 63). Erosion driven by storm events (individual or clustered) is the primary factor in beach fluctuation. Therefore, the widely used probability relationship for storm demand on NSW beaches of Gordon (1987) and subsequent studies (Callaghan et al. 2008, 2013) were used to shape the gamma distribution (Kinsela et al. 2017). The distribution accommodates the potential for coincident storm erosion and other drivers of beach fluctuation, such as influences from climate variability (for example, beach rotation and headland sand bypassing). The distribution has been evaluated against available extreme beach erosion mapping data previously, in which the 1% annual

exceedance probability level fluctuation volume (250 m<sup>3</sup>/m) was found to be consistent with the positions of the significant historical erosion scarps (Kinsela et al. 2017).

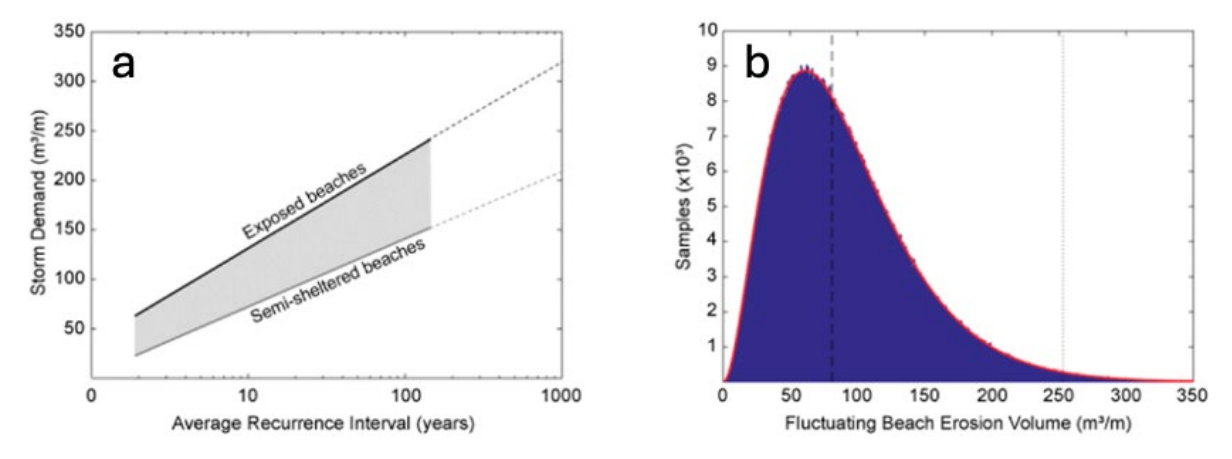


Figure 63 (a) Average recurrence interval for storm-driven beach erosion volumes (m³/m) on exposed and semi-sheltered NSW beaches and (b) the gamma probability distribution for fluctuating beach erosion

Sources: (a) Gordon (1987); (b) Kinsela et al. (2017).

The gamma distribution for fluctuating erosion was scaled for each beach sector using the nearshore extreme wave statistics calculated for each sector described in Appendix A.3: Wave climate. For example, the beach fluctuation distributions for the 4 sectors of the Wooli embayment are compared to the most exposed sector in the region, which captures increased sheltering from waves moving from north to south within the bay, due to the combined influences of headlands and offshore reefs (Figure 60), as shown in Figure 64(a) (nsw073a), Figure 64(b) (nsw073b), Figure 64(c) (nsw073c) and Figure 64(d) (nsw074).

The scaling was applied across 10 regions along the NSW coastline, covering the 9 primary sediment compartments, with the southern compartment (nsw09) divided into 2 regions because of its alongshore length and varying wave climates between the northern and southern portions. Within each region, all beach sectors were scaled against the most exposed sector in that region. This approach acknowledges that understanding of the probability relationship for storm-driven beach fluctuation remains limited by spatiotemporal sampling biases in historical observation data, and thus it would not be prudent to imply from the modelled wave statistics that one region is more exposed to coastal erosion than another.

The sampled (and scaled) fluctuating beach erosion volume within each model simulation was applied to the alongshore-averaged sector onshore profile, reflecting the fully accreted sediment volume, which comprised the backshore profile and accreted beach face profile spanning between the backshore line and baseline. Thus, the simulated erosion distances are measured relative to the present-day accreted beach state.

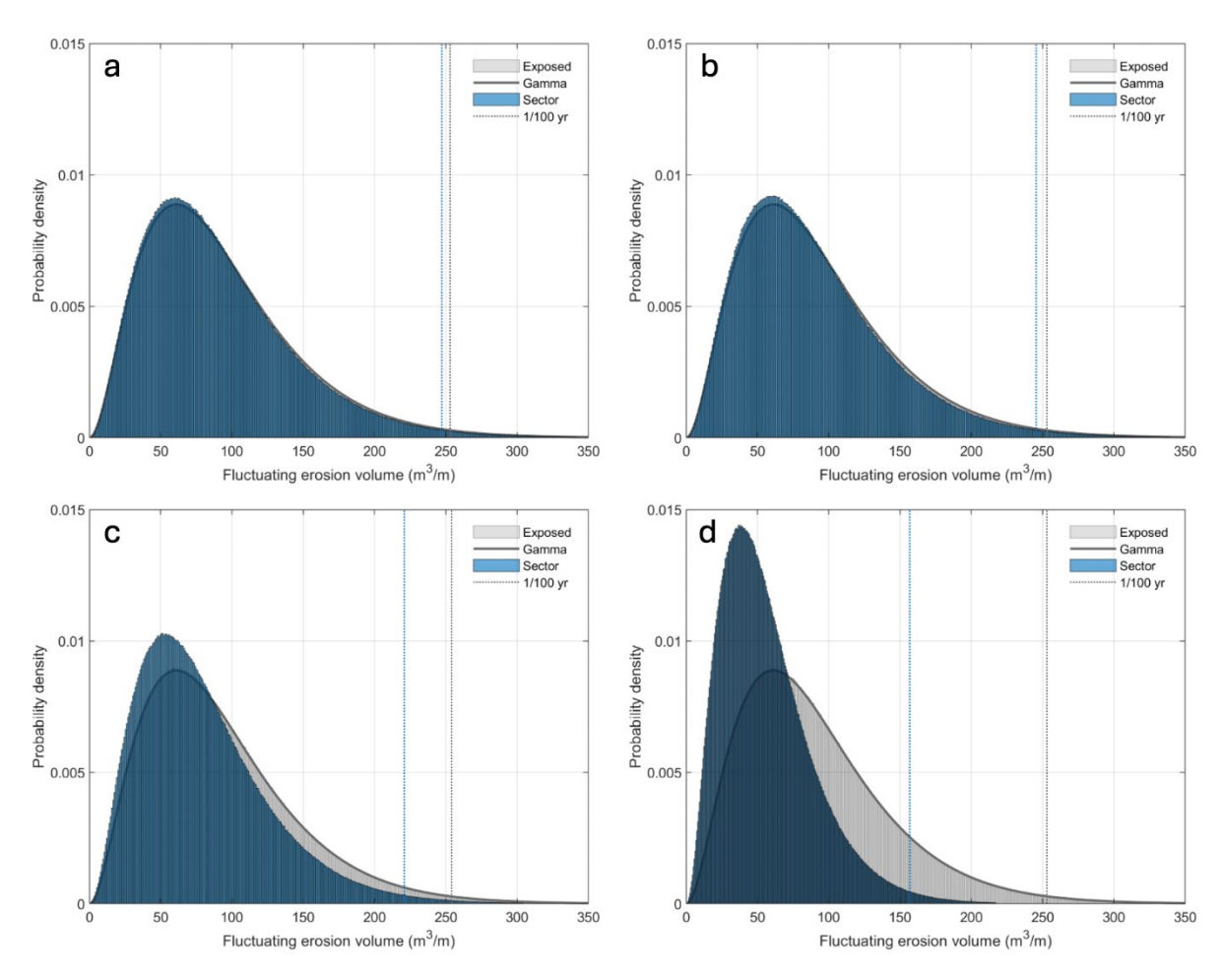


Figure 64 Example scaling of the fluctuating beach erosion gamma probability distribution in Wooli embayment sectors (a) nsw073a, (b) nsw073b, (c) nsw073c and (d) nsw074, showing the effect of sheltering from waves in the south in reducing the potential fluctuation volume

## Sediment budget imbalance

When a sustained historical shoreline recession trend is observed on NSW beaches, it implies that the sediment budget for that beach is imbalanced. This imbalance may arise from the inherited geomorphology of the surrounding coastline and ongoing stabilisation of sediment distributions with Holocene sea levels, or from human interventions in coastal systems (for example, river entrance training). The most notable examples occur on drift-aligned coasts with leaky headlands, such as the mid-north to northern NSW coasts, where significantly more sand may be exiting the system than entering it.

<u>Figure 65</u> illustrates an example of the potential sources and sinks influencing the sediment budget at Terrigal–Wamberal Beach, an embayed setting on the NSW Central Coast. If all sources and sinks are inactive or balance out to a net zero change in sediment availability at the beach over the long term, the shoreline will remain stable on average over time. This does not preclude fluctuations in shoreline position landwards and seawards with erosion-recovery cycles. If the sediment losses to sinks were to exceed gains from sources, however, the shoreline may gradually recede on average

over time, amidst the fluctuation cycles. SLR can activate sinks in systems that previously had a balanced sediment budget, driving a new phase of shoreline recession (Appendix A.3: Response to sea level rise).

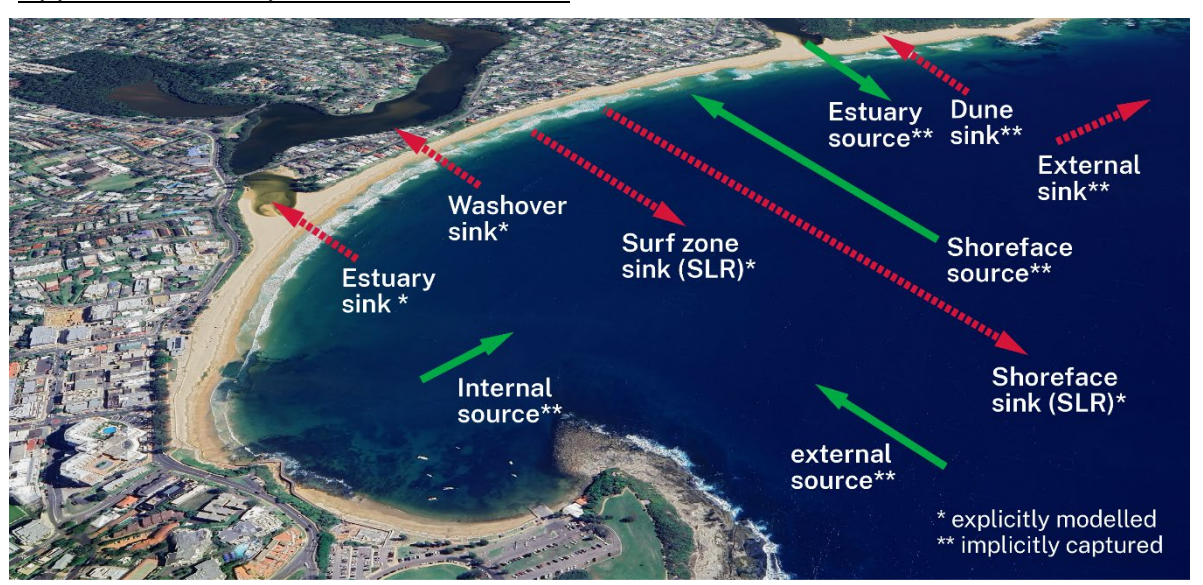


Figure 65 Hypothetical sediment budget components for Terrigal-Wamberal Beach

The influence of sediment budget imbalances on shoreline change trends was consistently investigated using satellite shoreline mapping spanning multiple decades. Examples of satellite mapped shorelines at 3 different NSW beaches with contrasting historical trends are shown in <a href="Figure 66">Figure 66</a>. Both DEA Coastlines (Bishop-Taylor et al. 2021) and CoastSat (Vos et al. 2019a, 2019b) satellite-derived shoreline change datasets were analysed to derive statistics (mean, minimum, maximum, standard deviation) for historical shoreline change within each beach sector, dating back to 1988 (commencement of Landsat satellite record).

Historical rates of shoreline change from satellite data were converted to sediment volumes by calculating the average elevation of the accreted beachface for each sector, which was determined as the average of the backshore and baseline elevations (Appendix A.3: Onshore geomorphology). The potential for sediment budget imbalance was then incorporated into the modelling as a probabilistic annual rate of sediment volume change. For example, the sector annual rates of beach volume change for the 3 examples are shown in <a href="Figure 66">Figure 66</a> covering the range of DEA Coastlines and CoastSat annual rates of change for each sector. It was presumed that any trends present in the recent historical record will persist indefinitely and that they are independent of any other erosion components.

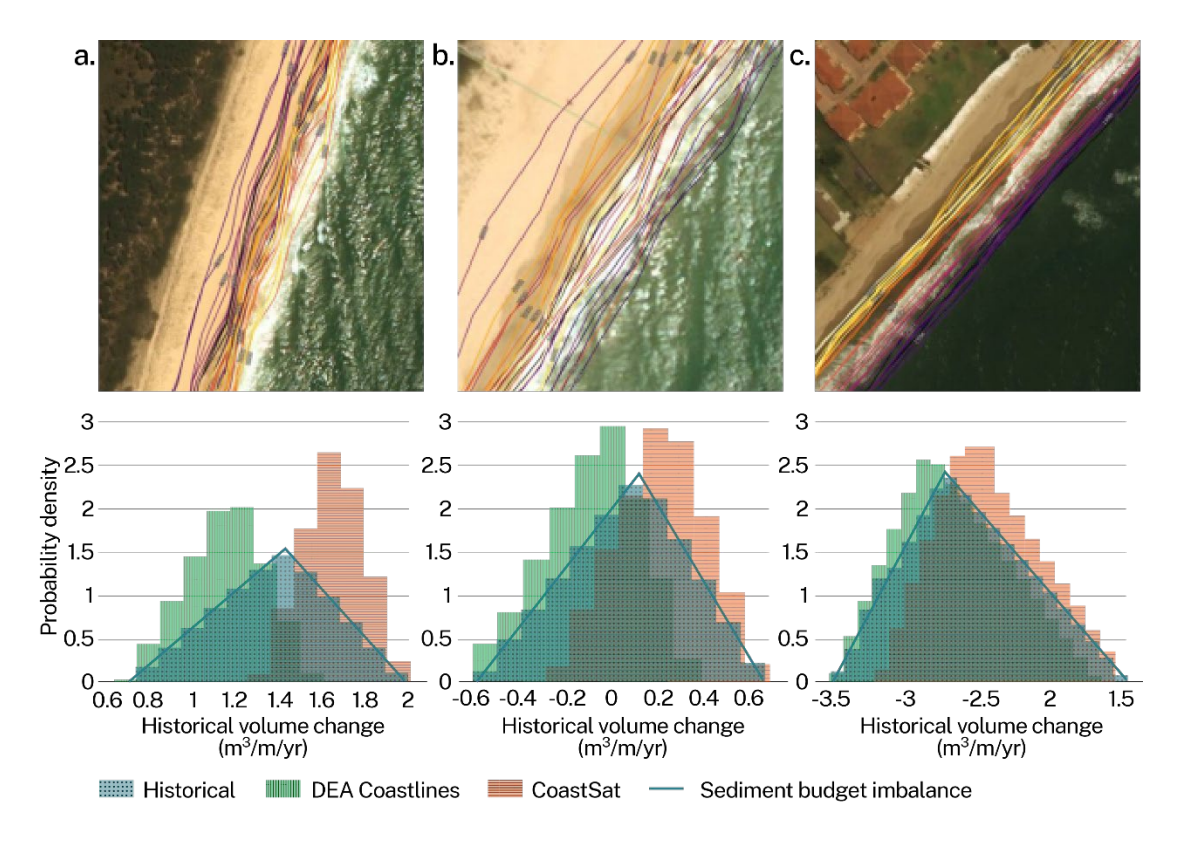


Figure 66 Example of historical shoreline change, as captured by annual average shoreline positions from DEA Coastlines for (a) accreting, (b) stationary and (c) receding settings with cool colours being older and warm colours recent shorelines. The corresponding model probability distributions for annual rates of beach-volume change due to sediment budget imbalance (blue) is also shown for each sector, spanning the ranges derived from DEA Coastlines and CoastSat data (grey)

### Response to sea level rise

SLR may generate new potential for coastal sediment accumulation on the shoreface by increasing the water depth and thus reducing wave-driven transport at the seabed (<u>Figure 67</u>). This shift means that sand transported offshore during storms that previously returned during calm conditions may not fully return to replenish the beach, resulting in a gradual long-term sediment-volume loss and shoreline recession (<u>Figure 10</u>). Importantly, a response of the nearshore-shoreface seabed to SLR represents one component (<u>Figure 65</u>) of the sediment budget system, which may be offset (or enhanced) by other factors, depending on the setting.

The modelled response to SLR comprises 3 components. The first follows the method of raising the upper shoreface (including beachface) profile by the magnitude of SLR and translating it landwards to a point where the sediment volume eroded from the beach/dunes and that deposited on the shoreface are balanced, as is shown in Figure 68, where *R* is the translation distance. This method, originally proposed by Bruun (1962), offers a reasonable approximation of one component of the beach system response to SLR, but it should not be solely relied on in settings where other sediment budget dynamics are known or suspected to be active (Rosati et al. 2013; Dean and

Houston 2013). For example, other potential sediment budget components, as illustrated in Figure 65, could influence the response.

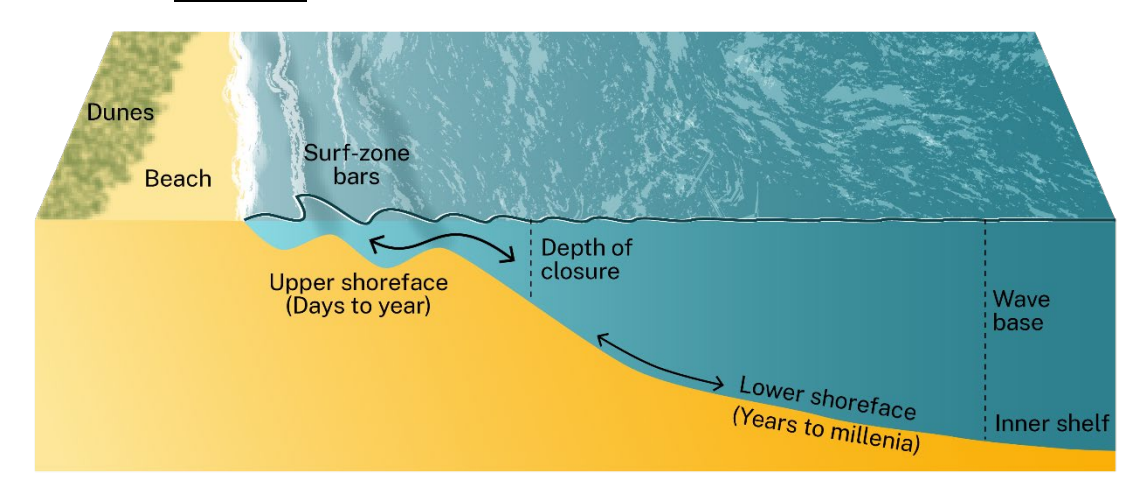


Figure 67 Illustration of beach, upper shoreface and lower shoreface profile morphology typical of NSW beaches

Source: Anthony and Aagaard (2020).

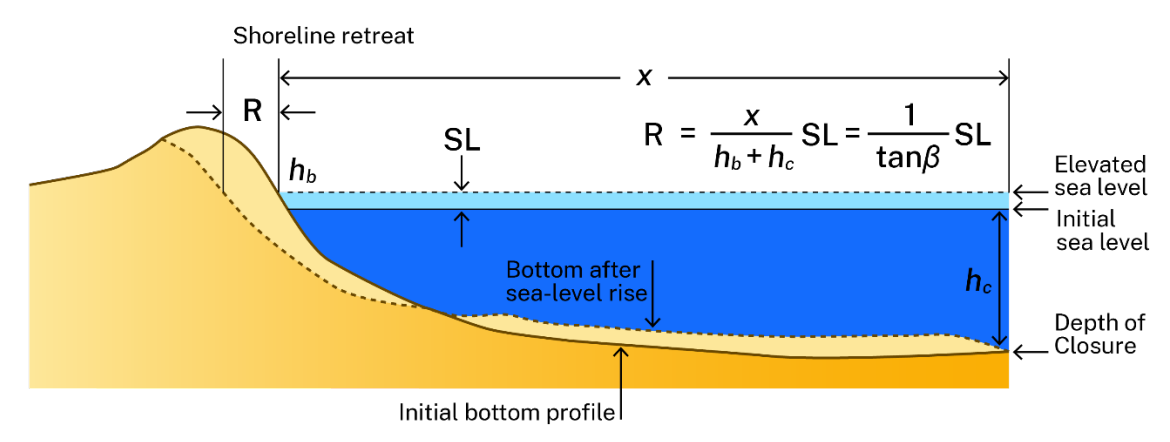


Figure 68 Illustration of the profile translation method for modelling beach erosion and shoreface deposition due to sea level rise

Note: The depth of closure represents the seaward limit of significant profile change at an annual timescale, while changes in the lower shoreface may occur over longer timescales. Source: FitzGerald et al. (2008).

The offshore extent of complete and instantaneous (that is, within the forecast period) seabed response to SLR, often referred to as the depth of closure or simply closure depth (Figure 68), is an important parameter as it influences the gradient of the beach system that is applied in the profile translation method. Importantly, the closure depth is not a limit of potential beach-shoreface sediment exchange but is intended to approximate the extent of complete seabed profile response in any given year (Anthony and Aagaard 2020; Cowell and Kinsela 2018). Over longer timescales, such as the forecasts considered here, there remains potential for significant sediment exchange beyond the closure depth (Figure 68).

The closure depth for each beach sector was calculated using the annual average extreme nearshore wave height,  $H_{sx}$ , derived from long-term nearshore wave data

(<u>Appendix A.3: Wave climate</u>), following the inner shoal zone limit formula proposed by Hallermeier (1980). The method approximates the limit of seabed change on an annual timescale (Nicholls et al. 1998).

The translation component of modelled beach response to SLR was calculated in each simulation using randomly sampled SLR, the sector closure depth based on local nearshore wave data, and the aggregated <u>onshore</u> and <u>offshore geomorphology</u> for each sector, from which the profile width and height were derived. The translation profiles extended from the mapped backshore line to the closure depth. The beachdune erosion volume ( $V_B$ ) corresponding to the translation distance was derived from the onshore sediment profiles and liberated dune sand above the translated backshore position returned to the system to conserve the sediment volume balance.

The second component of modelled beach response to SLR accounts for potential loss of sand from the eroding beach and dunes to the lower shoreface, beyond the closure depth (<u>Figure 68</u>). This was modelled by applying similar profile translation concepts within a volume-based approach, in which the lower shoreface sink generated by SLR ( $V_s$ ) was calculated between the upper shoreface closure depth ( $h_c$ ) and active shoreface depth limit ( $h_a$ ), which lies between  $h_c$  and the lower shoreface depth limit ( $h_c$ ) (Figure 69).

Similar to the way that SLR probability distributions increase in width for each future forecast year, the probability distribution of active shoreface depth limits ( $h_a$ ) increases to reflect the increased potential for loss of beach sand to the lower shoreface over longer forecast timescales (Cowell and Kinsela 2018). This is shown in <u>Figure 70</u>, where the width of an example  $h_a$  probability distribution increases for longer forecast horizons.

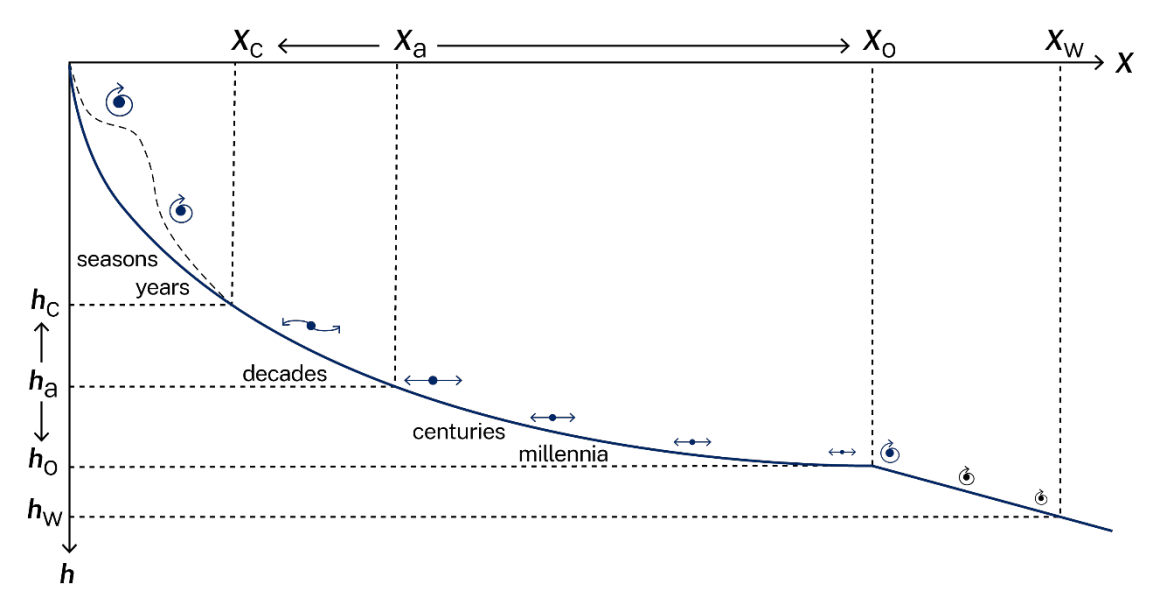


Figure 69 Illustration of shoreface zones linked to timescales of evolution, showing the active shoreface extent increasing as h<sub>a</sub> becomes deeper for longer timescales. Source: Cowell and Kinsela (2018)

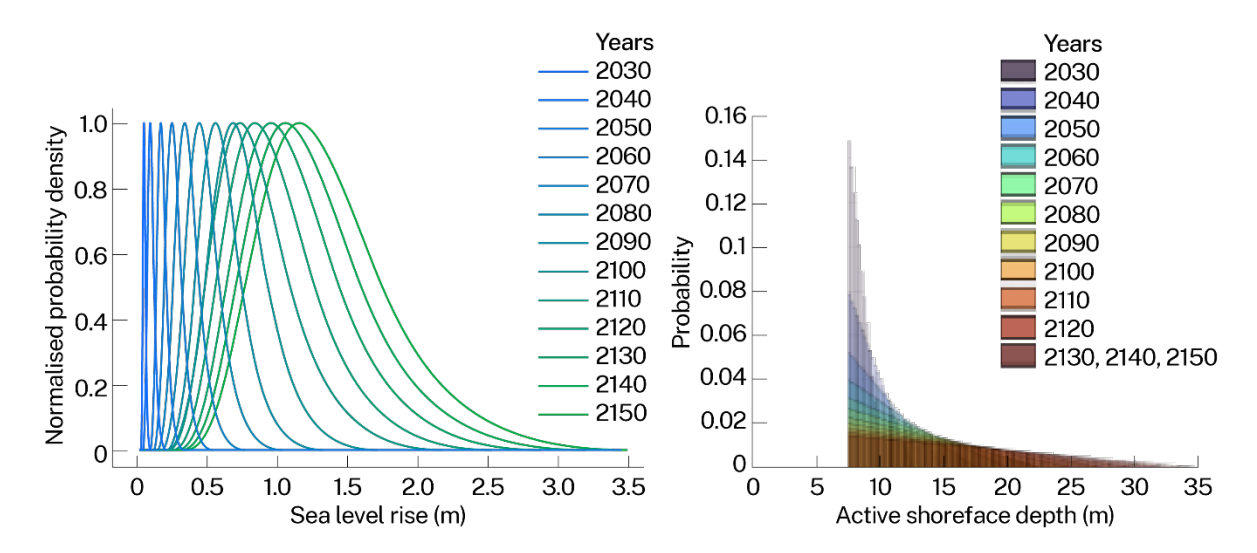


Figure 70 Example input probability distributions for (a) sea level rise (m), 2030 to 2150, and for (b) the active shoreface depth limit  $h_a$ , which increases with the timescale from the upper shoreface closure depth (lower bound) to a maximum 35 m water depth

The lower shoreface sink volume ( $V_s$ ) was treated independently of the upper shoreface profile translation, except for correlated sampling of SLR in each Monte Carlo simulation. The upper bound of the active shoreface depth limit ( $h_a$ ) increased with forecast year to a maximum water depth of 35 m (Figure 70), with the response potential reducing linearly from the upper shoreface closure depth to the maximum  $h_a$  value.

As outlined in Appendix A.3: Offshore geomorphology, the potential for sediment deposition across the shoreface is restricted to areas of sedimentary seabed. The depth-based sediment cover across each sector-average offshore profile was used to scale the lower shoreface sink volume, reflecting the response potential of the seabed in each sector. Consequently, beach sectors with reef-dominated seabed will have lower potential  $V_s$  than sediment-dominated sectors. The potential burial of rocky reefs by an aggrading seabed was not considered, as with the magnitudes of SLR considered, the impediment to deposition in the moderate-high energy wave climate setting would likely persist. The  $V_s$  calculated therefore depended on the SLR scenario and active shoreface depth distributions, as well as both the geometry and sediment cover of the sector-average offshore seabed profile.

The third component of modelled beach response to SLR accounts for potential sediment loss to estuary sinks (flood-tide deltas) as sea levels rise (Figure 65). Observations and modelling elsewhere suggest that flood-tide deltas can aggrade during rising sea levels (Eysink 1990; Van Goor et al. 2003). This was modelled following a similar approach to Kinsela et al. (2017), where the estuary sediment sink is calculated using the mapped flood-tide delta surface area ( $A_D$ ) and sampled SLR.

The potential range of the estuary sink volume ( $V_D$ ) spans from zero (no response) to an upper bound proportionate to the total flood-tide delta surface area multiplied by the sampled SLR (complete response), with a linearly decaying response rate across the

delta. This approach allows for partial response due to morphodynamic hysteresis (lagged response), recognising that estuary delta responses often lag behind modifications to tidal inlet hydrodynamics. The approach assumes that estuary deltas do not advance further into estuaries (inland) over forecast timescales or deflate from increased hydrodynamic scouring.

# Model summary

The modelled components of coastal erosion described <u>above</u> can be simplified into 5 sediment-volume change terms ( $V_F$ ,  $V_H$ ,  $V_T$ ,  $V_S$  and  $V_E$ ) that sum to the total erosion volume ( $V_R$ ), while allowing for the accreted beachface volume ( $V_B$ ) and volume of dune sand liberated by translation ( $V_L$ ) of the beach-upper shoreface profile, which both reduce the erosion volume applied landward of the backshore position ( $X_D$ ).

The historical volume change rate (underlying change trend) term ( $V_H$ ) may be either positive (erosion) or negative (accretion), whereas the remaining 4 erosion terms ( $V_F$ ,  $V_T$ ,  $V_S$  and  $V_E$ ) are always negative. Thus, the underlying change trend, representing any sediment budget imbalance, may moderate the other erosion components, particularly in settings where a historical trend of beach accretion and shoreline progradation is well established.

<u>Figure 71</u> illustrates the combining of the volume terms above in the model, in which the translation distance of the beach-upper shoreface ( $R_T$ ) is calculated from sector-average morphology, following the approach outlined in <u>Figure 68</u>. From this, the translation volume ( $V_T$ ) and liberated dune sand volume ( $V_L$ ) are derived. The balance of these and the other volume terms is then used to calculate  $V_R$ , from which the total erosion distance ( $R_V$ ) can be derived using the sector-average onshore morphology and sediment profile volume.

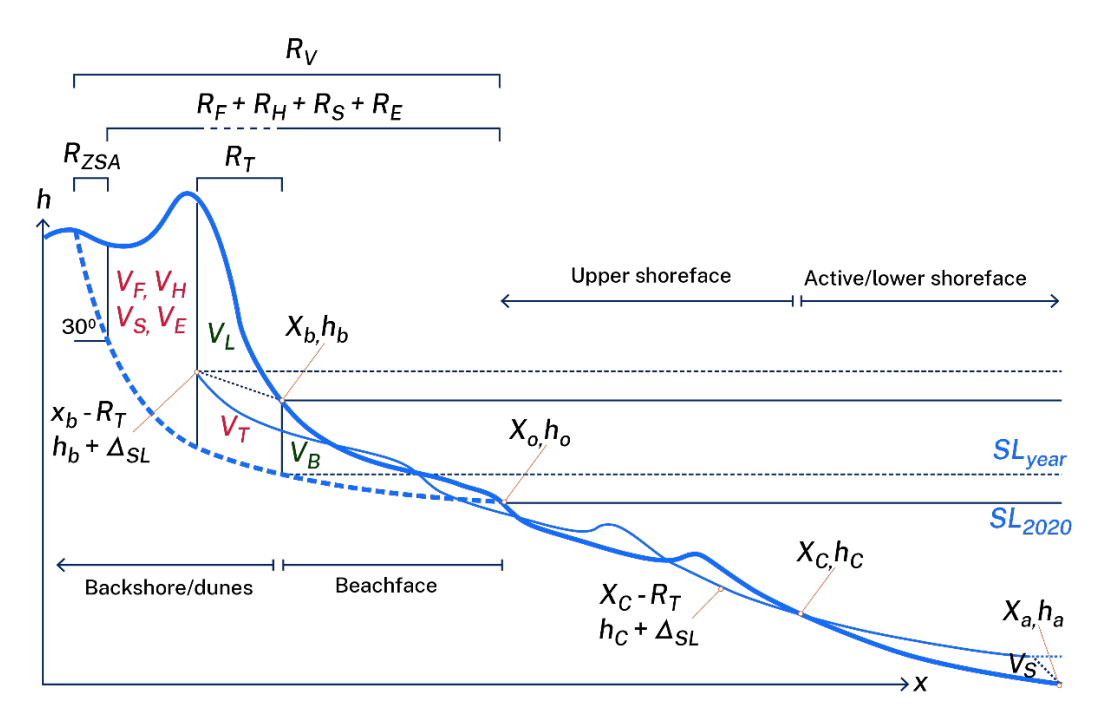


Figure 71 Schematic of the coastal erosion model components applied to a generalised coastal profile

Note: The diagram is not to scale, with the dune, beach and upper shoreface emphasised for clarity and vertical exaggeration applied.

Also shown in <u>Figure 71</u> are the locations of key model features, including the backshore line  $(x_b, h_b)$ , baseline  $(x_o, h_o)$ , upper shoreface depth limit or closure depth  $(x_c, h_c)$ , and the active shoreface depth limit  $(x_a, h_a)$ . The erosion distances also include an allowance for dune slumping  $(R_{ZSA})$  following erosion, assuming that the eroded substrate collapses to a natural slope consistent with the angle of repose. The zone of slope adjustment method of Nielsen et al. (1992) is applied, using an angle of repose for unconsolidated sand of 30°.

Each term in the general equation above, and thus  $V_R$ , is calculated within the Monte Carlo simulations (n = 2 million) for each scenario by randomly sampling model inputs from their respective input probability distributions.

For example, <u>Figure 72</u> shows the historical rate, estuary sink, translation distance, and shoreface sink sample distributions for Wooli Beach sector (nsw073b, <u>Figure 60</u>) for the SSP3-7.0 scenario at the year 2090. All components are ultimately expressed as sediment volumes per metre of shoreline (m³/m) following methods described above, with annual rates multiplied over years from 2020 to the forecast year.

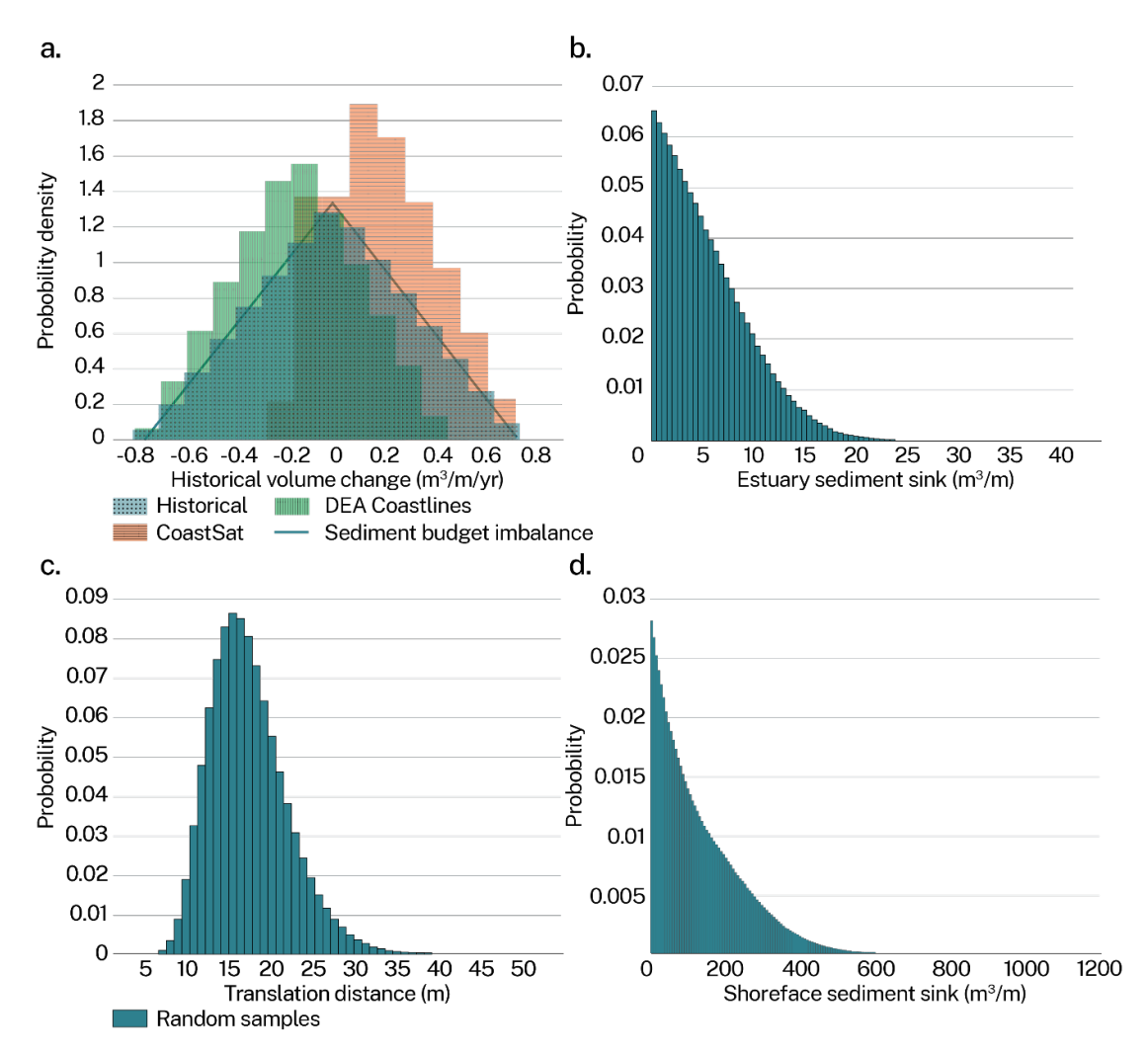


Figure 72 The Wooli Beach sector nsw073b for the scenario SSP3-7.0 in 2090 showing

(a) modelled historical volume change of coastal erosion, (b) modelled estuary sediment sink, (c) modelled coastal erosion translation distance, and

(d) modelled shoreface sediment sink

The model inputs and components sampled and calculated during each Monte Carlo simulation for both present (beach fluctuation only) and future scenarios are summarised in <u>Table 3</u> (beach fluctuation), <u>Table 4</u> (sediment budget imbalance), and Table 5 (response to SLR). The spatial scale and form of each input are also provided.

Table 3 Summary of key variables in the volume-based coastal erosion model – beach fluctuation

Model input	Notation	Units	Scale	Form
extreme significant wave height	$H_{\text{sx}}$	m	sector	scalar
wave sheltering coefficient	C <sub>F</sub>	-	sector	scalar
fluctuating beach erosion volume	$V_{F}$	m³/m	sector	gamma

Table 4 Summary of key variables in the volume-based coastal erosion model – sediment budget imbalance

Sediment budget imbalance				
DEA Coastlines historical change rates	-	-	sector	statistics
CoastSat historical change rates	-	-	sector	statistics
historical beach change volume	$V_{H}$	m³/m/yr	sector	gamma

Table 5 Summary of key variables in the volume-based coastal erosion model – response to sea level rise

Model input	Notation	Units	Scale	Form
sea level rise	SL	m	compartment	log normal
beach width	X <sub>o</sub> - X <sub>b</sub>	m	sector	scalar
upper shoreface width	X <sub>c</sub> - X <sub>o</sub>	m	sector	scalar
backshore beach elevation	$x_b$ , $h_b$	m	sector	scalar
baseline position	x <sub>o</sub> , h <sub>o</sub>	m	sector	scalar
upper shoreface closure depth	x <sub>c</sub> , h <sub>c</sub>	m	sector	scalar
active shoreface depth limit	x <sub>a</sub> , h <sub>a</sub>	m	sector	gamma
estuary flood-tide delta areas	$A_D$	m <sup>2</sup>	compartment	scalar
beach translation volume	$V_T$	m³/m	sector	scalar
lower shoreface sink volume	Vs	m³/m	sector	gamma
flood-tide delta sink volume	VE	m³/m	sector	triangular

# Hazard projections

## **Probability distributions**

The coastal erosion model generates a probability distribution of potential beach change for each beach sector, corresponding to each SSP scenario and forecast year. This approach allows for coastal erosion forecasts covering the feasible range of potential coastal change and expressed in terms of their probability of occurring within the combined range of component uncertainty. Coastal erosion hazard mapping is then prepared for each SSP scenario and forecast year, corresponding to selected exceedance probability levels (50%, 10%, 1% and 0.1%).

Model output probability distributions for the Wooli embayment beach sectors (<u>Figure 60</u>) under the SSP3-7.0 scenario in 2090 are shown in <u>Figure 73</u>a (nsw073a), <u>Figure 73</u>b (nsw073b), <u>Figure 73</u>c (nsw073c) and <u>Figure 73</u>d (nsw074). The plots show that the cumulative erosion volume is consistent across all Wooli Beach sectors (nsw073a-c), as these components are shared along the continuous beaches. However, the total erosion volume at each sector varies due to differences in exposure to

fluctuating erosion at each sector (see <u>Appendix A.3: Beach fluctuation</u>). In comparison, the more sheltered Jones Beach (nsw074, <u>Figure 73</u>d) has lower cumulative and fluctuating erosion components, resulting in a lower sector total erosion volume.

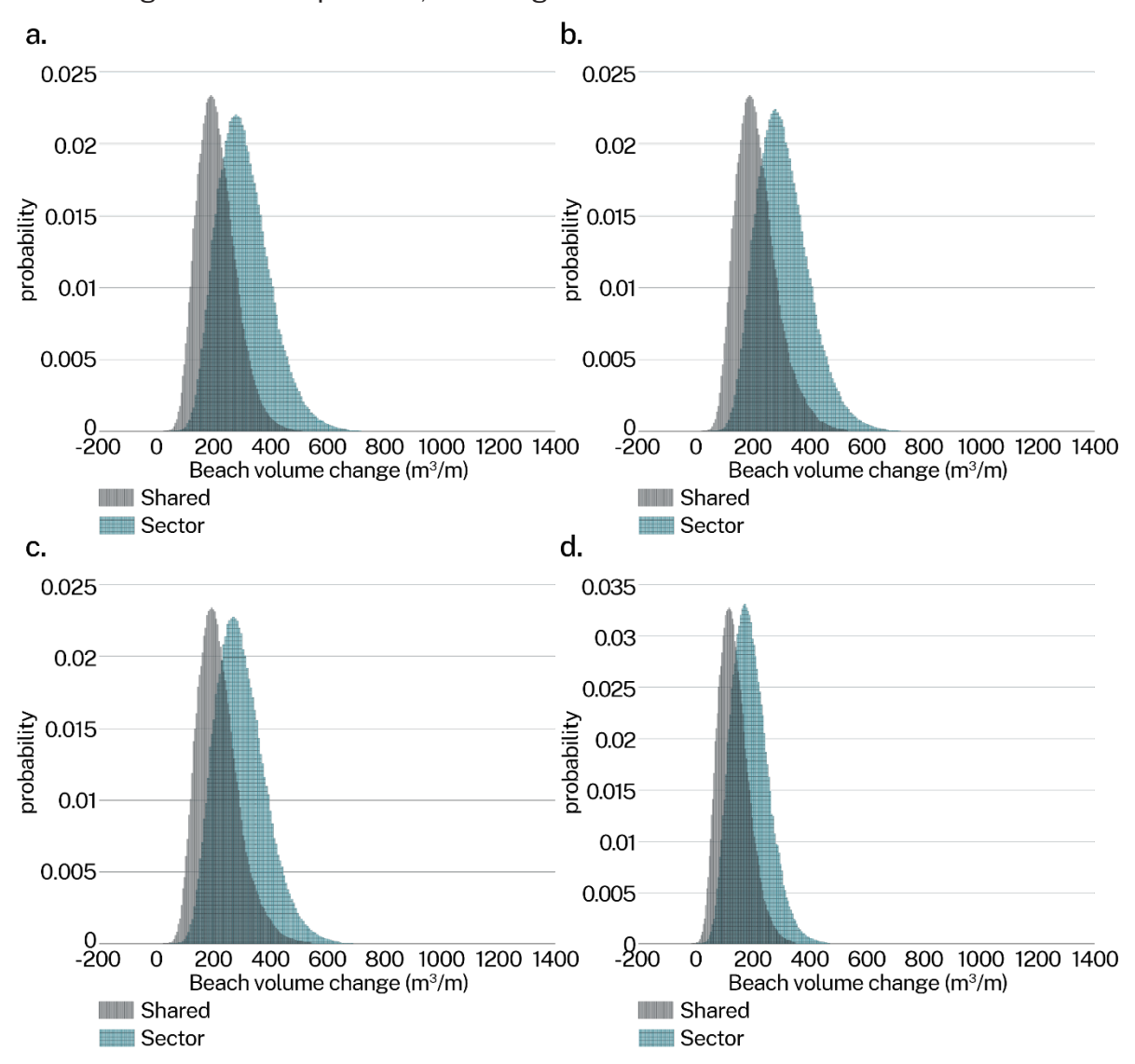


Figure 73 Modelled beach volume change for Wooli embayment sector (a) nsw073a, (b) nsw073b, (c) nsw073c and (d) nsw074 for scenario SSP3-7.0 in 2090

The sector total beach volume change for each SSP scenario, forecast year and probability level is converted into a shoreline change distance, measured from the model baselines, using the sector-average onshore sediment profile for each beach sector, which captures the geomorphology within each sector. This is illustrated in Figure 10, highlighting the erosion distance (R) corresponding to the calculated sediment volume loss (V), depending on the profile topography and cumulative sediment volume.

## Mapping

Coastal erosion hazard mapping and exposure statistics have been prepared for selected exceedance probability levels (50%, 10%, 1%, 0.1%) for the present (baseline)

and for each of the SSP scenarios considered for forecast years at decadal increments from 2030 to 2150. The mapping dataset comprises distinct mapped erosion hazard areas for each of the 726 open coast and 32 bay/estuary beach sectors modelled. The individual hazard areas for each beach sector have been merged within each primary sediment compartment, resulting in output dataset variants for each compartment.

The present-day (2020) erosion hazard zones include only the beach fluctuation component (see Appendix A.3: Beach fluctuation), which reflects the potential range of temporary variations in the beach–dune volume and shoreline position that may persist for months to years (Figure 2). The erosion hazard zones for future forecasts include beach fluctuation and the cumulative components of coastal erosion, capturing the total beach–dune volume and shoreline position change due to shoreline recession and storm or cyclical erosion impacts.

<u>Figure 74</u> provides an example of coastal erosion hazard mapping for the central sector of Wooli Beach (nsw073b), as shown in <u>Figure 60</u>. The total potential erosion hazard zones are mapped to the 0.1% exceedance probability level for the present-day and for the SSP3-7.0 future scenario in 2090. Selected 10% and 1% exceedance probability level shoreline positions for the present and future scenarios are mapped as lines, depicting the feasible range of coastal erosion for each scenario and shoreline positions corresponding to selected probabilities.

As the scope of the coastal erosion modelling is limited to areas with substrate that is known or suspected to be unconsolidated or otherwise erodible sediment, and thus modelling uses the sediment profile for each sector (see <a href="Appendix A.3: Onshore geomorphology">Appendix A.3: Onshore geomorphology</a>), areas classified as bedrock at the surface or bedrock-mantling dunes in the <a href="NSW coastal quaternary geology mapping">NSW coastal quaternary geology mapping</a> dataset (Appendix B: Datasets) have been omitted from the erosion mapping. As such, the coastal erosion mapping should always be viewed in conjunction with the state-wide bedrock mapping layer for context.

For SSP1-2.6, SSP2-4.5, SSP3-7.0 and SSP5-8.5, where beach barriers are predicted to be entirely eroded through to backbarrier estuaries, land areas on the landward side of the estuaries have not been mapped as exposed. This is because the behaviour of coastal sand barriers following breaching or total destruction is complex and beyond the scope of the modelling approach. Foreshore areas on the landward sides of estuaries may be exposed to coastal erosion hazards in such cases, depending on the extent of barrier breaching and overall barrier behaviour alongshore.

For low-confidence SSP5-8.5, foreshore areas landward of estuaries that become exposed to ocean processes following barrier breaching are considered exposed, given much higher SLR that would at the least expose such areas to ocean inundation and otherwise enable rapid shoreline transgression. Therefore, coastal erosion and estuarine inundation mapping for the relevant SSP scenarios and forecast years should be viewed together, to provide an indicative understanding of compounding erosion and inundation hazards where the present-day coastal morphology may be significantly modified by ocean processes.



Figure 74 Coastal erosion mapping for Wooli Beach showing the modelled potential erosion extent for the 10% and 1% exceedance probability at present (2020) and for the SSP3-7.0 scenario in 2090

# A.4 Coastal overwash

# Approach

For the first time in NSW, this study identifies locations of sandy coastline likely to experience coastal overwash: the combined effects of astronomical tides, storm surge, wave runup and future SLR. State-wide analyses have been undertaken using high-resolution 100-m spaced transects, covering over 800 km of sandy coastline. Inundation of rocky environments along headlands is excluded from the analyses, as the complex overwash dynamics in these settings require detailed modelling approaches that are not practical on a state-wide level.

Conceptually, coastal overwash occurs when coastal total water levels exceed the local backbeach elevation (for example, the dune crest in <u>Figure 75</u>). Following the definition by Serafin et al. (2017), coastal *total water level (TWL)* can be defined as the combination of still water level (*SWL*) and wave runup (*R*),

$$TWL = SWL + R$$

Still water levels account for variations due to astronomical tides and non-tidal residuals (storm surge, coastal trapped waves, El Niño/La Niña effects, Eastern Australian Current, and so on), and can be obtained from ocean tide gauges. Wave runup (R) – the vertical excursion of waves at the shoreline – includes time-averaged (wave setup) and oscillating components of the water line (swash). Runup levels are typically estimated using empirical parametrisations that are forced with wave data and a representative foreshore beach slope ( $\beta$ , Figure 75).

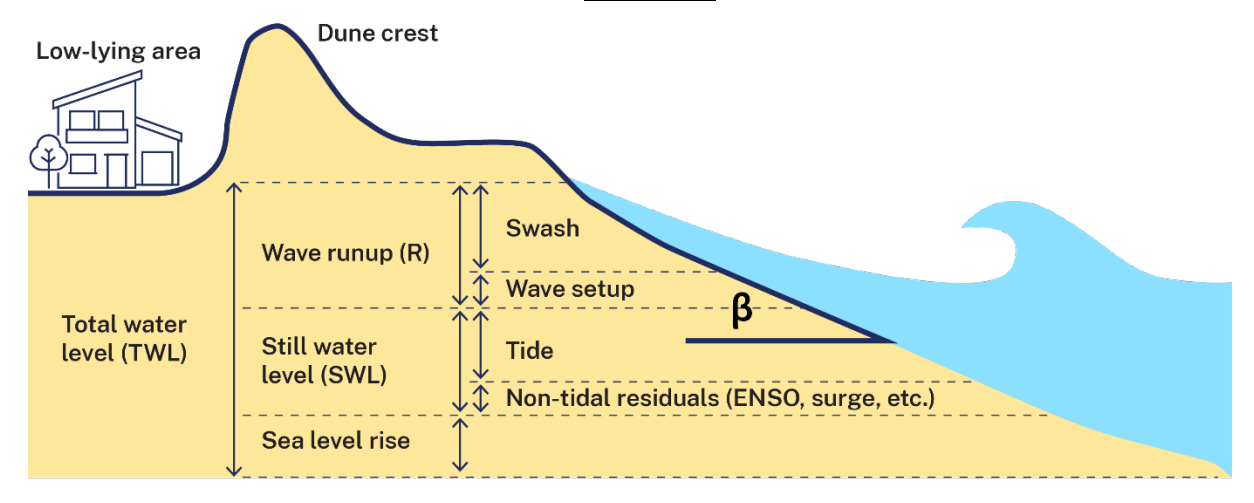


Figure 75 Total water level components that contribute to coastal overwash

In the future, total water levels will be amplified by rising sea levels (SLR),

$$TWL = SWL + R + SLR$$

Future SLR will result in increasing TWL, which over time, will result in increasing frequency of overtopping in locations subject to inundation now, as well as in new locations that will need to be identified. To identify these locations, this study assesses the current and future likelihood of coastal overwash across a high-resolution spatial

domain along the NSW coast. The method employed is shown in <u>Figure 76</u> and detailed in the following sections.

Briefly, simulations of historical (1990–2020) TWL at approximately 8,650 100-m spaced transects were calculated using tide gauges, a novel nearshore wave transformation tool, and site-specific probabilistic beach slope distributions. Probabilistic time series of historical TWL were generated using extreme value analysis (EVA). TWL magnitudes (with confidence bands) for different probability levels are compared to local backbeach inundation thresholds (such as dune and seawall crests) to classify the likelihood of current coastal overwash. Results were summarised in a simple traffic-light inundation impact scale (cyan meaning *likely inundation*, green *potential inundation*, and blue *unlikely inundation*). Future overwash (shown as inundation) likelihoods were incorporated into the analysis using probability distributions of SLR, following a Monte Carlo approach.

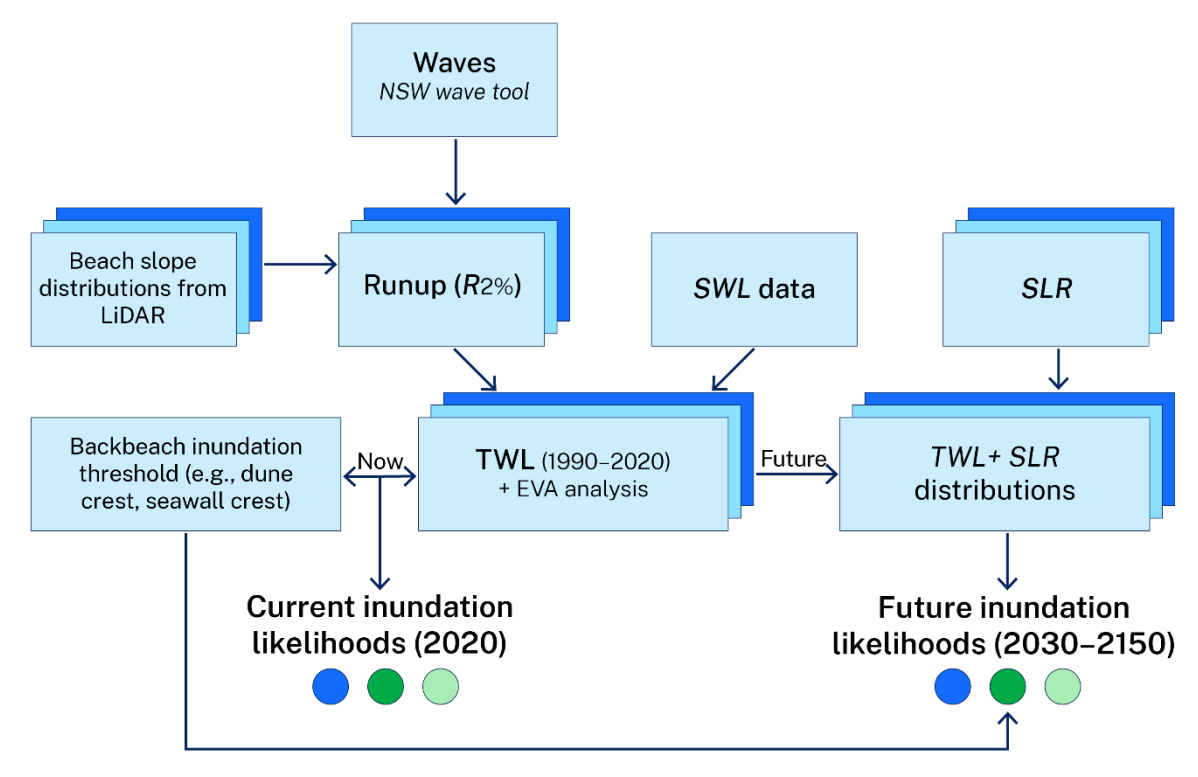


Figure 76 Coastal overwash hazard assessment method at the transect scale (100-m spaced transects)

#### Data

#### Beach transects dataset

The NSW sandy coastline was discretised into 100-m shore-normal transects along plan view shorelines representative of the mean high-water line (Smartline dataset in Hazelwood 2009). In total, 8,649 *major* transects were generated, covering 546 open coast sandy beaches. Additionally, a higher resolution 10-m spaced *minor* transect dataset was generated for higher-resolution beach slope calculations using LiDAR datasets, as detailed in Appendix A.4: Beach slope distributions from LiDAR.

#### Historical still water level (SWL) dataset

The contribution of astronomical tides and non-tidal residuals to TWL was obtained from the dataset of oceanic water levels presented in Viola et al. (2021). This dataset provides time series of (at least hourly) SWLs across several open coast tide gauge stations in NSW, sourced from the Bureau of Meteorology and Manly Hydraulics Laboratory (MHL). Table 6 summarises the tidal gauge stations used in this study. The period from 1990 to 2020 was selected due to data gaps before 1990. Data was limited to 2020, consistent with the baseline of SLR projections (see Appendix A.2 Sea level rise). SWL data was linearly detrended such that any long-term trend is removed from the signals while preserving higher frequency variability (hourly to inter-annual). Each 100-m spaced transect is assigned to the data from the nearest tidal gauge location.

Table 6 Location of ocean tide gauges used within the coastal overwash modelling methodology

Station name	Latitude	Longitude
Tweed Offshore	-28.18	153.59
Crowdy Head	-31.83	152.75
Sydney Harbour	-33.82	151.25
Jervis Bay	-35.12	150.70
Eden Boat Harbour	-37.07	149.90

#### Beach slope distributions from LiDAR

Beach slope distributions derived from available LiDAR topographic datasets were used to calculate probabilistic runup (*R*) contributions to TWL. To provide a broader sample of potential spatiotemporal beach slope variability at each *major* 100-m transect, distributions were sampled from beach slopes covering 10 transects of a higher resolution 10-m spaced *minor* dataset (see Appendix A.4: Beach transects dataset). A 100-m spatial window aimed to include the alongshore variability associated with localised effects, such as beach cusps and rip horns (Harley et al. 2011). Similarly, data from several LiDAR flights were included to incorporate the uncertainty associated with the high temporal beach slope variability and rapid transitions of intermediate beachtype morphologies in NSW (McLean et al. 2023; Phillips et al. 2019; Wright and Short 1984).

Beach slopes were estimated from cross-shore profiles using linear regression, with the berm crest (around 2 m AHD: Kinsela et al. 2017), and mean sea level (around 0 m AHD) serving as the landward and seaward limits, respectively. High resolution topographic data from regional scale airborne LiDAR flights (1 to 5 m horizontal resolution, around 0.3 m vertical accuracy) were employed for this purpose. Figure 77 shows the distribution of available LiDAR surveys (counts, horizontal axis) at individual 100-m spaced transects. A minimum of 2 and maximum of 13 LiDAR datasets – per transect – were available during the 2007–2023 period. LiDAR data is periodically uploaded to the NSW photogrammetry website as new LiDAR data becomes available. For simplicity,

beach slope distributions were modelled as a normal distribution, with the mean and standard deviation derived from the historical data.

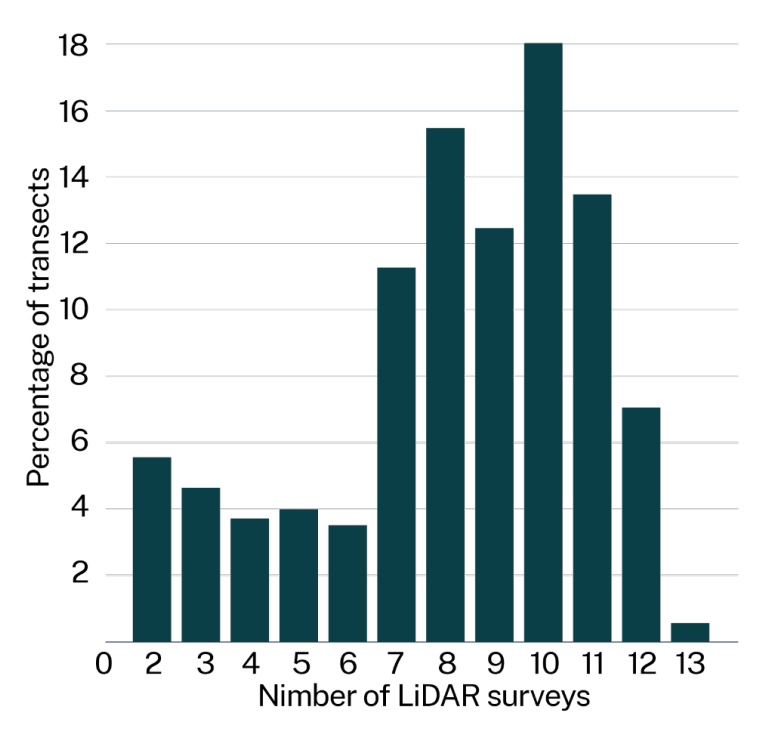


Figure 77 Distribution of available LiDAR surveys (2007–2023) across 8,649 100-m spaced transects

#### Wave data: NSW Nearshore wave tool

To account for nearshore wave modifications and the sheltering effects of headlands, a novel high-resolution nearshore wave tool (NSW Nearshore wave tool) was employed to transfer offshore wave data to the 10-m contour, every 250 m of coastline. This tool is based on a WAVEWATCHIII model forced by ERA5 wind fields (Hersbach et al. 2020). Calibration of the model was performed against existing offshore wave buoy data and more recent, roughly yearly, deployments of inshore wave data from SOFAR Spotter buoys spanning more than 10 locations across NSW (Kinsela et al. 2024).

The outputs from this wave tool include hourly time series of nearshore wave data concurrent with available SWL data (1990–2020, Appendix A.4: <u>Historical still water level (SWL) dataset</u>). Nearshore wave information at the 10-m contour (for example, significant wave height at 10 m depth,  $H_{s,10}$ ) was reverse shoaled to deep water conditions using linear wave theory to comply with the requirements of runup formulas (for example,  $H_0, L_0$ ; see Appendix A.4: <u>Runup model selection</u>). Each 100-m transect was assigned to the nearest wave tool output location and manually verified in a GIS environment.

# Runup model selection

Numerous wave runup formulas for sandy coastlines have been developed over the past few decades (da Silva et al. 2020). These formulas typically estimate the elevation exceeded by 2% of the waves ( $R_{2\%}$ ) over some period, typically one hour, using deep

water wave data ( $H_0$ ,  $L_0$ ) and the foreshore beach slope ( $\beta$ ). To evaluate the accuracy and applicability of several runup models and long-term average beach slopes derived from LiDAR, a regional scale dataset of storm runup debris lines was used (Shoalhaven Heads to Newcastle) over 4 storm events (between October 2014 and July 2020), as presented in Figure 78.

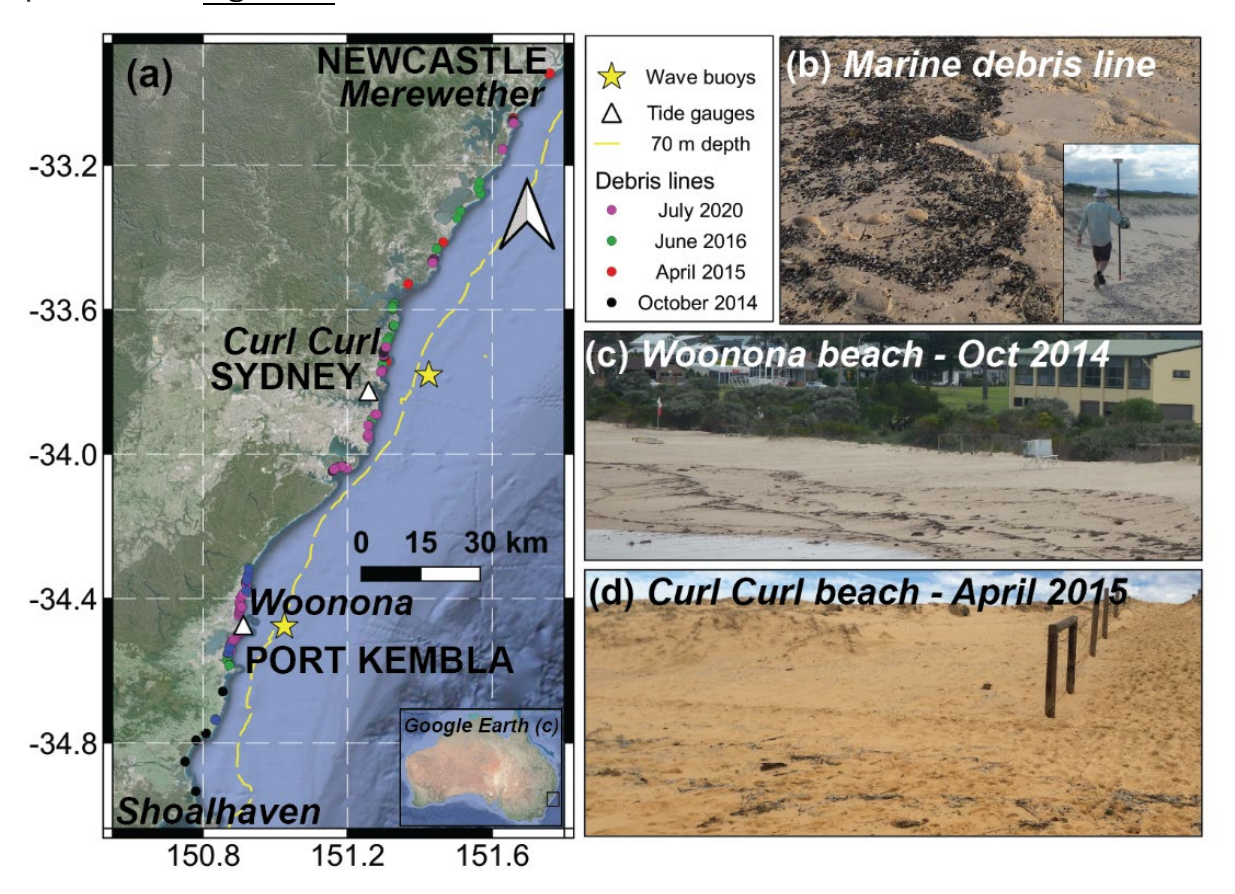


Figure 78

(a) Geographical distribution of marine debris line measurements after 4 storm events in October 2014, April 2015, June 2016 and July 2020 (see legend).

(b) Example of marine debris line and RTK-GNSS monitoring. Marine debris line examples for (c) Woonona beach near Port Kembla and (d) Curl Curl beach in Sydney

Regional scale marine debris observations were benchmarked against peaks in modelled *TWL = SWL + R* time series, using several runup formulas. Marine debris observations were averaged at 100-m windows alongshore to match the resolution of the available *major* transects and average beach slopes (see Appendix A.4: Beach slope distributions from LiDAR). In total, 472 marine debris line observations – covering 40 beaches – were available to compare with extreme TWL estimations. SWLs were sourced from tide gauges in Sydney and Port Kembla. Wave data from offshore wave buoys was transferred to the nearshore with the NSW wave transformation tool (see Appendix A.4: Wave data: NSW Nearshore wave tool). Beach slopes (with uncertainty) and wave data were used to force 7 runup formulas for model evaluation. These models included 2 formulas commonly used in coastal hazards studies in NSW (Hedges and Mase 2004; Nielsen and Hanslow 1991), as well as 3 models (Atkinson et al. 2017; Holman 1986; Vousdoukas et al. 2012) that performed similarly well in a previous

assessment by Atkinson et al. (2017). The remaining 2 models include the widely used formula by Stockdon et al. (2006) and a recent machine learning model (Power et al. 2019).

Details of the model-data comparison can be found in <u>Appendix D: Runup formula selection</u>. These analyses indicated that employing historical LiDAR-derived beach slopes between mean sea level (MSL, around 0 m AHD) and berm crest (2 m AHD) resulted in variable model skill (performance) across different formulas (for example, model bias ranged from around 0.1 m to a few metres). The model that showed the lowest root mean squared error (RMSE, around 0.5 m) and lowest bias (around 0.2 m) was the formula proposed by Atkinson et al. (2017):

$$R_{2\%} = 0.92 \tan(\beta) \sqrt{H_o L_o} + 0.16 H_o$$

Notably, this model was developed using data from 11 beaches in southeast Australia and consisted of a 'model of models' which fitted a runup parametrisation to the predictions from several existing runup models. As a result, this model has been selected to calculate the runup contributions to TWLs.

## Current coastal overwash likelihoods

## Historical total water level time series

Total water level time series (TWL = SWL + R) were calculated over the 1990–2020 period using data from ocean tide gauges (Appendix A4: <u>Historical still water level (SWL) dataset</u>) and the Atkinson et al. (2017) runup formula (see Appendix A.4: <u>Runup model selection</u>). To provide a broad range of probable historical total water levels, runup time series (R) were calculated n = 1,000 times using ensemble members from randomly generated beach slope distributions (see Appendix A.4: <u>Beach slope distributions from LiDAR</u>). This resulted in 1,000 TWL time series – per transect – that reflect the local to regional variability in TWL from varying beach slopes and wave conditions in NSW.

A sensitivity analysis to determine the adequate number of ensembles (*n*) is presented in <u>Appendix E: Coastal overwash ensembles</u>. Briefly, this analysis showed that using more ensemble members (n > 1,000) resulted in no improved modelling accuracy, while fewer than 1,000 members resulted in under sampling issues.

## Backbeach overwash thresholds

Conceptually, coastal overwash and subsequent inundation occurs when total water levels exceed a local backbeach overwash threshold (for example, a dune crest, as in <u>Figure 75</u>). Selecting appropriate thresholds is essential to determine the likelihoods of coastal overwash. Each transect was first classified into one of 4 different *backbeach archetypes* (<u>Table 7</u>), describing the feature located behind the active beach and the position of the backbeach overwash threshold.

Table 7 Backbeach archetype classification system

Backbeach archetype	Description	Overwash threshold
Dune	Active beaches that are backed by natural or modified dunes	Dune crest
ICOLL	Beaches backed by ICOLLs, also including dune portions backed by waterways near ICOLL entrances	Berm crest
Cliff	Beaches backed by rocky cliffs. Note that this archetype does not include cliff environments that directly face the open coast along rocky headlands	Cliff top, or maximum elevation across transect domain
Structure	Beaches backed by coastal structures (e.g. seawalls) that are typically lower than the elevation of natural dunes	Structure elevation (e.g. seawall crest)

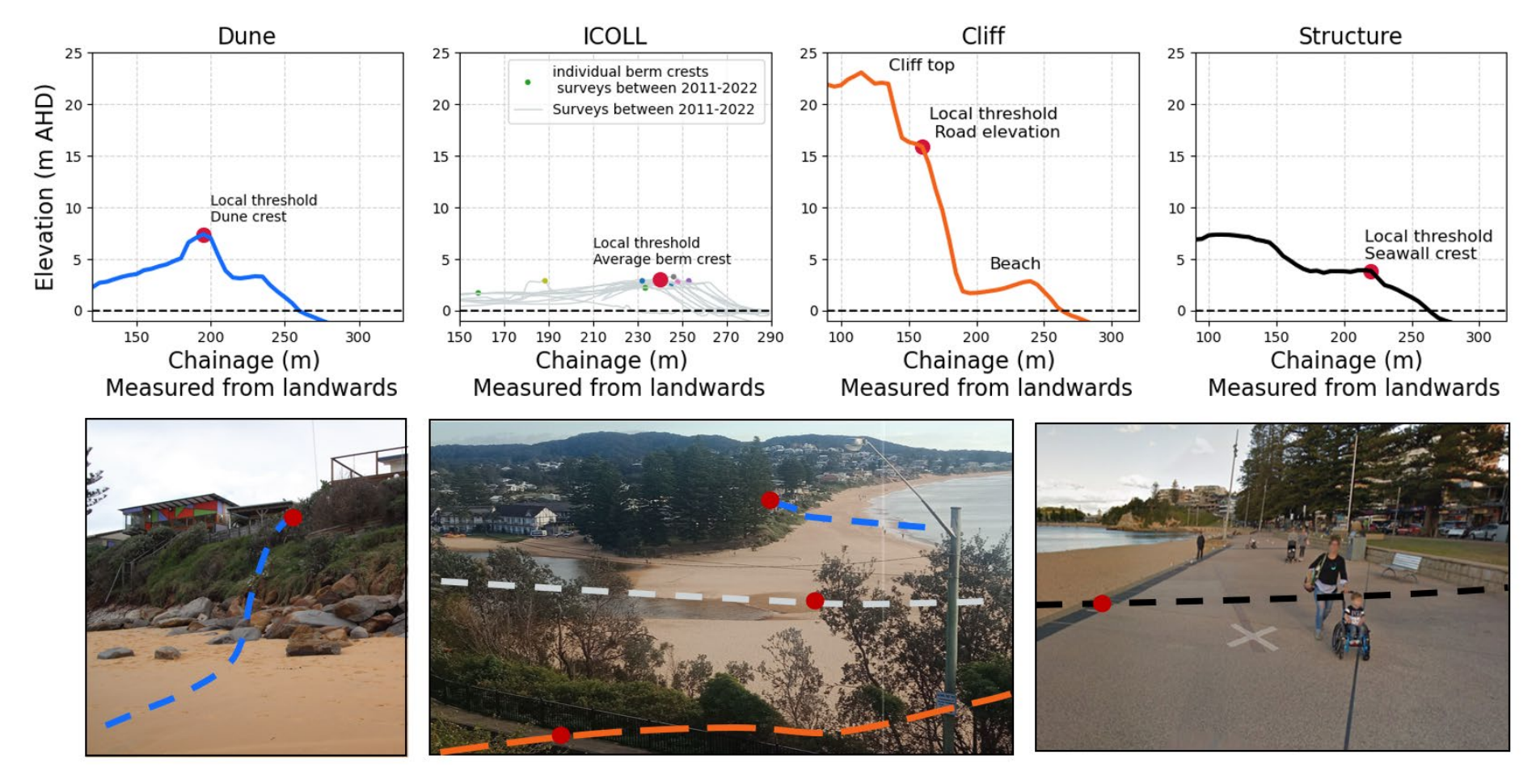
<u>Figure 79</u> exemplifies these archetypes along 4 transects at Wamberal–Terrigal Beach (Central Coast). The left to right panels show LiDAR profiles for dune, ICOLL, cliff and structure archetypes, as well as selected backbeach overwash thresholds. Topographic data from the 2018 Marine LiDAR dataset – the most recently available bare earth statewide dataset – is employed for this purpose. To account for the transient nature of ICOLL entrances, the elevation threshold was calculated as the average berm crest from all available historical LiDAR flights (Appendix A.4: <u>Beach slope distributions from LiDAR</u>).

As a fundamental limitation of this study, it was assumed that the elevation of these thresholds remains unchanged over time. The potential future evolution of these systems, particularly for dunes and berms at lagoon entrances, is beyond the scope of this first-pass state-wide analysis.

## Extreme value analysis (EVA)

EVA of historical TWLs was performed to determine expected TWL magnitudes for different probability levels. Following existing EVA assessments of deepwater wave data in NSW (e.g. Shand et al. 2011), generalised extreme value distributions (GEV) were fitted to yearly TWL maxima.

EVA was repeated n = 1,000 times per transect, providing TWL magnitudes for different probability levels (AEP = 1%, 5%, 20% and 100%) and confidence bands, which are obtained empirically from the associated ensemble members (Figure 80).



Upper panels: examples of cross-shore transects representing coastal archetypes in New South Wales. Horizontal axes indicate chainage, measured from the most landward location of the transect (0 m). Lower panels: corresponding images showcasing each archetype. Photos (left to right): DCCEEW, CoastSnap citizen science program, and Google Maps

## Overwash likelihoods - traffic light approach

To determine coastal overwash likelihoods, TWL exceedance levels for different probability levels (for example, 1% AEP) were compared with local backbeach overwash thresholds (such as a dune crest) and classified into 1 of 3 likelihoods, as defined in <a href="Table 8">Table 8</a>. In this classification, the upper limit of the likely TWL range (83%) defines instances of *likely overwash*, whereas less likely extreme TWL occurrences (99% exceedance) mark the limit where overwash likelihoods shift from *potential* to *unlikely*.

Table 8 Classification of coastal overwash likelihoods

Overwash likelihood	Condition
Likely overwash	Upper limit of total water level (TWL) likely range (83rd percentile) exceeds backbeach inundation threshold
Potential overwash	Backbeach threshold between 83rd and 99th (extreme) TWL percentiles
Unlikely overwash	Backbeach threshold exceeds extreme TWL (99th percentile)

Panels (a) and (b) of <u>Figure 80</u> illustrate this classification for a 1% AEP TWL distribution, where the elevation of some local backbeach overwash threshold falls between the 83rd and 99th percentiles of the 1% AEP TWL distribution, suggesting that this transect is currently experiencing *potential overwash*.

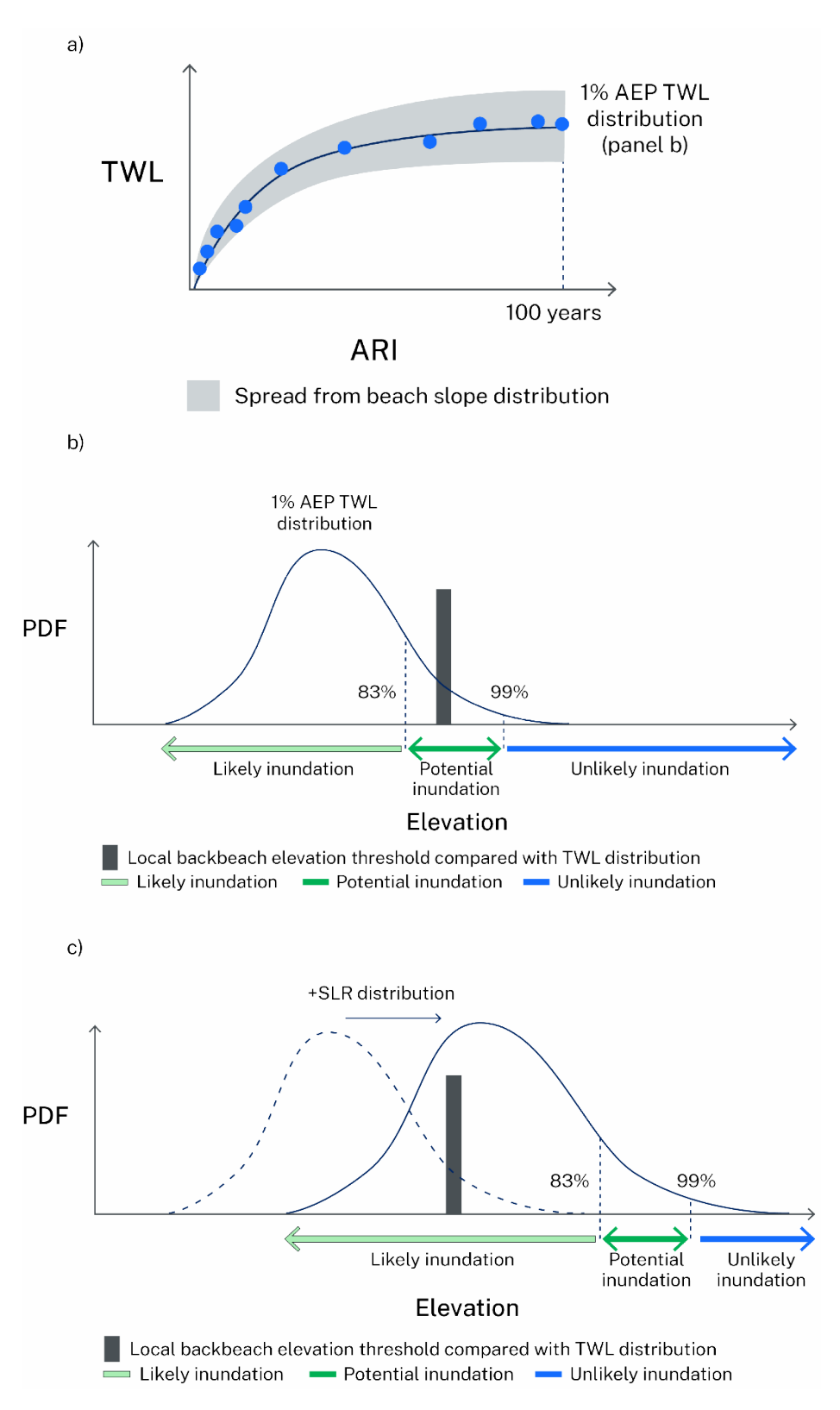


Figure 80 Diagram showing extreme value analysis (EVA) of total water level (TWL) time series using block maxima (1990 to 2020) used for calculating the transect-based overwash (shown as inundation) likelihood scale. The distribution of the 1% AEP (100-year) TWL in (a) is used in (b) to define the overwash (shown as inundation) impacts based on TWL percentiles and local backbeach overwash thresholds. (c) The method is repeated for future scenarios, where SLR distributions are added to the original TWL distribution on a Monte-Carlo basis

## Future coastal overwash likelihoods

Estimating future coastal overwash likelihoods was performed similarly to present conditions. Distributions of historical extreme value TWL (e.g. <u>Figure 80(b)</u>) were combined with SLR distributions (n = 1,000 ensemble members), following a Monte Carlo type approach (<u>Figure 80(c)</u>) and compared with backbeach overwash thresholds. In the previous example, a transect classified as having *potential overwash* would experience *likely overwash* impacts in the future. The underlying assumptions of this approach include wave and SWL stationarity, as well as unchanged backbeach elevation thresholds.

# Results and mapping

Analyses were performed at the state-wide level (8,649 transects) for present (1990-2020) and future (2030 to 2150) conditions, considering several scenarios at decadal timeframes. Results first provide a state-wide picture of current overwash likelihoods, followed by regional analysis – that is, the 9 primary sediment compartments (Thom et al. 2018) – and a local scale example. Then, similar results are presented for future conditions.

As detailed in <u>Section 2.2</u>, coastal overwash is a temporary and transient process driving localised coastal flooding adjacent to areas of overwash. Thus, it is not appropriate to map areas of inundation using a static 'bathtub' approach, as it is commonly performed in tide-only inundation studies. Therefore, this first-pass study provides mapping output with the location of 100-m spaced transects and corresponding overwash likelihood only, highlighting locations that are likely experiencing overwash both now and into the future. It is expected that the vulnerable sites identified in this study will undergo a more detailed process-based modelling approach under the Coastal Management Framework.

# A.5 Estuarine inundation

#### Hazard overview

Previous studies have shown that extensive development adjacent to NSW estuaries is exposed to potential inundation as sea levels rise (OEH 2018; Hanslow et al. 2018). Many coastal towns in NSW already experience street inundation (commonly referred to as 'sunny day flooding' or 'nuisance inundation') during higher tides, and the frequency of these events has been increasing (Hague et al. 2020, 2022; Hanslow et al. 2019, 2023), particularly in areas where mitigation measures such as installing stormwater gates or flaps have not yet been implemented. These sites are mostly located in the lower reaches of estuaries where exposure to open coast processes like wave setup and runup is reduced, as is exposure to the floods that typically affect upper estuarine settings (Hanslow et al. 2019).

At present, this inundation is primarily driven by both astronomic tides and tidal anomalies resulting from weather and oceanic processes. However, it is not necessarily associated with extreme storm conditions – that is, it is typically observed during 'normal' weather – hence the term 'sunny day flooding'. As sea levels rise, this type of

inundation will increasingly occur under astronomic tide conditions alone (Hague et al. 2022). Over time, as sea levels continue to rise, inundation events are expected to become both higher and more frequent. These events will also last longer, eventually resulting in permanent inundation of low-lying areas.

This study's approach is focused on addressing the chronic aspects of inundation within estuaries, examining water levels at annual exceedance levels and below. Effects of rainfall-related flooding were not considered, as a more detailed modelling method is required to assess the effects of SLR on flood related processes (in other words, they cannot simply be combined because changes in sea level will affect flood wave propagation further upstream).

# **Approach**

In this study, the exposure to estuarine inundation of existing properties and infrastructure adjacent to NSW estuaries was assessed under the range of SLR scenarios outlined in Appendix A.2 Sea level rise.

The study adopted an intermediate complexity approach to modelling and mapping water levels within estuaries. This approach was based primarily on the use of measured data from individual tide gauges and used a surface fitting method which allows for variation in water levels both between and within individual estuaries. The method improves on simple 'bathtub' approaches used in previous national assessments but is less complex than hydrodynamic modelling for each estuary. To improve communication of current inundation frequency, this study adopted a daily water level exceedance approach, rather than relying on astronomic tidal planes used in the previous NSW state-wide estuary tidal inundation exposure assessment (OEH 2018; Hanslow et al. 2018).

Daily maximum empirical frequency distributions derived from water level gauge data for 96 estuaries (MHL 2019) were used to present current estuarine water levels. In ungauged estuaries, data from similar nearby estuaries was used, while for ICOLLs, an averaged exceedance distribution was applied, scaled according to measured berm elevation.

Potential future water levels were calculated at decadal intervals for each SLR scenario by adding SLR randomly sampled from each of the log-normal distributions outlined in Appendix A.2 Sea level rise. In estuaries with available hydrodynamic models, potential changes to high tides were considered, associated with changes to tide dynamics as sea levels increase.

The water surface mapping method used an interpolated water level surface created from the gauge data. These water level surfaces were overlaid on digital elevation models derived from high-resolution LiDAR elevation data. The resulting spatial model of inundation improves the representation of current inundation hazard extent and allows for improved assessment of the inundation hazard associated with potential SLR.

### Data

#### Terrain data

For this project, the best available digital elevation data for each estuary catchment were used. In all areas, a 5-m digital elevation model (DEM) was used, derived from LiDAR data collected progressively by NSW Spatial Services over the past couple of decades (DCS Spatial Services 2020). These DEMs are publicly available via the ELVIS data portal (ICSM 2021) and have a horizontal accuracy of 0.8 m and vertical accuracy of 0.3 m (95% CI), meeting the Intergovernmental Committee on Surveying and Mapping's guidelines for digital elevation data. To improve mapping workflow performance, the DEM of each estuary catchment was constrained by limiting the elevation to areas below 10 m AHD (Figure 81).

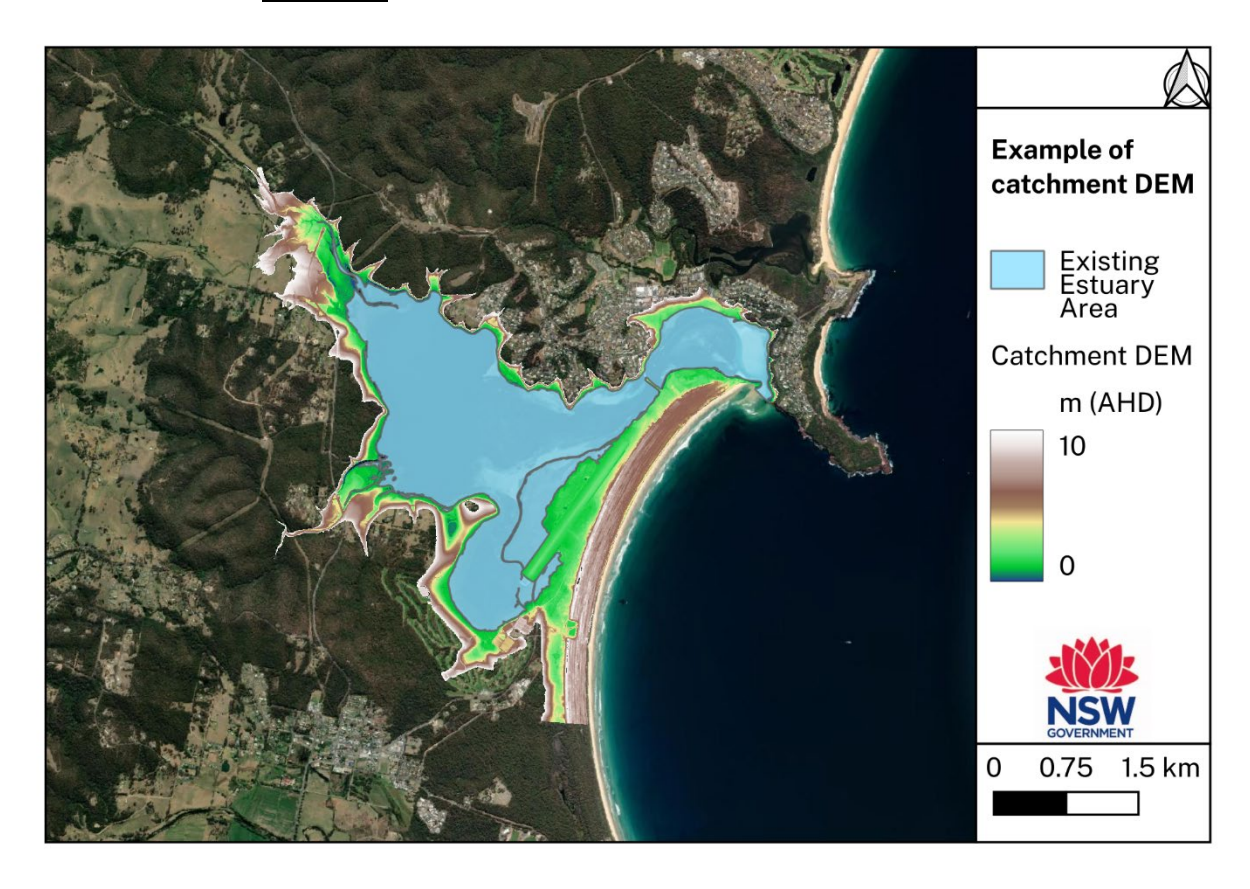


Figure 81 Plot showing an example of a truncated estuary catchment digital elevation model (DEM) (i.e. areas below 10 m AHD) for Merimbula Lake

#### Water level data

Water levels were sourced from available tide gauge data from Manly Hydraulics Laboratory, which operates the NSW tide gauge network for the Department of Climate Change, Energy, the Environment and Water. This includes data from 8 tide gauges that are considered fully representative of the ocean tides along the NSW coast (see <u>Figure 82</u>, with details shown in Table 9). Further, water levels across NSW are recorded at approximately 213 gauge locations within the tidally influenced parts of 96 estuaries

(MHL 2019), as shown in <u>Figure 82</u> and detailed in Appendix F: NSW estuarine tidal water level gauges.

Table 9 Ocean tide gauges in New South Wales: station name, Australian Water Resources Code (AWRC) number, latitude, longitude and duration of operation

Station name	AWRC	Latitude	Longitude	Duration (yrs)
Coffs Harbour	205470	-30.30287	153.14614	36.4
Crowdy Head	208471	-31.83871	152.75001	37.6
Shoal Bay	209474	-32.71967	152.17565	37.6
Patonga	212440	-33.55098	151.27462	30.9
Sydney	213470	-33.82546	151.25853	35.6
Jervis Bay	216470	-35.12195	150.70744	35.9
Ulladulla	216471	-35.35767	150.47653	15.4
Eden Boat Harbour	220470	-37.07124	149.90829	36.6

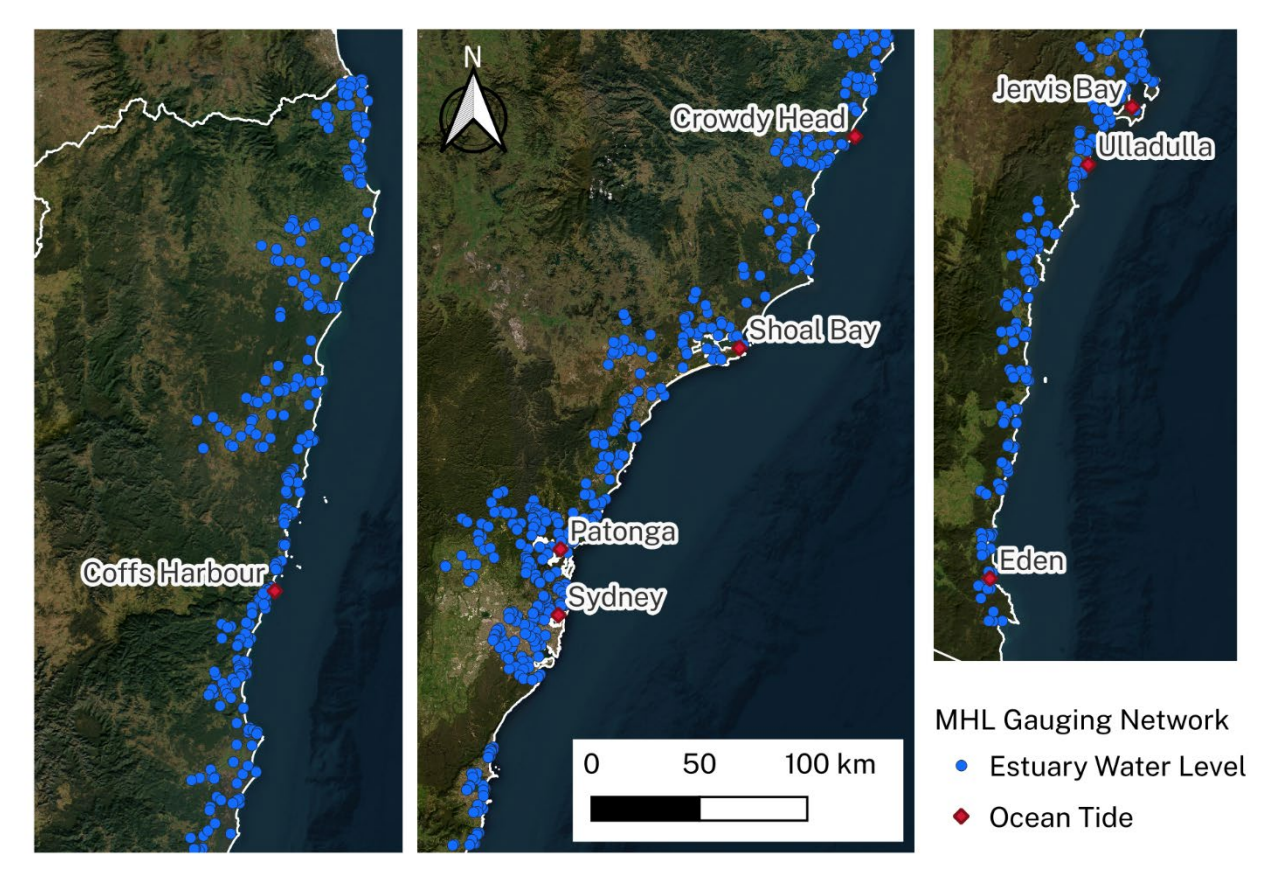


Figure 82 Map showing location of NSW Manly Hydraulics Laboratory (MHL) tide and water level gauging network

The majority of water level records at these gauge locations span 30 years or more (Appendix F: NSW estuarine tidal water level gauges and Figure 83) and are ongoing.

However, in some instances, it was necessary to use shorter records and records from decommissioned sites to ensure maximum spatial coverage where possible.

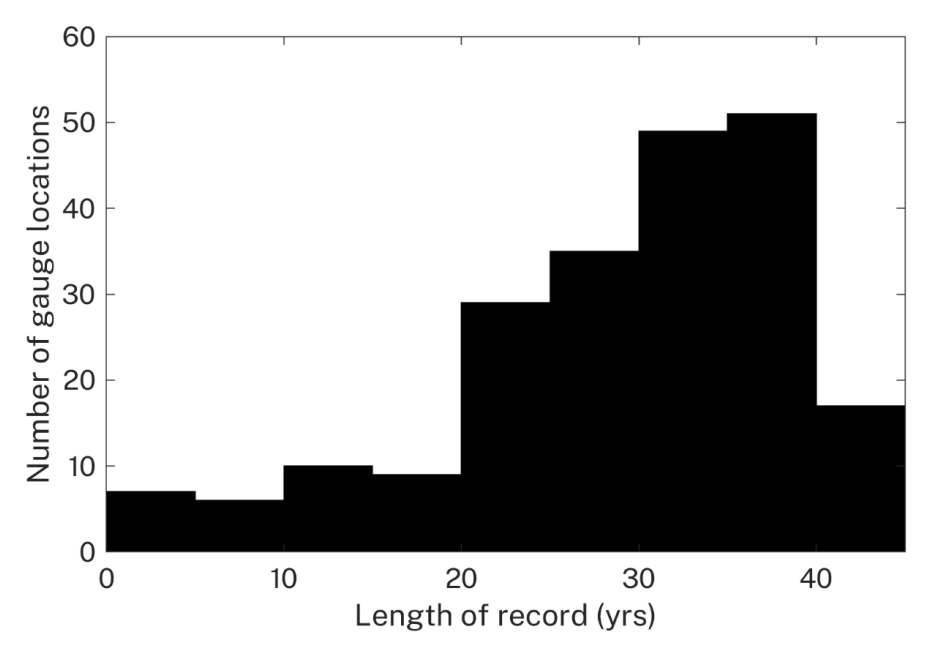


Figure 83 Histogram showing length (number of years) of water level records at NSW gauge locations

## Water levels

#### Current water levels

Water level records from the current gauge locations, including ocean tide locations, were obtained from the beginning of records until the beginning of July 2022. As each gauge dataset includes the effects of SLR, linear detrending was applied to adjust each water level distribution to be representative of 2020 – that is, the early part of each record is lifted to make the overall dataset representative of the water level in 2020. The purpose of this adjustment is to remove any constant rate long-term trends in the data (changes due to SLR) without removing inter-annual variability from the time series.

Water levels in the upstream reaches of many estuaries are often influenced by terrestrial floods, which can have considerable impacts, even at an annual recurrence interval basis. To remove these effects, a threshold method following Palmer et al. (2024) was implemented. This technique uses the interquartile range (IQR) and the third quartile (Q3) statistics, calculated from the water level record to define a flood peak threshold as Q3 + 1.5 × IQR (Tukey 1977). A flood event is defined as a period when the non-tidal residuals (recorded water level minus tidal predictions) exceed a threshold (the Q3 of the non-tidal residuals) for more than 6 hours. If the maximum water level during an event exceeds the flood peak threshold, then the water levels during that event are removed from the time series.

Daily maximum, mean and minimum water levels from these adjusted records were then extracted and used to calculate a set of empirical cumulative density functions (ECDF), as illustrated in Figure 84.

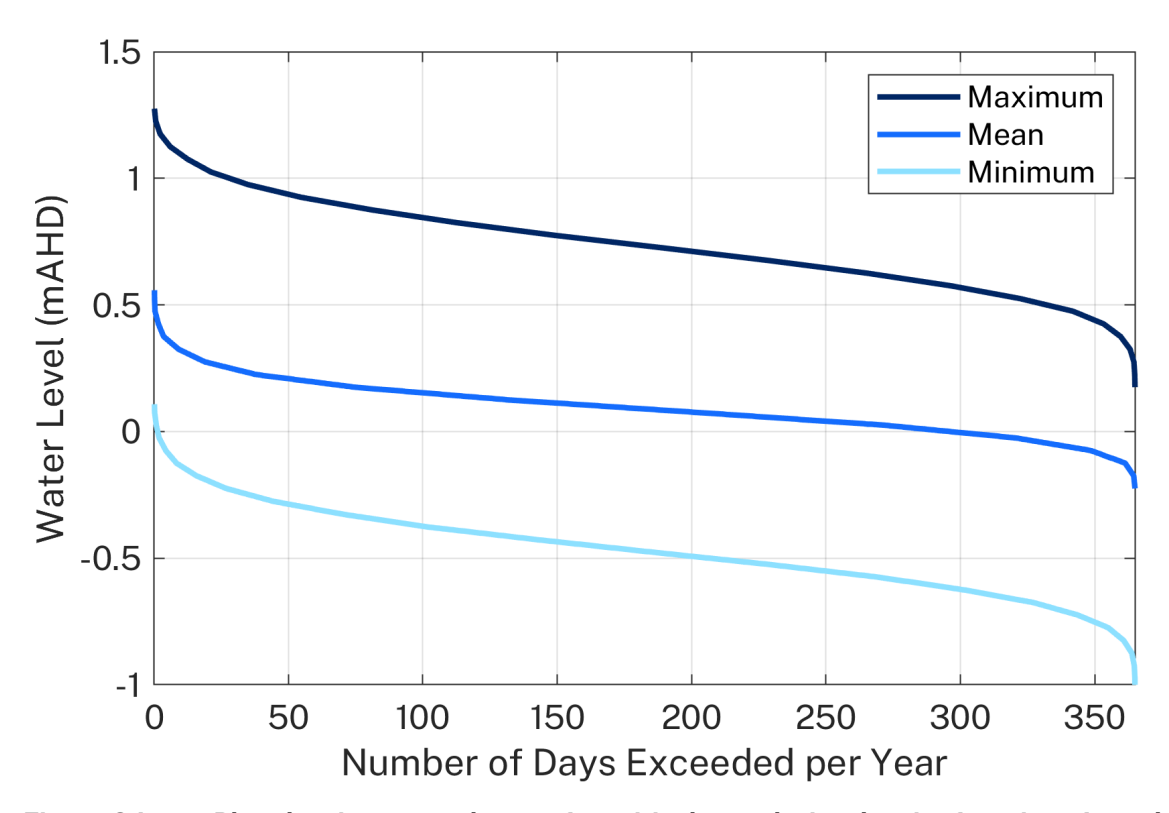


Figure 84 Plot showing example set of empirical cumulative density functions from daily estuarine water level gauge data

The ECDF for the ocean tide gauge locations were also calculated (see <u>Figure 85</u> for daily maximum ECDF). These show a slight increase in water levels along the NSW coast (that is, water levels are higher in the north of the state), consistent with MHL (2018). The daily maximum ECDF from the nearest ocean tide gauge location was used as the ocean boundary for each given estuary. From each daily maximum ECDF, 4 daily exceedance statistics were extracted for mapping current water levels:

- f1 = 1 day/year (annual)
- f2 = 3.6 days/year (1% days exceeded)
- f3 = 36.5 days/year (10% days exceeded)
- f4 = 182.5 days/year (50% days exceeded).

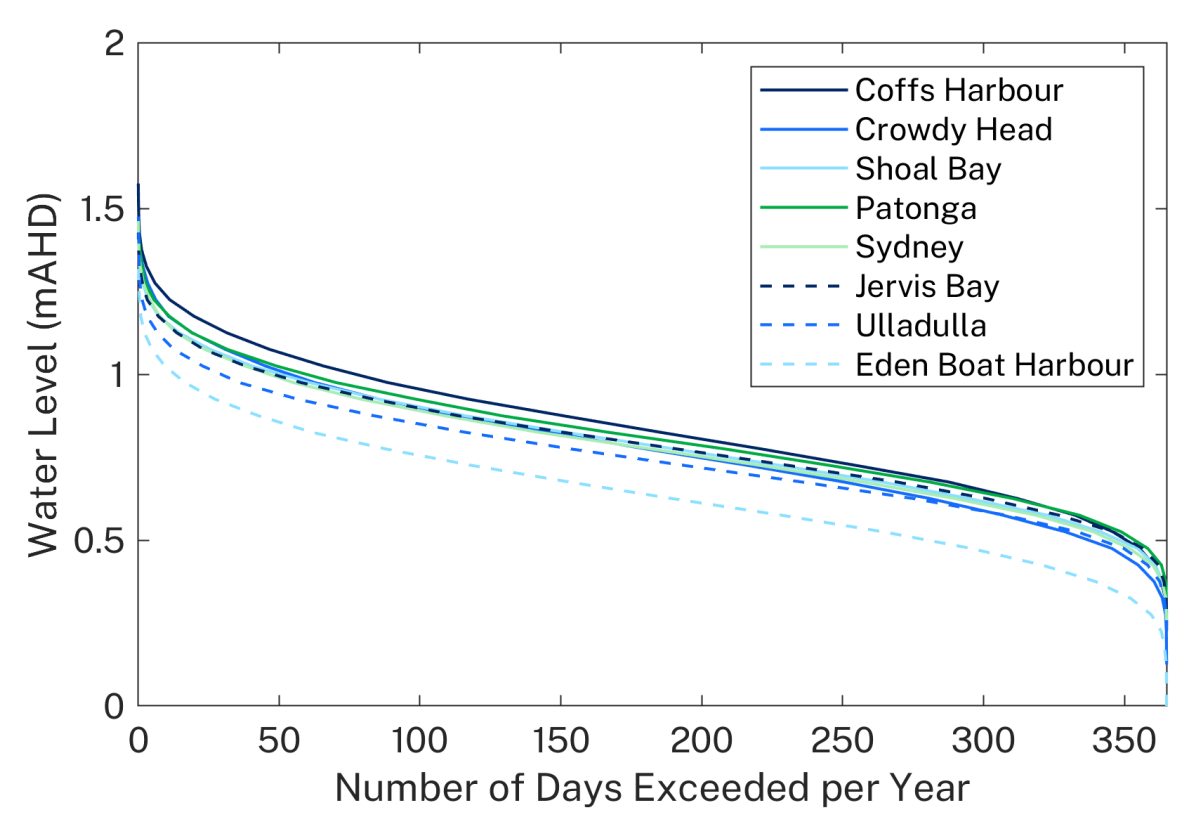


Figure 85 Plot showing empirical cumulative density functions from daily maximum data at 8 NSW ocean gauge locations

Water levels also vary by estuary type, as shown in the first NSW state-wide estuary tidal inundation exposure assessment (OEH 2018). Figure 86 provides some examples of this variation. In this figure, drowned river valley estuaries, such as the Hawkesbury River, exhibit tidal amplification, tidal lake estuaries, represented by Lake Macquarie, exhibit significant tidal attenuation, riverine estuaries, such as the Tweed River, show initial tidal attenuation followed by amplification, while ICOLLs such as Lake Wollumboola exhibit a broader range of water levels owing to their respective berm levels.

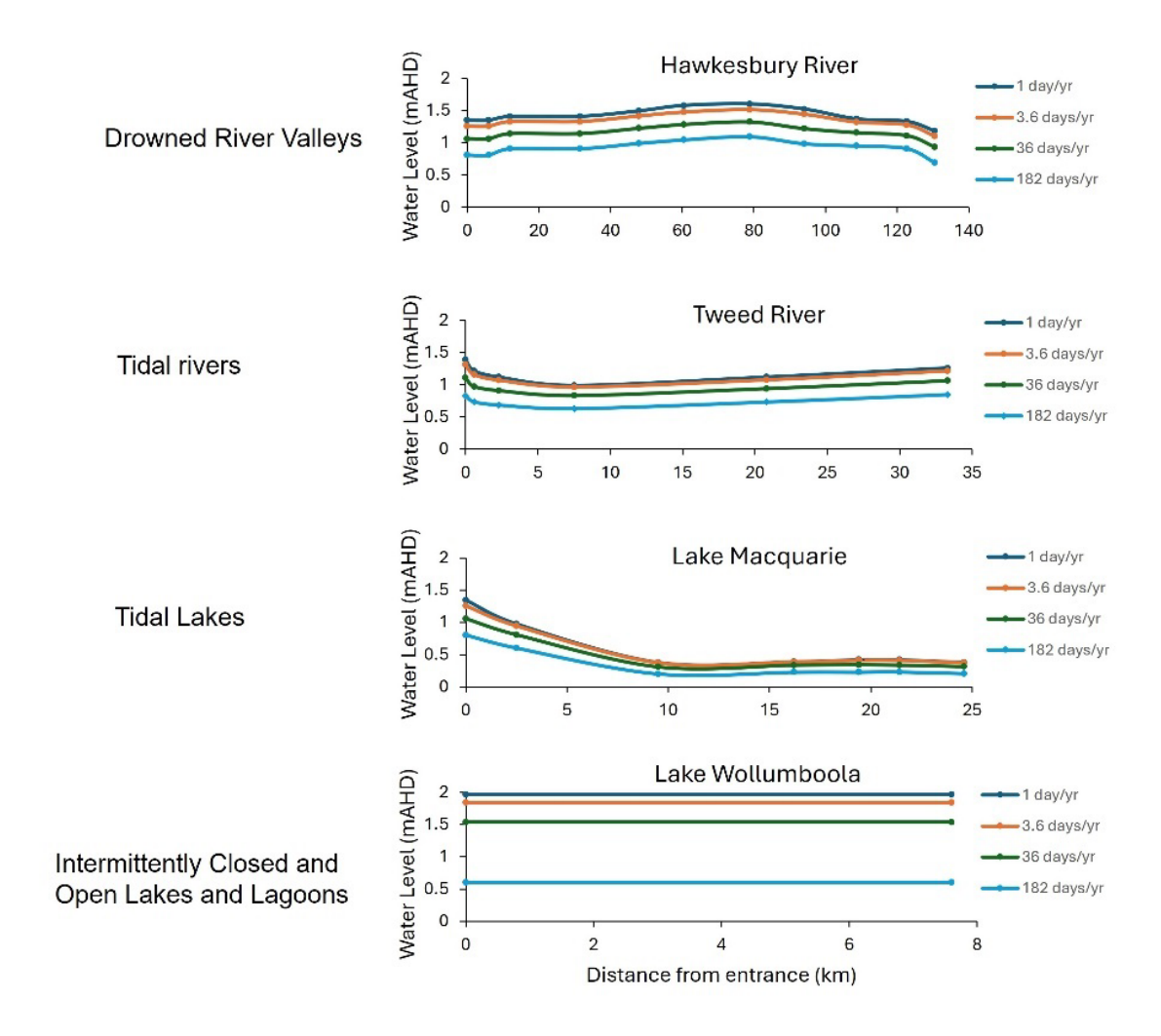


Figure 86 Examples of water levels in different estuary types

For the small number of NSW estuaries (excluding non-gauged ICOLLs, NGIs) without water level gauge data, nearby gauged estuaries of the same type were selected as proxies. Virtual gauge locations were then chosen in each of the 13 non-gauged estuaries, based on the scaled distance from the estuary entrance of the gauges in the proxy estuary, and the appropriate ECDF was assigned to each. The extraction of the exceedance statistics then proceeded as for the gauged estuaries.

For NGIs, a method similar to that used in the first NSW state-wide estuary tidal inundation exposure assessment (OEH 2018) was implemented. In this case, generic non-dimensional ECDFs were determined using water level records from all ICOLLs with gauge data. These non-dimensional ECDFs were then scaled for each NGI using the maximum berm height as the maximum water level, following OEH (2018). Berm heights for each NGI were obtained from available LiDAR and survey data. As with other non-gauged estuaries, virtual gauge locations were chosen within each NGI to enable mapping of the exceedance levels.

All these data were compiled into a state-wide water level information database for use in the GIS water surface modelling (see Appendix A.5: Water surface model).

#### Future water levels

As outlined in <u>Appendix A.2 Sea level rise</u>, probability distributions were used to account for uncertainty in SLR for each scenario and timeframe. In order to obtain water level ECDFs for each future scenario and timeframe, the probability distributions were randomly sampled and added to current water level records. In addition, to take into account potential changes in the tidal dynamics under SLR, an amplification/dampening factor, as outlined in Appendix A.5: <u>Potential changes to tides</u>, was also applied for the 12 modelled estuaries (Table 10).

The ECDFs of the daily maximums for all gauge locations were then recalculated using these adjusted water level records for each SLR scenario and timeframe, and 4 exceedance levels equivalent to the current water level case were extracted for mapping.

An example of the calculation of probability density and ECDF of daily maximums for a water level gauge location is shown in Figure 87.

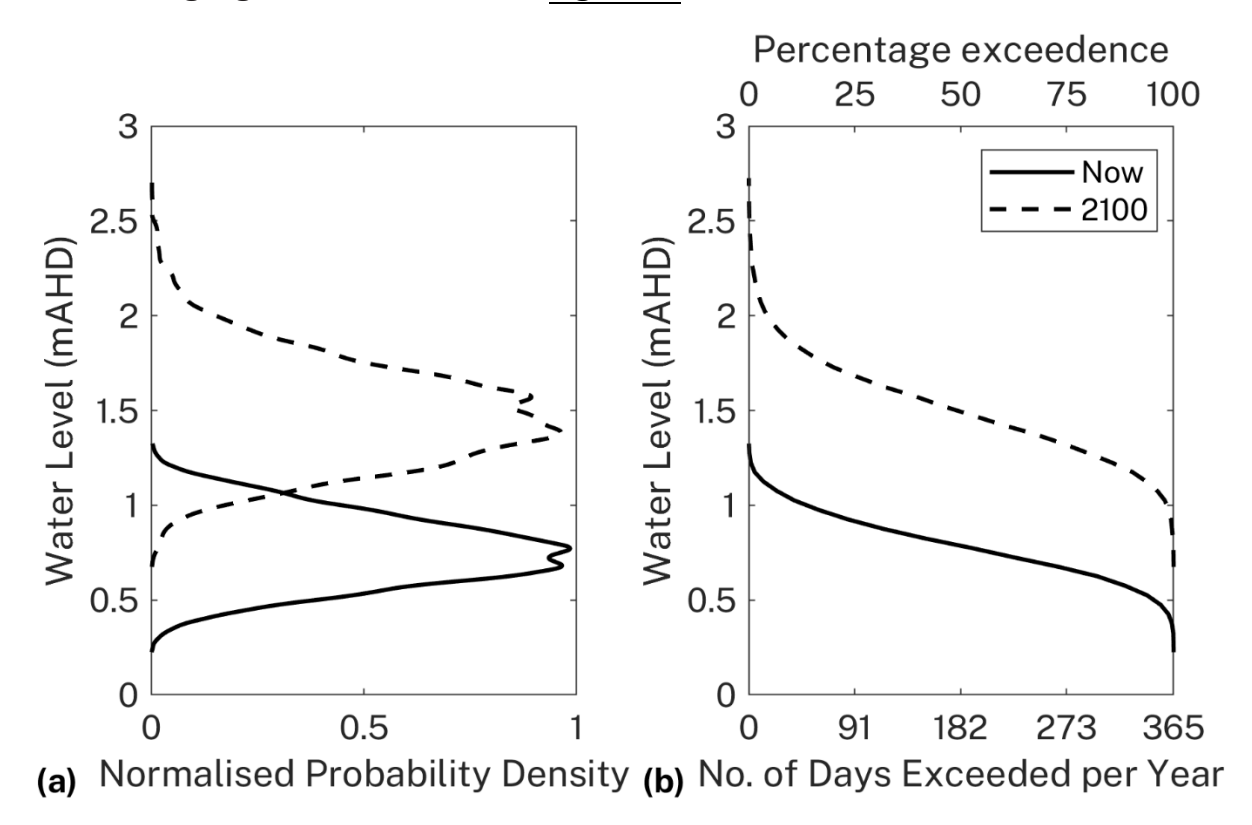


Figure 87 Water level frequency distributions for a gauge in a non-modelled estuary for a current (2020) and future case (2100; SSP3-7.0), showing (a) normalised probability density and (b) empirical cumulative density function

In the case of non-gauged estuaries, including the NGI, the processes outlined in the previous section were repeated using the ECDF produced for each SLR scenario and timeframe.

All these data were then added to the state-wide water level information database for use in the GIS water surface modelling.

## Potential changes to tides

To accommodate potential future changes to tides (amplification, dampening, or a mix of both), detailed hydrodynamic modelling for selected estuaries was used. The primary aim was to formulate an 'amplification/dampening factor', with positive values highlighting a rise in maximum water levels and negative values denoting a reduction in maximum water levels under a SLR scenario, that considers the interaction of SLR and tidal processes within different estuary types.

A set of pre-existing calibrated hydrodynamic models for 12 estuaries in NSW was used to explore the potential impacts of various SLR scenarios on their longitudinal maximum water levels. A list of these models together with the references related to the model creation and calibration as well as their state-wide geographical distribution are presented in Table 10.

For these sites, the models were run with constant SLR scenarios of 0 m, 0.5 m, 1 m and 2 m – except in the Lake Macquarie and Lake Illawarra where only SLR scenarios of 0 m, 0.5 m and 1 m were investigated due to model boundary limitations. For all models and scenarios tested, the maximum water levels were extracted along the main stem (branch) of each estuary to gain insights into the amplification/dampening factors in these estuaries.

Table 10 A list of 12 estuary models collated from different sources to gain understanding on changes to maximum water level along different NSW estuaries and under different sea level rise (SLR) scenarios

No.	Estuary	Estuary type	Numerical model	SLR scenario (m)
1	Tweed River	Barrier river	RMA-2ª	0, 0.5, 1, 2
2	Richmond River	Barrier river	RMA-2ª	0, 0.5, 1, 2
3	Clarence River	Barrier river	RMA-2ª	0, 0.5, 1, 2
4	Macleay River	Barrier river	RMA-2ª	0, 0.5, 1, 2
5	Hastings River	Barrier river	RMA-2ª	0, 0.5, 1, 2
6	Manning River	Barrier river	RMA-2ª	0, 0.5, 1, 2
7	Hunter River	Barrier river	RMA-2 <sup>a,b</sup>	0, 0.5, 1, 2
8	Lake Macquarie	Lake	Telemac2D°	0, 0.5, 1
9	Lake Illawarra	Lake	RMA-2 <sup>d</sup>	0, 0.5, 1
10	Botany Bay (including Cooks and Georges rivers)	Lake, barrier river and drowned valley	RMA-2 <sup>e</sup>	0, 0.5, 1, 2
11	Shoalhaven River	Barrier river	RMA-2ª	0, 0.5, 1, 2

No.	Estuary	Estuary type	Numerical model	SLR scenario (m)
12	Sydney Harbour (including Port Jackson, Middle Harbour Creek, Lane Cove River, and Parramatta River)	Drowned valley	RMA-2 <sup>e</sup>	0, 0.5, 1, 2

Sources: a. UNSW Water Research Laboratory (WRL); b. Hunter Water Corporation; c. Schneider et al. (2016); d. Manly Hydraulics Laboratory (MHL); e. Sydney Water Corporation.

An example of the output from this modelling is shown in <u>Figure 88</u> for the Clarence River. This model was developed by UNSW WRL using the RMA-2 numerical package. Here, the maximum water levels associated with each of the SLR scenarios are plotted along the length of the main channel together with the percentage change in the normalised maximum water level. Maximum water levels exhibit amplification as sea levels rise with peak increases around 25 km to 40 km away from the entrance, corresponding roughly with peak attenuation of the current maximum water level.

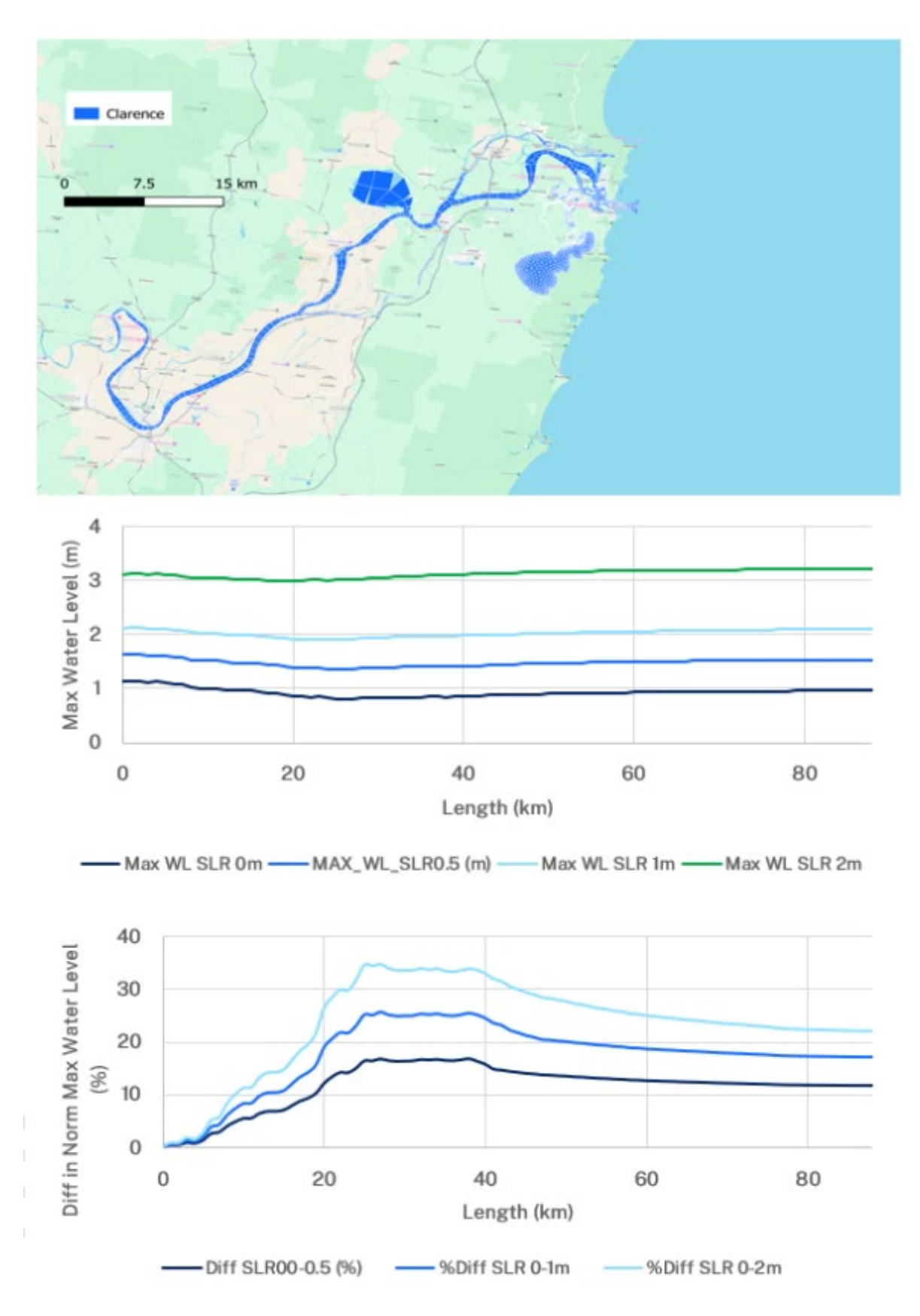


Figure 88 Model grid and output for the Clarence River in Northern NSW, showing maximum water levels extending from the river mouth to the tidal limit for each sea level rise scenario along with the percent difference in the normalised maximum water level

Results of the detailed modelling were applied to the measured water level data at each of these estuaries, taking into account the location of the gauge with respect to the modelled amplification/dampening. To accommodate the possibility that morphological setting represents only one of several potential future scenarios – that is, there may be some morphological changes (such as accretion or erosion) in the estuaries under SLR – the modelling results were used as the near upper limit (3 standard deviations or 3 sigma) of the amplification/dampening factor which is represented using a normal distribution, with no change at the lower limit.

### **Mapping**

To map the extent of inundation within the NSW estuaries, a GIS-based model was developed, consisting of 2 main parts: the water surface model and the inundation model, and using QGIS (QGIS Development Team 2023) and Arc Desktop geoprocessing and spatial analysis functions (ESRI 2021). A flow chart outlining the structure of the model is shown in Figure 89.

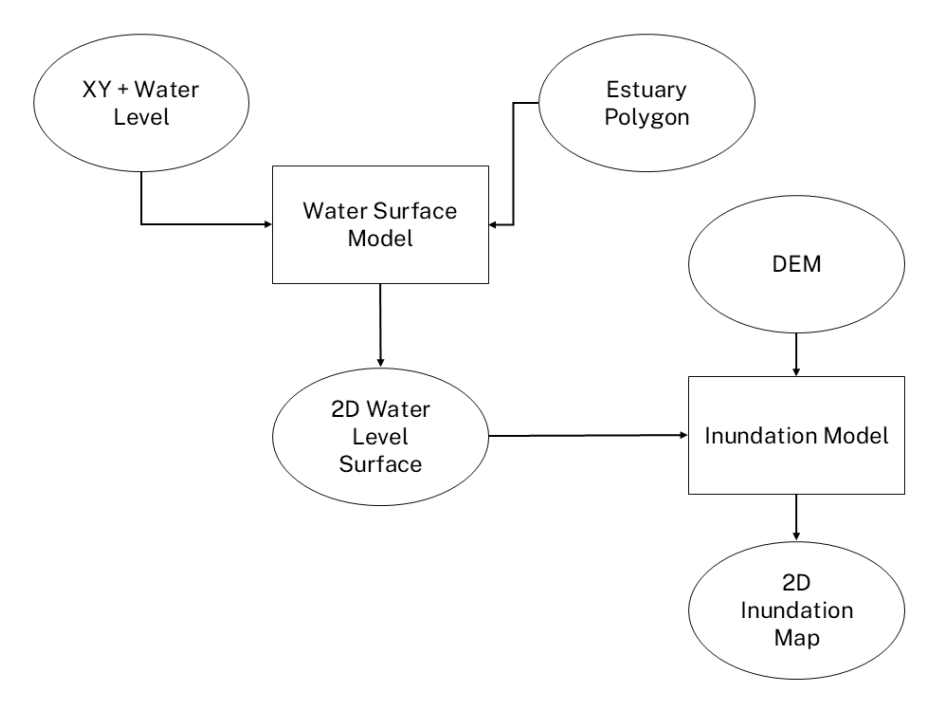


Figure 89 Flow chart showing simplified structure of GIS-based estuarine inundation model

#### Water surface model

The GIS-based water surface model was used to generate an estuary wide 2D water level surface (WLS) analogous to the method outlined in Foulsham et al. (2012). In this study, the water levels were based on frequency of occurrence (see Appendix A.5: <a href="Water levels">Water levels</a>) rather than harmonic tidal planes. For a given estuary, the water level information was extracted from the water level information database (Appendix A.5: <a href="Current water levels">Current water levels</a>), which includes both ocean tide and estuary gauge water levels, as well as the tidal limit locations.

An area of analysis (AOA) for each estuary was then created by buffering the estuary's spatial boundary (OEH 2013) by 200 m, while constraining the extent within the estuary's catchment area. A surface was then created from the water level information for the various frequency of occurrences using a minimum curvature spline technique, with the AOA boundary serving as a barrier. An example of the resulting surface is shown in Figure 90.

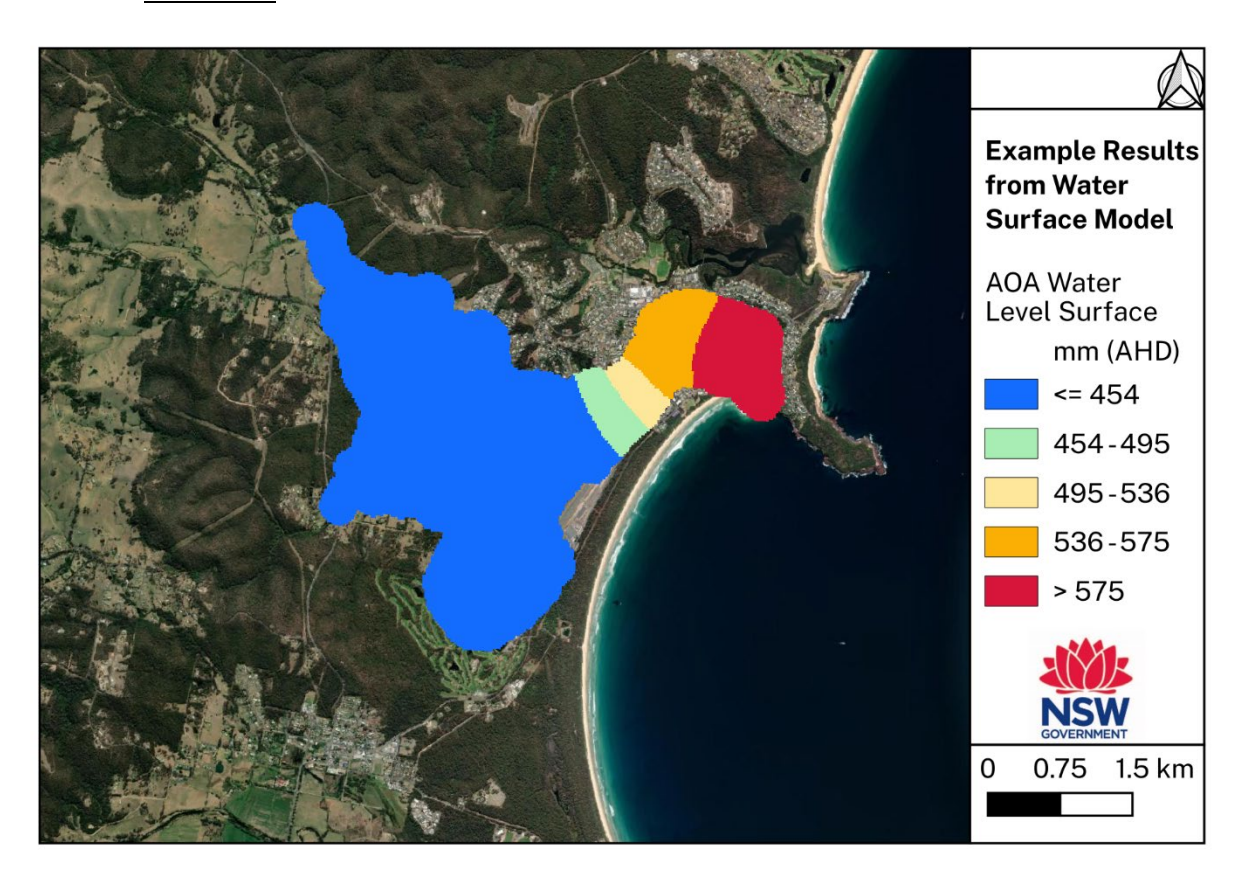


Figure 90 Map showing example results from water surface model, area of analysis (AOA) water level surface (mm AHD)

The AOA water level surface was then intersected with the estuary boundary to create an estuary boundary water level. This representation of the water level surface along the estuary boundary was projected across the estuary catchment by assigning each point in the catchment the value of the nearest boundary water level, measured using straight-line distance, that is, Euclidean allocation (Shih and Wu 2004). An example of the resultant 2D WLS is shown in <a href="Figure 91">Figure 91</a>. An exception to this method is the embayed (EM) type estuaries where the exceedances extracted from the daily maximum ECDF of adjacent ocean tidal water level were used throughout, that is, a constant WLS over the extent of the embayment.

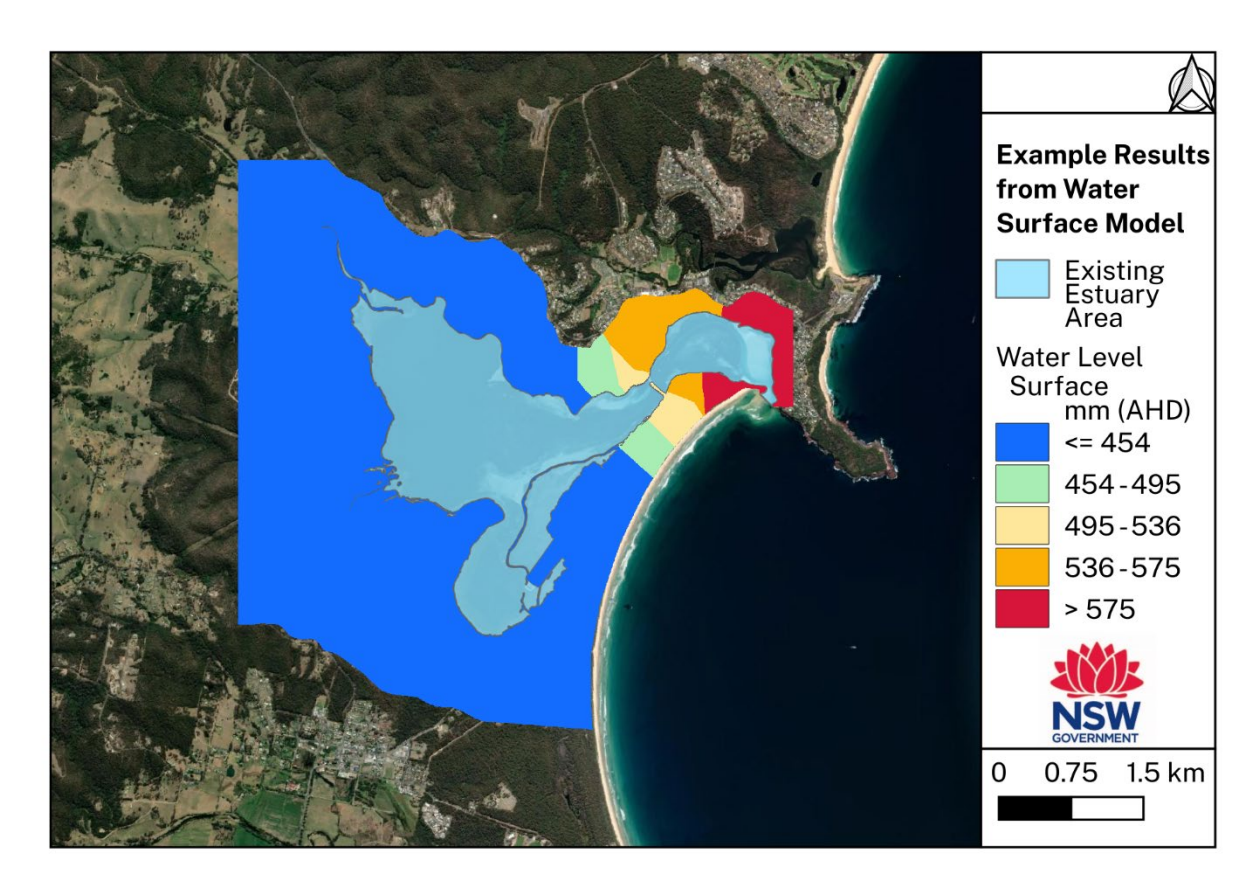


Figure 91 Map showing example results from the water surface model, final water level surface (mm AHD)

#### Inundation model

The WLS created using the water surface model was then used as one of the inputs to the GIS-based inundation model which estimates the spatial extent of tidal inundation for a given estuary. A DEM of the estuary catchment was compiled from available data and constrained to elevations below 10 m AHD (Appendix A.5: <u>Terrain data, Figure 81</u>). The WLS was then spatially joined to the DEM, and the inundation status calculated by assessing whether the WLS height is higher or lower than the elevation at each data point, producing a raw estuarine inundation polygon layer.

The final step in the inundation model considered the flow path of the existing estuary water body and differentiated non-connected low-lying areas of inundation from connected areas within the estuary catchment. In reality, non-connected areas may be connected through infrastructure such as the storm water system, although no state-wide datasets are presently available which would allow for ready identification of drainage connectivity. Therefore, the inundation polygon layer was modified so that isolated areas of inundation, defined as areas more than a given distance (nominally 5 m) from the existing estuary water body, were split and an auxiliary inundation polygon layer was created. This process resulted in 2 polygon layers for each model run, the primary and isolated inundation polygon layers (see Figure 92).

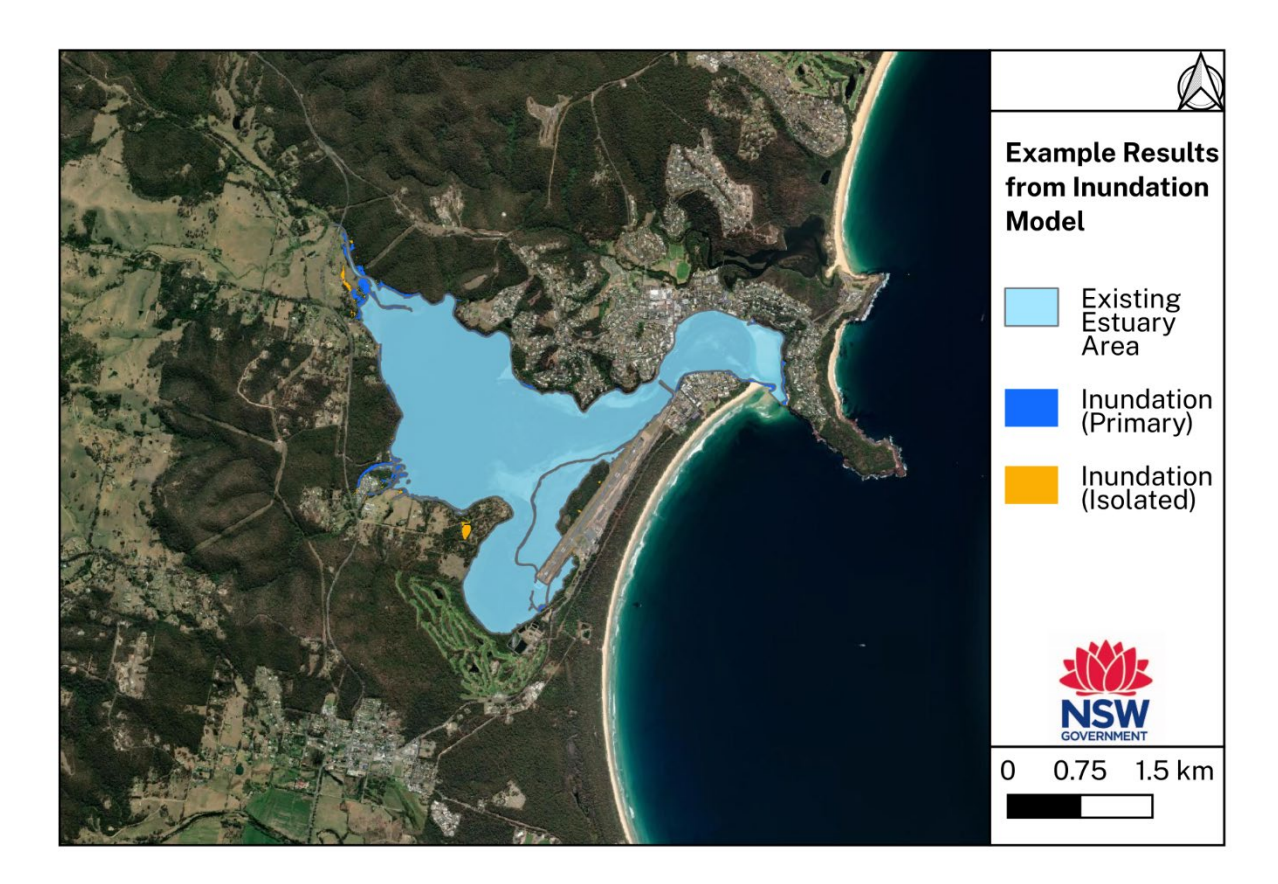


Figure 92 Plot showing example of primary and isolated estuarine inundation polygon layers

The final map layer outputs include 2 polygon layers of inundation extent associated with current and potential future scenarios at several inundation exceedance frequencies (1 day/year, 3.6 days/year (1% of days), 36 days/year (10% of days), and 182 days/year (50% of days)) and at decadal intervals from 2020 to 2150 (Appendix A.2 Sea level rise). The exception is low-confidence SSP5-8.5, where only the 2 lower exceedance frequencies (36 days/year and 182 days/year) are mapped for the latter years, owing to limitations in the DEMs.

# A.6 Exposure

## Approach to generating exposure statistics

To estimate the numbers and area of assets potentially impacted by inundation and erosion along the NSW coast, GIS processing in python and in ArcMap 10.8.2 (ESRI 2021) was used to overlay and intersect generated hazard extent layers with existing asset layers. Exposure to inundation and erosion was reported both as totals for NSW and by beach/estuary. Methods for calculating counts and areas vary according to asset type (see <u>Table 11</u>). For each asset and hazard, bar plots were generated to indicate state-wide exposure totals.

#### Exposure to coastal erosion

For erosion hazards, the hazard areas extend landward from the present-day beach berm position (2 m AHD) for an accreted beach state, up to the inland extent of erosion predicted for each SLR scenario. Each combination of forecast horizon, SLR scenario and exceedance probability level produced a unique hazard area reflecting future shoreline changes due to coastal erosion.

#### **Exposure to inundation**

For each estuary and SLR scenario, 4 series of statistics are reported for the intersecting inundation hazard and asset features. These statistics represent combined primary and isolated inundation extents for the following exceedance statistics: 182.5 days/year (50%), 36.5 days/year (10%), 3.6 days/year (1%) and 1 day/year (annual).

# **Building footprints**

Building footprints were acquired from the *Geoscape buildings* product (Geoscape Australia 2023), a commercial dataset updated quarterly. This dataset consists of polygons of roof outlines, which have been digitised through a combination of manual and automated processes from satellite and aerial imagery for buildings greater than 9 m². Each building is linked to a planning zone and includes an address count attribute, which details the number of addresses associated with each building. Where the exposure of a building to either estuarine inundation or erosion was less than 5 m², it was classed as nuisance exposure and was excluded from building and address counts.

## Transport infrastructure

Road and rail segments are vector data sourced from the Transport Theme of the NSW Government <u>Spatial collaboration portal</u>. These data are held and maintained within the Foundation Spatial Data Framework (DCS Spatial Services 2020). The statistics generated for transport infrastructure exposure to hazard extents include lengths of road and rail segments, counts of airports, and lengths of runways.

## Aboriginal heritage assets

Statistics on the number of Aboriginal heritage sites were obtained from the <u>Aboriginal</u> <u>heritage information system</u> (OEH n.d.), which is a point dataset. The total number of recorded sites exposed to each hazard extent is reported by estuary and by beach.

#### Critical infrastructure

Statistics on critical infrastructure were derived from vector data available on the NSW Government *Spatial collaboration portal*. The statistics were generated for the following critical infrastructure:

- school and university facilities
- hospitals
- emergency services (police, fire and SES stations)
- correctional centre and courthouse facilities.

Table 11 Summary of statistics generated for exposure to inundation and erosion hazards

Asset type	Data source	Last modified	Statistics generated
Building footprints	Geoscape buildings (Geoscape 2023)	September 2023	Building count and address count by planning zone
Transport infrastructure	NSW foundation spatial data framework	April 2023	Lengths of road, rail and runways; count of airports
Aboriginal heritage sites	Aboriginal heritage information management system (OEH n.d.)	June 2021	Total number of recorded sites exposed
Critical infrastructure assets	NSW foundation spatial data framework	Emergency services: November 2021 Health: December 2023 Education: May 2023 Justice: February 2022	Counts of schools and universities, hospitals, correctional facilities and courthouses, and emergency services facilities
Electricity transmission lines	NSW foundation spatial data framework	March 2023	Lengths of overhead and underground lines

# Appendix B: Datasets

Datasets used in the coastal hazard modelling and mapping are set out in <u>Table 12</u> (coastal geomorphology), <u>Table 13</u> (historical beach and shoreline change), <u>Table 14</u> (coastal waves), and <u>Table 15</u> (coastal water levels).

Table 12 Coastal geomorphology datasets

Dataset	Dates	Custodian
NSW terrestrial airborne LiDAR mapping	2010-2014	DCS Spatial Services
NSW seamless coastal LiDAR topography–bathymetry	2018	DCCEEW (NSW)
NSW multibeam echosounder coastal seabed bathymetry	2008 to present	DCCEEW (NSW)
NSW coastal seabed landforms classification mapping	2020	DCCEEW (NSW)
NSW repeat airborne LiDAR beach surveys (UNSW)	2015 to present	DCCEEW (NSW)
NSW coastal quaternary geology mapping	2015	NSW Resources
Smartline coastal geomorphology	2009	Geoscience Australia
Australian coastal sediment compartments	2015	Geoscience Australia

DCCEEW (NSW) = Department of Climate Change, Energy, the Environment and Water; UNSW = University of New South Wales.

Table 13 Historical beach and shoreline change datasets

Dataset	Dates	Custodian
NSW beach profile database historical photogrammetry	1970s to present	DCCEEW (NSW)
Digital Earth Australia Coastlines satellite shoreline mapping	1988 to present	Geoscience Australia
CoastSat satellite shoreline mapping	1988 to present	UNSW

DCCEEW (NSW) = Department of Climate Change, Energy, the Environment and Water; UNSW = University of New South Wales.

Table 14 Coastal waves datasets

Dataset	Dates	Custodian
NSW deep-water ocean waverider buoy observations/statistics	1970s to present	MHL/DCCEEW
NSW nearshore coastal wave buoy observations/statistics	2016 to present	DCCEEW (NSW)

Dataset	Dates	Custodian
NSW Nearshore wave transformation tool wave hindcast	1957 to present	DCCEEW (NSW)

DCCEEW (NSW) = Department of Climate Change, Energy, the Environment and Water; MHL = Manly Hydraulics Laboratory.

Table 15 Coastal water levels datasets

Dataset	Dates	Custodian
NSW ocean tide gauge observations/statistics	1970s to present	MHL/DCCEEW
(IPCC) AR6 regional sea level rise projections	Present to 2150	IPCC

DCCEEW (NSW) = Department of Climate Change, Energy, the Environment and Water; IPCC = Intergovernmental Panel on Climate Change; MHL = Manly Hydraulics Laboratory.

# Appendix C: Beaches modelled

<u>Table 16</u> presents the beaches modelled in the coastal erosion hazard assessment arranged by primary and secondary compartment, with the number of model beach sectors and reference tide gauge for sea level rise projections also listed.

Table 16 Beaches modelled by primary and secondary compartment, number of sectors and tide gauge

Primary compartment	Secondary compartment	Beach	Sectors	Tide gauge
nsw01	nsw010101	nsw002	3	Tweed River
nsw01	nsw010101	nsw003	3	Tweed River
nsw01	nsw010101	nsw004	3	Tweed River
nsw01	nsw010101	nsw005	1	Tweed River
nsw01	nsw010101	nsw006	3	Tweed River
nsw01	nsw010101	nsw008	3	Brunswick River
nsw01	nsw010101	nsw009	3	Brunswick River
nsw01	nsw010101	nsw010	3	Brunswick River
nsw01	nsw010101	nsw011	3	Brunswick River
nsw01	nsw010101	nsw012	3	Brunswick River
nsw01	nsw010101	nsw013	3	Brunswick River
nsw01	nsw010102	nsw016	3	Brunswick River
nsw01	nsw010102	nsw021	3	Brunswick River
nsw01	nsw010102	nsw022	1	Brunswick River
nsw01	nsw010102	nsw024	3	Brunswick River
nsw01	nsw010102	nsw025	3	Brunswick River
nsw01	nsw010102	nsw026	1	Brunswick River
nsw01	nsw010102	nsw027	1	Brunswick River
nsw01	nsw010102	nsw028	1	Brunswick River
nsw01	nsw010103	nsw029	5	Yamba
nsw01	nsw010104	nsw033	1	Yamba
nsw01	nsw010104	nsw034	1	Yamba
nsw01	nsw010104	nsw035	5	Yamba
nsw01	nsw010104	nsw036	3	Yamba

Primary compartment	Secondary compartment	Beach	Sectors	Tide gauge
nsw01	nsw010104	nsw037	3	Yamba
nsw01	nsw010104	nsw038	1	Yamba
nsw01	nsw010104	nsw039	3	Yamba
nsw01	nsw010104	nsw040	3	Yamba
nsw01	nsw010104	nsw041	1	Yamba
nsw01	nsw010104	nsw043	1	Yamba
nsw02	nsw010201	nsw044	3	Yamba
nsw02	nsw010201	nsw045	3	Yamba
nsw02	nsw010201	nsw046	1	Yamba
nsw02	nsw010201	nsw047	1	Yamba
nsw02	nsw010201	nsw048	1	Yamba
nsw02	nsw010201	nsw049	3	Yamba
nsw02	nsw010201	nsw051	3	Yamba
nsw02	nsw010201	nsw052	3	Yamba
nsw02	nsw010201	nsw053	3	Yamba
nsw02	nsw010201	nsw055	3	Yamba
nsw02	nsw010201	nsw056	3	Yamba
nsw02	nsw010201	nsw060	3	Yamba
nsw02	nsw010201	nsw063	3	Yamba
nsw02	nsw010201	nsw064	1	Yamba
nsw02	nsw010201	nsw068	3	Yamba
nsw02	nsw010201	nsw070	1	Yamba
nsw02	nsw010201	nsw073	3	Coffs Harbour
nsw02	nsw010201	nsw074	1	Coffs Harbour
nsw02	nsw010202	nsw077	3	Coffs Harbour
nsw02	nsw010202	nsw078	3	Coffs Harbour
nsw02	nsw010202	nsw079	3	Coffs Harbour
nsw02	nsw010202	nsw081	3	Coffs Harbour
nsw02	nsw010202	nsw082	1	Coffs Harbour
nsw02	nsw010202	nsw083	3	Coffs Harbour
nsw02	nsw010202	nsw086**	1	Coffs Harbour
nsw02	nsw010202	nsw087**	1	Coffs Harbour

Primary compartment	Secondary compartment	Beach	Sectors	Tide gauge
nsw02	nsw010202	nsw089	3	Coffs Harbour
nsw02	nsw010202	nsw090	2	Coffs Harbour
nsw02	nsw010202	nsw091	3	Coffs Harbour
nsw02	nsw010202	nsw092	3	Coffs Harbour
nsw02	nsw010202	nsw093	3	Coffs Harbour
nsw02	nsw010203	nsw094	3	Coffs Harbour
nsw02	nsw010203	nsw095	1	Coffs Harbour
nsw02	nsw010203	nsw097	3	Coffs Harbour
nsw02	nsw010203	nsw098	3	Coffs Harbour
nsw02	nsw010203	nsw099	1	Coffs Harbour
nsw02	nsw010203	nsw100	1	Coffs Harbour
nsw02	nsw010203	nsw101	1	Coffs Harbour
nsw02	nsw010203	nsw103	1	Coffs Harbour
nsw02	nsw010203	nsw104	1	Coffs Harbour
nsw02	nsw010203	nsw105	1	Coffs Harbour
nsw02	nsw010203	nsw107	1	Coffs Harbour
nsw02	nsw010203	nsw109	3	Coffs Harbour
nsw02	nsw010203	nsw110	1	Coffs Harbour
nsw02	nsw010204	nsw113	3	Coffs Harbour
nsw02	nsw010204	nsw114	3	Coffs Harbour
nsw02	nsw010204	nsw115	3	Coffs Harbour
nsw02	nsw010204	nsw116	3	Coffs Harbour
nsw02	nsw010204	nsw117	3	Coffs Harbour
nsw02	nsw010204	nsw118	3	Coffs Harbour
nsw02	nsw010204	nsw119	1	Coffs Harbour
nsw02	nsw010204	nsw120	3	Coffs Harbour
nsw02	nsw010204	nsw123	3	Coffs Harbour
nsw02	nsw010204	nsw124	1	Coffs Harbour
nsw02	nsw010205	nsw129	3	Coffs Harbour
nsw02	nsw010205	nsw130	1	Coffs Harbour
nsw02	nsw010205	nsw132	3	Coffs Harbour
nsw02	nsw010205	nsw133	3	Coffs Harbour

Primary compartment	Secondary compartment	Beach	Sectors	Tide gauge
nsw02	nsw010205	nsw134	3	Coffs Harbour
nsw02	nsw010205	nsw135	3	Port Macquarie
nsw02	nsw010205	nsw137	3	Port Macquarie
nsw03	nsw010301	nsw139	1	Port Macquarie
nsw03	nsw010301	nsw144	5	Port Macquarie
nsw03	nsw010301	nsw150	3	Port Macquarie
nsw03	nsw010301	nsw152	3	Port Macquarie
nsw03	nsw010301	nsw153	3	Port Macquarie
nsw03	nsw010301	nsw154	3	Port Macquarie
nsw03	nsw010301	nsw156	3	Port Macquarie
nsw03	nsw010301	nsw157	1	Port Macquarie
nsw03	nsw010301	nsw159	3	Port Macquarie
nsw03	nsw010301	nsw161	1	Port Macquarie
nsw03	nsw010302	nsw171	1	Port Macquarie
nsw03	nsw010302	nsw172	3	Port Macquarie
nsw03	nsw010302	nsw173	3	Port Macquarie
nsw03	nsw010302	nsw174	3	Port Macquarie
nsw03	nsw010302	nsw178	3	Port Macquarie
nsw03	nsw010302	nsw182	3	Port Macquarie
nsw03	nsw010302	nsw184	5	Port Macquarie
nsw03	nsw010303	nsw185	3	Port Macquarie
nsw03	nsw010303	nsw186	3	Port Macquarie
nsw03	nsw010303	nsw187	3	Port Macquarie
nsw03	nsw010303	nsw188	3	Port Macquarie
nsw03	nsw010303	nsw189	3	Port Macquarie
nsw03	nsw010303	nsw192	3	Port Macquarie
nsw03	nsw010304	nsw194	1	Port Stephens
nsw03	nsw010304	nsw195	3	Port Stephens
nsw03	nsw010304	nsw196	1	Port Stephens
nsw03	nsw010304	nsw197	1	Port Stephens
nsw03	nsw010304	nsw198	3	Port Stephens
nsw04	nsw020101	nsw204	3	Port Stephens
		·		

Primary compartment	Secondary compartment	Beach	Sectors	Tide gauge
nsw04	nsw020101	nsw206	1	Port Stephens
nsw04	nsw020101	nsw208	3	Port Stephens
nsw04	nsw020101	nsw209	3	Port Stephens
nsw04	nsw020101	nsw210	3	Port Stephens
nsw04	nsw020101	nsw216	3	Port Stephens
nsw04	nsw020101	nsw217	1	Port Stephens
nsw04	nsw020102	nsw218	3	Port Stephens
nsw04	nsw020102	nsw219	3	Port Stephens
nsw04	nsw020102	nsw220	3	Port Stephens
nsw04	nsw020102	nsw221	3	Port Stephens
nsw04	nsw020102	nsw222	3	Port Stephens
nsw04	nsw020102	nsw223	5	Port Stephens
nsw04	nsw020103	nswPS01*	1	Port Stephens
nsw04	nsw020103	nswPS15*	1	Port Stephens
nsw04	nsw020104	nsw224	1	Port Stephens
nsw04	nsw020104	nsw226	1	Port Stephens
nsw04	nsw020104	nsw227	1	Port Stephens
nsw04	nsw020104	nsw228	1	Port Stephens
nsw04	nsw020104	nsw230	3	Port Stephens
nsw04	nsw020104	nsw231	3	Port Stephens
nsw04	nsw020104	nsw232	3	Port Stephens
nsw04	nsw020104	nsw234	1	Port Stephens
nsw04	nsw020105	nsw239	6	Port Stephens
nsw05	nsw020201	nsw242	3	Port Stephens
nsw05	nsw020201	nsw245	3	Port Stephens
nsw05	nsw020201	nsw248	3	Port Stephens
nsw05	nsw020201	nsw249	3	Port Stephens
nsw05	nsw020201	nsw250	5	Port Stephens
nsw05	nsw020201	nsw254	3	Port Stephens
nsw05	nsw020201	nsw255****	1	Port Stephens
nsw05	nsw020201	nsw259	3	Port Stephens
nsw05	nsw020201	nsw268	3	Fort Denison

Primary compartment	Secondary compartment	Beach	Sectors	Tide gauge
nsw05	nsw020201	nsw269	3	Fort Denison
nsw05	nsw020202	nsw273	1	Fort Denison
nsw05	nsw020202	nsw274	3	Fort Denison
nsw05	nsw020202	nsw275	3	Fort Denison
nsw05	nsw020202	nsw276	1	Fort Denison
nsw05	nsw020202	nsw278	1	Fort Denison
nsw05	nsw020202	nsw280	3	Fort Denison
nsw05	nsw020202	nsw281	1	Fort Denison
nsw05	nsw020202	nsw282	1	Fort Denison
nsw05	nsw020202	nsw283	3	Fort Denison
nsw05	nsw020202	nsw284	3	Fort Denison
nsw05	nsw020202	nsw285	5	Fort Denison
nsw05	nsw020202	nsw287	3	Fort Denison
nsw05	nsw020202	nsw288	3	Fort Denison
nsw06	nsw020301	nsw292	3	Fort Denison
nsw06	nsw020301	nsw293	1	Fort Denison
nsw06	nsw020301	nsw297*	1	Fort Denison
nsw06	nsw020301	nsw298*	1	Fort Denison
nsw06	nsw020301	nswBB01*	1	Fort Denison
nsw06	nsw020302	nsw300	3	Fort Denison
nsw06	nsw020302	nsw301	1	Fort Denison
nsw06	nsw020302	nsw302	1	Fort Denison
nsw06	nsw020302	nsw303	1	Fort Denison
nsw06	nsw020302	nsw304	3	Fort Denison
nsw06	nsw020302	nsw306	1	Fort Denison
nsw06	nsw020302	nsw307	3	Fort Denison
nsw06	nsw020302	nsw310	3	Fort Denison
nsw06	nsw020302	nsw311	1	Fort Denison
nsw06	nsw020302	nsw314	3	Fort Denison
nsw06	nsw020302	nsw315	3	Fort Denison
nsw06	nsw020302	nsw316	1	Fort Denison
nsw06	nsw020302	nsw317	3	Fort Denison

Primary compartment	Secondary compartment	Beach	Sectors	Tide gauge
nsw06	nsw020304	nsw320	3	Fort Denison
nsw06	nsw020304	nsw322	1	Fort Denison
nsw06	nsw020304	nsw323	1	Fort Denison
nsw06	nsw020304	nsw326	1	Fort Denison
nsw06	nsw020304	nsw327	3	Fort Denison
nsw06	nsw020305	nsw332	1	Fort Denison
nsw06	nsw020305	nsw334	3	Fort Denison
nsw06	nsw020305	nsw335	1	Fort Denison
nsw06	nsw020305	nswPH07*	1	Fort Denison
nsw06	nsw020305	nsw339*	1	Fort Denison
nsw07	nsw020401	nsw341	1	Fort Denison
nsw07	nsw020401	nsw342	1	Fort Denison
nsw07	nsw020401	nsw343	1	Fort Denison
nsw07	nsw020401	nsw344	1	Port Kembla
nsw07	nsw020401	nsw346	1	Port Kembla
nsw07	nsw020401	nsw347	1	Port Kembla
nsw07	nsw020401	nsw352	1	Port Kembla
nsw07	nsw020401	nsw358	1	Port Kembla
nsw07	nsw020401	nsw359	1	Port Kembla
nsw07	nsw020401	nsw362	1	Port Kembla
nsw07	nsw020401	nsw363	1	Port Kembla
nsw07	nsw020401	nsw364	1	Port Kembla
nsw07	nsw020401	nsw365	3	Port Kembla
nsw07	nsw020401	nsw366	3	Port Kembla
nsw07	nsw020401	nsw367	3	Port Kembla
nsw07	nsw020402	nsw368	1	Port Kembla
nsw07	nsw020402	nsw369	3	Port Kembla
nsw07	nsw020402	nsw370	3	Port Kembla
nsw07	nsw020402	nsw371	1	Port Kembla
nsw07	nsw020402	nsw373	3	Port Kembla
nsw07	nsw020403	nsw379	3	Port Kembla
nsw07	nsw020403	nsw380	3	Port Kembla

Primary compartment	Secondary compartment	Beach	Sectors	Tide gauge
nsw07	nsw020403	nsw381	3	Port Kembla
nsw07	nsw020403	nsw383	2	Port Kembla
nsw07	nsw020404	nsw388	1	Port Kembla
nsw07	nsw020404	nsw389	3	Port Kembla
nsw07	nsw020404	nsw390	3	Port Kembla
nsw07	nsw020404	nsw392	3	Port Kembla
nsw07	nsw020404	nsw394	1	Port Kembla
nsw07	nsw020404	nsw395	1	Port Kembla
nsw07	nsw020404	nsw396	1	Port Kembla
nsw07	nsw020404	nsw397	3	Port Kembla
nsw07	nsw020404	nsw399	1	Port Kembla
nsw07	nsw020405	nsw400	3	Jervis Bay
nsw07	nsw020405	nsw401	3	Jervis Bay
nsw07	nsw020405	nsw402	3	Jervis Bay
nsw07	nsw020405	nsw403	3	Jervis Bay
nsw07	nsw020405	nsw404	3	Jervis Bay
nsw07	nsw020405	nsw405	3	Jervis Bay
nsw08	nsw020502	nsw420*	1	Jervis Bay
nsw08	nsw020502	nsw421*	1	Jervis Bay
nsw08	nsw020502	nsw422*	1	Jervis Bay
nsw08	nsw020502	nsw425*	1	Jervis Bay
nsw08	nsw020502	nsw431*	1	Jervis Bay
nsw08	nsw020502	nsw433*	1	Jervis Bay
nsw08	nsw020502	nsw434*	1	Jervis Bay
nsw08	nsw020503	nsw439	1	Jervis Bay
nsw08	nsw020504	nsw446	1	Jervis Bay
nsw08	nsw020504	nsw447	1	Jervis Bay
nsw08	nsw020504	nsw448	1	Jervis Bay
nsw08	nsw020504	nsw449	3	Jervis Bay
nsw08	nsw020504	nsw451	3	Jervis Bay
nsw08	nsw020504	nsw454	3	Jervis Bay
nsw08	nsw020504	nsw459	3	Jervis Bay

nsw08         nsw020505         nsw462         3         Jervis Bay           nsw08         nsw020505         nsw463         3         Jervis Bay           nsw08         nsw020505         nsw465         3         Jervis Bay           nsw08         nsw020505         nsw466         3         Jervis Bay           nsw08         nsw020505         nsw468         3         Jervis Bay           nsw08         nsw020506         nsw476         3         Jervis Bay           nsw08         nsw020506         nsw477         3         Jervis Bay           nsw08         nsw020506         nsw478         3         Jervis Bay           nsw08         nsw020506         nsw479         3         Jervis Bay           nsw08         nsw020506         nsw482***         3         Jervis Bay           nsw08         nsw020506         nsw482***         3         Jervis Bay           nsw08         nsw020506         nsw485         1         Jervis Bay           nsw08         nsw020506         nsw487         1         Jervis Bay           nsw08         nsw020506         nsw488         1         Jervis Bay           nsw08         nsw020506         nsw491<	Primary compartment	Secondary compartment	Beach	Sectors	Tide gauge
nsw08         nsw020505         nsw465         3         Jervis Bay           nsw08         nsw020505         nsw466         3         Jervis Bay           nsw08         nsw020505         nsw467         3         Jervis Bay           nsw08         nsw020506         nsw476         3         Jervis Bay           nsw08         nsw020506         nsw477         3         Jervis Bay           nsw08         nsw020506         nsw477         3         Jervis Bay           nsw08         nsw020506         nsw477         3         Jervis Bay           nsw08         nsw020506         nsw479         3         Jervis Bay           nsw08         nsw020506         nsw482***         3         Jervis Bay           nsw08         nsw020506         nsw483         1         Jervis Bay           nsw08         nsw020506         nsw485         1         Jervis Bay           nsw08         nsw020506         nsw488         1         Jervis Bay           nsw08         nsw020506         nsw489         3         Jervis Bay           nsw08         nsw020506         nsw491         1         Jervis Bay           nsw08         nsw020506         nsw492 <td>nsw08</td> <td>nsw020505</td> <td>nsw462</td> <td>3</td> <td>Jervis Bay</td>	nsw08	nsw020505	nsw462	3	Jervis Bay
nsw08         nsw020505         nsw466         3         Jervis Bay           nsw08         nsw020505         nsw467         3         Jervis Bay           nsw08         nsw020506         nsw476         3         Jervis Bay           nsw08         nsw020506         nsw477         3         Jervis Bay           nsw08         nsw020506         nsw478         3         Jervis Bay           nsw08         nsw020506         nsw479         3         Jervis Bay           nsw08         nsw020506         nsw482***         3         Jervis Bay           nsw08         nsw020506         nsw483         1         Jervis Bay           nsw08         nsw020506         nsw485         1         Jervis Bay           nsw08         nsw020506         nsw487         1         Jervis Bay           nsw08         nsw020506         nsw488         1         Jervis Bay           nsw08         nsw020506         nsw489         3         Jervis Bay           nsw08         nsw020506         nsw491         1         Jervis Bay           nsw08         nsw020506         nsw492         3         Jervis Bay           nsw08         nsw020506         nsw493 <td>nsw08</td> <td>nsw020505</td> <td>nsw463</td> <td>3</td> <td>Jervis Bay</td>	nsw08	nsw020505	nsw463	3	Jervis Bay
nsw08         nsw020505         nsw467         3         Jervis Bay           nsw08         nsw020506         nsw468         3         Jervis Bay           nsw08         nsw020506         nsw476         3         Jervis Bay           nsw08         nsw020506         nsw477         3         Jervis Bay           nsw08         nsw020506         nsw478         3         Jervis Bay           nsw08         nsw020506         nsw482***         3         Jervis Bay           nsw08         nsw020506         nsw483         1         Jervis Bay           nsw08         nsw020506         nsw485         1         Jervis Bay           nsw08         nsw020506         nsw487         1         Jervis Bay           nsw08         nsw020506         nsw488         1         Jervis Bay           nsw08         nsw020506         nsw489         3         Jervis Bay           nsw08         nsw020506         nsw490         1         Jervis Bay           nsw08         nsw020506         nsw491         1         Jervis Bay           nsw08         nsw020506         nsw493         1         Jervis Bay           nsw08         nsw020506         nsw494 <td>nsw08</td> <td>nsw020505</td> <td>nsw465</td> <td>3</td> <td>Jervis Bay</td>	nsw08	nsw020505	nsw465	3	Jervis Bay
nsw08         nsw020505         nsw468         3         Jervis Bay           nsw08         nsw020506         nsw476         3         Jervis Bay           nsw08         nsw020506         nsw477         3         Jervis Bay           nsw08         nsw020506         nsw478         3         Jervis Bay           nsw08         nsw020506         nsw479         3         Jervis Bay           nsw08         nsw020506         nsw482***         3         Jervis Bay           nsw08         nsw020506         nsw485         1         Jervis Bay           nsw08         nsw020506         nsw487         1         Jervis Bay           nsw08         nsw020506         nsw488         1         Jervis Bay           nsw08         nsw020506         nsw489         3         Jervis Bay           nsw08         nsw020506         nsw490         1         Jervis Bay           nsw08         nsw020506         nsw491         1         Jervis Bay           nsw08         nsw020506         nsw492         3         Jervis Bay           nsw08         nsw020506         nsw493         1         Jervis Bay           nsw08         nsw020506         nsw495 <td>nsw08</td> <td>nsw020505</td> <td>nsw466</td> <td>3</td> <td>Jervis Bay</td>	nsw08	nsw020505	nsw466	3	Jervis Bay
nsw08         nsw020506         nsw476         3         Jervis Bay           nsw08         nsw020506         nsw477         3         Jervis Bay           nsw08         nsw020506         nsw478         3         Jervis Bay           nsw08         nsw020506         nsw482***         3         Jervis Bay           nsw08         nsw020506         nsw483         1         Jervis Bay           nsw08         nsw020506         nsw485         1         Jervis Bay           nsw08         nsw020506         nsw487         1         Jervis Bay           nsw08         nsw020506         nsw488         1         Jervis Bay           nsw08         nsw020506         nsw489         3         Jervis Bay           nsw08         nsw020506         nsw490         1         Jervis Bay           nsw08         nsw020506         nsw491         1         Jervis Bay           nsw08         nsw020506         nsw492         3         Jervis Bay           nsw08         nsw020506         nsw491         1         Jervis Bay           nsw08         nsw020506         nsw491         1         Jervis Bay           nsw08         nsw020506         nsw495 <td>nsw08</td> <td>nsw020505</td> <td>nsw467</td> <td>3</td> <td>Jervis Bay</td>	nsw08	nsw020505	nsw467	3	Jervis Bay
nsw08         nsw020506         nsw477         3         Jervis Bay           nsw08         nsw020506         nsw478         3         Jervis Bay           nsw08         nsw020506         nsw479         3         Jervis Bay           nsw08         nsw020506         nsw482***         3         Jervis Bay           nsw08         nsw020506         nsw483         1         Jervis Bay           nsw08         nsw020506         nsw487         1         Jervis Bay           nsw08         nsw020506         nsw488         1         Jervis Bay           nsw08         nsw020506         nsw489         3         Jervis Bay           nsw08         nsw020506         nsw490         1         Jervis Bay           nsw08         nsw020506         nsw491         1         Jervis Bay           nsw08         nsw020506         nsw492         3         Jervis Bay           nsw08         nsw020506         nsw493         1         Jervis Bay           nsw08         nsw020506         nsw494         1         Jervis Bay           nsw08         nsw020506         nsw497         1         Jervis Bay           nsw08         nsw020506         nsw508 <td>nsw08</td> <td>nsw020505</td> <td>nsw468</td> <td>3</td> <td>Jervis Bay</td>	nsw08	nsw020505	nsw468	3	Jervis Bay
nsw08         nsw020506         nsw478         3         Jervis Bay           nsw08         nsw020506         nsw479         3         Jervis Bay           nsw08         nsw020506         nsw482***         3         Jervis Bay           nsw08         nsw020506         nsw483         1         Jervis Bay           nsw08         nsw020506         nsw485         1         Jervis Bay           nsw08         nsw020506         nsw487         1         Jervis Bay           nsw08         nsw020506         nsw489         3         Jervis Bay           nsw08         nsw020506         nsw489         3         Jervis Bay           nsw08         nsw020506         nsw491         1         Jervis Bay           nsw08         nsw020506         nsw492         3         Jervis Bay           nsw08         nsw020506         nsw493         1         Jervis Bay           nsw08         nsw020506         nsw494         1         Jervis Bay           nsw08         nsw020506         nsw495         1         Jervis Bay           nsw08         nsw020506         nsw498         1         Jervis Bay           nsw08         nsw020506         nsw508 <td>nsw08</td> <td>nsw020506</td> <td>nsw476</td> <td>3</td> <td>Jervis Bay</td>	nsw08	nsw020506	nsw476	3	Jervis Bay
nsw08         nsw020506         nsw479         3         Jervis Bay           nsw08         nsw020506         nsw482***         3         Jervis Bay           nsw08         nsw020506         nsw483         1         Jervis Bay           nsw08         nsw020506         nsw485         1         Jervis Bay           nsw08         nsw020506         nsw487         1         Jervis Bay           nsw08         nsw020506         nsw489         3         Jervis Bay           nsw08         nsw020506         nsw490         1         Jervis Bay           nsw08         nsw020506         nsw491         1         Jervis Bay           nsw08         nsw020506         nsw492         3         Jervis Bay           nsw08         nsw020506         nsw493         1         Jervis Bay           nsw08         nsw020506         nsw494         1         Jervis Bay           nsw08         nsw020506         nsw495         1         Jervis Bay           nsw08         nsw020506         nsw497         1         Jervis Bay           nsw08         nsw020506         nsw508         1         Jervis Bay           nsw08         nsw020506         nsw512 <td>nsw08</td> <td>nsw020506</td> <td>nsw477</td> <td>3</td> <td>Jervis Bay</td>	nsw08	nsw020506	nsw477	3	Jervis Bay
nsw08         nsw020506         nsw482***         3         Jervis Bay           nsw08         nsw020506         nsw483         1         Jervis Bay           nsw08         nsw020506         nsw485         1         Jervis Bay           nsw08         nsw020506         nsw487         1         Jervis Bay           nsw08         nsw020506         nsw488         1         Jervis Bay           nsw08         nsw020506         nsw489         3         Jervis Bay           nsw08         nsw020506         nsw490         1         Jervis Bay           nsw08         nsw020506         nsw491         1         Jervis Bay           nsw08         nsw020506         nsw492         3         Jervis Bay           nsw08         nsw020506         nsw493         1         Jervis Bay           nsw08         nsw020506         nsw494         1         Jervis Bay           nsw08         nsw020506         nsw495         1         Jervis Bay           nsw08         nsw020506         nsw497         1         Jervis Bay           nsw08         nsw020506         nsw508         1         Jervis Bay           nsw08         nsw020506         nsw512 <td>nsw08</td> <td>nsw020506</td> <td>nsw478</td> <td>3</td> <td>Jervis Bay</td>	nsw08	nsw020506	nsw478	3	Jervis Bay
nsw08         nsw020506         nsw483         1         Jervis Bay           nsw08         nsw020506         nsw485         1         Jervis Bay           nsw08         nsw020506         nsw487         1         Jervis Bay           nsw08         nsw020506         nsw488         1         Jervis Bay           nsw08         nsw020506         nsw489         3         Jervis Bay           nsw08         nsw020506         nsw491         1         Jervis Bay           nsw08         nsw020506         nsw492         3         Jervis Bay           nsw08         nsw020506         nsw493         1         Jervis Bay           nsw08         nsw020506         nsw494         1         Jervis Bay           nsw08         nsw020506         nsw495         1         Jervis Bay           nsw08         nsw020506         nsw497         1         Jervis Bay           nsw08         nsw020506         nsw508         1         Jervis Bay           nsw08         nsw020506         nsw508         1         Jervis Bay           nsw08         nsw020506         nsw512         3         Jervis Bay           nsw08         nsw020506         nsw513	nsw08	nsw020506	nsw479	3	Jervis Bay
nsw08         nsw020506         nsw485         1         Jervis Bay           nsw08         nsw020506         nsw487         1         Jervis Bay           nsw08         nsw020506         nsw488         1         Jervis Bay           nsw08         nsw020506         nsw489         3         Jervis Bay           nsw08         nsw020506         nsw490         1         Jervis Bay           nsw08         nsw020506         nsw491         1         Jervis Bay           nsw08         nsw020506         nsw492         3         Jervis Bay           nsw08         nsw020506         nsw493         1         Jervis Bay           nsw08         nsw020506         nsw494         1         Jervis Bay           nsw08         nsw020506         nsw495         1         Jervis Bay           nsw08         nsw020506         nsw497         1         Jervis Bay           nsw08         nsw020506         nsw508         1         Jervis Bay           nsw08         nsw020506         nsw508         1         Jervis Bay           nsw08         nsw020506         nsw512         3         Jervis Bay           nsw08         nsw020506         nsw513	nsw08	nsw020506	nsw482***	3	Jervis Bay
nsw08         nsw020506         nsw487         1         Jervis Bay           nsw08         nsw020506         nsw488         1         Jervis Bay           nsw08         nsw020506         nsw489         3         Jervis Bay           nsw08         nsw020506         nsw490         1         Jervis Bay           nsw08         nsw020506         nsw491         1         Jervis Bay           nsw08         nsw020506         nsw492         3         Jervis Bay           nsw08         nsw020506         nsw493         1         Jervis Bay           nsw08         nsw020506         nsw494         1         Jervis Bay           nsw08         nsw020506         nsw495         1         Jervis Bay           nsw08         nsw020506         nsw497         1         Jervis Bay           nsw08         nsw020506         nsw508         1         Jervis Bay           nsw08         nsw020506         nsw509         1         Jervis Bay           nsw08         nsw020506         nsw512         3         Jervis Bay           nsw08         nsw020506         nsw513         1         Jervis Bay           nsw08         nsw020506         nsw514	nsw08	nsw020506	nsw483	1	Jervis Bay
nsw08         nsw020506         nsw488         1         Jervis Bay           nsw08         nsw020506         nsw489         3         Jervis Bay           nsw08         nsw020506         nsw490         1         Jervis Bay           nsw08         nsw020506         nsw491         1         Jervis Bay           nsw08         nsw020506         nsw492         3         Jervis Bay           nsw08         nsw020506         nsw493         1         Jervis Bay           nsw08         nsw020506         nsw494         1         Jervis Bay           nsw08         nsw020506         nsw495         1         Jervis Bay           nsw08         nsw020506         nsw497         1         Jervis Bay           nsw08         nsw020506         nsw508         1         Jervis Bay           nsw08         nsw020506         nsw509         1         Jervis Bay           nsw08         nsw020506         nsw512         3         Jervis Bay           nsw08         nsw020506         nsw513         1         Jervis Bay           nsw08         nsw020506         nsw514         1         Jervis Bay           nsw09         nsw020601         nsw520	nsw08	nsw020506	nsw485	1	Jervis Bay
nsw08         nsw020506         nsw489         3         Jervis Bay           nsw08         nsw020506         nsw490         1         Jervis Bay           nsw08         nsw020506         nsw491         1         Jervis Bay           nsw08         nsw020506         nsw492         3         Jervis Bay           nsw08         nsw020506         nsw493         1         Jervis Bay           nsw08         nsw020506         nsw494         1         Jervis Bay           nsw08         nsw020506         nsw495         1         Jervis Bay           nsw08         nsw020506         nsw498         1         Jervis Bay           nsw08         nsw020506         nsw508         1         Jervis Bay           nsw08         nsw020506         nsw509         1         Jervis Bay           nsw08         nsw020506         nsw512         3         Jervis Bay           nsw08         nsw020506         nsw513         1         Jervis Bay           nsw08         nsw020506         nsw514         1         Jervis Bay           nsw09         nsw020601         nsw517         1         Jervis Bay           nsw09         nsw020601         nsw520	nsw08	nsw020506	nsw487	1	Jervis Bay
nsw08         nsw020506         nsw490         1         Jervis Bay           nsw08         nsw020506         nsw491         1         Jervis Bay           nsw08         nsw020506         nsw492         3         Jervis Bay           nsw08         nsw020506         nsw493         1         Jervis Bay           nsw08         nsw020506         nsw494         1         Jervis Bay           nsw08         nsw020506         nsw495         1         Jervis Bay           nsw08         nsw020506         nsw497         1         Jervis Bay           nsw08         nsw020506         nsw508         1         Jervis Bay           nsw08         nsw020506         nsw509         1         Jervis Bay           nsw08         nsw020506         nsw512         3         Jervis Bay           nsw08         nsw020506         nsw512         3         Jervis Bay           nsw08         nsw020506         nsw513         1         Jervis Bay           nsw08         nsw020506         nsw514         1         Jervis Bay           nsw09         nsw020601         nsw517         1         Jervis Bay           nsw09         nsw020601         nsw520	nsw08	nsw020506	nsw488	1	Jervis Bay
nsw08         nsw020506         nsw491         1         Jervis Bay           nsw08         nsw020506         nsw492         3         Jervis Bay           nsw08         nsw020506         nsw493         1         Jervis Bay           nsw08         nsw020506         nsw494         1         Jervis Bay           nsw08         nsw020506         nsw495         1         Jervis Bay           nsw08         nsw020506         nsw497         1         Jervis Bay           nsw08         nsw020506         nsw508         1         Jervis Bay           nsw08         nsw020506         nsw508         1         Jervis Bay           nsw08         nsw020506         nsw512         3         Jervis Bay           nsw08         nsw020506         nsw513         1         Jervis Bay           nsw08         nsw020506         nsw514         1         Jervis Bay           nsw09         nsw020601         nsw517         1         Jervis Bay           nsw09         nsw020601         nsw520         1         Jervis Bay	nsw08	nsw020506	nsw489	3	Jervis Bay
nsw08         nsw020506         nsw492         3         Jervis Bay           nsw08         nsw020506         nsw493         1         Jervis Bay           nsw08         nsw020506         nsw494         1         Jervis Bay           nsw08         nsw020506         nsw495         1         Jervis Bay           nsw08         nsw020506         nsw497         1         Jervis Bay           nsw08         nsw020506         nsw508         1         Jervis Bay           nsw08         nsw020506         nsw509         1         Jervis Bay           nsw08         nsw020506         nsw512         3         Jervis Bay           nsw08         nsw020506         nsw513         1         Jervis Bay           nsw08         nsw020506         nsw514         1         Jervis Bay           nsw09         nsw020601         nsw517         1         Jervis Bay           nsw09         nsw020601         nsw520         1         Jervis Bay	nsw08	nsw020506	nsw490	1	Jervis Bay
nsw08         nsw020506         nsw493         1         Jervis Bay           nsw08         nsw020506         nsw494         1         Jervis Bay           nsw08         nsw020506         nsw495         1         Jervis Bay           nsw08         nsw020506         nsw497         1         Jervis Bay           nsw08         nsw020506         nsw498         1         Jervis Bay           nsw08         nsw020506         nsw508         1         Jervis Bay           nsw08         nsw020506         nsw512         3         Jervis Bay           nsw08         nsw020506         nsw512         3         Jervis Bay           nsw08         nsw020506         nsw513         1         Jervis Bay           nsw08         nsw020506         nsw514         1         Jervis Bay           nsw09         nsw020601         nsw517         1         Jervis Bay           nsw09         nsw020601         nsw520         1         Jervis Bay	nsw08	nsw020506	nsw491	1	Jervis Bay
nsw08         nsw020506         nsw494         1         Jervis Bay           nsw08         nsw020506         nsw495         1         Jervis Bay           nsw08         nsw020506         nsw497         1         Jervis Bay           nsw08         nsw020506         nsw498         1         Jervis Bay           nsw08         nsw020506         nsw508         1         Jervis Bay           nsw08         nsw020506         nsw512         3         Jervis Bay           nsw08         nsw020506         nsw513         1         Jervis Bay           nsw08         nsw020506         nsw514         1         Jervis Bay           nsw09         nsw020601         nsw517         1         Jervis Bay           nsw09         nsw020601         nsw520         1         Jervis Bay	nsw08	nsw020506	nsw492	3	Jervis Bay
nsw08         nsw020506         nsw495         1         Jervis Bay           nsw08         nsw020506         nsw497         1         Jervis Bay           nsw08         nsw020506         nsw498         1         Jervis Bay           nsw08         nsw020506         nsw508         1         Jervis Bay           nsw08         nsw020506         nsw512         3         Jervis Bay           nsw08         nsw020506         nsw512         3         Jervis Bay           nsw08         nsw020506         nsw513         1         Jervis Bay           nsw08         nsw020506         nsw514         1         Jervis Bay           nsw09         nsw020601         nsw517         1         Jervis Bay           nsw09         nsw020601         nsw520         1         Jervis Bay	nsw08	nsw020506	nsw493	1	Jervis Bay
nsw08         nsw020506         nsw497         1         Jervis Bay           nsw08         nsw020506         nsw498         1         Jervis Bay           nsw08         nsw020506         nsw508         1         Jervis Bay           nsw08         nsw020506         nsw509         1         Jervis Bay           nsw08         nsw020506         nsw512         3         Jervis Bay           nsw08         nsw020506         nsw513         1         Jervis Bay           nsw08         nsw020506         nsw514         1         Jervis Bay           nsw09         nsw020601         nsw517         1         Jervis Bay           nsw09         nsw020601         nsw520         1         Jervis Bay	nsw08	nsw020506	nsw494	1	Jervis Bay
nsw08         nsw020506         nsw498         1         Jervis Bay           nsw08         nsw020506         nsw508         1         Jervis Bay           nsw08         nsw020506         nsw509         1         Jervis Bay           nsw08         nsw020506         nsw512         3         Jervis Bay           nsw08         nsw020506         nsw513         1         Jervis Bay           nsw08         nsw020506         nsw514         1         Jervis Bay           nsw09         nsw020601         nsw517         1         Jervis Bay           nsw09         nsw020601         nsw520         1         Jervis Bay	nsw08	nsw020506	nsw495	1	Jervis Bay
nsw08         nsw020506         nsw508         1         Jervis Bay           nsw08         nsw020506         nsw509         1         Jervis Bay           nsw08         nsw020506         nsw512         3         Jervis Bay           nsw08         nsw020506         nsw513         1         Jervis Bay           nsw08         nsw020506         nsw514         1         Jervis Bay           nsw09         nsw020601         nsw517         1         Jervis Bay           nsw09         nsw020601         nsw520         1         Jervis Bay	nsw08	nsw020506	nsw497	1	Jervis Bay
nsw08         nsw020506         nsw509         1         Jervis Bay           nsw08         nsw020506         nsw512         3         Jervis Bay           nsw08         nsw020506         nsw513         1         Jervis Bay           nsw08         nsw020506         nsw514         1         Jervis Bay           nsw09         nsw020601         nsw517         1         Jervis Bay           nsw09         nsw020601         nsw520         1         Jervis Bay	nsw08	nsw020506	nsw498	1	Jervis Bay
nsw08         nsw020506         nsw512         3         Jervis Bay           nsw08         nsw020506         nsw513         1         Jervis Bay           nsw08         nsw020506         nsw514         1         Jervis Bay           nsw09         nsw020601         nsw517         1         Jervis Bay           nsw09         nsw020601         nsw520         1         Jervis Bay	nsw08	nsw020506	nsw508	1	Jervis Bay
nsw08         nsw020506         nsw513         1         Jervis Bay           nsw08         nsw020506         nsw514         1         Jervis Bay           nsw09         nsw020601         nsw517         1         Jervis Bay           nsw09         nsw020601         nsw520         1         Jervis Bay	nsw08	nsw020506	nsw509	1	Jervis Bay
nsw08         nsw020506         nsw514         1         Jervis Bay           nsw09         nsw020601         nsw517         1         Jervis Bay           nsw09         nsw020601         nsw520         1         Jervis Bay	nsw08	nsw020506	nsw512	3	Jervis Bay
nsw09         nsw020601         nsw517         1         Jervis Bay           nsw09         nsw020601         nsw520         1         Jervis Bay	nsw08	nsw020506	nsw513	1	Jervis Bay
nsw09 nsw020601 nsw520 1 Jervis Bay	nsw08	nsw020506	nsw514	1	Jervis Bay
·	nsw09	nsw020601	nsw517	1	Jervis Bay
nsw09 nsw020601 nsw522 1 Jervis Bay	nsw09	nsw020601	nsw520	1	Jervis Bay
	nsw09	nsw020601	nsw522	1	Jervis Bay

Primary compartment	Secondary compartment	Beach	Sectors	Tide gauge
nsw09	nsw020602	nsw524*	1	Jervis Bay
nsw09	nsw020602	nsw526*	1	Jervis Bay
nsw09	nsw020602	nsw529*	1	Jervis Bay
nsw09	nsw020602	nsw530*	1	Jervis Bay
nsw09	nsw020602	nsw531*	1	Jervis Bay
nsw09	nsw020602	nsw532*	1	Jervis Bay
nsw09	nsw020602	nsw533*	1	Jervis Bay
nsw09	nsw020602	nsw534*	1	Jervis Bay
nsw09	nsw020602	nsw535*	1	Jervis Bay
nsw09	nsw020602	nsw537*	1	Jervis Bay
nsw09	nsw020602	nsw538*	1	Jervis Bay
nsw09	nsw020603	nsw543	1	Jervis Bay
nsw09	nsw020603	nsw545	1	Jervis Bay
nsw09	nsw020603	nsw547	1	Jervis Bay
nsw09	nsw020603	nsw552	1	Jervis Bay
nsw09	nsw020603	nsw557	3	Jervis Bay
nsw09	nsw020603	nsw558	1	Jervis Bay
nsw09	nsw020603	nsw559	1	Jervis Bay
nsw09	nsw020603	nsw560	3	Jervis Bay
nsw09	nsw020603	nsw562	3	Jervis Bay
nsw09	nsw020603	nsw566	3	Jervis Bay
nsw09	nsw020603	nsw567	3	Jervis Bay
nsw09	nsw020603	nsw568	1	Jervis Bay
nsw09	nsw020603	nsw571	1	Jervis Bay
nsw09	nsw020603	nsw577	3	Jervis Bay
nsw09	nsw020604	nsw579	3	Jervis Bay
nsw09	nsw020604	nsw581	1	Eden
nsw09	nsw020604	nsw582	1	Eden
nsw09	nsw020604	nsw583	1	Eden
nsw09	nsw020604	nsw585	3	Eden
nsw09	nsw020604	nsw586	1	Eden
nsw09	nsw020604	nsw588	1	Eden

Primary compartment	Secondary compartment	Beach	Sectors	Tide gauge
nsw09	nsw020604	nsw589	1	Eden
nsw09	nsw020604	nsw590	3	Eden
nsw09	nsw020604	nsw592	1	Eden
nsw09	nsw020604	nsw593	1	Eden
nsw09	nsw020604	nsw594	1	Eden
nsw09	nsw020604	nsw596	1	Eden
nsw09	nsw020604	nsw597	1	Eden
nsw09	nsw020604	nsw599	1	Eden
nsw09	nsw020604	nsw603	1	Eden
nsw09	nsw020604	nsw604	1	Eden
nsw09	nsw020604	nsw606	1	Eden
nsw09	nsw020604	nsw607	1	Eden
nsw09	nsw020604	nsw608	2	Eden
nsw09	nsw020604	nsw609	3	Eden
nsw09	nsw020605	nsw616	1	Eden
nsw09	nsw020605	nsw618	3	Eden
nsw09	nsw020605	nsw619	3	Eden
nsw09	nsw020605	nsw621	3	Eden
nsw09	nsw020605	nsw622	1	Eden
nsw09	nsw020605	nsw624	1	Eden
nsw09	nsw020605	nsw625	1	Eden
nsw09	nsw020605	nsw627	1	Eden
nsw09	nsw020605	nsw632	3	Eden
nsw09	nsw020605	nsw633	1	Eden
nsw09	nsw020605	nsw635	1	Eden
nsw09	nsw020605	nsw636	1	Eden
nsw09	nsw020605	nsw637	3	Eden
nsw09	nsw020606	nsw641	1	Eden
nsw09	nsw020606	nsw646	1	Eden
nsw09	nsw020606	nsw647	1	Eden
nsw09	nsw020606	nsw650**	1	Eden
nsw09	nsw020606	nsw651	1	Eden

Primary compartment	Secondary compartment	Beach	Sectors	Tide gauge
nsw09	nsw020606	nsw652	1	Eden
nsw09	nsw020606	nsw655	1	Eden
nsw09	nsw020606	nsw656	1	Eden
nsw09	nsw020606	nsw659	3	Eden
nsw09	nsw020607	nsw664	3	Eden
nsw09	nsw020607	nsw668	3	Eden
nsw09	nsw020607	nsw671	3	Eden
nsw09	nsw020607	nsw676	3	Eden
nsw09	nsw020608	nsw680	3	Eden
nsw09	nsw020608	nsw684*	1	Eden
nsw09	nsw020608	nsw685*	1	Eden
nsw09	nsw020608	nsw688*	1	Eden
nsw09	nsw020608	nsw689*	1	Eden
nsw09	nsw020608	nsw692*	1	Eden
nsw09	nsw020608	nsw695*	1	Eden
nsw09	nsw020608	nsw699*	1	Eden
nsw09	nsw020609	nsw708	1	Eden
nsw09	nsw020610	nsw710	3	Eden
nsw09	nsw020610	nsw711	3	Eden
nsw09	nsw020611	nsw715	3	Eden
nsw09	nsw020611	nsw716	3	Eden
nsw09	nsw020611	nsw718	1	Eden
nsw09	nsw020611	nsw720	1	Eden
nsw09	nsw020611	nsw721	1	Eden

<sup>\*</sup> Bay/estuary beach.

<sup>\*\*</sup> No sediment dune profile.

<sup>\*\*\*</sup> No sediment dune profile for nsw482c.

<sup>\*\*\*\*</sup> Modelled with nsw254c.

# Appendix D: Runup formula selection

Extreme total water level observations from 4 separate storm events, in October 2014, April 2015, June 2016 and July 2020, at 40 alongshore-variable embayed beaches were inferred from swash lens deposits (strandline of marine debris) and used to benchmark several runup models (<u>Figure 93</u>). The offshore significant wave height ( $H_s$ ) peaked between 6 m and 8 m.

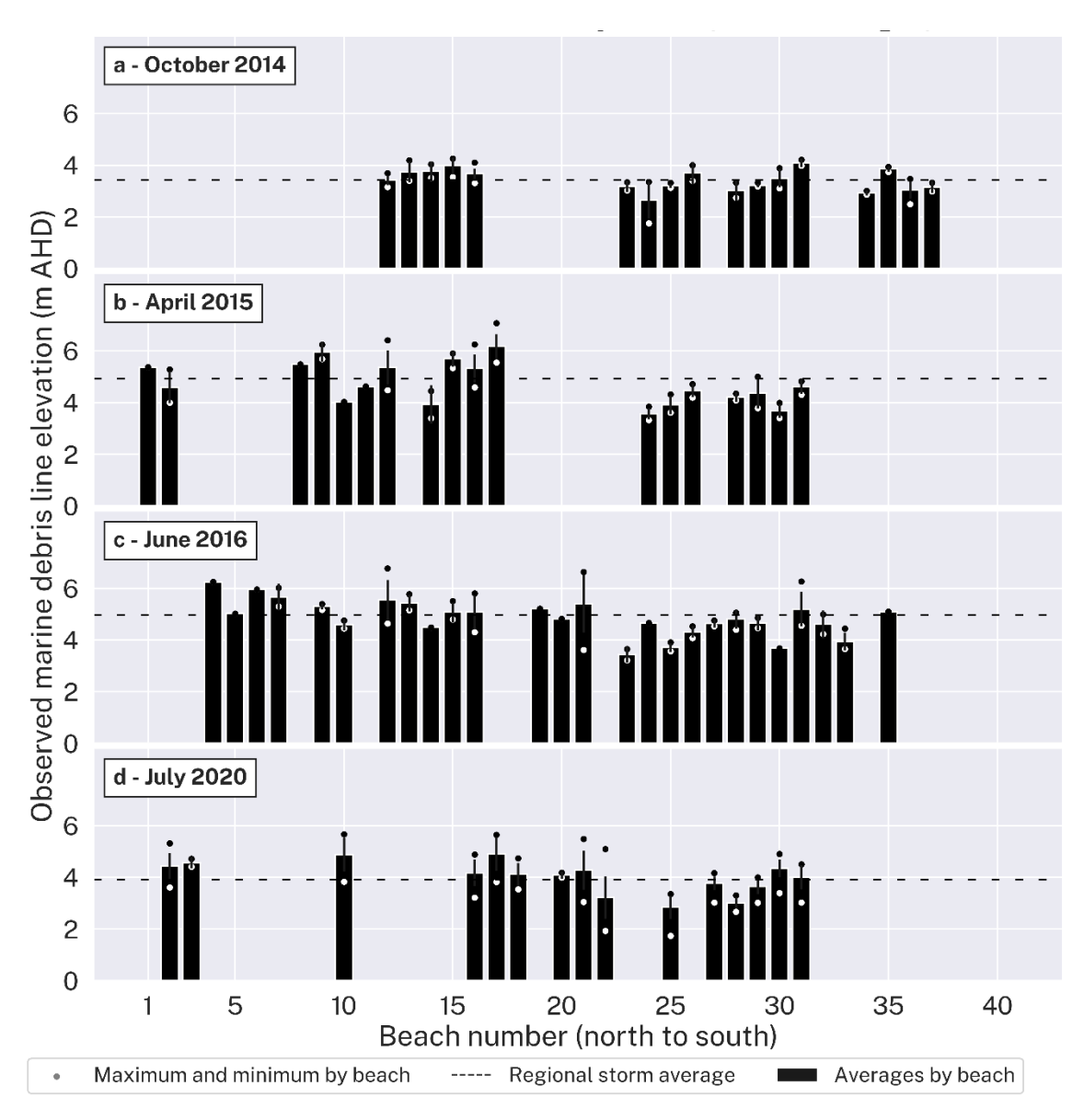


Figure 93 Regional observations of total water levels (TWLs) from marine debris lines after 4 storm events along 40 individual beaches

Key: Horizontal dashed lines show the regional average. Bars show the intra-beach average and standard deviation (black lines). Coloured and white dots indicate the maximum and minimum measurement by beach.

Extreme TWLs were modelled using the expression:

$$TWL = SWL + R$$

where *SWL* is still water level and *R* is wave runup.

Still water levels (SWL) were obtained directly from nearby tide gauges and wave runup ( $R_{2\%}$ ) levels were estimated from several empirical parametrisations. Based on previous investigations, 7 models were selected for this purpose. These included 2 formulas (Hedges and Mase 2004; Nielsen and Hanslow 1991) that are commonly used in coastal hazards studies in NSW and 3 models that previously performed similarly well during small to moderate wave conditions in this region (Atkinson et al. 2017; Holman 1986; Vousdoukas et al. 2012). The remaining 2 models include the widely used formula by Stockdon et al. (2006) and a recent machine learning model that included storm data within its development (Power et al. 2019).

Three specifications of average beach slopes were tested, including:

- beach slopes from LiDAR, calculated between the mean sea level and berm height (0 to 2 m AHD)
- 2. beach slopes from LiDAR, calculated between the mean sea level and the mean high-water springs at this region (0 to 0.7 m AHD)
- 3. satellite-derived beach slopes from the CoastSat dataset (Vos et al. 2020).

The accuracy of 7 empirical runup models and 3 specifications of beach slope are summarised in Figure 94. Model performance (coefficient of determination  $R_2$ , root mean square error (RMSE) and bias) is calculated for the entire dataset. Horizontal axes indicate different runup models according to their year of publication. Results show higher  $R_2$  for beach slopes calculated between the mean sea level and berm, for all formulas, but similar in terms of RMSE and bias across different formulations. The RMSE varies from around 0.5 m (e.g. Atkinson et al. 2017) to up to 2 m (Hedges and Mase 2004). Additionally, some formulas overestimate the TWL magnitude (e.g. Hedges and Mase 2004; Power et al. 2019), while others result in a negligible bias (e.g. Atkinson et al. 2017). Overall, the model that resulted in better combined statistics ( $R_2 \sim 0.6$ , RMSE  $\sim 0.8$  m, bias  $\sim 0.1$ ) was the formula proposed by Atkinson et al. (2017) for beach slopes from LiDAR (MSL/berm):

$$R_{2\%} = 0.92 \tan(\beta) \sqrt{H_o L_o} + 0.16 H_o$$

Fortuitously, this model was developed with data from 11 beaches in southeast Australia and consisted of a 'model-of-models' that fitted a runup parametrisation to the predictions from several existing runup models. This model has been selected for statewide estimations of runup levels.

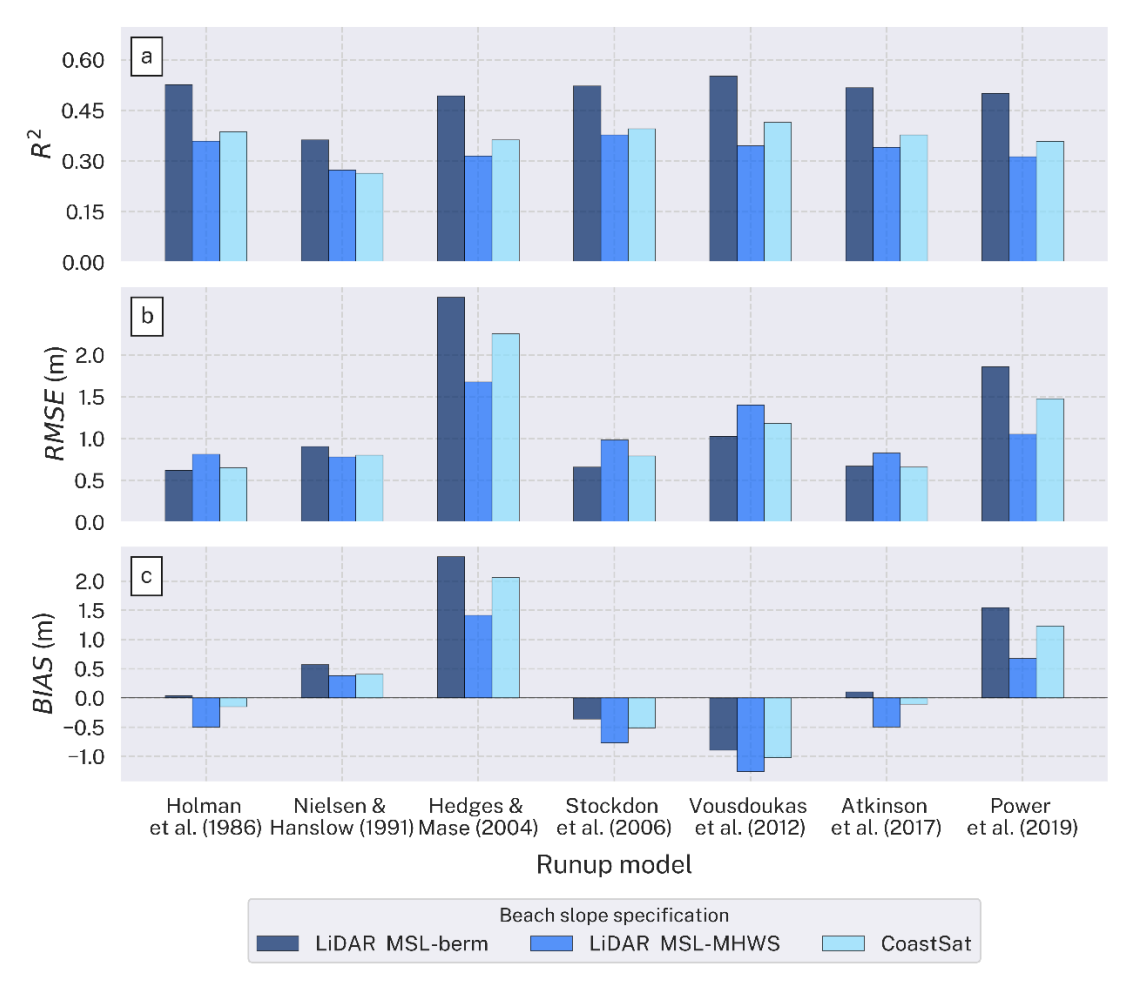


Figure 94 Summary statistics of total water level modelling (TWL = SWL + R, 472 observations) for 3 beach slope specifications and 7 runup formulas across 4 storm events

MHWS = mean high water springs; MSL = mean sea level;  $R^2$  = coefficient of determination; RMSE = root mean square error.

Note: Different runup formulas are ordered from left to right according to their year of publication.

# Appendix E: Coastal overwash ensembles

The adequate number of ensembles (n) that balances under-sampling issues and computational resources was determined with the following method. Recalling that the coastal overwash impacts were assessed by comparing different total water level (TWL) exceedances with the elevation of backbeach overwash thresholds from LiDAR, we compared the vertical accuracy of the employed LiDAR (0.3 m) with the variability (represented as the standard deviation) of different exceedance levels from 50 model realisations, for several ensemble sizes ( $n = 5 \text{ to } 5,000, \underline{Figure 95}$ ). This showed that the variability in TWLs (for 50%, 83% and 99% exceedances) is below the LiDAR accuracy for ensemble sizes of 200 or more ( $n \ge 200$ ). Furthermore, the model sensitivity associated with the 99% exceedances changes more slowly for ensembles greater than 1,000 (n > 1,000; std ~0.1 m). Balancing the computational effort against reduction in variance for larger numbers of ensembles, the ensemble size selected for the statewide assessment of coastal overwash was n = 1,000.

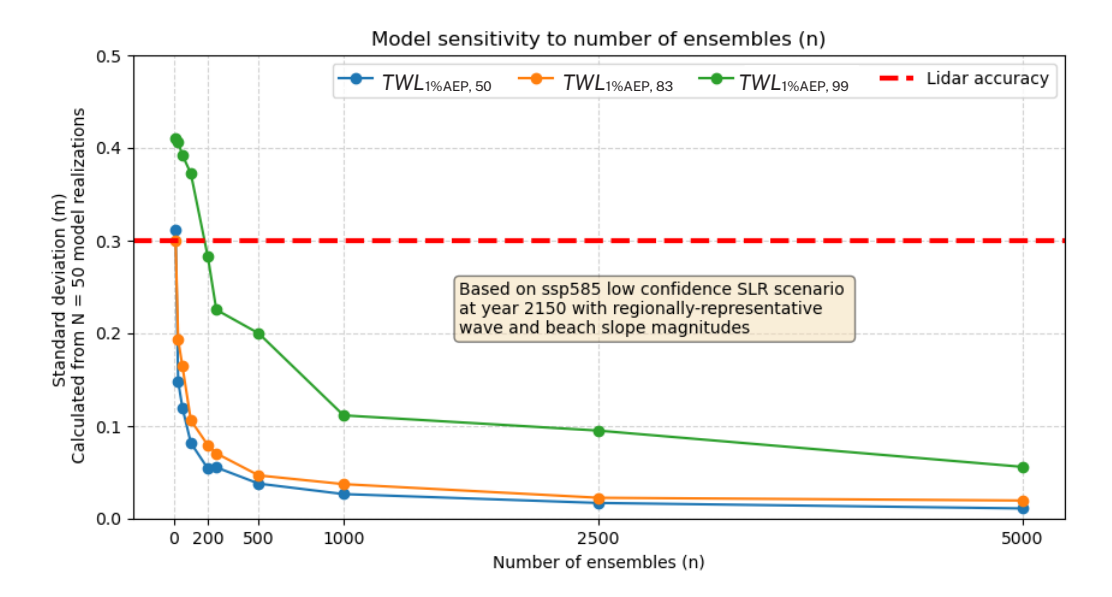


Figure 95 Model sensitivity to number of ensembles based on comparing the LiDAR accuracy with the variability (standard deviation) of different total water level exceedances for different numbers of ensemble members

AEP = annual exceedance probability; TWL = total water level.

# Appendix F: NSW estuarine tidal water level gauges

Table 17 shows details of NSW estuarine tidal water level gauging locations.

Table 17 NSW estuarine tidal water level gauging locations by Australian Water Resource Code (AWRC) number, latitude, longitude and duration of operation

Estuary No.	Name	Estuary	AWRC	Latitude	Longitude	Duration (yrs)
1	Tweed Entrance South	Tweed River	201472	-28.17064	153.55119	36.3
1	Cobaki	Tweed River	201448	-28.17664	153.50268	35.4
1	Dry Dock	Tweed River	201428	-28.19367	153.51673	35.4
1	Terranora	Tweed River	201447	-28.20142	153.49883	35.4
1	Letitia 2A	Tweed River	201429	-28.18295	153.55329	35.5
1	Barneys Point	Tweed River	201426	-28.22536	153.55148	36.2
1	Tumbulgum	Tweed River	201432	-28.27725	153.46061	37.8
1	Murwillumbah Bridge	Tweed River	201465	-28.32840	153.40010	20.5
1	Kynnumboon	Tweed River	201422	-28.31451	153.38944	32.7
2	Bogangar	Cudgen Creek	202416	-28.32705	153.55800	37.4
2	Kingscliff	Cudgen Creek	202418	-28.25966	153.58177	38.0
4	Mooball Creek	Mooball Creek	202435	-28.39191	153.56647	2.2
5	Brunswick Heads	Brunswick River	202403	-28.53703	153.55277	37.2
5	Orana Bridge	Brunswick River	202475	-28.51581	153.54788	20.5
5	Billinudgel	Brunswick River	202400	-28.50162	153.52679	37.3
5	Mullumbimby	Brunswick River	202402	-28.55002	153.49663	38.8
9	Ballina Breakwall	Richmond River	203425	-28.87538	153.58443	37.1

Estuary No.	Name	Estuary	AWRC	Latitude	Longitude	Duration (yrs)
9	Missingham Bridge	Richmond River	203465	-28.86874	153.57587	19.5
9	Byrnes Point	Richmond River	203461	-28.87377	153.52669	32.4
9	Wardell	Richmond River	203468	-28.95341	153.46470	20.6
9	Woodburn	Richmond River	203412	-29.07103	153.34193	37.6
9	Tucombil Highway Bridge	Richmond River	203480	-29.08458	153.33856	33.4
9	Rocky Mouth Creek	Richmond River	203432	-29.09603	153.32626	28.6
9	Bungawalbin	Richmond River	203450	-29.03346	153.27761	20.6
9	Bungawalbin Creek	Richmond River	2034133	-29.13985	153.17026	7.7
9	Coraki	Richmond River	203403	-28.98380	153.28723	35.4
9	East Gundurimba	Richmond River	203427	-28.84571	153.26689	43.2
9	Tuncester	Richmond River	203443	-28.79575	153.24020	43.2
9	Woodlawn College	Richmond River	203402	-28.78541	153.30254	43.2
11	Evans River Fishing Co-op	Evans River	203462	-29.12240	153.43429	26.2
11	Iron Gates	Evans River	203475	-29.12370	153.40808	25.7
11	Tucombil Floodgate*	Evans River	203434	-29.09291	153.34965	24.0
13	Yamba	Clarence River	204454	-29.42896	153.36206	36.8
13	Oyster Channel	Clarence River	204451	-29.43070	153.31412	20.5
13	Maclean	Clarence River	204410	-29.45603	153.19593	33.3
13	Lawrence	Clarence River	204453	-29.49697	153.10584	20.5

Estuary No.	Name	Estuary	AWRC	Latitude	Longitude	Duration (yrs)
13	Tyndale	Clarence River	204465	-29.56663	153.12987	20.5
13	The Avenue Downstream	Clarence River	204476	-29.70283	153.07416	20.5
13	Brushgrove	Clarence River	204406	-29.56792	153.07751	33.6
13	Ulmarra	Clarence River	204480	-29.63097	153.02682	20.6
13	Grafton	Clarence River	204400	-29.69380	152.93165	35.8
13	Rogans Bridge	Clarence River	204414	-29.61922	152.88445	29.8
13	Palmers Island Bridge	Clarence River	204426	-29.43212	153.26579	21.4
13	Lake Wooloweyah	Clarence River	204485	-29.47757	153.34184	13.6
16	Sandon River Entrance*	Sandon River	2044113	-29.67670	153.32726	0.8
16	Candole Creek Junction*	Sandon River	2044144	-29.68482	153.30167	0.6
17	Wooli Entrance	Wooli River	205462	-29.89032	153.26597	32.0
17	Wooli Caravan Park	Wooli River	205463	-29.85010	153.25417	32.2
18	Red Rock	Corindi River	205450	-29.98311	153.22722	19.2
23	Woolgoolga Lake	Woolgoolga Lake	205455	-30.10570	153.19815	16.0
26	Moonee Creek	Moonee Creek	205435	-30.20075	153.15535	20.7
28	Coffs Creek Highway Bridge	Coffs Creek	205439	-30.29323	153.11605	42.4
29	Newports Creek	Boambee Creek	205460	-30.32089	153.10419	32.5
29	Boambee	Boambee Creek	205438	-30.33757	153.08150	43.3
29	Boambee Creek Downstream*	Boambee Creek	205459	-30.33923	153.09398	16.0

Estuary No.	Name	Estuary	AWRC	Latitude	Longitude	Duration (yrs)
29	Boambee Entrance	Boambee Creek	205475	-30.35323	153.10297	18.2
30	Bonville	Bonville Creek	205480	-30.36852	153.04137	13.7
32	Repton	Bellinger River	205403	-30.44216	153.02456	34.9
32	Urunga	Bellinger River	205407	-30.49093	153.01285	29.6
32	Upstream Newry Island	Bellinger River	205458	-30.50527	152.97881	33.6
35	Deep Creek	Deep Creek	205485	-30.61169	153.00264	21.1
36	Stuarts Island Downstream	Nambucca River	205466	-30.65561	152.99498	31.1
36	Macksville	Nambucca River	205416	-30.70609	152.92045	40.0
36	Utungun	Nambucca River	205414	-30.72970	152.85167	31.6
36	Bowraville Downstream	Nambucca River	205425	-30.65436	152.86189	14.4
36	Warrell Creek	Nambucca River	205490	-30.73218	152.91629	13.2
37	South West Rocks	Macleay River	206456	-30.89009	153.01714	35.1
37	Smithtown	Macleay River	206406	-31.01583	152.94720	37.2
37	Kempsey	Macleay River	206402	-31.08150	152.84418	39.8
37	Aldavilla Downstream	Macleay River	206459	-31.08253	152.78317	32.8
39	Saltwater Lagoon	Saltwater Creek (Fredrickton )	206460	-30.88979	153.06402	18.8
40	Hat Head	Korogoro Creek	206465	-31.05778	153.05725	19.3
41	Crescent Head Killick Creek	Killick Creek	207452	-31.18741	152.97590	22.1

Estuary No.	Name	Estuary	AWRC	Latitude	Longitude	Duration (yrs)
43	Port Macquarie	Hastings River	207420	-31.42683	152.91113	37.2
43	Green Valley	Hastings River	207406	-31.27359	152.85730	30.4
43	Telegraph Point	Hastings River	207415	-31.32365	152.80116	33.6
43	Settlement Point	Hastings River	207418	-31.40677	152.90149	37.2
43	Dennis Bridge Downstream	Hastings River	207444	-31.40738	152.82111	29.0
43	Wauchope Railway Bridge	Hastings River	207401	-31.45273	152.73682	37.6
44	Lake Cathie	Cathie Creek	207441	-31.54778	152.85421	30.7
46	North Haven	Camden Haven	207423	-31.64036	152.82213	36.6
46	West Haven	Camden Haven	207437	-31.63712	152.79609	36.6
46	Laurieton	Camden Haven	207425	-31.65538	152.79878	32.7
46	Lakewood	Camden Haven	207475	-31.62975	152.76227	21.4
46	Watson Taylors Lake	Camden Haven	207480	-31.71539	152.74224	21.4
47	Harrington	Manning River	208425	-31.87487	152.68552	35.8
47	Croki	Manning River	208404	-31.87710	152.59390	31.3
47	Dumaresq Island	Manning River	208430	-31.90065	152.51700	21.7
47	Taree	Manning River	208410	-31.91702	152.45724	37.6
47	Wingham	Manning River	208400	-31.87532	152.37155	33.8
47	Farquhar Inlet	Manning River	208415	-31.94110	152.59525	35.7
50	Forster	Wallis Lake	209402	-32.17399	152.50821	37.2

Estuary No.	Name	Estuary	AWRC	Latitude	Longitude	Duration (yrs)
50	Tuncurry Downstream	Wallis Lake	209401D	-32.15900	152.47364	37.7
50	Pacific Palms Wharf	Wallis Lake	209406	-32.33303	152.52611	37.7
51	Tarbuck Bay	Smiths Lake	209465	-32.37477	152.48493	27
52	Bulahdelah	Myall River	209460	-32.41391	152.20708	37.6
52	Bombah Point	Myall River	209475	-32.50558	152.30464	21.8
52	Tea Gardens	Myall River	209480	-32.66889	152.16518	14.4
53	Karuah	Karuah River	209485	-32.65489	151.97005	13.4
55	Mallabula Point	Port Stephens	209461	-32.72087	152.01580	30.8
56	Stockton Bridge	Hunter River	210456	-32.88488	151.78381	38.4
56	Hexham Bridge	Hunter River	210448	-32.81767	151.68144	42.9
56	Raymond Terrace	Hunter River	210452	-32.75338	151.74418	43.1
56	Seaham	Hunter River	210462	-32.66341	151.73235	27.4
56	Green Rocks	Hunter River	210432	-32.72771	151.69227	43.7
56	Morpeth	Hunter River	210430	-32.72396	151.62970	38.1
56	McKimms Corner	Hunter River	210455	-32.71955	151.59350	37.0
56	Belmore Bridge	Hunter River	210458	-32.72946	151.55387	30.9
56	Oakhampton Railway Bridge	Hunter River	210475	-32.69518	151.56908	27.4
56	Hinton Bridge	Hunter River	210410	-32.71392	151.64816	43.7
56	Dunmore	Hunter River	210409	-32.68069	151.60569	43.8
56	Paterson Railway Bridge	Hunter River	210406	-32.59832	151.61790	39.6
56	Wallis Creek Upstream	Hunter River	210428	-32.73718	151.57432	33.1
58	Marmong Point	Lake Macquarie	211460	-32.97742	151.61940	36.9
58	Cockle Railway Station	Lake Macquarie	211455	-32.94279	151.62204	38.2
58	Belmont	Lake Macquarie	211461	-32.04025	151.65370	37.0

Estuary No.	Name	Estuary	AWRC	Latitude	Longitude	Duration (yrs)
58	Swansea Channel	Lake Macquarie	211462	-33.08679	151.64087	27.2
58	Kalang Road	Lake Macquarie	211475	-33.07865	151.48828	29.6
58	Morisset	Lake Macquarie	211480	-33.10024	151.47516	38.4
61	Wallarah Creek Bridge	Tuggerah Lake	211420	-33.21769	151.50749	29.0
61	Toukley	Tuggerah Lake	211401	-33.26350	151.52481	38.2
61	Lees Bridge	Tuggerah Lake	211425	-33.32538	151.42800	30.0
61	Long Jetty	Tuggerah Lake	211418	-33.35724	151.48194	31.6
61	Tumbi Umbi	Tuggerah Lake	211419	-33.36219	151.44493	29.1
62	Wamberal Lagoon	Wamberal Lagoon	212450	-33.42711	151.44598	29.8
63	Terrigal Bridge	Terrigal Lagoon	212455	-33.44147	151.44091	29.9
64	Avoca Lagoon	Avoca Lake	212452	-33.46407	151.42975	29.9
65	Cockrone Lake	Cockrone Lake	212453	-33.49291	151.42666	29.9
66	Manns Road	Brisbane Waters	211435	-33.40167	151.34282	27.2
66	Erina	Brisbane Waters	212436	-33.43244	151.38806	27.2
66	Punt Bridge	Brisbane Waters	212433	-33.43821	151.35960	29.2
66	Ettalong	Brisbane Waters	212423	-33.51709	151.34197	37.1
66	Koolewong 2	Brisbane Waters	2124301	-33.47616	151.32423	37.7
67	Spencer	Hawkesbury River	212431	-33.45714	151.14684	31.1
67	Gunderman Caravan Park	Hawkesbury River	212429	-33.44086	151.05757	31.1

Estuary No.	Name	Estuary	AWRC	Latitude	Longitude	Duration (yrs)
67	Webbs Creek	Hawkesbury River	212408	-33.38746	150.98234	41.9
67	Colo Junction	Hawkesbury River	212407	-33.43769	150.88315	25.0
67	Sackville	Hawkesbury River	212406	-33.49333	150.88164	43.0
67	Ebenezer	Hawkesbury River	212427	-33.54747	150.89309	33.6
67	Windsor	Hawkesbury River	212426	-33.60493	150.81841	35.6
67	Freemans Reach	Hawkesbury River	212410	-33.56987	150.78074	43.1
70	Ocean Street Bridge	Narrabeen Lagoon	213408D	-33.70379	151.30475	28.7
70	Narrabeen Bridge	Narrabeen Lagoon	213422	-33.71218	151.29678	28.7
71	Dee Why	Dee Why Lagoon	213424	-33.74594	151.30206	27.1
72	Curl Curl	Curl Curl Lagoon	213426	-33.76622	151.29489	31.7
73	Riverview Parade	Manly Lagoon	213413	-33.78403	151.27733	33.1
73	Queenscliff Bridge	Manly Lagoon	213414	-33.78316	151.28230	32.6
74	Roseville Bridge*	Middle Harbour Creek	2134127	-33.77417	151.20433	0.8
75	Fullers Bridge	Lane Cove River	213476	-33.79292	151.15690	7.0
76	Silverwater Bridge	Parramatta River	213435	-33.82453	151.05156	11.1
78	Tempe Bridge	Cooks River	213415	-33.92861	151.15748	31.7
78	Illawarra Road Bridge	Cooks River	213420	-33.92269	151.14256	21.8
78	Canterbury Road Bridge	Cooks River	213411	-33.91341	151.11725	31.6
79	Como Bridge	Georges River	213425	-33.99700	151.07086	22.2

Estuary No.	Name	Estuary	AWRC	Latitude	Longitude	Duration (yrs)
79	Picnic Point Downstream	Georges River	213410D	-33.98235	151.00018	31.2
79	Milperra	Georges River	213405	-33.92752	150.97933	42.6
79	Lansdowne Bridge	Georges River	213402	-33.89034	150.96741	35.5
79	Lansvale	Georges River	213401	-33.89959	150.95758	42.7
79	Irelands Bridge	Georges River	213407	-33.90488	150.94320	35.2
79	Scrivener Street	Georges River	213404	-33.92229	150.93526	42.6
81	Bundeena	Port Hacking	214452	-34.08268	151.15090	8.4
89	Bellambi Lagoon	Bellambi Lake	214488	-34.37606	150.91964	10.6
90	Towradgi Creek Upstream	Towradgi Creek	214477	-34.38092	150.90743	31.1
91	Fairy Creek Downstream	Fairy Creek	214404	-34.41363	150.89295	38.1
94	Koonawarra Bay	Lake Illawarra	214440	-34.50424	150.82656	29.2
94	Cudgeree Bay 2	Lake Illawarra	2144101	-34.53019	150.86287	35.4
94	Lake Illawarra Entrance	Lake Illawarra	214417	-34.53741	150.87053	31.8
94	Macquarie Rivulet	Lake Illawarra	214402	-34.54679	150.78562	38.4
95	Little Lake Entrance	Elliot Lake	214467	-34.56099	150.86634	30.9
96	Minnamurra	Minnamurra River	214442	-34.62161	150.84588	21.2
99	Werri Lagoon	Werri Lagoon	214445	-34.72744	150.83737	20.7
100	Gerroa	Crooked River	215410	-34.77105	150.80817	24.2
101	Crookhaven Heads	Shoalhaven River	215408	-34.90534	150.75940	31.2

Estuary No.	Name	Estuary	AWRC	Latitude	Longitude	Duration (yrs)
101	Shoalhaven Heads	Shoalhaven River	215470	-34.85461	150.74534	32.2
101	Hay Street	Shoalhaven River	215415	-34.85972	150.72979	21.3
101	Terara	Shoalhaven River	215420	-34.86345	150.62896	21.7
101	Nowra Bridge	Shoalhaven River	215411	-34.86517	150.60240	32.7
101	Gradys Caravan Park	Shoalhaven River	215430	-34.87088	150.46288	17.2
101	Greenwell Point	Shoalhaven River	215417	-34.90728	150.73648	34.4
102	Wollumboola	Wollumbool a Lake	215454	-34.93840	150.76468	31.8
103	Currarong Creek	Currarong Creek	216405	-35.01746	150.82049	27.5
107	Huskisson*	Currambene Creek	216472	-33.03333	150.66667	6.4
113	Island Point	St Georges Basin	216415	-35.09738	150.59467	31.8
113	Sussex Inlet	St Georges Basin	216412	-35.16948	150.59425	22.5
114	Swan Lake	Swan Lake	216425	-35.19526	150.56057	23.3
117	Lake Conjola Downstream	Conjola Lake	216420D	-35.26918	150.50027	30.6
118	Narrawallee Inlet	Narrawallee Inlet	216430	-35.30068	150.46871	29.7
122	Burrill Lake Bridge	Burrill Lake	216435	-35.38800	150.44518	31.5
123	Tabourie Lake	Tabourie Lake	216440	-35.44095	150.40343	30.6
128	Durras Lake	Durras Lake	216445	-35.64388	150.29743	22.5
132	Princess Jetty	Clyde River	216410	-35.70381	150.17783	37.4
132	Nelligen	Clyde River	216453	-35.65150	150.14329	29.1
135	George Bass Drive	Tomaga River	216455	-35.82604	150.17845	26.7

Estuary No.	Name	Estuary	AWRC	Latitude	Longitude	Duration (yrs)
138	Moruya Bridge	Moruya River	217410	-35.90804	150.08240	26.0
138	Moruya Hospital	Moruya River	217402	-35.90351	150.07116	32.6
142	Coila Lake	Coila Lake	218405	-36.04867	150.13910	27.3
143	Tuross Head	Tuross River	218410	-36.06402	150.12321	29.0
149	Narooma Wharf*	Wagonga Inlet	218420	-36.21508	150.13069	11.0
149	Barlows Bay	Wagonga Inlet	218415	-36.20919	150.10196	26.7
149	Regatta Point	Wallaga Lake	219405	-36.36961	150.06723	29.6
157	Bermagui	Bermagui River	219470	-36.42633	150.07148	35.8
162	Wapengo Downstream*	Wapengo Lagoon	219420	-36.61259	150.01888	6.4
162	Wapengo Upstream*	Wapengo Lagoon	219421	-36.60058	150.01023	6.4
164	Nelson Lagoon*	Nelson Lagoon	219433	-36.68588	149.98940	3.7
165	Bega River	Bega River	219410	-36.70261	149.97786	22.5
168	Back Lagoon	Back Lagoon	219415	-36.88357	149.91566	14.2
169	Merimbula Wharf	Merimbula Lake	220410	-36.89295	149.90980	32.2
169	Merimbula Lake	Merimbula Lake	220405	-36.89168	149.87845	32.2
170	Pambula Lake	Pambula River	220415	-36.96578	149.88390	32.2
171	Lake Curalo	Curalo Lagoon	220420	-37.05227	149.90595	15.9
175	Towamba River Upstream*	Towamba River	220450	-37.11482	149.90910	2.0
175	Bundian Crossing*	Towamba River	220451	-37.11456	149.89509	1.7
180	Wonboyn Lake	Wonboyn River	220452	-37.24937	149.91831	25.7

* Denotes decommissioned gauge location.		

## Appendix G: Coastal erosion exposure under SSP5-8.5 (medium-confidence) and SSP5-8.5 (low-confidence) scenarios

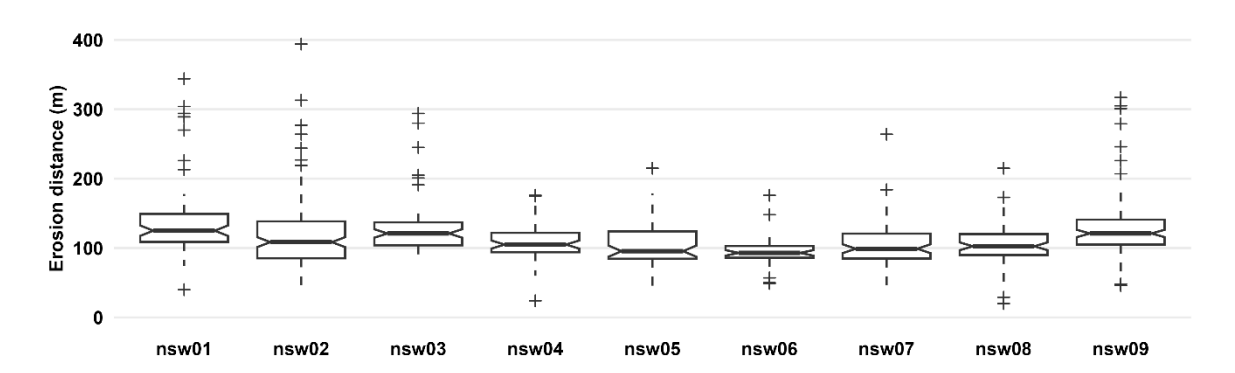
To offer a complete picture of potential SLR impacts for decision-makers and stakeholders with low risk tolerance, results on (future) exposure to coastal erosion under SSP5-8.5 medium- and low-confidence scenarios are provided in this appendix in Figure 96 through Figure 106.

Exposure statistics for coastal erosion under present-day (2020) conditions are shown in Table 18.

Table 18 Exposure statistics for coastal erosion under present-day conditions at 1% exceedance probability level

Asset	Statistic
Buildings	657
Addresses	1,919
Airports	0
Runways	0 km
Critical infrastructure sites	0
Electricity transmission lines	14 km
Aboriginal cultural heritage assets	288
Transport infrastructure – railway	0.02 km
Transport infrastructure – roads	22 km
Transport infrastructure – pathways	35 km

a.



b.

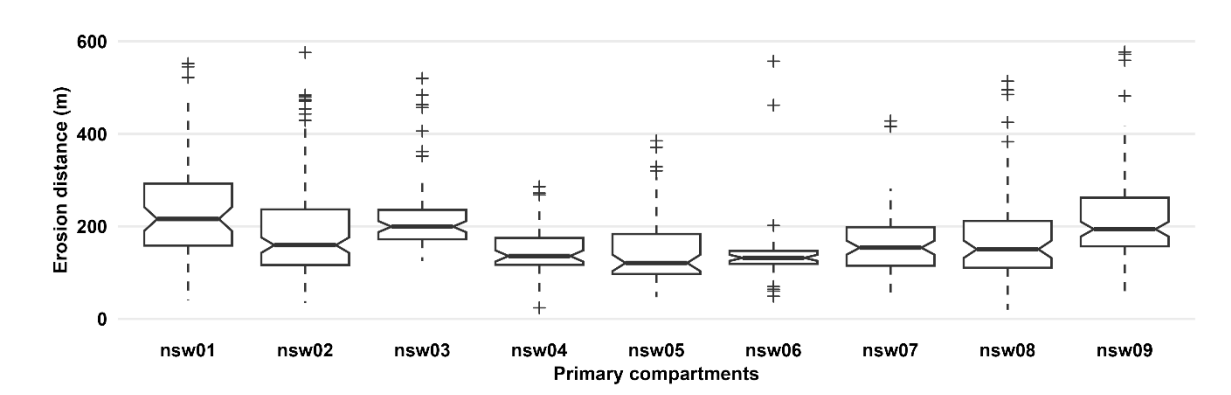


Figure 96 Box plots summarising modelled shoreline erosion distances at a 1% exceedance probability level in 2100 for (a) SSP5-8.5 medium-confidence and (b) SSP5-8.5 low-confidence scenarios

Note: The y-axis scales differ and may have been limited for illustrative clarity.

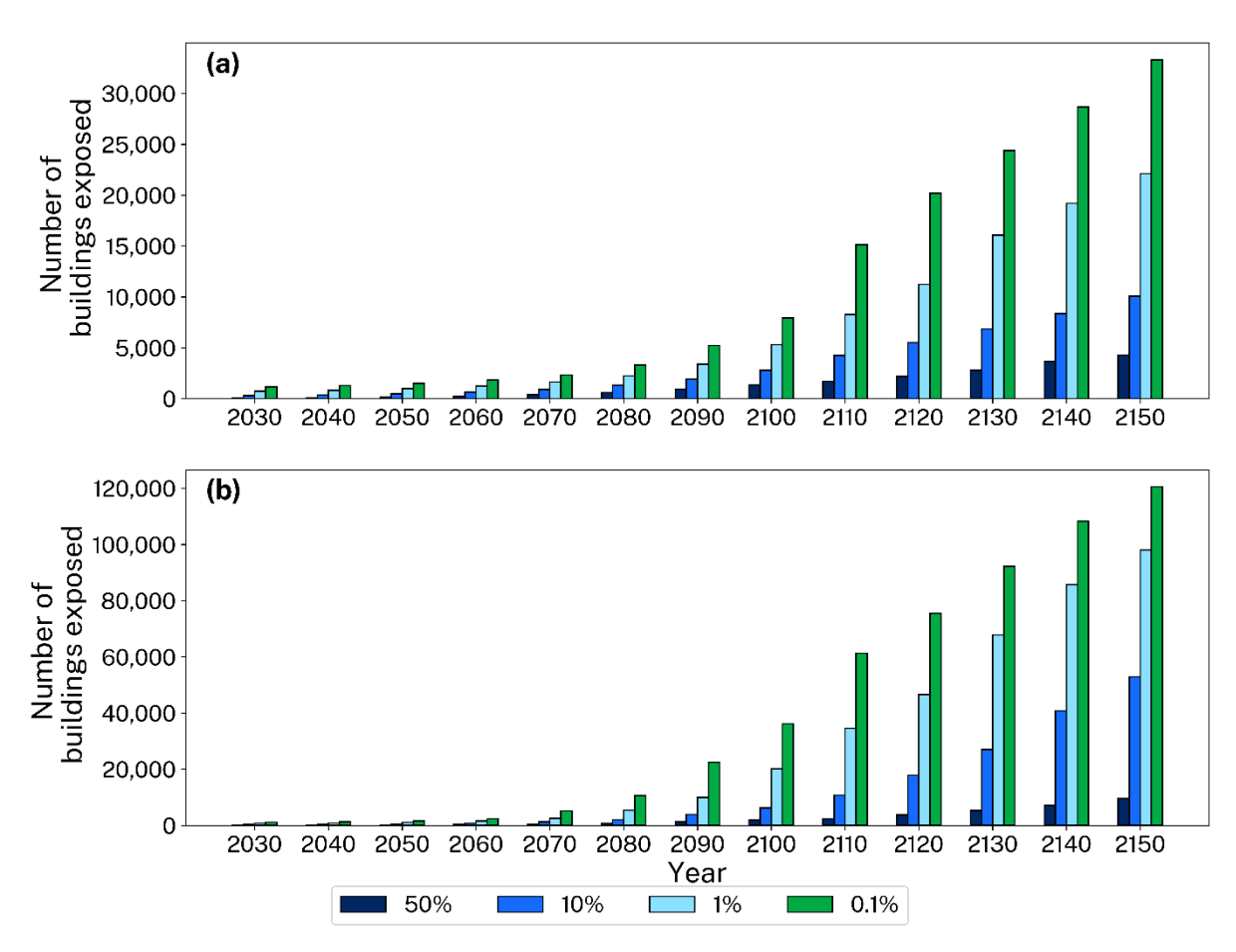


Figure 97 State-wide building counts exposed to coastal erosion over time at different exceedance probability levels (0.1%, 1%, 10%, and 50%) associated with (a) medium-confidence SSP5-8.5 and (b) low-confidence SSP5-8.5 scenarios Note: The scales on y-axes are different.

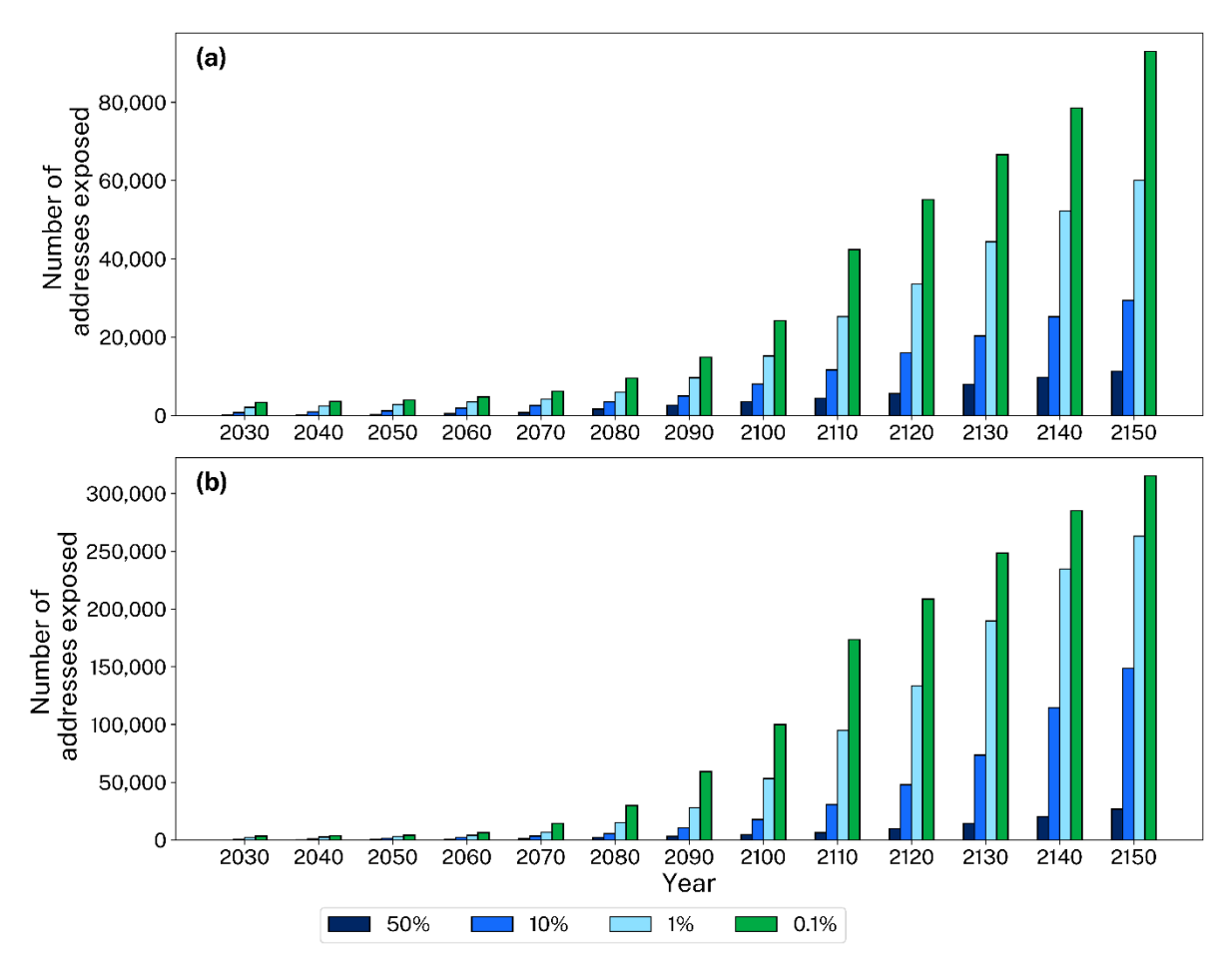


Figure 98 State-wide address counts exposed to coastal erosion over time at different exceedance probability levels (0.1%, 1%, 10%, and 50%) associated with (a) medium-confidence SSP5-8.5 and (b) low-confidence SSP5-8.5 scenarios Note: The scales on y-axes are different.

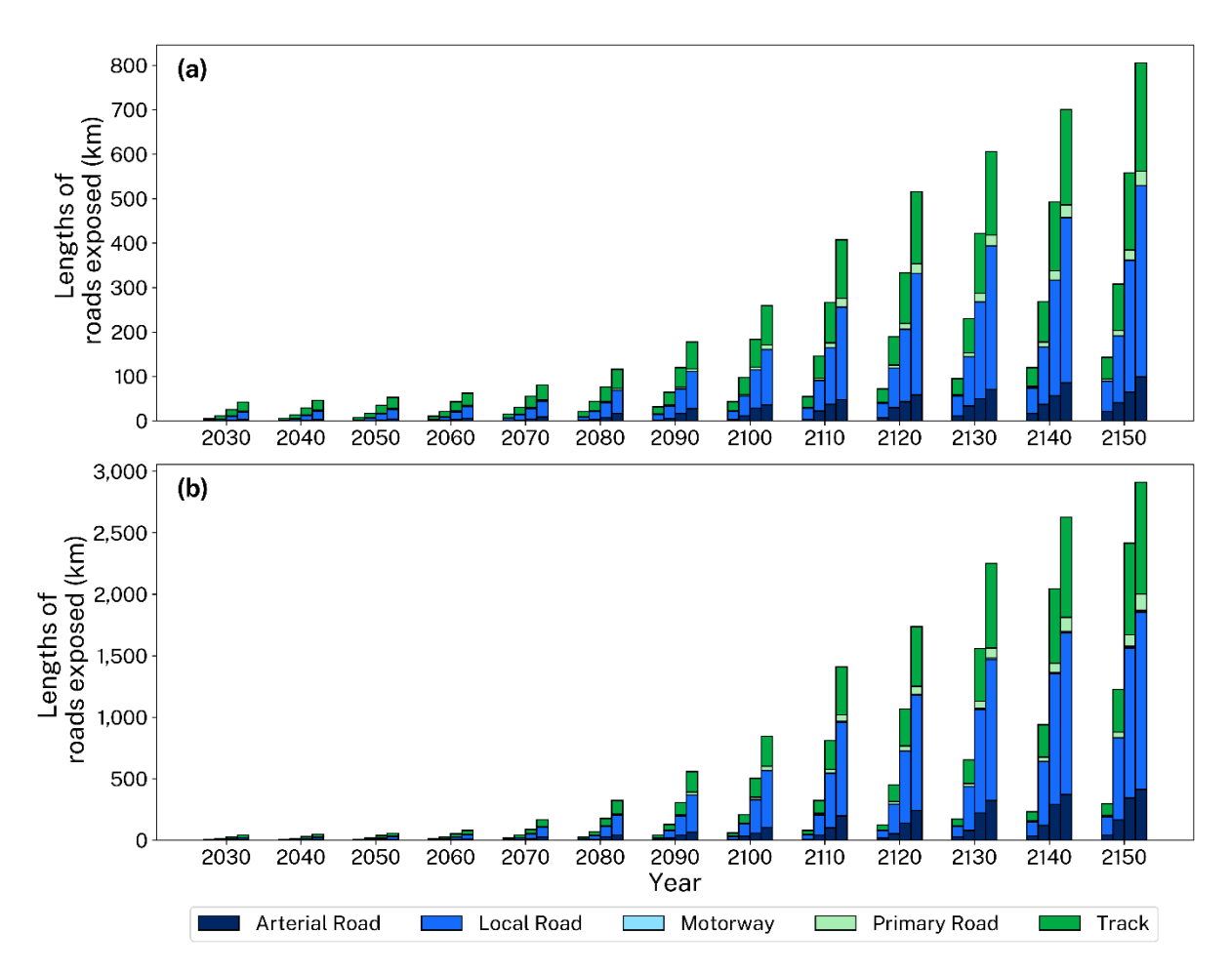


Figure 99 State-wide road lengths (km) by type exposed to coastal erosion over time at different exceedance probability levels (from right to left: 0.1%, 1%, 10%, and 50%) associated with (a) medium-confidence SSP5-8.5 and (b) low-confidence SSP5-8.5 scenarios

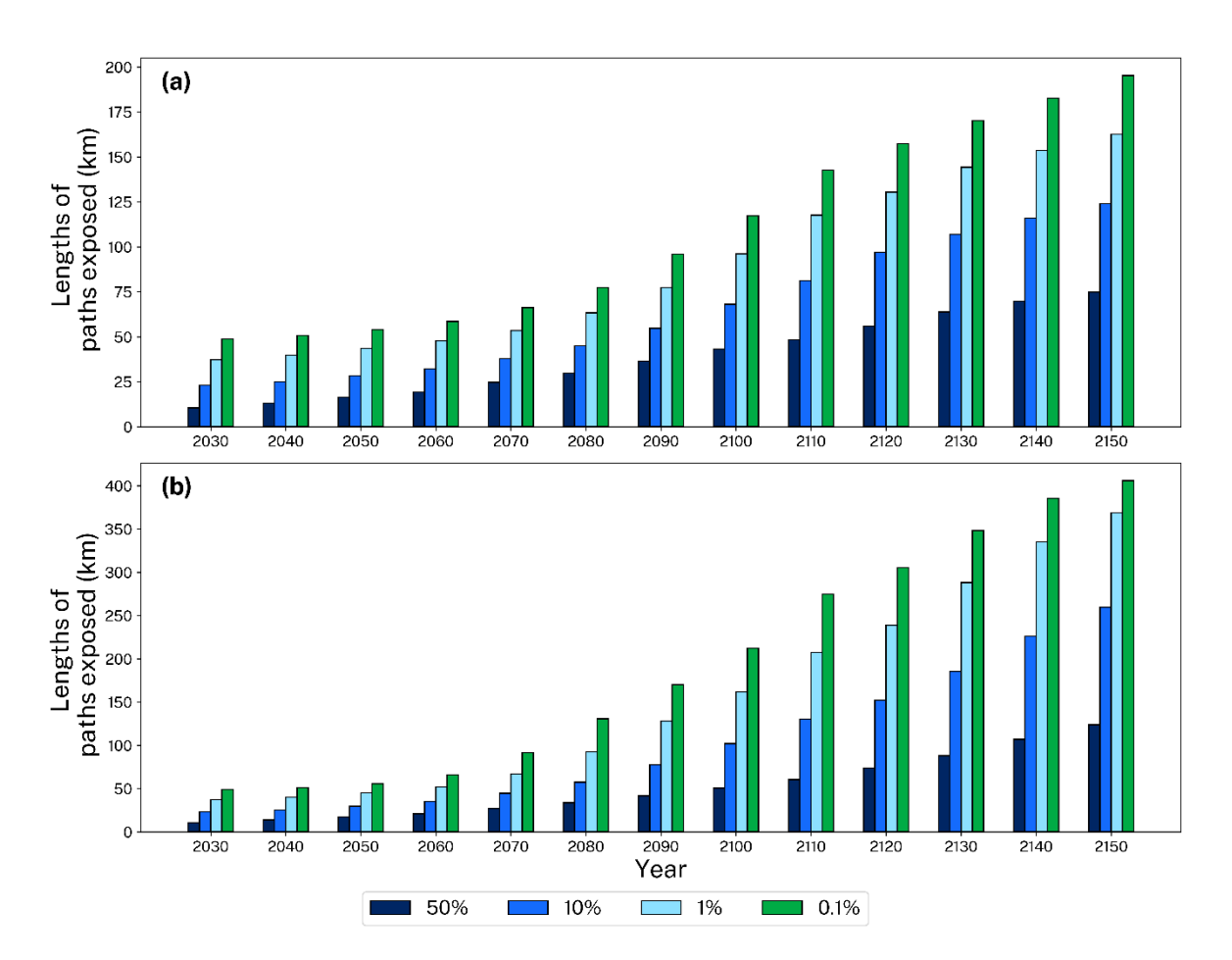


Figure 100 State-wide path lengths (km) exposed to coastal erosion over time at different exceedance probability levels (0.1%, 1%, 10%, and 50%) associated with (a) medium-confidence SSP5-8.5 and (b) low-confidence SSP5-8.5 scenarios

Note: The scales on the y-axes are different.

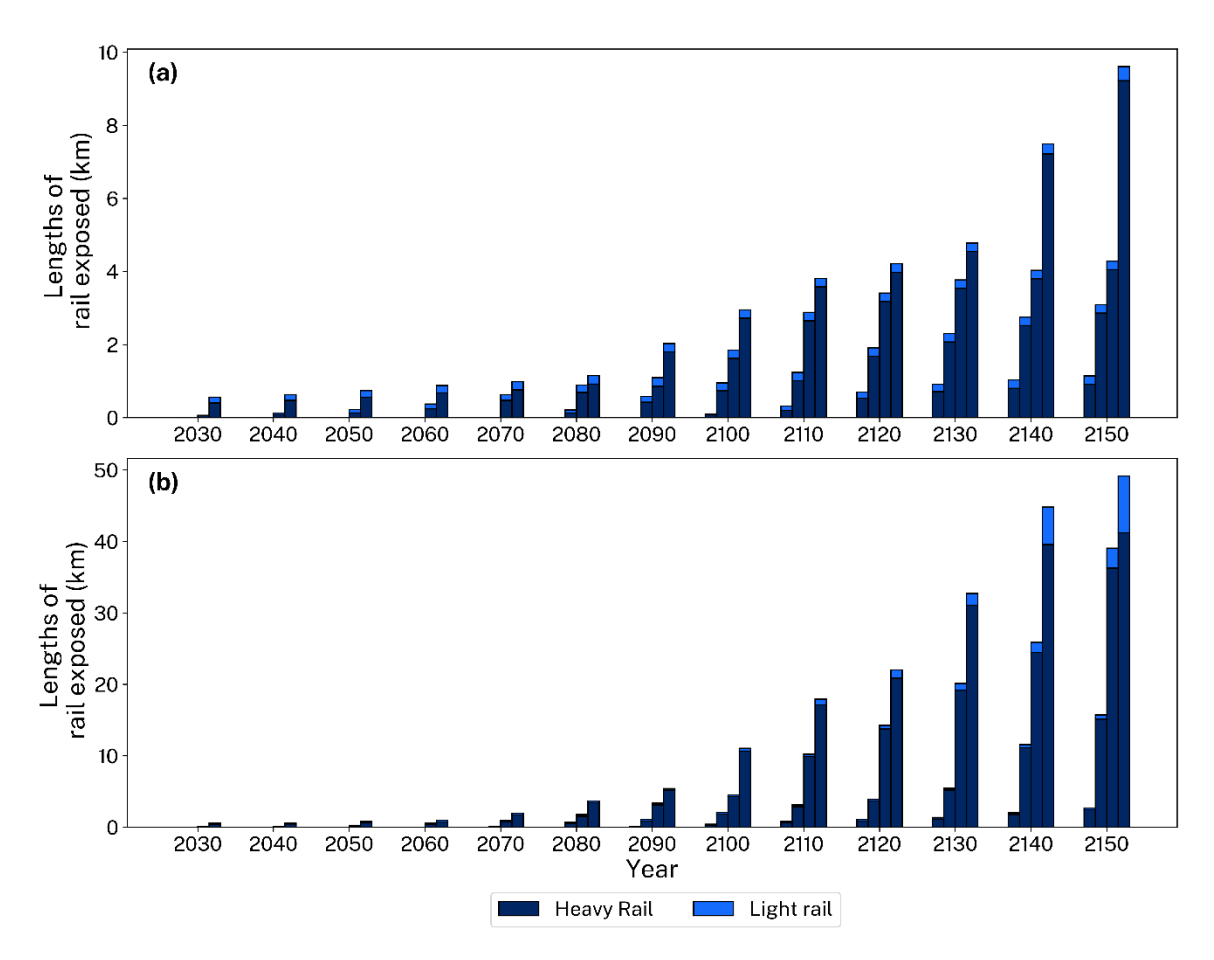


Figure 101 State-wide rail lengths (km) exposed by type to coastal erosion over time at different exceedance probability levels (from right to left: 0.1%, 1%, 10%, and 50%) associated with (a) medium-confidence SSP5-8.5 and (b) low-confidence SSP5-8.5 scenarios

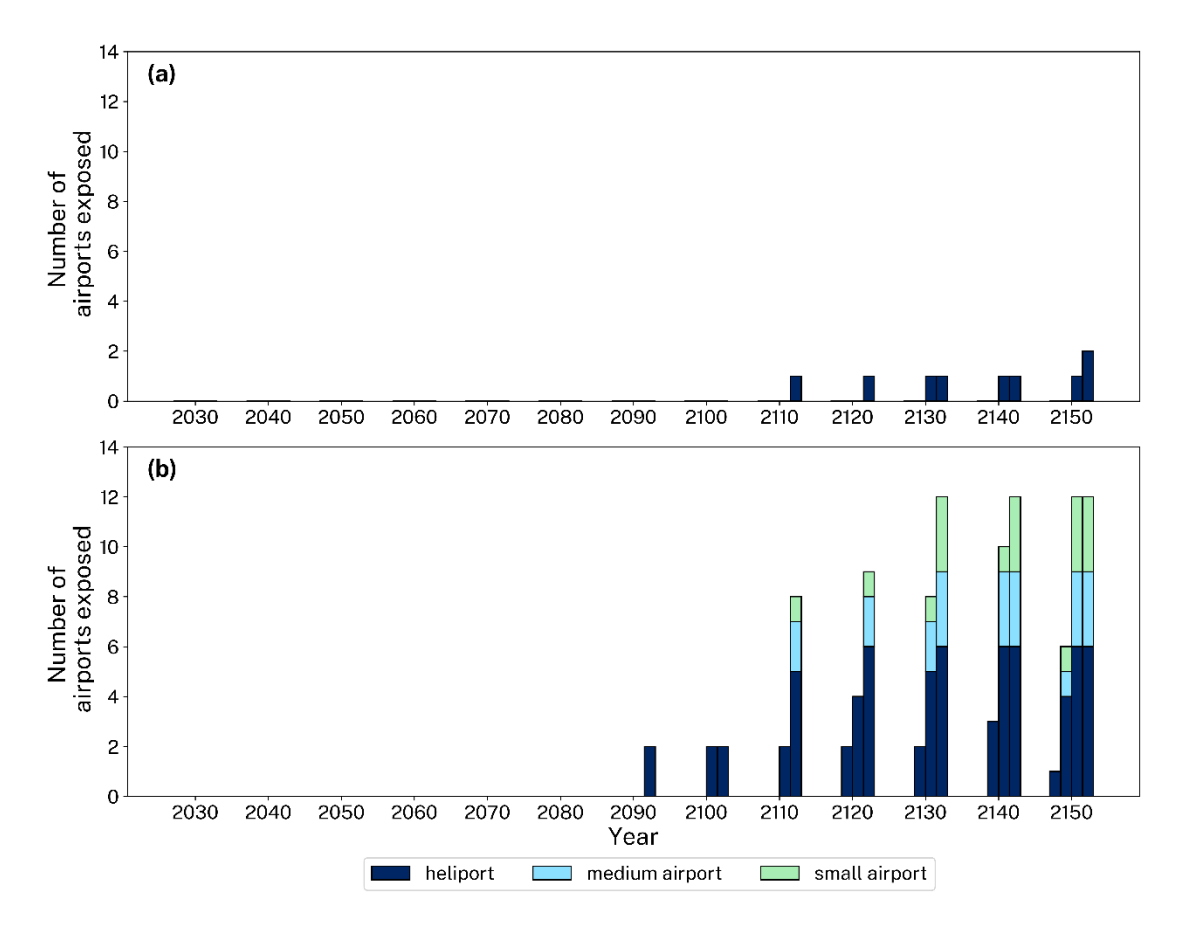


Figure 102 State-wide airports by type exposed to coastal erosion over time at different exceedance probability levels (from right to left: 0.1%, 1%, 10%, and 50%) associated with (a) medium-confidence SSP5-8.5 and (b) low-confidence SSP5-8.5 scenarios

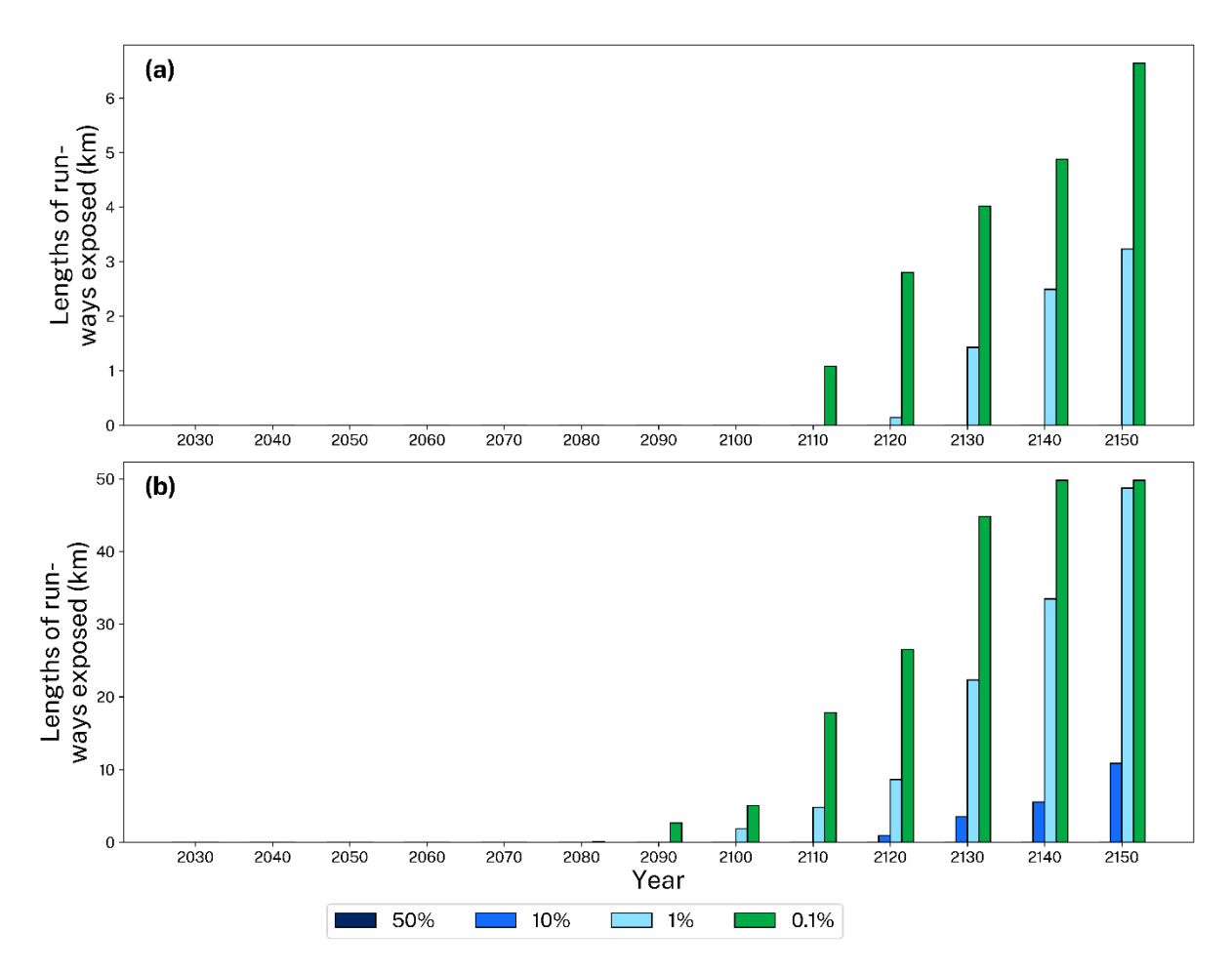


Figure 103 State-wide runway lengths (km) exposed to coastal erosion over time at different exceedance probability levels (0.1%, 1%, 10%, and 50%) associated with (a) medium-confidence SSP5-8.5 and (b) low-confidence SSP5-8.5 scenarios

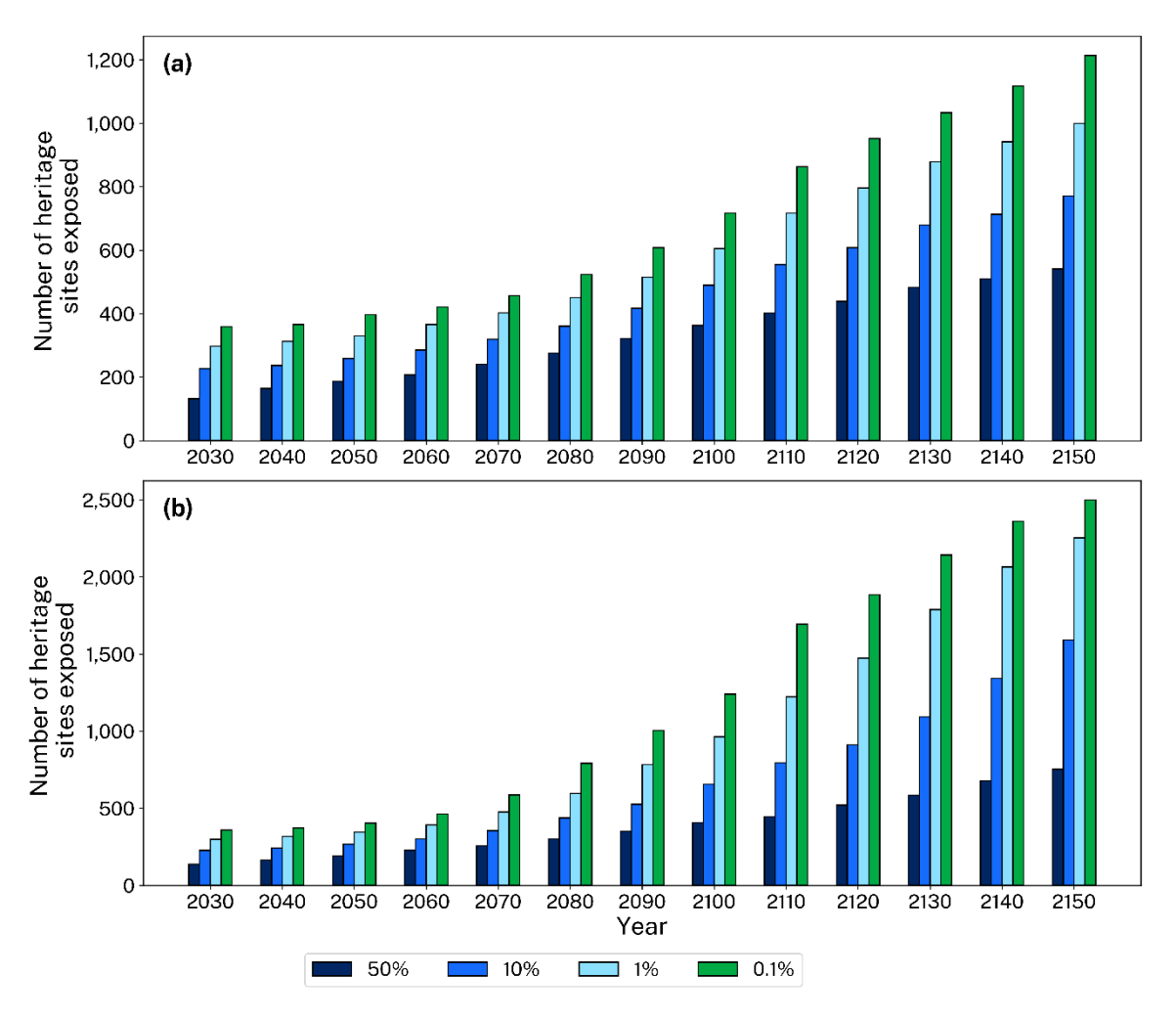


Figure 104 State-wide Aboriginal cultural heritage sites exposed to coastal erosion over time at different exceedance probability levels (0.1%, 1%, 10%, and 50%) associated with (a) medium-confidence SSP5-8.5 and (b) low-confidence SSP5-8.5 scenarios

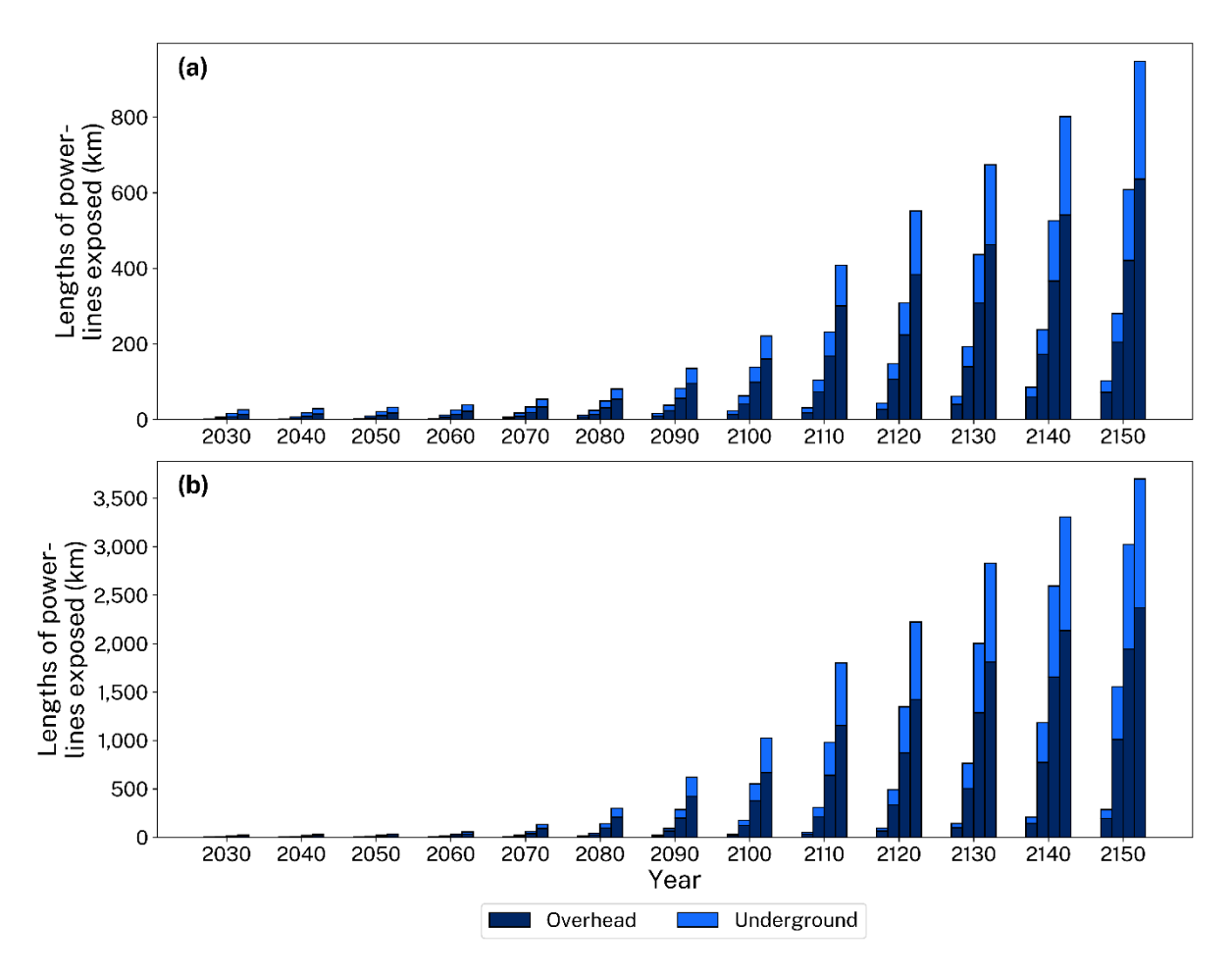


Figure 105 State-wide lengths (km) of electricity transmission lines, by type, exposed to coastal erosion over time at different exceedance probability levels (from right to left: 0.1%, 1%, 10%, and 50%) associated with (a) medium-confidence SSP5-8.5 and (b) low-confidence SSP5-8.5 scenarios

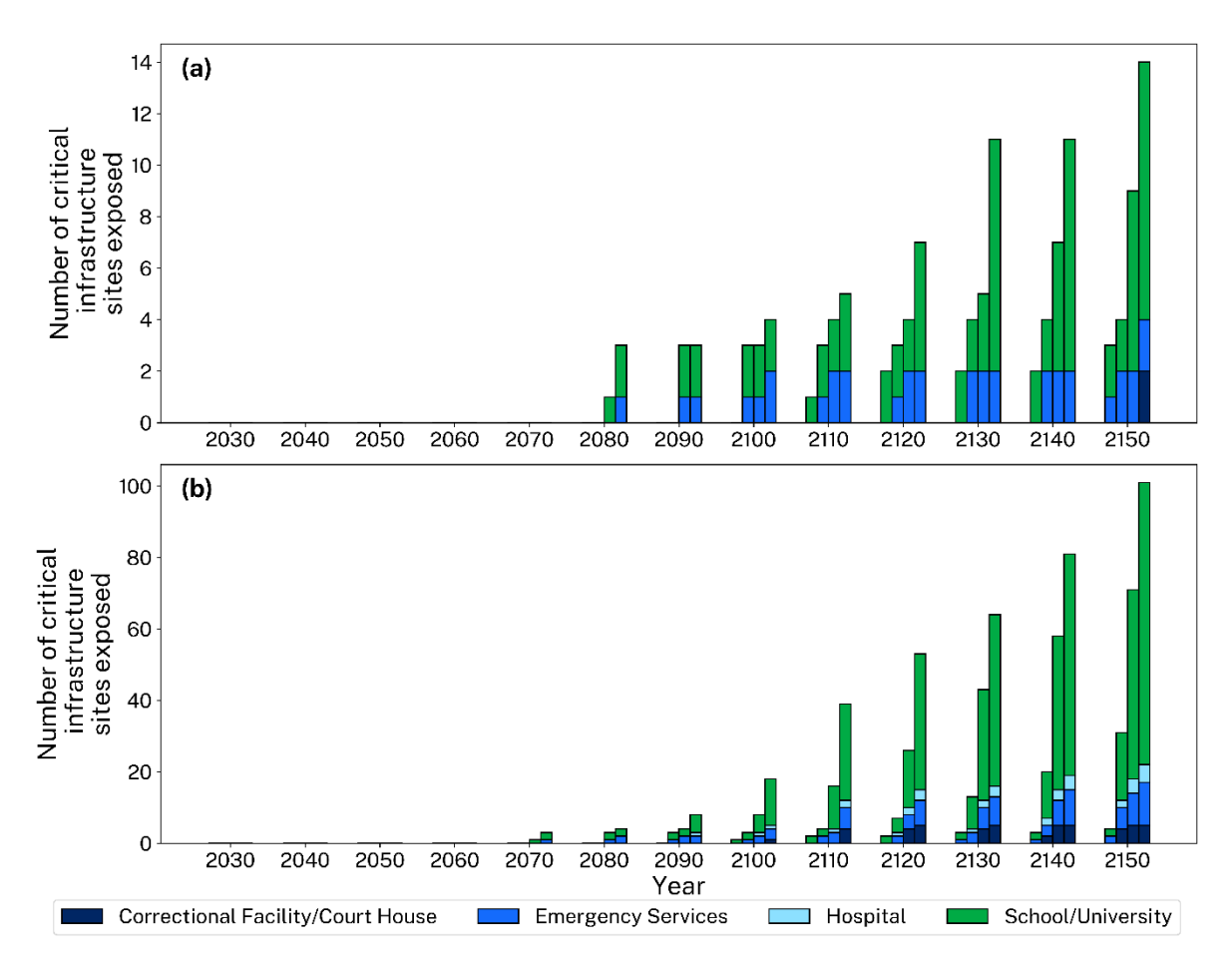


Figure 106 State-wide critical infrastructure assets, by type, exposed to coastal erosion over time at different exceedance probability levels (from right to left: 0.1%, 1%, 10%, and 50%) associated with (a) medium-confidence SSP5-8.5 and (b) low-confidence SSP5-8.5 scenarios

## Appendix H: Results of coastal overwash for various SSP scenarios and exceedance probability levels

<u>Table 19</u> shows likelihoods, in both percentage and kilometres, of coastal overwash for various SSP scenarios and annual exceedance probability levels from 2020 to 2150.

Table 19 Results of coastal overwash for various SSP scenarios and probability levels from 2020 to 2150

Year	SSP scenario	AEP (%)	Unlikely overwash (%)	Unlikely overwash (km)	Potential overwash (%)	Potential overwash (km)	Likely overwash (%)	Likely overwash (km)
2020	SSP1-2.6	1	89	773	5	41	6	51
2030	SSP1-2.6	1	89	770	5	42	6	53
2040	SSP1-2.6	1	89	768	5	42	6	55
2050	SSP1-2.6	1	88	766	5	42	7	57
2060	SSP1-2.6	1	88	763	5	44	7	58
2070	SSP1-2.6	1	88	758	5	46	7	61
2080	SSP1-2.6	1	87	755	6	48	7	62
2090	SSP1-2.6	1	87	751	6	50	7	64
2100	SSP1-2.6	1	86	747	6	52	8	66
2110	SSP1-2.6	1	85	736	7	59	8	70
2120	SSP1-2.6	1	85	732	7	61	8	72
2130	SSP1-2.6	1	83	722	8	67	9	76
2140	SSP1-2.6	1	83	715	8	72	9	78
2150	SSP1-2.6	1	82	707	9	76	9	82
2020	SSP1-2.6	5	91	789	4	35	5	41
2030	SSP1-2.6	5	91	786	4	36	5	43
2040	SSP1-2.6	5	91	785	4	36	5	44
2050	SSP1-2.6	5	91	782	4	37	5	46
2060	SSP1-2.6	5	90	779	4	38	6	48
2070	SSP1-2.6	5	89	776	5	40	6	49
2080	SSP1-2.6	5	89	772	5	42	6	51
2090	SSP1-2.6	5	89	770	5	43	6	52

Year	SSP scenario	AEP (%)	Unlikely overwash (%)	Unlikely overwash (km)	Potential overwash (%)	Potential overwash (km)	Likely overwash (%)	Likely overwash (km)
2100	SSP1-2.6	5	89	765	5	44	6	56
2110	SSP1-2.6	5	88	759	5	47	7	59
2120	SSP1-2.6	5	87	754	6	50	7	61
2130	SSP1-2.6	5	86	744	7	57	7	64
2140	SSP1-2.6	5	85	738	7	61	8	66
2150	SSP1-2.6	5	84	729	8	68	8	68
2020	SSP1-2.6	20	92	802	4	30	4	33
2030	SSP1-2.6	20	92	801	4	30	4	34
2040	SSP1-2.6	20	92	799	4	31	4	35
2050	SSP1-2.6	20	92	796	4	32	4	37
2060	SSP1-2.6	20	92	793	4	34	4	38
2070	SSP1-2.6	20	91	790	4	35	5	40
2080	SSP1-2.6	20	91	789	4	34	5	42
2090	SSP1-2.6	20	91	786	4	36	5	43
2100	SSP1-2.6	20	91	782	4	38	5	45
2110	SSP1-2.6	20	89	774	5	43	6	48
2120	SSP1-2.6	20	89	772	5	43	6	50
2130	SSP1-2.6	20	88	764	6	49	6	52
2140	SSP1-2.6	20	88	758	6	52	6	55
2150	SSP1-2.6	20	86	751	7	58	7	56
2020	SSP1-2.6	100	96	835	2	14	2	16
2030	SSP1-2.6	100	96	834	2	14	2	17
2040	SSP1-2.6	100	96	832	2	15	2	18
2050	SSP1-2.6	100	96	830	2	16	2	19
2060	SSP1-2.6	100	96	829	2	16	2	20
2070	SSP1-2.6	100	96	827	2	17	2	21
2080	SSP1-2.6	100	95	826	2	17	3	22
2090	SSP1-2.6	100	95	825	2	18	3	22
2100	SSP1-2.6	100	95	822	2	19	3	24
2110	SSP1-2.6	100	94	817	3	23	3	25
2120	SSP1-2.6	100	94	815	3	24	3	26

Year	SSP scenario	AEP (%)	Unlikely overwash (%)	Unlikely overwash (km)	Potential overwash (%)	Potential overwash (km)	Likely overwash (%)	Likely overwash (km)
2130	SSP1-2.6	100	94	810	3	27	3	28
2140	SSP1-2.6	100	94	805	3	30	3	30
2150	SSP1-2.6	100	92	803	4	31	4	31
2020	SSP2-4.5	1	89	774	5	40	6	51
2030	SSP2-4.5	1	89	771	5	41	6	53
2040	SSP2-4.5	1	89	769	5	42	6	54
2050	SSP2-4.5	1	88	764	5	43	7	58
2060	SSP2-4.5	1	88	760	5	45	7	60
2070	SSP2-4.5	1	88	756	5	47	7	62
2080	SSP2-4.5	1	86	748	6	51	8	66
2090	SSP2-4.5	1	86	743	6	53	8	69
2100	SSP2-4.5	1	85	735	7	58	8	72
2110	SSP2-4.5	1	84	725	7	61	9	79
2120	SSP2-4.5	1	82	713	8	68	10	84
2130	SSP2-4.5	1	81	702	9	75	10	88
2140	SSP2-4.5	1	79	687	10	84	11	94
2150	SSP2-4.5	1	77	672	11	93	12	100
2020	SSP2-4.5	5	91	789	4	34	5	42
2030	SSP2-4.5	5	91	786	4	36	5	43
2040	SSP2-4.5	5	91	784	4	37	5	44
2050	SSP2-4.5	5	91	781	4	38	5	46
2060	SSP2-4.5	5	90	777	4	39	6	49
2070	SSP2-4.5	5	89	774	5	40	6	51
2080	SSP2-4.5	5	89	770	5	41	6	54
2090	SSP2-4.5	5	88	765	5	42	7	58
2100	SSP2-4.5	5	88	755	5	48	7	62
2110	SSP2-4.5	5	87	746	6	54	7	65
2120	SSP2-4.5	5	85	738	7	58	8	69
2130	SSP2-4.5	5	83	725	8	66	9	74
2140	SSP2-4.5	5	83	715	8	72	9	78
2150	SSP2-4.5	5	80	700	10	82	10	83

Year	SSP scenario	AEP (%)	Unlikely overwash (%)	Unlikely overwash (km)	Potential overwash (%)	Potential overwash (km)	Likely overwash (%)	Likely overwash (km)
2020	SSP2-4.5	20	93	802	3	30	4	33
2030	SSP2-4.5	20	92	800	4	31	4	34
2040	SSP2-4.5	20	92	798	4	32	4	35
2050	SSP2-4.5	20	92	796	4	32	4	37
2060	SSP2-4.5	20	91	793	4	33	5	39
2070	SSP2-4.5	20	91	789	4	34	5	42
2080	SSP2-4.5	20	91	784	4	36	5	45
2090	SSP2-4.5	20	91	779	4	39	5	47
2100	SSP2-4.5	20	89	775	5	40	6	50
2110	SSP2-4.5	20	89	766	5	45	6	54
2120	SSP2-4.5	20	87	758	6	49	7	58
2130	SSP2-4.5	20	86	747	7	57	7	61
2140	SSP2-4.5	20	86	736	7	64	7	65
2150	SSP2-4.5	20	84	722	8	73	8	70
2020	SSP2-4.5	100	96	835	2	14	2	16
2030	SSP2-4.5	100	96	833	2	15	2	17
2040	SSP2-4.5	100	96	832	2	16	2	17
2050	SSP2-4.5	100	96	830	2	16	2	19
2060	SSP2-4.5	100	96	828	2	17	2	20
2070	SSP2-4.5	100	95	826	2	17	3	22
2080	SSP2-4.5	100	95	823	2	19	3	23
2090	SSP2-4.5	100	95	821	2	19	3	25
2100	SSP2-4.5	100	94	817	3	22	3	26
2110	SSP2-4.5	100	94	812	3	25	3	28
2120	SSP2-4.5	100	93	806	3	28	4	31
2130	SSP2-4.5	100	92	800	4	32	4	33
2140	SSP2-4.5	100	92	791	4	38	4	36
2150	SSP2-4.5	100	91	784	5	43	4	38
2020	SSP3-7.0	1	89	774	5	40	6	51
2030	SSP3-7.0	1	89	771	5	41	6	53
2040	SSP3-7.0	1	89	768	5	42	6	55

Year	SSP scenario	AEP (%)	Unlikely overwash (%)	Unlikely overwash (km)	Potential overwash (%)	Potential overwash (km)	Likely overwash (%)	Likely overwash (km)
2050	SSP3-7.0	1	88	764	5	43	7	58
2060	SSP3-7.0	1	88	759	5	46	7	60
2070	SSP3-7.0	1	87	752	6	49	7	64
2080	SSP3-7.0	1	86	743	6	53	8	69
2090	SSP3-7.0	1	85	733	7	58	8	74
2100	SSP3-7.0	1	84	721	7	63	9	81
2110	SSP3-7.0	1	82	705	8	72	10	88
2120	SSP3-7.0	1	80	687	9	82	11	96
2130	SSP3-7.0	1	77	667	11	95	12	103
2140	SSP3-7.0	1	75	648	12	103	13	114
2150	SSP3-7.0	1	73	624	13	117	14	124
2020	SSP3-7.0	5	91	789	4	35	5	41
2030	SSP3-7.0	5	91	786	4	36	5	43
2040	SSP3-7.0	5	91	783	4	38	5	44
2050	SSP3-7.0	5	90	779	5	40	5	46
2060	SSP3-7.0	5	89	775	5	40	6	50
2070	SSP3-7.0	5	89	771	5	42	6	52
2080	SSP3-7.0	5	88	765	5	43	7	57
2090	SSP3-7.0	5	88	757	5	46	7	62
2100	SSP3-7.0	5	86	744	6	54	8	67
2110	SSP3-7.0	5	84	729	7	62	9	74
2120	SSP3-7.0	5	83	712	8	72	9	81
2130	SSP3-7.0	5	80	694	10	83	10	88
2140	SSP3-7.0	5	78	677	11	92	11	96
2150	SSP3-7.0	5	76	652	12	107	12	106
2020	SSP3-7.0	20	93	802	3	30	4	33
2030	SSP3-7.0	20	93	800	3	30	4	35
2040	SSP3-7.0	20	92	798	4	31	4	36
2050	SSP3-7.0	20	92	794	4	33	4	38
2060	SSP3-7.0	20	91	791	4	34	5	40
2070	SSP3-7.0	20	91	786	4	36	5	43

Year	SSP scenario	AEP (%)	Unlikely overwash (%)	Unlikely overwash (km)	Potential overwash (%)	Potential overwash (km)	Likely overwash (%)	Likely overwash (km)
2080	SSP3-7.0	20	91	780	4	39	5	46
2090	SSP3-7.0	20	89	774	5	41	6	50
2100	SSP3-7.0	20	88	764	5	44	7	57
2110	SSP3-7.0	20	87	751	6	53	7	61
2120	SSP3-7.0	20	85	736	7	62	8	67
2130	SSP3-7.0	20	84	718	8	73	8	74
2140	SSP3-7.0	20	82	706	9	78	9	81
2150	SSP3-7.0	20	79	681	11	95	10	89
2020	SSP3-7.0	100	96	835	2	14	2	16
2030	SSP3-7.0	100	96	833	2	15	2	17
2040	SSP3-7.0	100	96	832	2	15	2	18
2050	SSP3-7.0	100	96	831	2	15	2	19
2060	SSP3-7.0	100	96	828	2	16	2	21
2070	SSP3-7.0	100	95	825	2	18	3	22
2080	SSP3-7.0	100	95	822	2	19	3	24
2090	SSP3-7.0	100	94	816	3	22	3	27
2100	SSP3-7.0	100	94	810	3	25	3	30
2110	SSP3-7.0	100	93	802	3	30	4	33
2120	SSP3-7.0	100	92	791	4	37	4	37
2130	SSP3-7.0	100	90	782	5	43	5	40
2140	SSP3-7.0	100	89	771	6	50	5	44
2150	SSP3-7.0	100	87	753	7	62	6	50
2020	SSP5- 8.5 (med)	1	89	774	5	40	6	51
2030	SSP5- 8.5 (med)	1	89	770	5	42	6	53
2040	SSP5- 8.5 (med)	1	89	767	5	42	6	56
2050	SSP5- 8.5 (med)	1	88	763	5	44	7	58
2060	SSP5- 8.5 (med)	1	88	757	5	47	7	61

Year	SSP scenario	AEP (%)	Unlikely overwash (%)	Unlikely overwash (km)	Potential overwash (%)	Potential overwash (km)	Likely overwash (%)	Likely overwash (km)
2070	SSP5- 8.5 (med)	1	86	749	6	50	8	66
2080	SSP5- 8.5 (med)	1	86	738	6	56	8	71
2090	SSP5- 8.5 (med)	1	84	727	7	60	9	78
2100	SSP5- 8.5 (med)	1	82	710	8	68	10	87
2110	SSP5- 8.5 (med)	1	80	687	9	82	11	96
2120	SSP5- 8.5 (med)	1	77	664	11	95	12	106
2130	SSP5- 8.5 (med)	1	75	641	12	107	13	117
2140	SSP5- 8.5 (med)	1	70	609	15	128	15	128
2150	SSP5- 8.5 (med)	1	68	584	16	140	16	141
2020	SSP5- 8.5 (med)	5	91	789	4	34	5	42
2030	SSP5- 8.5 (med)	5	91	786	4	36	5	43
2040	SSP5- 8.5 (med)	5	91	783	4	37	5	45
2050	SSP5- 8.5 (med)	5	90	778	4	39	6	48
2060	SSP5- 8.5 (med)	5	89	774	5	41	6	50
2070	SSP5- 8.5 (med)	5	89	769	5	41	6	55
2080	SSP5- 8.5 (med)	5	88	762	5	43	7	60
2090	SSP5- 8.5 (med)	5	86	749	6	51	8	65
2100	SSP5- 8.5 (med)	5	85	735	7	57	8	73

Year	SSP scenario	AEP (%)	Unlikely overwash (%)	Unlikely overwash (km)	Potential overwash (%)	Potential overwash (km)	Likely overwash (%)	Likely overwash (km)
2110	SSP5- 8.5 (med)	5	83	712	8	72	9	81
2120	SSP5- 8.5 (med)	5	81	694	9	81	10	90
2130	SSP5- 8.5 (med)	5	77	670	11	95	12	100
2140	SSP5- 8.5 (med)	5	73	638	14	117	13	110
2150	SSP5- 8.5 (med)	5	71	613	15	131	14	121
2020	SSP5- 8.5 (med)	20	93	802	3	30	4	33
2030	SSP5- 8.5	20	92	800	4	31	4	34
2040	SSP5- 8.5 (med)	20	92	797	4	32	4	36
2050	SSP5- 8.5 (med)	20	92	793	4	33	4	39
2060	SSP5- 8.5 (med)	20	91	790	4	34	5	41
2070	SSP5- 8.5 (med)	20	91	784	4	36	5	45
2080	SSP5- 8.5 (med)	20	89	777	5	39	6	49
2090	SSP5- 8.5 (med)	20	89	769	5	42	6	54
2100	SSP5- 8.5 (med)	20	87	756	6	48	7	61
2110	SSP5- 8.5 (med)	20	85	737	7	62	8	66
2120	SSP5- 8.5 (med)	20	82	717	9	74	9	74
2130	SSP5- 8.5 (med)	20	80	699	10	83	10	83
2140	SSP5- 8.5 (med)	20	77	668	12	104	11	93

Year	SSP scenario	AEP (%)	Unlikely overwash (%)	Unlikely overwash (km)	Potential overwash (%)	Potential overwash (km)	Likely overwash (%)	Likely overwash (km)
2150	SSP5- 8.5 (med)	20	74	643	14	118	12	104
2020	SSP5- 8.5	100	96	836	2	13	2	16
2030	SSP5- 8.5 (med)	100	96	834	2	14	2	17
2040	SSP5- 8.5 (med)	100	96	832	2	15	2	18
2050	SSP5- 8.5 (med)	100	96	830	2	16	2	19
2060	SSP5- 8.5 (med)	100	95	826	2	17	3	22
2070	SSP5- 8.5	100	95	824	2	18	3	23
2080	SSP5- 8.5 (med)	100	95	820	2	20	3	25
2090	SSP5- 8.5 (med)	100	94	812	3	24	3	29
2100	SSP5- 8.5 (med)	100	93	803	3	29	4	33
2110	SSP5- 8.5	100	92	792	4	37	4	36
2120	SSP5- 8.5 (med)	100	90	780	5	44	5	41
2130	SSP5- 8.5 (med)	100	89	766	6	53	5	46
2140	SSP5- 8.5 (med)	100	86	743	8	69	6	53
2150	SSP5- 8.5 (med)	100	84	725	9	81	7	59
2020	SSP5- 8.5 (low)	1	89	774	5	40	6	51
2030	SSP5- 8.5 (low)	1	89	770	5	42	6	53
2040	SSP5- 8.5 (low)	1	89	766	5	43	6	56

Year	SSP scenario	AEP (%)	Unlikely overwash (%)	Unlikely overwash (km)	Potential overwash (%)	Potential overwash (km)	Likely overwash (%)	Likely overwash (km)
2050	SSP5- 8.5 (low)	1	88	759	5	46	7	60
2060	SSP5- 8.5 (low)	1	87	751	6	50	7	64
2070	SSP5- 8.5 (low)	1	85	735	7	59	8	71
2080	SSP5- 8.5 (low)	1	82	710	9	75	9	80
2090	SSP5- 8.5 (low)	1	77	672	12	100	11	93
2100	SSP5- 8.5 (low)	1	70	611	17	144	13	110
2110	SSP5- 8.5 (low)	1	58	498	27	234	15	133
2120	SSP5- 8.5 (low)	1	51	438	31	268	18	159
2130	SSP5- 8.5 (low)	1	35	303	40	344	25	218
2140	SSP5- 8.5 (low)	1	23	198	42	367	35	300
2150	SSP5- 8.5 (low)	1	14	128	42	360	44	377
2020	SSP5- 8.5 (low)	5	91	789	4	35	5	41
2030	SSP5- 8.5 (low)	5	91	786	4	35	5	44
2040	SSP5- 8.5 (low)	5	91	782	4	38	5	45
2050	SSP5- 8.5 (low)	5	89	777	5	40	6	48
2060	SSP5- 8.5 (low)	5	89	770	5	43	6	52
2070	SSP5- 8.5 (low)	5	87	756	6	49	7	60
2080	SSP5- 8.5 (low)	5	84	732	8	66	8	67

Year	SSP scenario	AEP (%)	Unlikely overwash (%)	Unlikely overwash (km)	Potential overwash (%)	Potential overwash (km)	Likely overwash (%)	Likely overwash (km)
2090	SSP5- 8.5 (low)	5	81	700	10	88	9	77
2100	SSP5- 8.5 (low)	5	74	641	15	131	11	93
2110	SSP5- 8.5 (low)	5	61	524	26	227	13	114
2120	SSP5- 8.5 (low)	5	53	458	31	271	16	136
2130	SSP5- 8.5 (low)	5	37	318	41	356	22	191
2140	SSP5- 8.5 (low)	5	23	205	45	387	32	273
2150	SSP5- 8.5 (low)	5	15	132	44	377	41	356
2020	SSP5- 8.5 (low)	20	93	803	3	30	4	32
2030	SSP5- 8.5 (low)	20	92	800	4	31	4	34
2040	SSP5- 8.5 (low)	20	92	797	4	32	4	36
2050	SSP5- 8.5 (low)	20	91	791	4	34	5	40
2060	SSP5- 8.5 (low)	20	91	784	4	37	5	44
2070	SSP5- 8.5 (low)	20	89	774	5	43	6	48
2080	SSP5- 8.5 (low)	20	88	753	6	56	6	56
2090	SSP5- 8.5 (low)	20	84	723	9	78	7	64
2100	SSP5- 8.5 (low)	20	77	668	14	118	9	79
2110	SSP5- 8.5 (low)	20	64	554	25	214	11	97
2120	SSP5- 8.5 (low)	20	56	478	31	270	13	117

Year	SSP scenario	AEP (%)	Unlikely overwash (%)	Unlikely overwash (km)	Potential overwash (%)	Potential overwash (km)	Likely overwash (%)	Likely overwash (km)
2130	SSP5- 8.5 (low)	20	39	333	42	367	19	165
2140	SSP5- 8.5 (low)	20	25	214	47	408	28	243
2150	SSP5- 8.5 (low)	20	16	138	46	397	38	330
2020	SSP5- 8.5 (low)	100	96	835	2	14	2	16
2030	SSP5- 8.5 (low)	100	96	834	2	14	2	17
2040	SSP5- 8.5 (low)	100	96	832	2	15	2	18
2050	SSP5- 8.5 (low)	100	96	828	2	16	2	21
2060	SSP5- 8.5 (low)	100	95	824	2	19	3	22
2070	SSP5- 8.5 (low)	100	94	815	3	24	3	26
2080	SSP5- 8.5 (low)	100	93	803	4	32	3	30
2090	SSP5- 8.5 (low)	100	91	783	5	47	4	35
2100	SSP5- 8.5 (low)	100	86	745	9	77	5	43
2110	SSP5- 8.5 (low)	100	76	652	18	158	6	55
2120	SSP5- 8.5 (low)	100	66	571	26	226	8	68
2130	SSP5- 8.5 (low)	100	46	396	42	366	12	103
2140	SSP5- 8.5 (low)	100	30	253	52	453	18	159
2150	SSP5- 8.5 (low)	100	18	156	55	476	27	233

AEP = annual exceedance probability; low = low-confidence; med = medium-confidence; SSP = shared socioeconomic pathway.

## Appendix I: Estuarine inundation exposure under SSP5-8.5 (medium-confidence) and SSP5-8.5 (low-confidence) scenarios

To offer a complete picture of potential SLR impacts for decision-makers and stakeholders with low risk tolerance, results on (future) exposure to estuarine inundation under SSP5-8.5 medium- and low-confidence scenarios are provided in this appendix in Figure 108 through Figure 122. Note that not all figures in this appendix include data for low-confidence SSP5-8.5 due to the limitations of the DEM.

Exposure statistics for estuarine inundation under present-day (2020) conditions are shown in Table 20.

Table 20 Exposure statistics for estuarine inundation under present-day conditions at one day/year (annual) frequency

Asset	Statistic
Buildings	3,345
Addresses	7,124
Airport(s)	1
Runways	3.5 km
Critical infrastructure sites	2
Electricity transmission lines	409 km
Aboriginal cultural heritage assets	611
Transport infrastructure – railway	2 km
Transport infrastructure – roads	357
Transport infrastructure – pathways	32 km

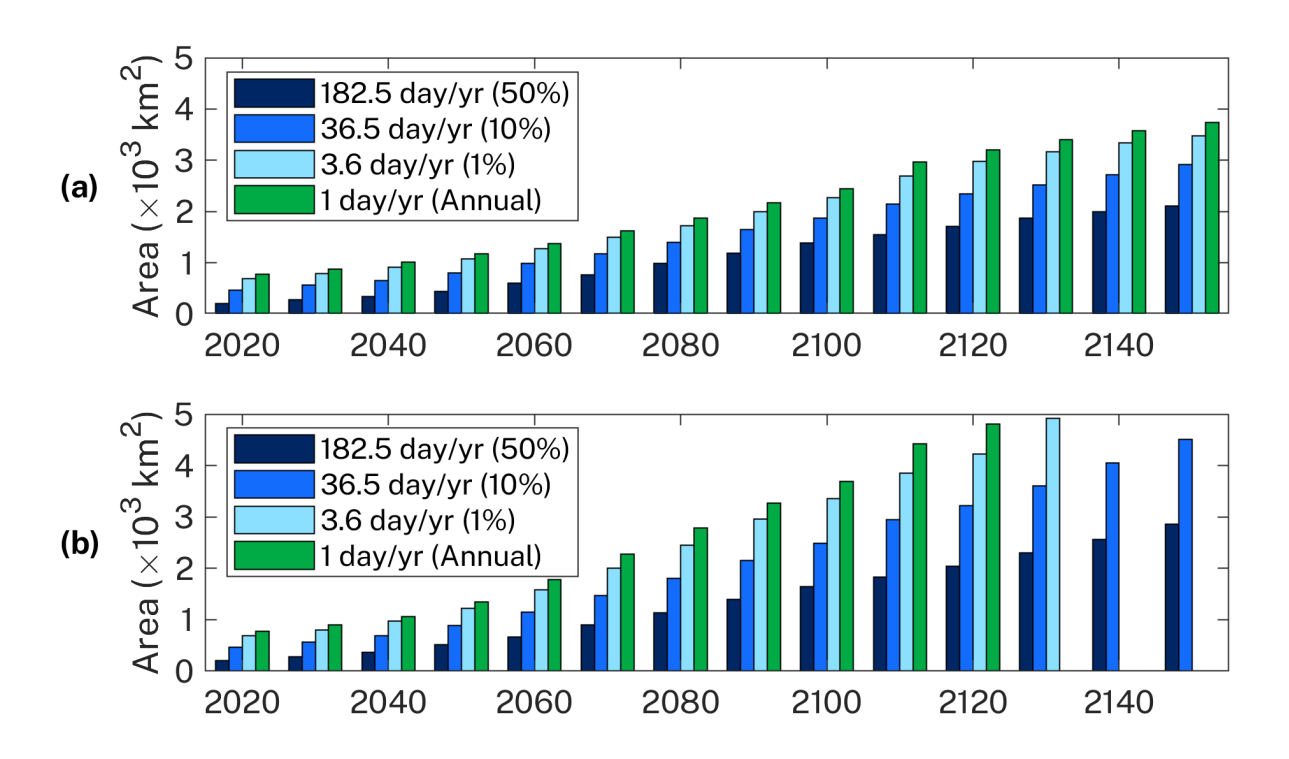


Figure 107 Bar charts of increasing inundated area for each exceedance inundation frequency and climate change scenario under (a) medium-confidence SSP5-8.5 and (b) low-confidence SSP5-8.5 scenarios

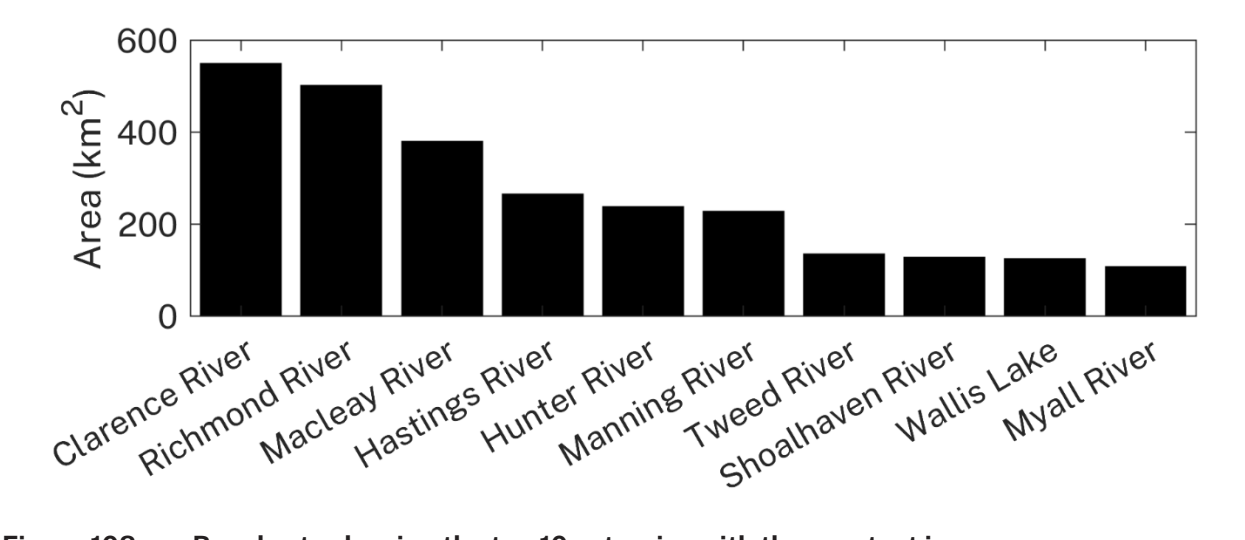


Figure 108 Bar charts showing the top 10 estuaries with the greatest increases on an annual exceedance frequency (1 day/year) in inundated area for medium-confidence SSP5-8.5

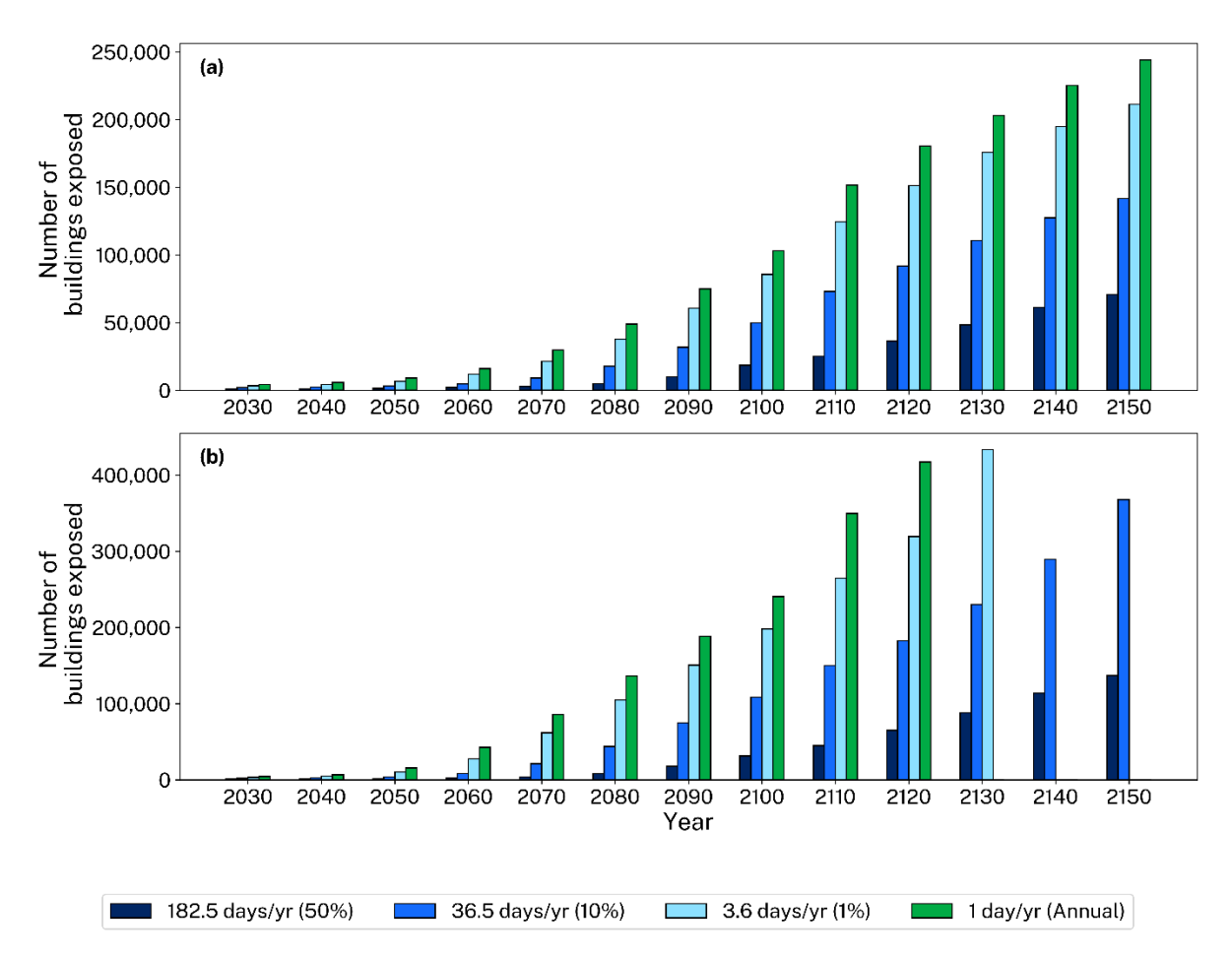


Figure 109 State-wide counts of buildings exposed to inundation over time at different exceedance frequencies associated with (a) medium-confidence SSP5-8.5 and (b) low-confidence SSP5-8.5 scenarios

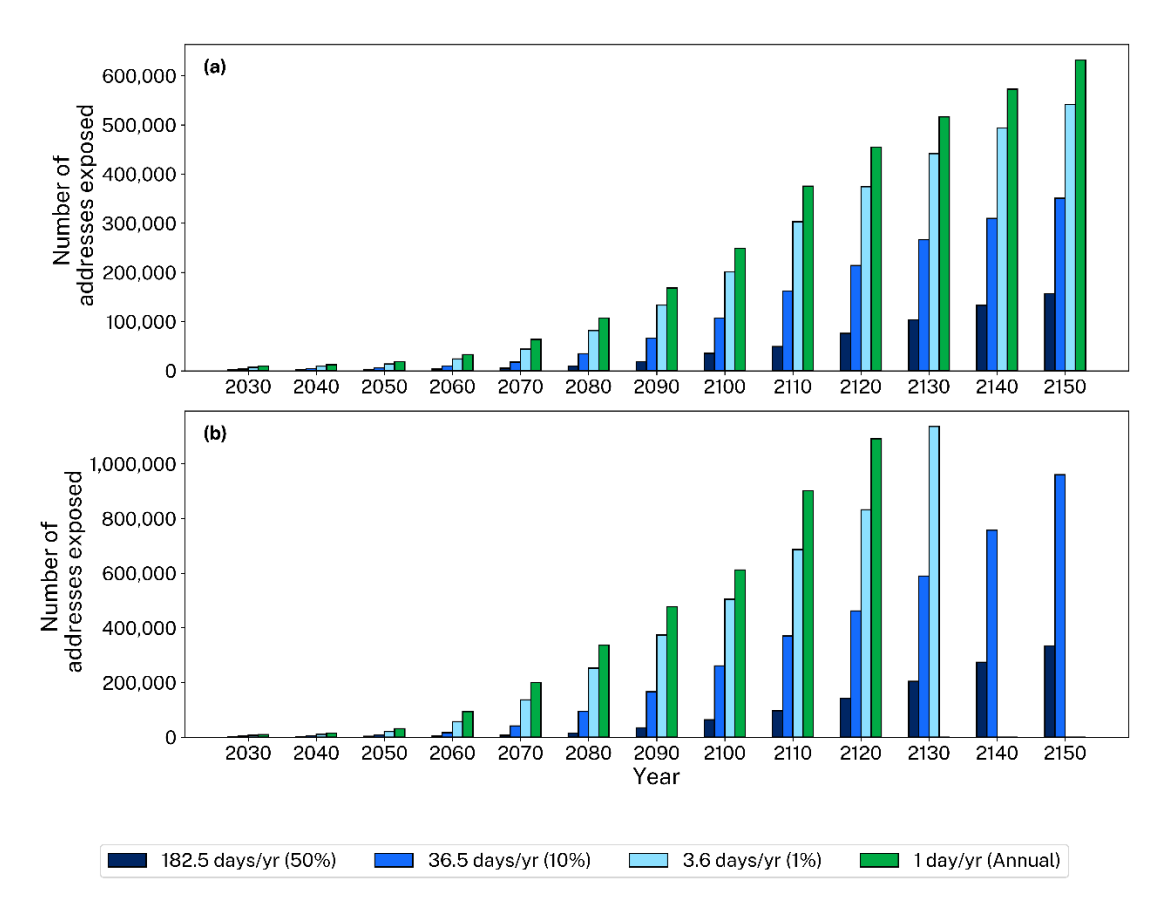


Figure 110 State-wide counts of addresses exposed to inundation over time at different exceedance frequencies associated with (a) medium-confidence SSP5-8.5 and (b) SSP5-8.5 low-confidence scenarios

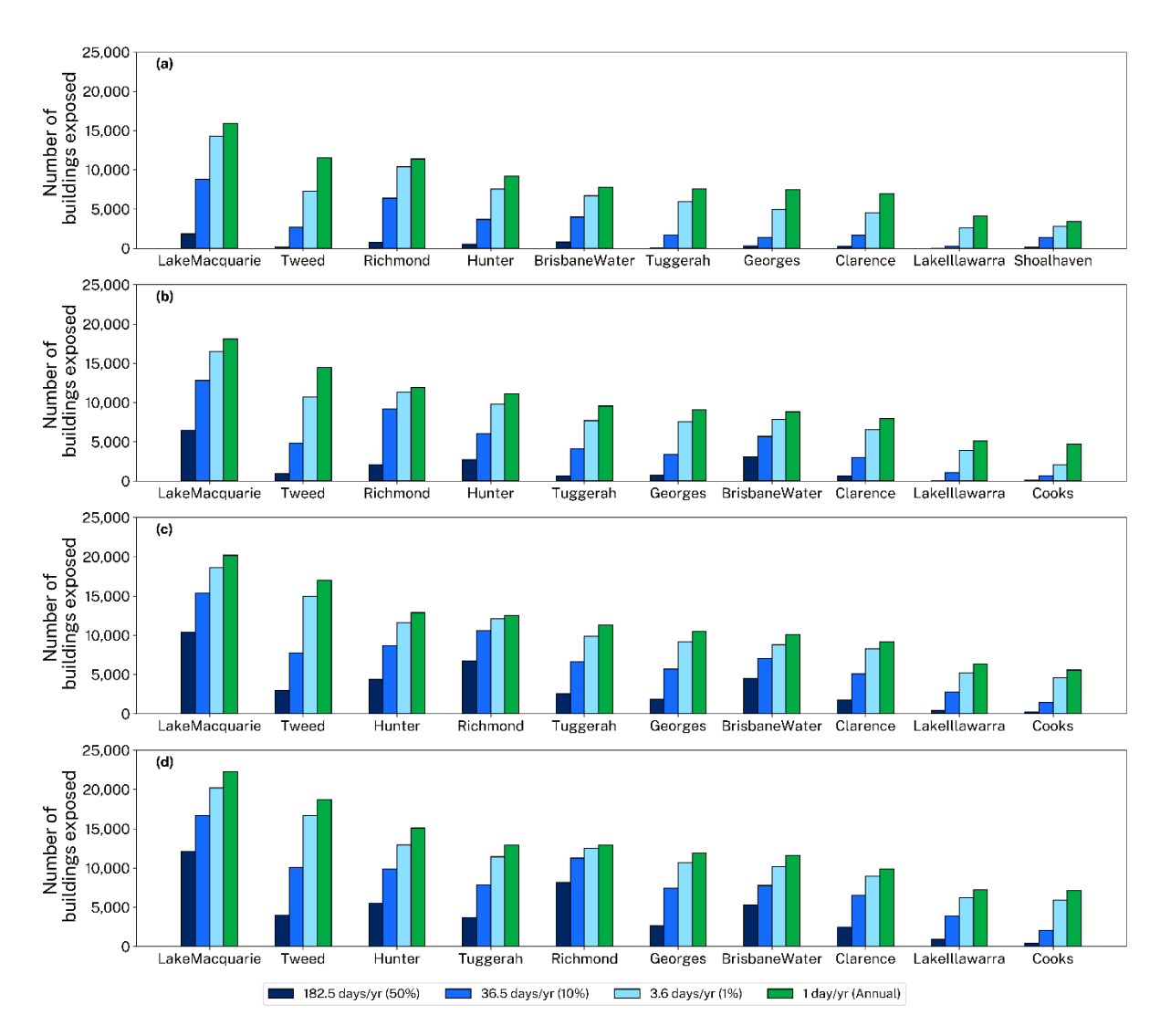


Figure 111 Bar plots of the 10 estuaries most exposed to inundation (defined in terms of building counts) in 2150 under (a) SSP1-2.6, (b) SSP2-4.5, (c) SSP3-7.0 and (d) medium-confidence SSP5-8.5 scenarios

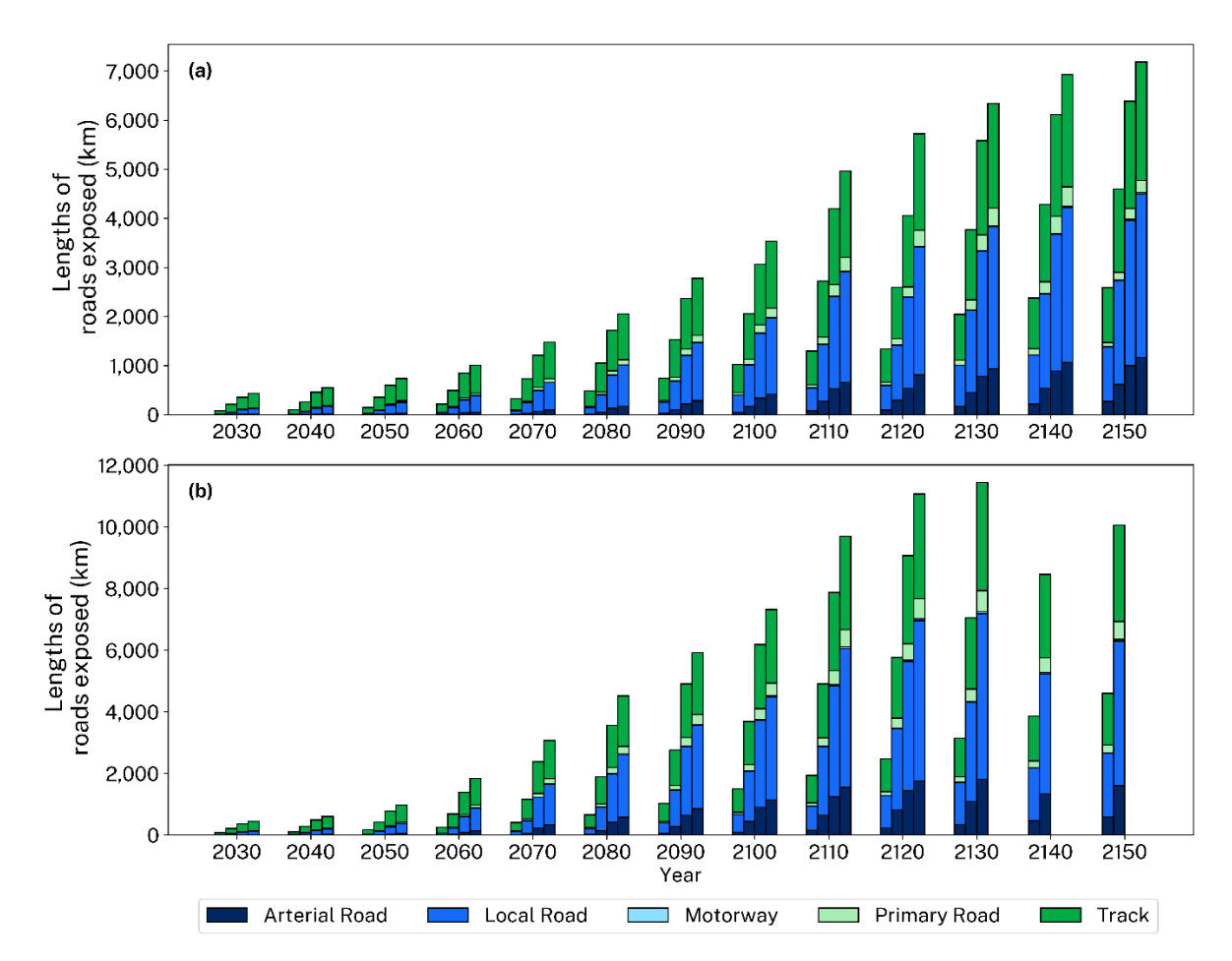


Figure 112 State-wide road lengths (km) by type exposed to inundation over time at different exceedance frequencies (from right to left: 1 day/year (annual), 3.6 days/year (1%), 36.5 days/year (10%), and 182.5 days/year (50%) exceedance) under (a) medium-confidence SSP5-8.5 and (b) SSP5-8.5 low-confidence scenarios

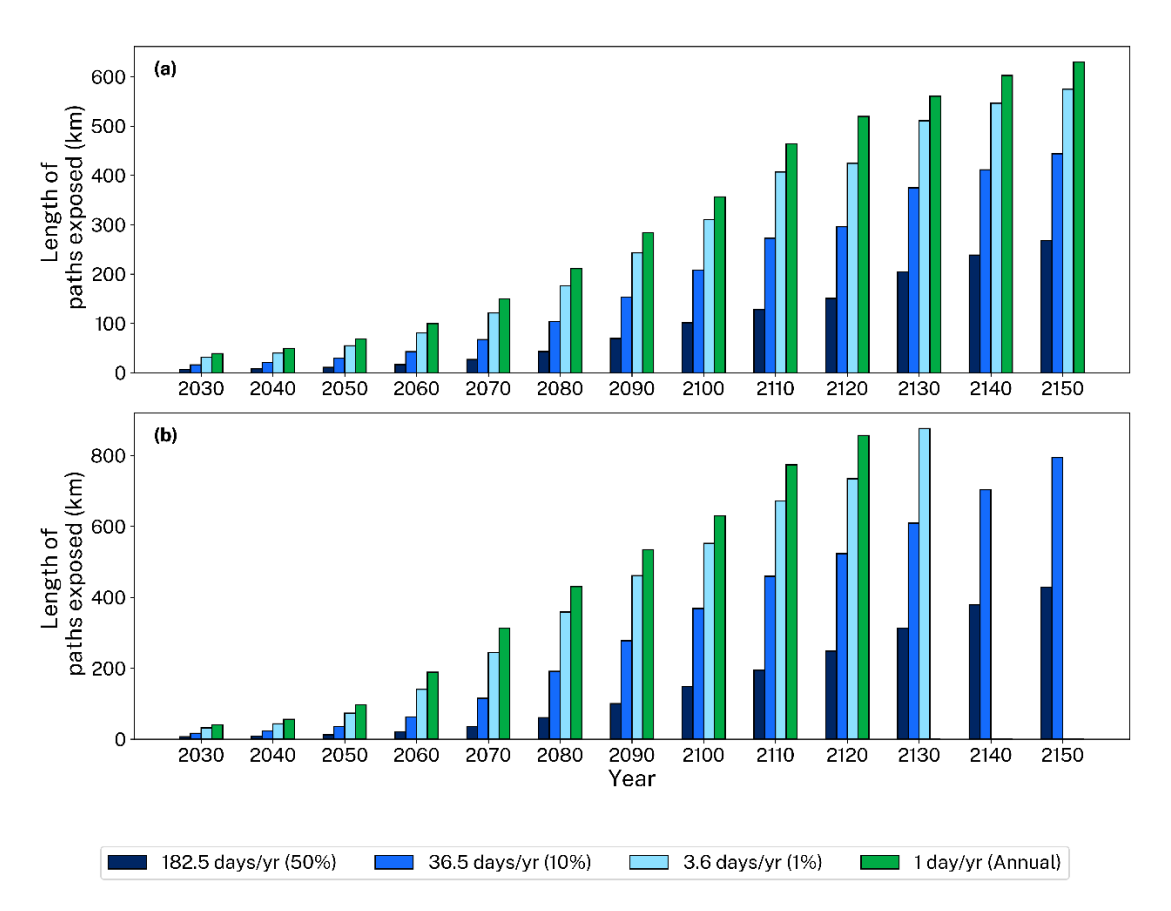


Figure 113 State-wide path lengths (km) exposed to inundation over time at different exceedance frequencies under (a) medium-confidence SSP5-8.5 and (b) low-confidence SSP5-8.5 scenarios

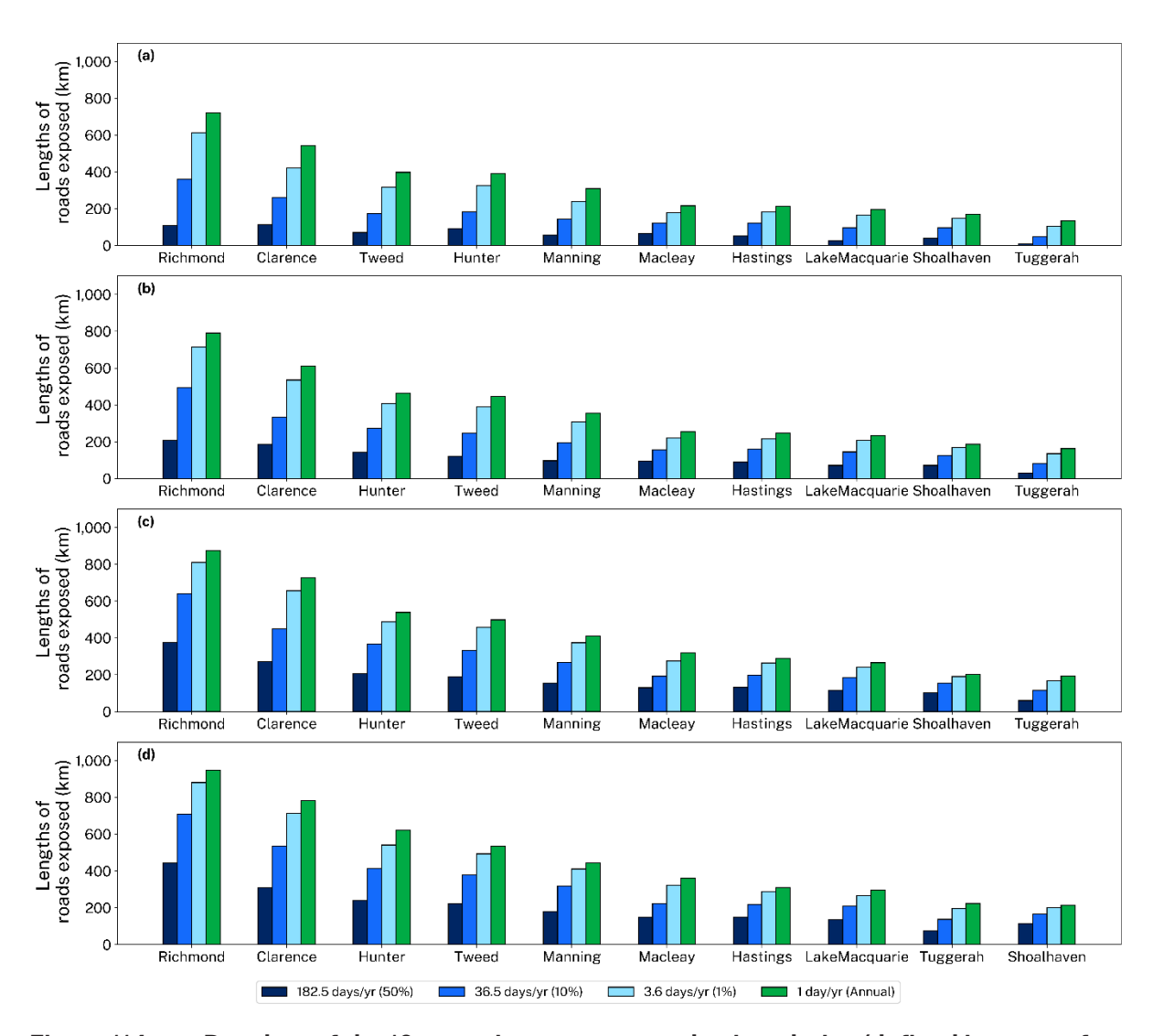


Figure 114 Bar plots of the 10 estuaries most exposed to inundation (defined in terms of road lengths) in 2150 associated with various exceedance frequencies under (a) SSP1-2.6, (b) SSP2-4.5, (c) SSP3-7.0 and (d) medium-confidence SSP5-8.5 scenarios

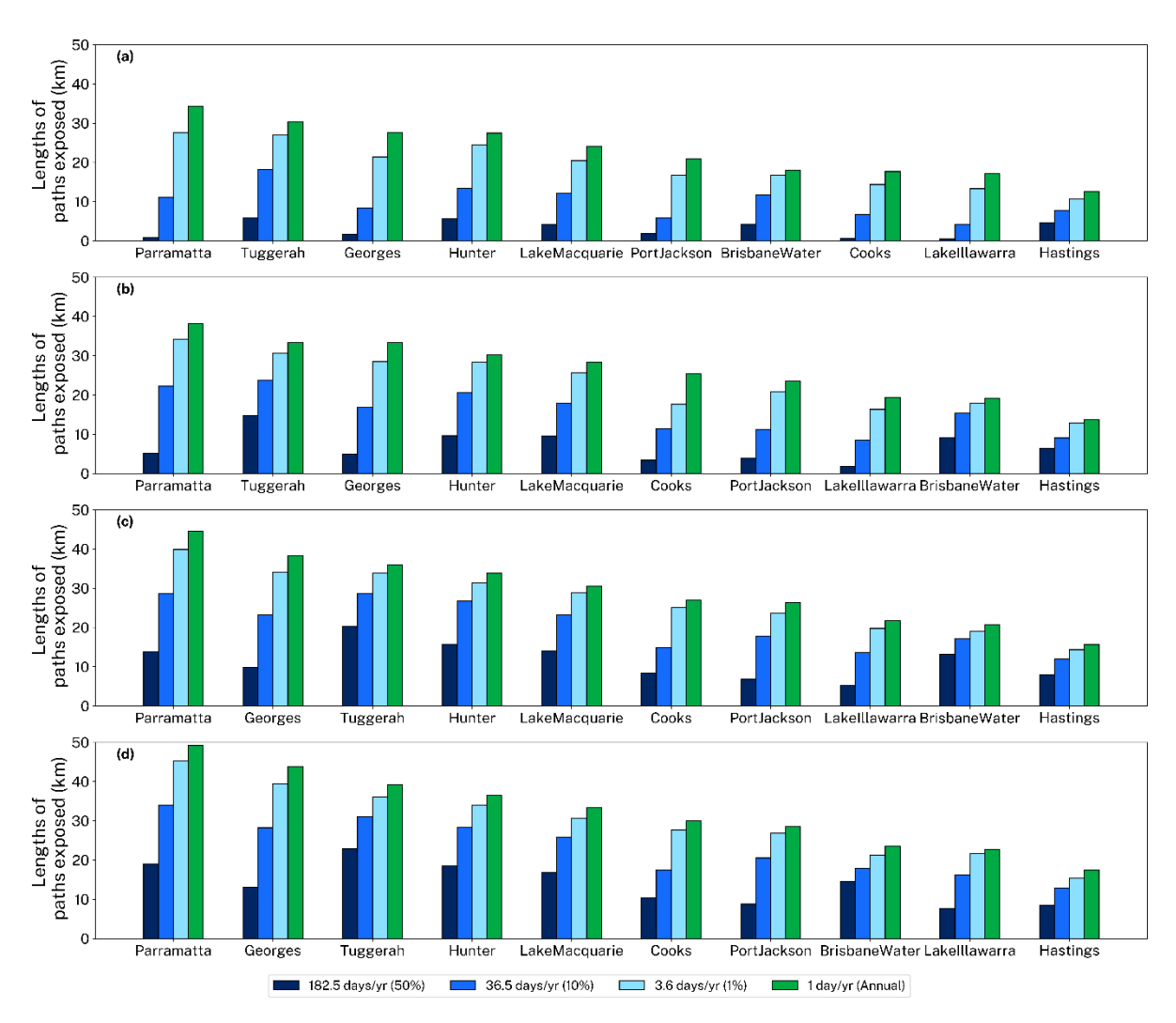


Figure 115 Bar plots of the 10 estuaries most exposed to inundation (defined in terms of path lengths) in 2150 associated with various exceedance frequencies under (a) SSP1-2.6, (b) SSP2-4.5, (c) SSP3-7.0 and (d) medium-confidence SSP5-8.5 scenarios

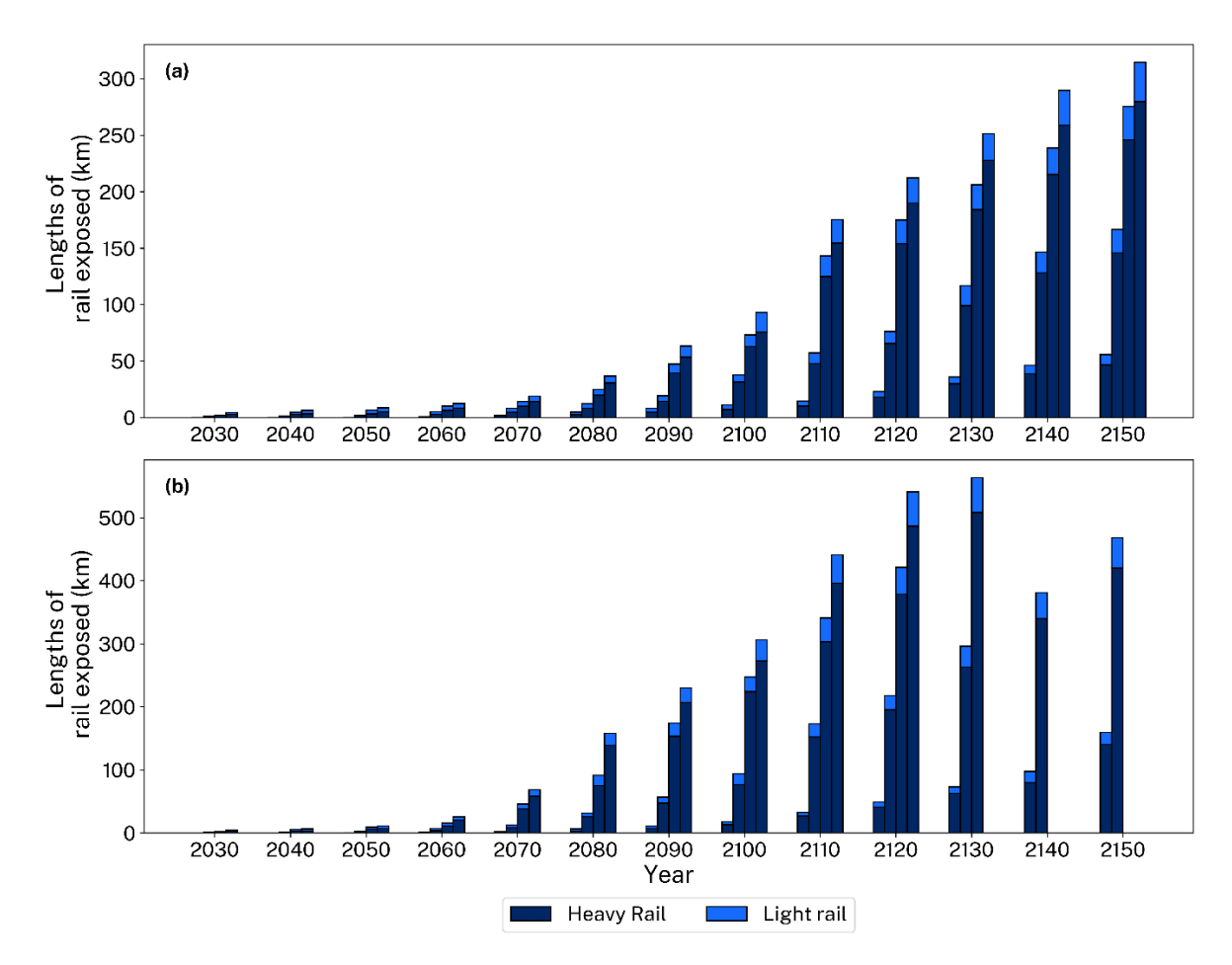


Figure 116 State-wide rail lengths (km) by type exposed to inundation over time at different exceedance frequencies (from right to left: 1 day/year (annual), 3.6 days/year (1%), 36.5 days/year (10%), and 182.5 days/year (50%) exceedance) associated with (a) under medium-confidence SSP5-8.5 and (b) low-confidence SSP5-8.5 scenarios

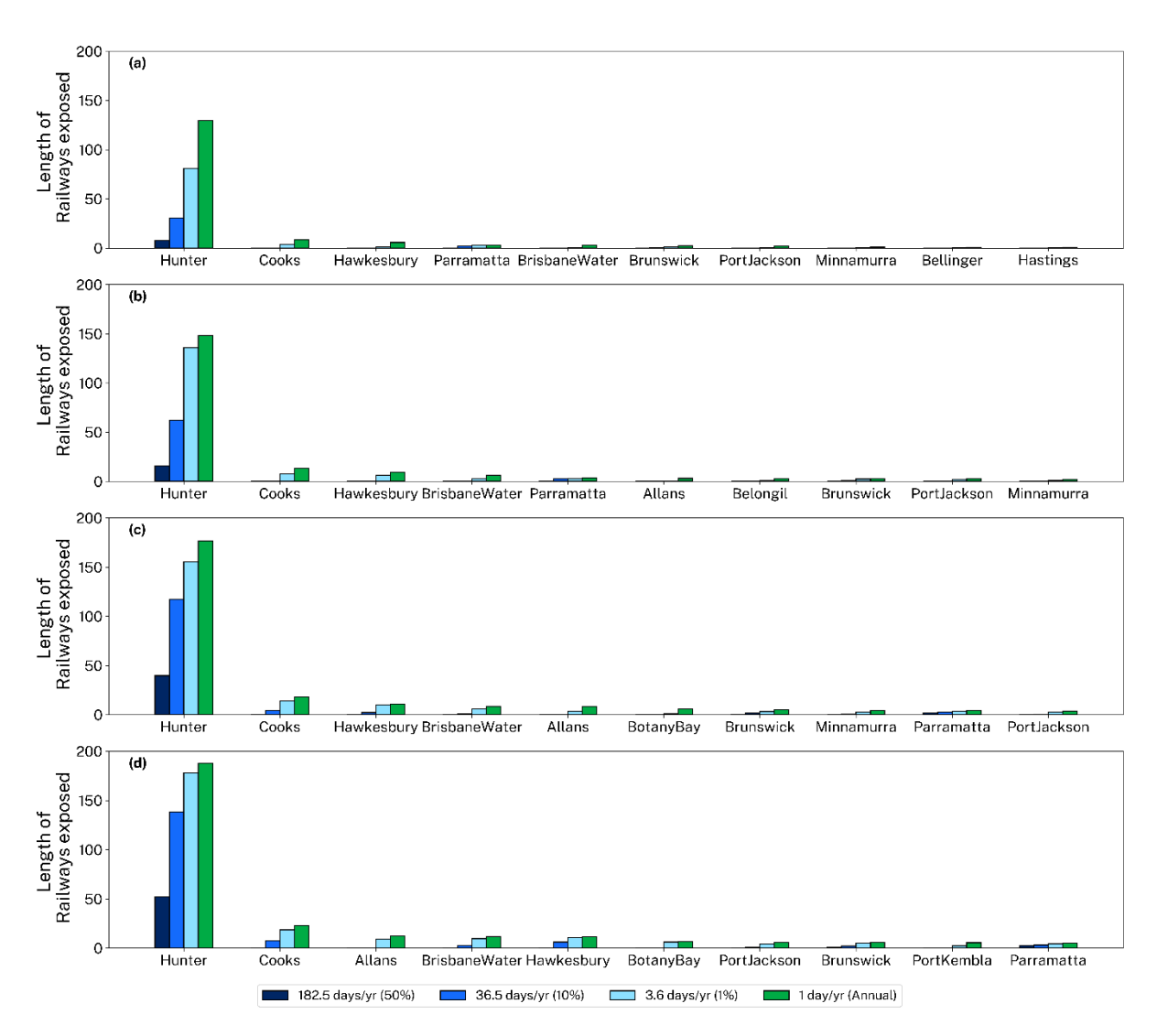


Figure 117 Bar plots of the 10 estuaries most exposed to inundation (defined in terms of rail lengths) in 2150 at different exceedance frequencies under (a) SSP1-2.6, (b) SSP2-4.5, (c) SSP3-7.0 and (d) medium-confidence SSP5-8.5 scenarios

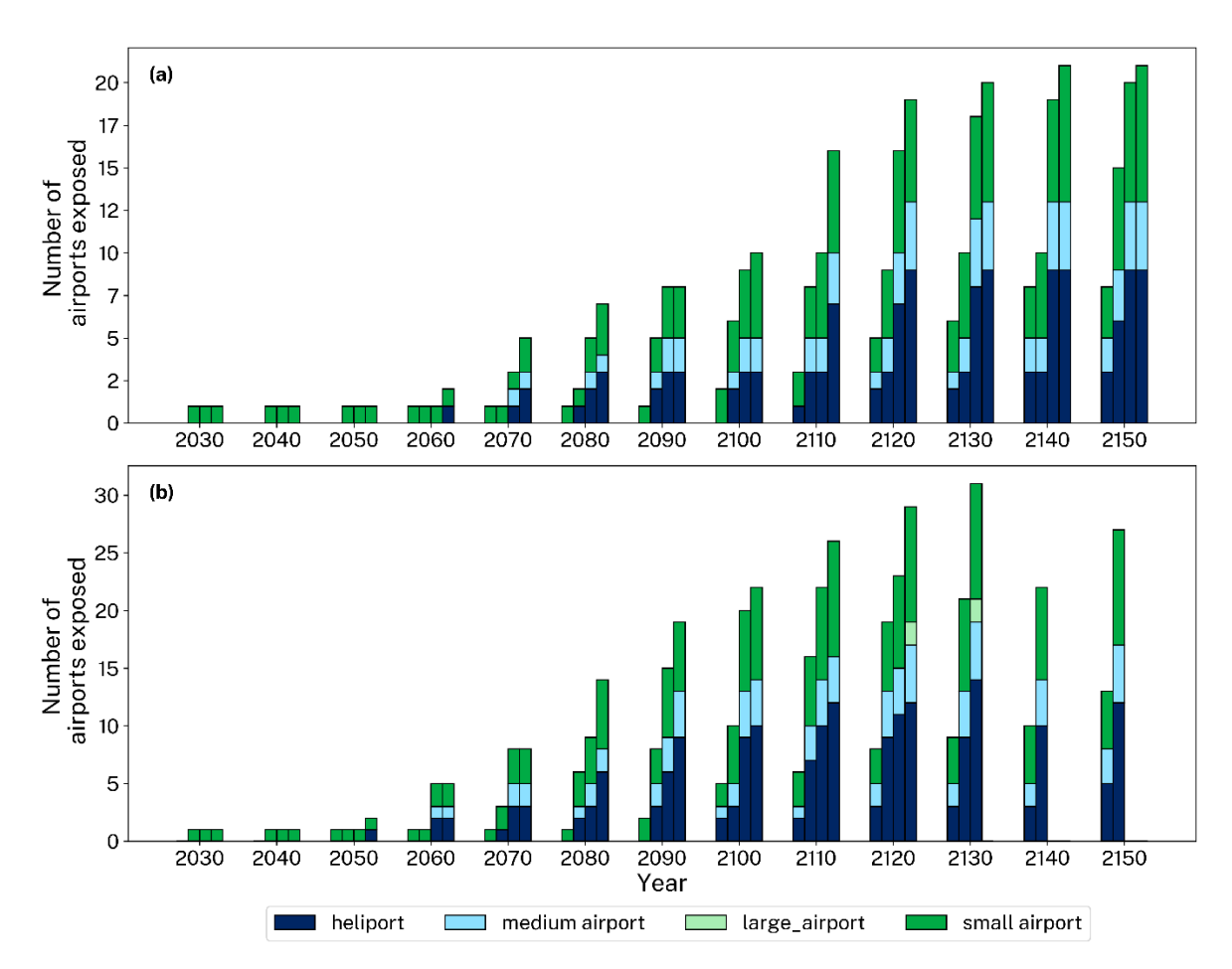


Figure 118 State-wide airports by type exposed to inundation over time at different exceedance frequencies (from right to left: 1 day/year (annual), 3.6 days/year (1%), 36.5 days/year (10%), and 182.5 days/year (50%) exceedance) under (a) medium-confidence SSP5-8.5 and (b) low-confidence SSP5-8.5 scenarios

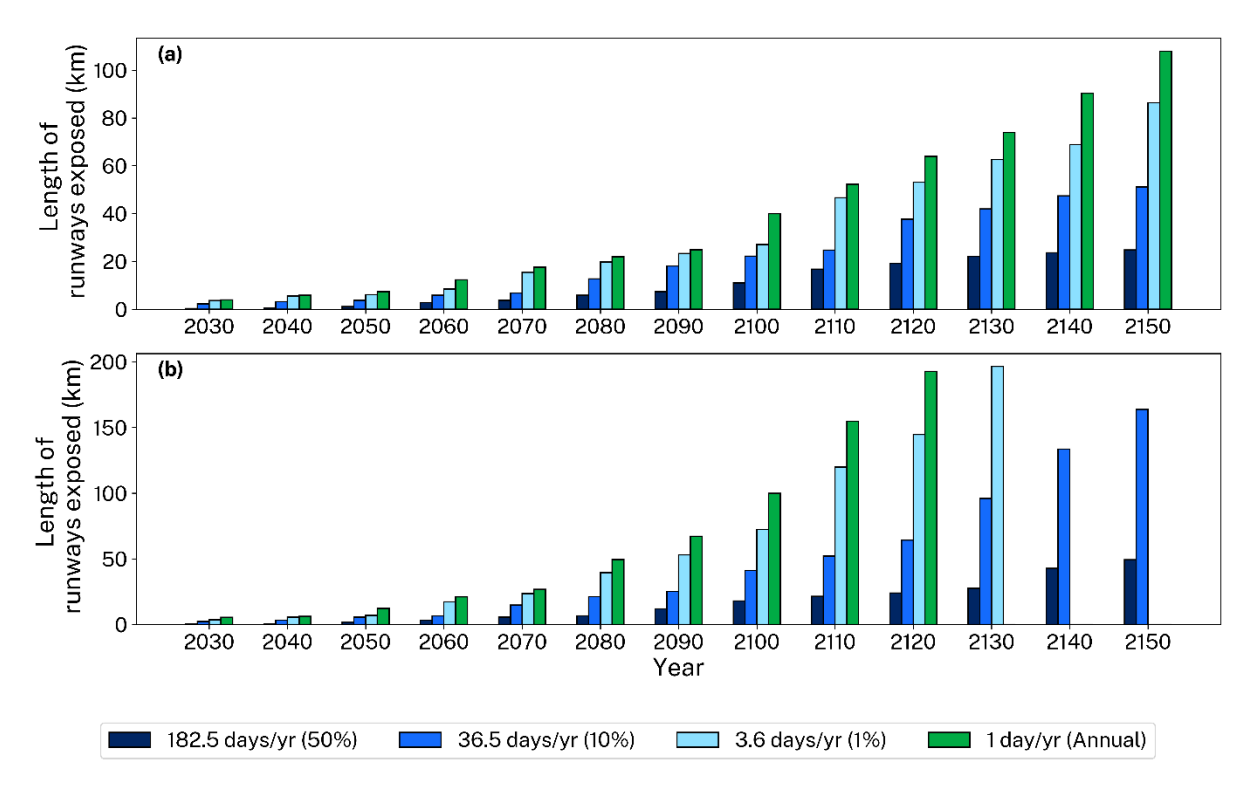


Figure 119 State-wide runway lengths (km) exposed to inundation over time at different exceedance frequencies under (a) medium-confidence SSP5-8.5 and (b) low-confidence SSP5-8.5 scenarios

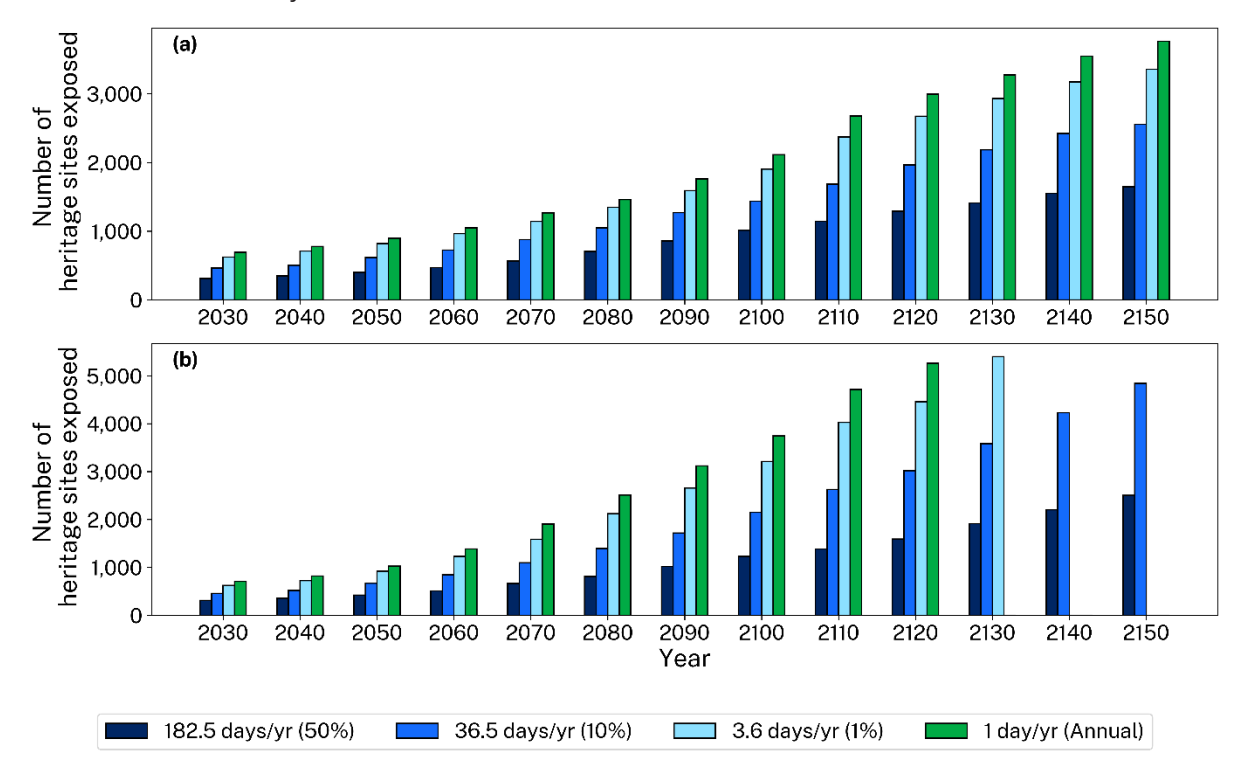


Figure 120 State-wide Aboriginal cultural heritage sites exposed to inundation over time at different exceedance frequencies under (a) medium-confidence SSP5-8.5 and (b) low-confidence SSP5-8.5 scenarios

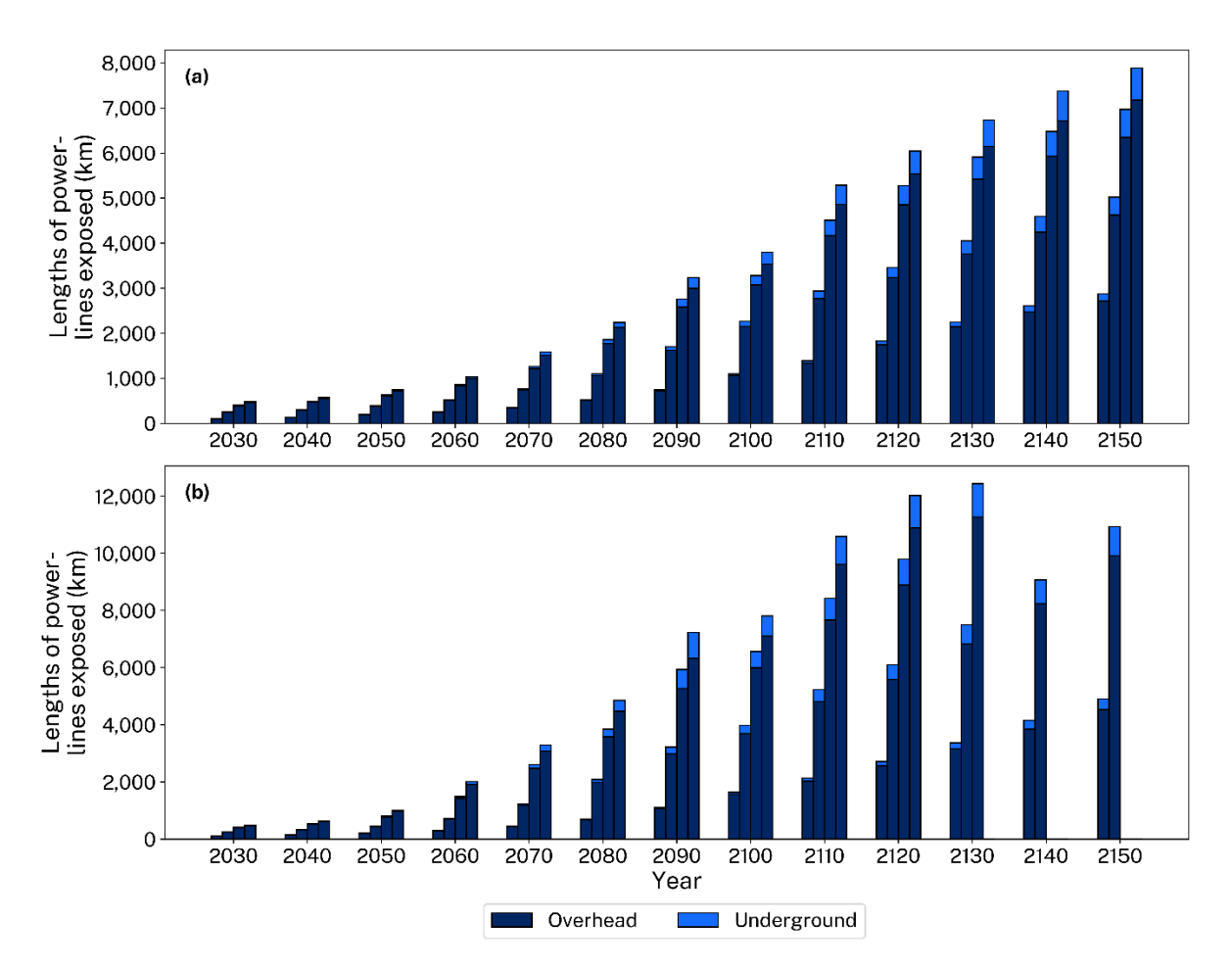


Figure 121 State-wide lengths (km) of electricity transmission lines, by type, exposed to inundation over time at different exceedance frequencies (from right to left: 1 day/year (annual), 3.6 days/year (1%), 36.5 days/year (10%), and 182.5 days/year (50%) exceedance) under (a) medium-confidence SSP5-8.5 and (b) low-confidence SSP5-8.5 scenarios

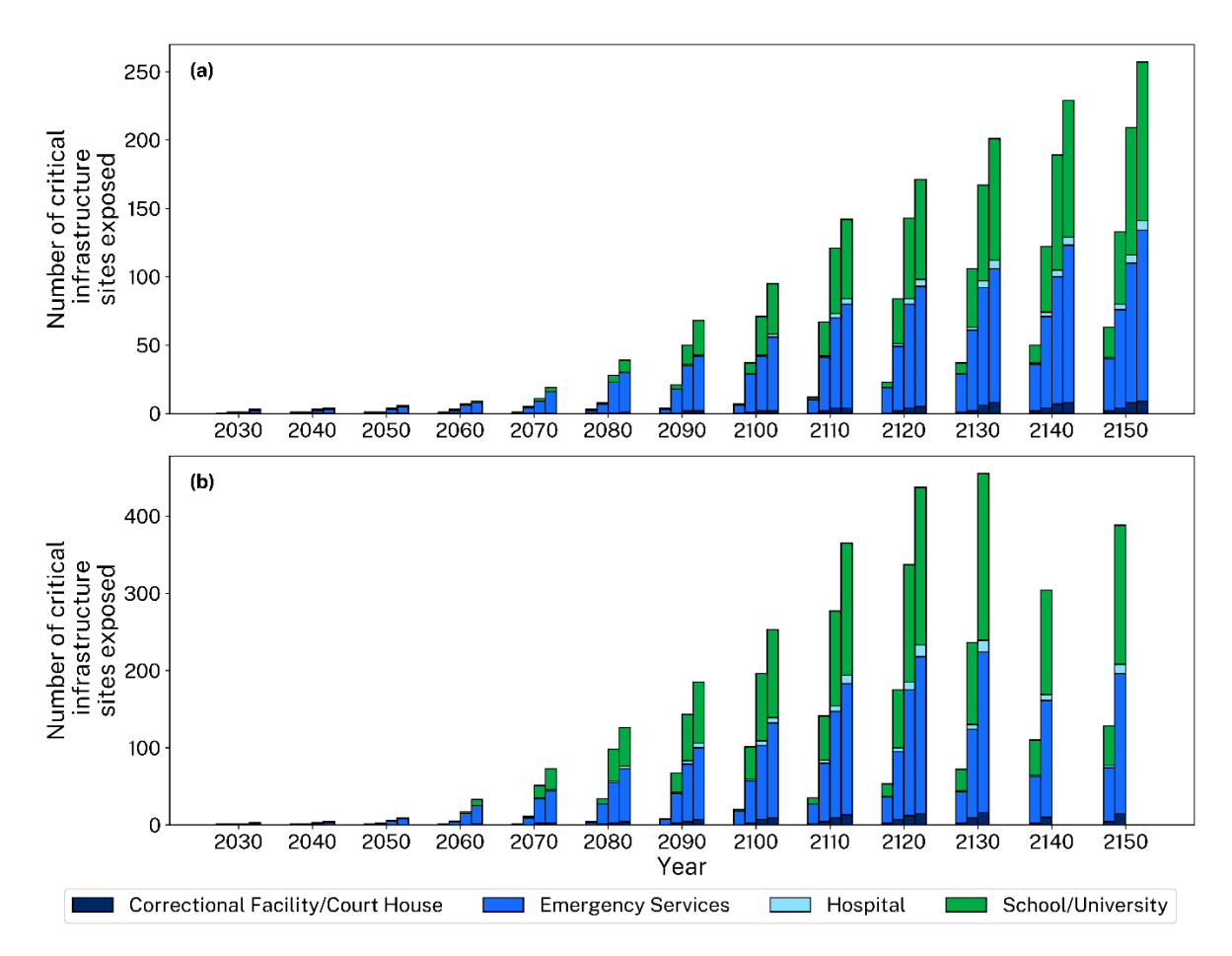


Figure 122 State-wide critical infrastructure assets, by category, exposed to inundation over time at different exceedance frequencies (from right to left: 1 day/year (annual), 3.6 days/year (1%), 36.5 days/year (10%), and 182.5 days/year (50%) exceedance) under (a) medium-confidence SSP5-8.5 and (b) low-confidence SSP5-8.5 scenarios